Design, Performance, and Analysis of an Automated Tool for Neuropathy Assessment on the Plantar Surface

by

Vitale Kyle Castellano

A dissertation submitted to the Graduate Faculty of
Auburn University
in partial fulfillment of the
requirements for the Degree of
Doctor of Philosophy

Auburn, Alabama
August 6, 2022

Keywords: Diabetic Peripheral Neuropathy, Threshold Sensitivity Assessment, Machine Design, Computer Numerical Control, Finite Element Analysis, Semmes-Weinstein Monofilament

Approved by

Michael Zabala, Chair, Assistant Professor of Mechanical Engineering
Robert L. Jackson, Professor of Mechanical Engineering
Chad Rose, Assistant Professor of Mechanical Engineering
Richard Sesek, Associate Professor of Industrial and Systems Engineering

Abstract

Diabetic peripheral neuropathy results in the loss of sensation in the hands and feet. Other symptoms such as numbness, burning, shooting pain, and electrical sensation have been reported. Individuals with this disease are at a greater risk of requiring amputations, as a result of unknowingly puncturing the soles of their feet leading to infection and ulceration. Tuning forks, electrodiagnostic equipment, and other novel inventions have been used to detect for neuropathy on the plantar surface, but the Semmes-Weinstein monofilament remains the most common tool. The monofilament is pressed against the plantar surface until it buckles, at which point it theoretically produces a maximum contact force, often expressed using grams of force. The most popular monofilament examines for the loss of protective sensation, designated at the threshold sensitivity of 10.0 grams of force. However, this tool's accuracy is subject to factors such as insertion rate, angle of insertion, diameter, length, human skin material properties, temperature, humidity, and even material fatigue. As such, the purpose of this dissertation is to demonstrate the practical concerns of the hand-applied Semmes-Weinstein monofilament assessment technique, present a novel diagnostic tool which automates the assessment protocol, and implement it in a clinical study to ascertain subjects' current degree of threshold sensitivity on the plantar surface.

Relevant background information is provided in Chapter 1, while Chapter 2 of this dissertation details a theoretical contact mechanics analysis of a hand-applied Semmes-Weinstein monofilament in contact with a human skin sample. Theoretical equations and finite element analysis are both used to explore the influence that monofilament diameter, insertion depth, and material skin properties have on the contact force, and corresponding normal stress at the center

of contact. Both a homogeneous isotropic and composite isotropic model are considered, the later includes the epidermis, dermis, and subcutaneous fat layers of human skin. The study resulted in 188 finite element analysis simulations, which after linear regression analysis led to the derivation of empirical equations. The equations relate contact force and normal stress at the center of contact to insertion depth, the epidermis stiffness, and dermis stiffness. The conclusions of this study were that small amounts of insertion depth can have a substantial impact on the contact force produced, and that the material properties of the epidermis and dermis layers are also impactful. These findings suggest that attention to application technique is recommended when interpreting the results while using the hand-applied monofilament for neuropathy assessment on the plantar surface. Furthermore the necessity for a force feedback loop used to measure the contact force during application is established.

After understanding the practical concerns of the hand-applied Semmes-Weinstein monofilament assessment, examined in a non-buckling simulation study, and the dependencies on external factors on the tool's accuracy, the development of an automated tool is presented in Chapter 3. This automated tool took the current commercially available 10.0-gram force Semmes-Weinstein monofilament and placed it in a robotic CNC device. The monofilament was moved into position with the use of belts and pulleys and was attached to an innovative probe subassembly. The probe subassembly used a stepper motor load cell feedback loop to constantly measure the contact force during insertion, until a prescribed value was achieved. The device used a new methodology which evaluated 13 locations per foot, grouped within three regions: toes, ball, and heel. The device was used at each location until the threshold sensitivity was determined, based

on the following force classifications: 0.35, 0.70, 2.0, 4.0, 6.0, 8.0, 10.0, and >10.0 grams of force. The methodology featured randomization, false positive checks, and documentation.

The automated tool was used in a clinical study that is presented in Chapters 4 and 5. Chapter 4 encompasses the device's force producing accuracy, a comparison to a hand-applied Semmes-Weinstein monofilament assessment, and linear regression analysis between subject's age, body mass index (BMI), ankle brachial index (ABI), fasting blood sugar (FBS), HbA1c and threshold sensitivity. The subjects examined in Chapter 4 were healthy control subjects, without type 2 diabetes mellitus. A Threshold Sensitivity Index (TSI) was calculated for each region, in addition to a TSI Norm. TSI Norm was representative of a subject's entire threshold sensitivity across 13 locations per foot. The automated tool's force producing accuracy was determined to be associated with the region the locations were within. The maximum average absolute errors were 0.5, 1.2, and 0.9 grams of force at the toe, ball, and heel locations, respectively. The toes demonstrated an average absolute error less than or equal to 0.4 grams of force at 98% of the locations evaluated, while the ball locations and heel locations were 84% and 60%, respectively. The 10.0 grams of force hand-applied monofilament was underdiagnosing 21% of the locations when compared to the automated device. Linear regression analysis found that the healthy control subjects attributed their threshold sensitivity (TSI Norm) to their age via significant linear regression (R^2=0.3422, P=0.004), while BMI, ABI, fasting blood sugar, and HbA1c were uncorrelated. Chapter 5 repeated the linear regression analysis between TSI Norm, age, BMI, ABI, fasting blood sugar, and HbA1c, for subjects with type 2 diabetes mellitus, with and without neuropathy symptoms. The subjects from Chapter 4 and 5 had ages, BMIs, and ABIs that where not significantly different when evaluated using ANOVAs. These subjects had

significantly different fasting blood sugars and HbA1c levels. Nonetheless, the study did not find a significant difference between each group's TSI Norm. The groups with type 2 diabetes did not correlate their threshold sensitivity to their age, BMI, ABI, fasting blood sugar, or HbA1c. This finding encourages the use of the automated tool for follow up screenings to monitor neuropathy disease progression on the plantar surface.

Chapter 6 details the development of the second iteration of the automated tool. Although the second prototype retained a similar gantry system and probe subassembly, improvements enhanced its structural rigidity and usability. Chapter 7 presents future studies that could be conducted in concert with the automated tool. Topics such as the effects of sex and time of year are encouraged, as well as determining locations that yield a better potential for earlier diagnosis. Using the automated tool for treatment monitoring would also be beneficial. Improvements to the control systems and the code that runs the automated tool are encouraged.

This dissertation presents the development and functionality of an automated tool for neuropathy assessment on the plantar surface. It was used in a clinical study, which concluded that threshold sensitivity is challenging to predict using age, BMI, ABI, fasting blood sugar, or HbA1c alone. With the automated tool threshold sensitivity can be documented and studied over time, which could provide both clinicians and their patients insights into the efficacy of treatments and disease progression.

Acknowledgements

I would like to thank Dr. Zabala for all of his advisement throughout my time at Auburn University. I would also like to thank my committee members Dr. Jackson, Dr. Rose, and Dr. Sesek for their support in my research and for serving on my defense. Their feedback towards my dissertation has been invaluable, and I am glad they were as enthusiastic about my research as I was. I would like to thank Dr. Burch and Dr. Commander for all of their support and insight throughout the development of this device. Dr. Burch has provided much of his engineering knowledge towards the device, while Dr. Commander has provided medical insight vital for the success of this project. I learned a great deal from both of them and am grateful for the opportunity to have worked beside them. I am grateful to Dr. Brock for being a good liaison between the Edward Via College of Osteopathic Medicine (VCOM) and Auburn University throughout this project. I am appreciative to VCOM for funding my research and for the support of their staff and faculty.

I am extremely appreciative for all my friends: Elliot Boerman, Jordan Coker, Austin Harris, Amelia Falcon, and Taylor Troutman for helping me get through my PhD and for always being there to support me. They were always there for me when I needed to be encouraged. Without their friendship, I am not sure I would have been able to finish this degree. I know I will be lifelong friends each of them.

Hayden Burch deserves a special acknowledgement for his time and commitment in this research project. He developed a good concept which served as the starting point for me when I began my graduate studies. We then came together and over the course of a summer we improved the

machine by developing a new method of applying the monofilament using a feedback loop between a stepper motor and a load cell. This device allowed the machine to be far more accurate and repeatable. Not only did I learn a great deal from him, but I also implemented many things he taught me about coding in other scripts and functions I wrote. I couldn't have done it without him and am grateful he worked so hard with me on this project.

Additionally, I would like to acknowledge Dr. Tippur for taking the time to meet with me and my dad when I was looking at graduate schools. Before I came to Auburn, he would always answer my questions regarding undergraduate courses I should take to better prepare myself for graduate school at Auburn. I also took many courses with Dr. Tippur and valued his availability for help outside of class and for challenging me to think critically about the course material. I appreciate the help I received from Shay Pilcher in manufacturing some of the components of my device. I need to also acknowledge Dr. Brady, Jake Neu, and the Auburn University IP Exchange for their guidance and assistance in filling the provisional and nonprovisional patent applications on the automated tool.

I am grateful to Auburn University and the Samuel Ginn College of Engineering for allowing me to not only get the opportunity to receive my Masters, but also my PhD in Mechanical Engineering. I was awarded an Auburn University Presidential Research Fellowship, which supported me during my PhD. Without this support I would have been unable to even begin my PhD.

I was fortunate to have meet and worked among Zac Young, Hayden Patterson, Mitch Owens, Daniel Mazur, Mit Patel, and Lydia Pass. Each are pursuing the American Dream and are doing it the right way by working hard yet staying humble. I wish each of them all the best in their future endeavors and know that they will achieve all of their goals and dreams.

During my research, I worked with a group of VCOM medical students who assisted with the clinical study that took place at Internal Medicine Associates, in Opelika, AL. Without Jessica Remy, Benjamin Harman, Yousef Nikzai, Austin Gould, David McGregor, David Axford, Chad Gibbs, Wesley Ortmann, Graham Trott, Nathan Anthony, Katie Allen, Raydeer Piromari, and Bradley Louis I would not have been able to collect data, and consequently would have been unable to write this dissertation. I would like to thank them all and wish them all the best as they begin to practice medicine.

Additionally, I would like to take the time to thank professors from my undergraduate education at Kennesaw State University (Southern Polytechnic State University), where I earned my Bachelor of Science in Mechanical Engineering Technology. I would like to thank Dr. Nasseri for taking me under her wing and teaching me what engineering research is all about. Together we conducted research in biomedical engineering and manufacturing engineering, working with her motivated me to pursue graduate education and I am glad I did. I became a better engineer because of her and will always be grateful to her. Next, I would like to acknowledge Professor Conrey for being a good mentor for me during my undergraduate studies and for all his advice and guidance. We had many good conversations and I always felt welcomed in the MET program because of him. I would like to thank Professor Turner for her support and always

answering my questions. Professor Turner was my statics professor and to this day I believe that statics it the foundation for engineering education and I am grateful to have learned from her. I also need to acknowledge Professor Sweigart for being my professor is so many engineering courses at SPSU. I spent many hours in his courses, but I feel that I became a better engineer from learning from him. Professor Winsor is also a professor I would like to thank, he is a fellow Auburn Alumni and because of him I was able to hone my SolidWorks skills which allowed me to become a professional at SolidWorks by obtaining the CSWP. He was also a fantastic professor and I always looked forward to his lectures. Other SPSU professors I would like to thank are Professor Emert, Dr. Russell, Dr. Stollberg, Dr. Ritter, Dr. Thackston, Professor Ilksoy, Professor Duff, Professor Jenkins, Dr. Trebits, and Dr. Pascu.

There are also a number of teachers from high school, middle school, and elementary school that I would like to acknowledge for working with me and instilling in me a passion for learning. They include Mrs. Stiers, Mrs. Stuler, Mr. Turner, Mr. Englebert, Mr. Tozier, Mrs. Whittaker, Mrs. Waddell, Mrs. Williams, Mr. Hamm, Mrs. Wilson, Mrs. Godby, Mr. Gathing, Mr. Miller, Mrs. Winkler, Mrs. Pickens, Mrs. Artzer, Mrs. Harrison, Mrs. Ingram, Mrs. Foster, Mr. Newton, Mrs. Waters, Mrs. McEntyre, Mrs. Reese, Mrs. Bialek, Mr. Cotton, Mrs. McGlumphy, Mrs. Hunt, Mrs. Woodring, Mrs. Stils, Mrs. Gravitt, Ms. Reis, and Mrs. Mallanace. In addition, I would like to acknowledge my 6th grade technology teacher, Mr. Taylor, who first introduced me to the area of STEM and for recognizing my hard work ethic. Since then, I always knew I would end up in a STEM field.

I need to sincerely thank Mr. Johnson, my high school engineering teacher and fellow Auburn Alumni. I learned so much from him both in the classroom and at Robotics Club. To this day I still use things he taught me. When building my machine I used 80/20 Aluminum profiles, which we used in Robotics Club. I thought of the idea of using a laser cutter to manufacture my acrylic plates from him, as we had one in high school and used it for various projects. I could never thank him enough for introducing me to the world of engineering, it is hard for me to believe that I would have pursued engineering in college and as a career path without him. Sometimes there is that one person in your life that makes a big difference and to me Mr. Johnson is that person. I will always remember him and continue to use the things he taught me throughout my life.

I would like to thank some close friends, starting with Ben Semmens and Cory Culberson for all of their support and camaraderie. I meet them the first week I was in Auburn, and shortly after we became good friends. We would often work together in class projects, and they are by far the best group I have been a part of. I would also like to thank Reed Rodich, Theresa Hardin, Grace Gray, and Sierra Eady for their support during my graduate studies. Next, I would like to thank Kurt Jacobson, Thomas Kosko, Tim Slaughter, Dan Homisak, Mushfequr Kotwal, Thomas Smith, Nathan Buck, Paul Schwan, Sams Khan, Daniel Bain, Taylor Bounds, and Herve Sobtaguim for their friendship.

Some other people I would like to thank are Dr. Jenkins, Dr. Beach, Dr. Sessions, Dr. Cofrancesco, and Dr. Cleaver for all of their support and help throughout my life. They were always there for me when I needed them the most and they always gave me peace of mind.

Lastly, I would like to thank my family for all of their love and support, especially during my time during my graduate studies. To my mother I would like to thank her for all of her support, for working with me when I was younger, and for being the best teacher I have ever had. Without her I would never have overcome my reading and learning disability, as well as my speech impediment when I was in elementary school. She helped me learn good study habits and better writing techniques that I still use to this day. To my father I would like to thank him for always supporting me and for always having fun with me. We bonded over fast cars, speakers, and fishing. We have always had an enjoyable time together as father and son fixing and building things. Both of my loving parents have always supported my academic aspirations and without them I would have never developed my work ethic which has taken me far. Additionally, I would like to thank my brother Kevin, my best friend, for always being there for me. We have always brought out the best in each other and I am glad he is my brother. I would like to thank my little buddy Rudy for always making me laugh and smile, even to this day. I would like to thank my grandfather and grandmother, Mario and Concetta Marino, for their love and support. Although I only got to spend a couple of years getting to know my grandfather, I would like to think he would have liked to see me become an engineer, as he worked with many. I never met my grandmother, she came to America from Italy as a little girl to escape fascism, and she is the bravest person I have ever heard of by doing so. I would also like to thank my grandparents, Vic and Val Castellano, for all of their love and support. They have always given kind words of encouragement and I am very grateful for them for always thinking of me. I would also like to thank my Zsi Zsi, Uncle Dan, and Zsi Zsi Fred for always thinking of me and for their love and support throughout my life. The three of them have always been there for me and my family and

I can’t wait to spend more time with them in the future. In addition, I would like to thank my Aunt Connie, Aunt Katie, Uncle John, Uncle Frank, and Aunt Pam for their love and support.

I think that in most people’s lives there is often one person that without, you would have turned out differently. However, I am fortunate and grateful to have many. From my family to my friends, and to my teachers I am a better person because of them and will always remember them for the kindness they have given me. Although this PhD was challenging in ways I wasn’t expecting, I still did it and I did it my way.

War Eagle!

Table of Contents

List of Tables

List of Figures

Chapter 1: Introduction and Background

1.1. Dissertation Overview

This dissertation addresses the current landscape of diabetic peripheral neuropathy on the plantar surface. Diabetic peripheral neuropathy is often attributed to the loss of sensation in the extremities, especially in older individuals with type 2 diabetes mellitus. As such this dissertation depicts the symptoms associated with neuropathy, as well as the current assessment techniques used for diagnosis and their inherent limitations. The hand-applied Semmes-Weinstein monofilament assessment is the gold standard for neuropathy assessment, but its accuracy has come into question in the literature examined. Finite element analysis is used to demonstrate the practical concerns when using hand-applied monofilaments. This justified the development of a diagnostic tool which automated the evaluation process and improved the assessment accuracy. The design is presented in this work, and a prototype was used in clinical study. The clinical study's results are divided into two areas of work, the first being the accuracy and threshold sensitivity assessment of subjects in a healthy non-diabetic control population. The second is the comparison of threshold sensitivities between the healthy control subjects and subjects with type 2 diabetes mellitus, with and without neuropathy symptoms. Linear regression analyses were performed between each subject's threshold sensitivity and their age, BMI, ABI, fasting blood sugar, and HbA1c to draw conclusions regarding if these characteristics can be used as a predictive factor in an individual's degree of sensation. Following this, a second prototype is introduced, as well as future directions where this research could be taken, not only to strengthen the findings, but to encourage the development of future treatments for neuropathy.

1.2. Neuropathy Disease Background

1.2.1. Origin and History

The loss of sensation in one's extremities is often attributed to peripheral neuropathy. By its definition it is the disease of nerves away from the brain, as "peripheral" is defined as anatomically beyond the brain, "neuro" is related to nerves, and "pathy" is disease [1]. Peripheral neuropathy is the most common type of neuropathy and is especially prevalent in the hands and feet of individuals with type 2 diabetes mellitus [2, 3, 4, 5]. The origins of diabetes have been recorded as far back as 1550 BC in Egypt, while the first recorded symptoms of diabetic neuropathy were recorded by Susruta in India, circa the 5th century AD [6, 7]. Marchal de Calvi reported on the link between neuropathy and diabetes in 1864 [6, 7]. Frederick William Pavy also noted the specific symptoms of "heavy legs", lightning pain, and numb feet in the 19th century [6]. The 20th century brought with it the discovery of insulin and that the development of neuropathy is impacted by glycemic control [6, 7].

1.2.2. Current Numbers and Trends

In 2019, it was reported by the International Diabetes Federation that there are 463 million adults with diabetes, with this number increasing to an estimated 700 million by 2045 [5]. Globally there are 40 to 60 million people who experience complications attributed to neuropathy [5]. It has been suggested that 50% of adults with diabetes will develop diabetic peripheral neuropathy during their lifetime [8]. Although much of the epidemiology of diabetic peripheral neuropathy is focused on older populations, it has also been reported that 26% of adolescents with type 2 diabetes also have peripheral neuropathy [8]. Individuals who have neuropathy are at a greater risk of developing foot ulcers, which are susceptible to infection and eventually may require amputations [9, 10]. To add to this, 15% of diabetics are at a risk of developing an ulcer and

there is a 10-to-20-fold increase in having a lower limb amputation than those without diabetes [5, 11]. There are approximately 80,000 lower limb amputations per year attributed to diabetic peripheral neuropathy [11]. Those who develop foot ulcers will experience an 85% chance of having an amputation, which occurs every 30 seconds worldwide [5, 12]. The cost for those who are diagnosed with painful diabetic peripheral neuropathy in the first year can exceed $16,000.00, which is double the cost for those diagnosed solely with diabetes mellitus [13]. The cost after the first year for those with painful neuropathy symptoms is approximately $14,000.00 per year [13, 14]. In 2002, the total annual cost of diabetic peripheral neuropathy in individuals with type 2 diabetes was approximately $14 billion in the US, while the cost of diabetes as a whole was $44 billion in 1997 [15]. As of 2017, the cost of diagnosed diabetes in the US has risen to $327 billion, which based on the previously cited literature indicates that the cost associated with diabetic neuropathy has increased substantially [16].

1.2.3. Type 2 Diabetes Mellitus and Neuropathy

It has often been reported that uncontrolled high blood sugar is what damages nerves and eventually causes diabetic peripheral neuropathy [17, 18]. High blood sugar can weaken the walls of capillaries, which in turn cuts off oxygen and nutrients to the nerves [17]. High blood sugar, or hyperglycemia, which takes the form of fasting blood sugar and HbA1c are used as the measure for the presence of diabetes [19]. Hyperglycemia has been linked to painful neuropathy symptoms [20]. Gaining control over blood sugar has been reported to slow down neuropathy in individuals with type 1 diabetes mellitus, but not those with type 2 diabetes mellitus [21]. However, in Bril's review, three separate studies found that glycemic control was not a strong factor in the progression of diabetic peripheral neuropathy for those with type 2 diabetes, but rather body mass index and high blood pressure are more likely [22]. High blood pressure and

insulin resistance have both been correlated to diabetic neuropathy [18]. Due to the presence of diabetic peripheral neuropathy, individuals often reduce their physical activity; consequently, this negatively impacts their vascular flow [23]. This reduction in vascular flow causes the peripheral edema, a buildup of fluid, to stagnate and can lead to an increased risk of infections [23, 24].

1.2.4. Symptoms

Neuropathy symptoms were reported in between 10% to 20% of individuals with diagnosed diabetes and between 40% and 60% of those with diagnosed diabetic neuropathy [11, 25]. Burning feet is often cited as one of the most common and persistent symptoms found in those with diabetic peripheral neuropathy [26]. Electrical sensation, shooting pain, and numbness have also all been reported as typical symptoms [27, 28, 29]. Others have described a loss of balance and difficulty walking, as well as poor sense to temperature [30]. Also prickling, tingling and weakness in the hands and feet have been described [30, 31]. Charcot's joint, although rare, is another complication, which occurs when a joint degrades due to nerve complications in the foot or ankle [32, 33]. "Diabetic foot" has been a moniker used to describe the loss of sensation in the feet for individuals who have been diagnosed with diabetic peripheral neuropathy [5]. Due to the loss of sensation and pain, an individual may puncture their foot by stepping on a sharp object without knowing it, causing an ulcer to form [9, 10, 34]. These diabetic foot ulcers can impact morbidity and mortality [35, 36, 37]. Boulton reported that those with diabetes and a history of ulceration are up to 50% more likely to develop additional foot ulcers in their lifetime [38].

1.3. Plantar Surface Anatomy

1.3.1. Anatomical References

The foot is made up of 28 bones, some of which include the talus, calcaneus, cuneiforms, metatarsals, and phalanges [39]. These can be grouped in two different ways, in regions and in columns. There are three regions of the foot, which are the hindfoot, midfoot, and forefoot [39]. Meanwhile there are two columns, the medical column (inward) and the lateral column (outward) [39]. There are five metatarsals and fourteen phalange bones in the foot, with the metatarsal heads being the main weight bearing surface of the foot [39]. Furthermore, the largest phalange is often referred to as the great toe or hallux [39]. The phalanges are either defined as the proximal phalanxes (closet to the ankle) or the distal phalanxes (farthest from the ankle) and are connected by either the proximal or distal interphalangeal joints [39]. The proximal phalanges and the metatarsals are joined together by the metatarsal-phalangeal joints [39]. The foot can also be broken down into the dorsum aspect (top) or the plantar aspect (bottom) [40]. The plantar fascia runs the distance from the calcaneus to the base of each of the five phalanges, but it is not a muscle, tendon, or nerve [39]. The plantar fascia is a strong fibrous tissue, located just beneath the skin, which provides protection to muscles located on the bottom of the foot and supports the arch of the foot [39, 41]. Relevant to this dissertation is the plantar aspect, or plantar surface, which has four distinct muscle layers, located beneath the plantar fascia [40].

1.3.2. Neurological References

The foot has five key nerves that run past the ankle, which can trace their origin to the lumbar spine [39]. The sciatic and femoral nerves comprise two branches that carry these five nerves past the ankle [39]. The femoral nerve leads to the saphenous nerve [39]. The sciatic nerve

precedes the tibial and peroneal nerves, where the peroneal nerve is further divided into the deep personal nerve and the superficial personal nerve [39]. The tibial nerve precedes the sural nerve, in addition to further branching off to form the medial plantar nerve and the lateral plantar nerve [39]. It is the medial plantar nerve and lateral plantar nerve that affect the sensitivity of the entire plantar surface and are responsible for innervating the muscles relevant to this aspect [39, 40]. In addition to these nerves there is the medial calcaneal nerve, which branches from the tibial nerve [42]. There is also the inferior calcaneal nerve which branches off the lateral plantar nerve [42]. A diagram of these neural connections is provided below in Figure 1-1, in addition to Figure 1-2, which shows approximate nerve locations on the plantar surface [42, 43].

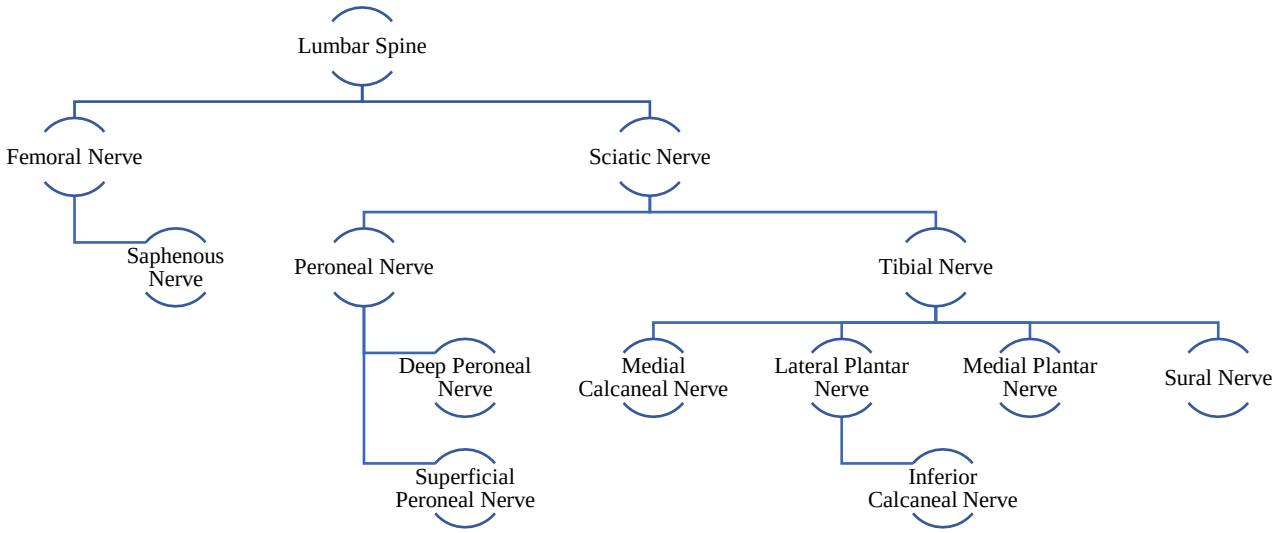

Figure 1-1: Nerve Branches Schematic of the Foot

Figure 1-2: Approximate Nerve Locations on the Plantar Surface[1]

[1] Medial Plantar Nerve (Purple), Lateral Plantar Nerve (Dark Green), Sural Nerve (Blue), Saphenous Nerve (Green), Medial Calcaneal Nerve (Orange)

1.4. Sensory Perception Tools and Methods

1.4.1. Survey Based Screening Tools

Questionnaire based evaluations have been used for the screening of DPN, such as the Michigan Neuropathy Screening Instrument (MNSI), the Neuropathy Symptom Score (NSS), the Neuropathy Disability Score (NDS), and the Neuropathy Impairment Score (NIS) [44, 45, 46, 47]. The MNSI is a very popular 15-item questionnaire relating to symptoms, in which the subject answers yes or no to each question [44, 46]. An MNSI score greater than or equal to 2.5 indicates the presence of diabetic peripheral neuropathy [44]. The MNSI test leads to the referral to a neurologist for further assessment with electrophysiological equipment [45, 46]. The NDS assessment is comprised of 35 items and has been used in the past, although a revised version has become more common [48]. The Toronto Clinical Scoring System (TCNS) includes the use of a symptoms score, reflex score, and sensory test score to screen for diabetic peripheral neuropathy [48]. The Norfolk Quality of Life Diabetic Neuropathy Questionnaire contains 35 questions, which the subject answers privately, and has been found to be effective in early diagnosis [49]. The composite scoring system known as the Clinical Neurological Examination (CNE) measures sensory signs and reflexes in the lower limbs through the use of light touch and vibration [48]. The Diabetic Neuropathy Examination (DNE) was derived from NDS, but only uses eight metrics, such as muscle strength, reflexes, and sensation on the index finger and big toe to evaluated for neuropathy [48].

1.4.2. Hand-Applied Semmes-Weinstein Monofilament Tool

The most common tool used for neuropathy assessment in the extremities is the Semmes-Weinstein monofilament. Originally horsehair filaments were used for sensation perception in the hands and feet in the 1800s, following which Semmes and Weinstein created nylon

monofilaments in the 1960s [50, 51]. They developed these monofilaments from a single fiber of nylon and were used on the palmar surfaces for individuals who sustained brain injuries [9, 52]. The principal behind them is that they are calibrated to produce a consistent buckling stress and minimize the effects of movement caused by the hand of the clinician during application [9, 53]. The Semmes-Weinstein monofilament is applied perpendicular to the skin, gradually increasing the contact force until it buckles, ideally making it a reproducible assessment [50, 52, 54]. An example of this technique can be found in Figure 1-3. Different buckling forces can be produced using different monofilaments, which range between 0.008 to 300 grams of force [29]. The monofilament gauge is often noted using an evaluator size, which is the logarithm of the force applied in grams [29, 51]. They work by using Weber's Law, which is the relationship between perceived sensation ratio to the stimulus intensity [52, 54]. Plantar threshold sensitivity can be grouped into 5 categories: normal (0.008-0.4 grams of force), diminished light touch (0.6-2.0 grams of force), diminished protective sensation (4.0-8.0 grams of force), loss of protective sensation (10.0-180.0 grams of force), and deep pressure sensation (300 grams of force) [29]. The 5.07 evaluator, which produces a buckling force of 10.0 grams of force, is the most widely used monofilament to measure threshold sensitivity [28, 29, 52]. Semmes-Weinstein monofilaments are chosen by clinicians because they are noninvasive, easy to use, quick, and inexpensive compared to other tools [9, 52].

a)

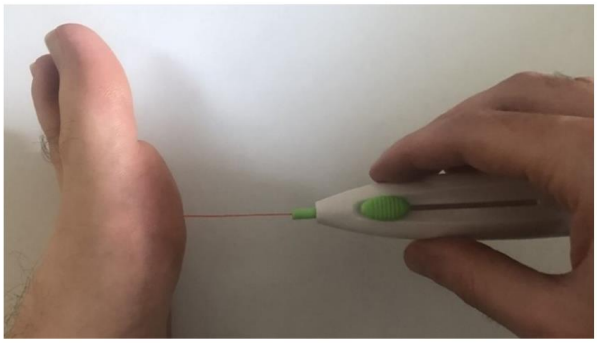

b)

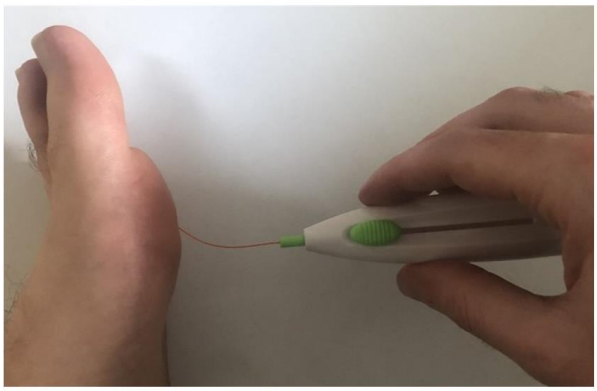

Figure 1-3: Hand-Applied Semmes-Weinstein Monofilament Procedure

a) Monofilament in initial contact with the plantar surface

b) Monofilament applied until buckling

1.4.3. Non-Monofilament Assessment Tools and Techniques

Non-monofilament assessment tools include the use of warm and cold stimuli, vibratory analysis, nerve conduction, and electrodiagnostic studies [9]. A popular non-monofilament assessment tool for neuropathy assessment has been the tuning fork. They apply a vibratory stimulus to the assessment location, the most popular being the 128 Hz tuning fork [4, 27, 29]. The fork itself is struck, after which the blunt end is applied to the skin causing vibration to propagate through the tool to the subject. The Vibratip™ is similar to the 128 Hz tuning fork, in which it applies a vibratory stimulus to assess an individual's threshold sensitivity [55]. A Tactile Circumferential Discriminator (TCD), which is a metal disk with eight protruding rods of increasing diameter,

has also been used to assess for neuropathy risk [56]. The TCD is applied by hand, similar to a Semmes-Weinstein monofilament, but lacks the buckling aspect, making it easy to use [56, 57]. Steel ball bearings of varying diameters, common in the field of tribology, have also been used for neuropathy assessment [58]. Subjects would walk barefoot on these ball bearings, which are attached to the plantar surface using a plaster [58]. The NeuroQuick device applies a cold stream of air to the skin, at varying velocities, to measure sensation threshold [59]. A device called a Neurometer® uses electrodes placed at either the big toe or ankle, to deliver current stimulations at specific frequencies [10]. Likewise, a Biothesiometer also applies a vibratory stimulus and has been effective in past studies [27, 38]. In a study that used a Biothesiometer among a diabetic population is was determined that those who had a baseline threshold above 25 volts were 7 times more likely to develop a foot ulcer than when evaluated using a lower voltage on the Biothesiometer [38]. An additional vibratory tool is the Neurothesiometer, which is considered an improvement over the Biothesiometer [60]. Another novel technique is by measuring the reflectance spectra, or the oxygen level of the skin, as a means of evaluating for neuropathy and ulcers [61]. Devices that measure an individual's sweat content have also been used for neuropathy assessment, also defined as sudomotor devices [57]. A sudomotor device known as a Neuropad uses sweat produced to measure healthy sensation perception [57, 62]. It works by using a color changing patch to signify the health of the subject [57, 62]. Another sudomotor tool is the Sudoscan, which works by having the subject place their hands and feet on stainless steel plates, used to analyze the subject's sweat [57, 63]. The NC-stat DPN is a handheld device used to evaluate the sural nerve conduction velocity and the sensory nerve action potential; it has been shown to screen for diabetic neuropathy [57, 64, 62]. Medoc's Quantitative Sensory Test (QST)

is another proposed tool to evaluate the sensory nerve function via the use of thermal, pressure, and or vibratory stimuli [65].

1.4.4. Automated Assessment Tools

Automated tools have been developed to more accurately assess a subject's threshold sensitivity, although documented quantitative data for these devices is lacking in the literature. A robotic device created by Wilasrumee et al. applied a 10.0-gram force Semmes-Weinstein monofilament on the plantar surface [66]. This device had good agreement with assessments performed using a hand-applied monofilament and tuning fork [66]. Another robotic tool was developed by Siddiqui et al., which also took a 10.0 grams of force Semmes-Weinstein monofilament and actuated it through a clear perforated hole plate, until it made contact with the subject's plantar surface [67, 68]. A handheld Semmes-Weinstein device, with a LED light indicator to signal when the monofilament had reached its 10.0 grams of force target, or if it was inadvertently applied greater than 11.0 grams of force, was also created by Spruce and Bowling [69]. This device countered the effects on monofilament fatigue and had improved repeatability to the commercially available Semmes-Weinstein monofilament [69]. The patent of Leung and Lau proposed a robotic solution for neuropathy assessment which used a solenoid to translate monofilaments through a perforated hole plate against the plantar surface [70]. Similarly, Ino et al. filed a patent on a device in which the subject's foot is subjected to not only a normal force, but a shear force to evaluate for sensation loss [71]. Snellenberg et al. patented an automated tool which used a micro servo to acuate a monofilament until it buckles, while also using a thermal imaging camera to evaluate potential areas of concern on the feet [72]. Spruce used a force transducer to apply a monofilament until a desired force was achieved, either using a handheld device or with the use of an automated tool similar to the other patents mentioned [73]. Only a

few of these automated devices reported accuracy data, which will be presented in Chapter 4 of this dissertation as a means of comparing the automated tool developed in this body of work.

1.5. Potential Shortcomings of Non-Automated Hand-Applied Tools

1.5.1. Accuracy Factors and Clinician Biases

The actual force produced as a result of applying the hand-applied monofilament until it buckles is dependent on a couple of factors. The rate of insertion in terms of impact velocity and the angle of insertion can factor into the accuracy [54]. Likewise, these monofilaments are susceptible to fatigue, in which after 10 applications its contact force has been decreased by 10% [54]. Lavery et al. not only found that some commercially available 10.0-gram monofilaments varied up to 30% of their buckling force when brand new, but also only remain effective for 7-9 days [74]. Although Lavery et al. demonstrated relatively stable behavior after the first application of the monofilament, at an accuracy of 30% this could potentially overlap between different monofilament evaluators, especially when considering monofilaments that produce 8.0 and 10.0 grams of force. It has also been reported that hand-applied monofilaments require 24 hours of inactivity to fully recover, before being capable of accurately applying their rated force [54, 69]. The environment, in terms of temperature and humidity, in which the monofilaments are kept also plays into the accuracy [50]. Not only can the diameter and length of the monofilaments influence the accuracy, but the overall quality of the nylon used to manufacture these devices is also important to the contact force accuracy [53]. It was observed that as the length of the monofilament decreased, the contact force produced upon buckling increased [75]. Chapter 2 of this dissertation explored how material properties of human skin are also influential on the accuracy of hand-applied monofilaments [76]. Moreover, the accuracy of hand-applied

monofilaments will be directly compared to the force producing accuracy of the automated tool in Chapter 4 of this dissertation.

1.5.2. Unstandardized Methodology

Dros et al. found that in their meta-analysis that there is a lack of standardization for the hand-applied monofilament assessment. Some studies have used one testing site, while others have used up to ten testing sites [9]. Three and five testing sites are also common, as well as also evaluating the dorsal aspect, otherwise known as the top of the foot between the toes [77]. Some studies will apply the monofilament between two and four times per location [77]. The great toe, or big toe, is often one of the most common sites evaluated, but there is no evidence in the literature to suggest that it is the most indicative location for sensation loss [77]. Although the 10.0-gram force rated monofilament is the most common hand-applied monofilament used, the 1.0, 2.0, and 75.0 grams of force monofilaments have also been cited, with the 2.0 grams of force monofilament having the potential for greater diagnosis of diabetic peripheral neuropathy [9, 77]. Ultimately, the use of monofilaments alone is not enough to diagnosis peripheral neuropathy, with additional evaluation techniques required to verify the individual's condition [9, 78].

1.6. Dissertation Motivation and Statement of Purpose

Neuropathy, especially in the presence of type 2 diabetes mellitus brings many complications. Although burning of the feet and numbness are prevalent symptoms, the formation of ulcers, resulting in amputations are what makes neuropathy life threatening. Sensation loss in the extremities, particularly the plantar surface, should not be overlooked and currently the Semmes-Weinstein monofilament assessment is the most common hand-applied assessment method. Other approaches have been used to assess for sensation loss and have compared well to the

hand-applied monofilament techniques, but their lack of accuracy validation still makes them challenging to recommend. Automated tools, which incorporate sensors and computer algorithms, can allow for increased accuracy and the removal of clinician biases. Paired with the ability to document sensation loss over the course of time, automated tools can evaluate the efficacy of treatments, allowing for unparalleled benefits when compared to standard tools and methods.

Therefore, the purpose of this dissertation is to demonstrate the practical concerns of the hand-applied Semmes-Weinstein monofilament assessment technique, present a novel diagnostic tool which automates the assessment protocol, and implement it in a clinical study to ascertain subjects' current degree of threshold sensitivity on the plantar surface.

1.7. Dissertation Objectives

There are six objectives related to this research project, which are each presented chronologically in a corresponding chapter in this dissertation. The first objective was to analyze the effects of monofilament diameter, insertion depth, and material skin properties on the contact force and normal stress produced. This was achieved through the use of theoretical contact mechanics and finite element simulations. The second objective was to introduce a proposed automated diagnostic tool solution for neuropathy assessment on the plantar surface. The design of the tool is presented, and its functionalities are detailed. The third objective of this dissertation was to conduct a performance analysis and a clinical evaluation of the automated tool in a healthy control group, absent of type 2 diabetes mellitus. This entailed not only determining the device's force producing accuracy, but also the quantification of research subjects' plantar threshold sensitivity. Linear regression analyses were used to compare each subject's threshold sensitivity

to their age, BMI, ABI, fasting blood sugar, and HbA1c to determine if a relationship existed between these variables in the healthy control population. The fourth objective was to evaluate and compare plantar threshold sensitivities between the healthy control subjects and subjects with type 2 diabetes mellitus, with and without neuropathy symptoms. A robust statistical analysis between the three populations was performed to draw conclusions as how type 2 diabetes mellitus and the presence of neuropathy symptoms impact sensation loss on the plantar surface. The fifth objective of this work is to propose and detail an improved design of the diagnostic tool. The sixth and final objective of this dissertation was to recommend future work and potential studies which could enhance the diagnostic tool and yield additional insights into neuropathy.

Chapter 2: Contact Mechanics Modeling of the Semmes-Weinstein Monofilament on the Plantar Surface

2.1. Abstract

Background: Neuropathy is a disease which results in the loss of sensation in the extremities. One method for assessing the degree of neuropathy is with a monofilament evaluator which buckles at a prescribed force depending on the filament diameter. However, as this assessment is conducted manually by the clinician, the true force delivered is not guaranteed. Therefore, the purpose of this study was to model the effects of both insertion depth and monofilament diameter on the contact force and normal stress produced on the plantar surface of the foot.

Methods: Theoretical contact mechanics equations were used to understand the relationship between insertion depth, monofilament diameter, and applied force. SolidWorks® Finite Element Analysis was used to evaluate a 0.5 mm diameter monofilament, which is reported to provide a contact force of 10.0 grams of force at the point of buckling, at various insertion depths. Two different Finite Element Analysis models were studied in this paper, a homogenous isotropic model and a composite isotropic model. A total of 188simulations were used in this study. A range of human skin elastic moduli were modeled to determine the effect imposed upon the contact force and normal stress produced by monofilament insertion. For the homogeneous isotropic model, the sample was modeled as a uniform block with an overall elastic modulus. The composite isotropic model was created using epidermis, dermis, and subcutaneous fat layers, each with its own specific thickness. A range of moduli were considered for the epidermis and dermis layers. The homogenous isotropic model was validated with the results of the theoretical calculations by comparing the percent error between the contact force and normal stress.

Consequently, the same simulation settings were used for both models. Regression analysis was used to analyze the composite isotropic results by using the regression coefficients and their corresponding epidermis and dermis elastic moduli. Linear, logarithmic, and power regressions were all considered. The overall fit of the data was examined by inspecting the R^2 values, which were between 0.52 and 0.99 for all regressions.

Results: The theoretical contact mechanics analysis show that higher levels of insertion and larger diameter monofilaments produce greater amounts of contact force. The normal stress increase with insertion depth but decrease with monofilament diameter. Increased values of human skin elastic modulus result in the contact force and normal stress being more sensitive to insertion depth, compared to lower values. The homogenous isotropic model had percent errors approximately between 2% and 8% when compared to the theoretical equations. Furthermore, after collecting all of the data from the composite isotropic model, regression analysis was used to derive empirical equations that represented both contact force and normal stress as functions of epidermis elastic modulus, dermis elastic modulus, and insertion depth. The empirical equations show that to produce exactly 10.0 grams of force upon contact the physician would have to insert the monofilament between 0.235 and 0.559 mm depending on the epidermis and dermis moduli.

Conclusions: The results show that slight differences in insertion depth and monofilament diameters have a large effect on the force delivered. Therefore, attention to application technique is recommended when interpreting the results obtained using hand-applied monofilaments

because of the variances of human skin properties among research subjects and the subsequent levels of applied force.

2.2. Introduction

Neuropathy is a disease, commonly associated with diabetes, which results in a loss of sensation on the plantar surfaces of the hands and feet. It is commonly known as “diabetic foot” and 40-60 million people suffer from challenges associated with neuropathy [5]. In a research survey conducted by Brouwer et al. they found that the most frequent symptom of neuropathy was burning feet [26]. Likewise, individuals tolerate numbness, electrical sensation, sensory loss, and shooting pain caused by neuropathy [27, 28, 29, 79]. Severe cases of neuropathy can result in an individual stepping on an object and unknowingly puncturing their foot as a result of their sensation loss [34]. These individuals are at a greater risk of ulceration [9, 10, 80]. The loss of protective sensation and mechanical loading during weight bearing activities, such as standing and walking, are contributing factors to the ulceration of individuals suffering from neuropathy [81]. In the worst cases, neuropathy can result in infection, amputation, and even death [10, 82]. The gold standard for assessing the degree of neuropathy is with the Semmes-Weinstein monofilament test. This method involves inserting a monofilament, similar to fishing line, noninvasively into human skin. These nylon monofilaments are calibrated to produce a consistent buckling stress and minimize the vibration of the clinician’s hand while it is being applied [9, 53]. The monofilaments are popular because they are noninvasive, quick, and easy to use [9, 52, 83]. There are many different gauges of these monofilament evaluators which reportedly produce different amounts of force at the point of buckling. However, the actual force produced by these monofilaments are extremely sensitive to many different parameters. For example, Chikai and Ino compared a manual monofilament assessment with an automated process looking at how insertion speed and angle affected measurements [54]. They found that after 10 applications of the monofilament the buckling force decayed by 10% of its initial value

[54]. They also found that the velocity and the insertion angle affected the buckling force in both automated and manual applications of the monofilament [54]. Haloua, Sierevelt, and Theuvenet found that these monofilaments are dependent on the temperature and the humidity in which they are stored, resulting in different buckling forces than advertised [50]. The length of the monofilament also influences the amount of force applied to the plantar surface of the foot [75]. Furthermore, an extensive literature review by Dros et al. found that there is a lack of standard testing methodology [9]. This, along with the lack of accuracy of this test, raises questions about its validity [9].

One of the most common monofilaments used produces an equivalent force of 10.0 grams when applied to the plantar surface of the foot to the point of buckling [28, 29, 52]. The monofilament is advertised to produce this force at the instant that it buckles but it is possible for it to exceed its rated value if it is over applied. If the monofilament is not applied normal to the surface than the force can be subdivided into more than one cartesian plane. The inability of the clinician to apply a consistent force presents challenges for assessment of disease progression and future treatments to combat this disease. Therefore, it is important to develop an understanding of the parameters that may affect the force applied by the monofilament and, therefore, why attention to application procedure is recommended when interpreting the results of the hand-applied monofilament assessment.

To this end, this modeling study examined how changes in the depth of insertion, the diameter of the monofilament, and skin material properties affects the amount of force and stress produced on the skin. Accordingly, this study was designed to ensure that the monofilament was applied

normal to the skin, i.e., normal to the plantar surface of the foot. This orientation of insertion is easily achieved with both theoretical equations and finite element analysis (FEA). Theoretical contact mechanics were used to show the dependence on the insertion depth for monofilaments of various diameters. Furthermore, FEA was conducted via SolidWorks® Simulation for the 10.0-gram rated monofilament. The FEA simulations were used to calculate the contact force and to measure the normal stress. The FEA results of this study were verified with theoretical results and were also subjected to a sensitivity analysis [84]. Ultimately the objective of this study was to determine the effects of monofilament diameter, insertion depth, and skin materials properties on the force produced as a result of monofilament contact against the skin.

2.3. Methods

2.3.1. Theoretical Equations

In this study, theoretical contact mechanics equations were chosen that would best demonstrate the effect of insertion depth on the force and stress produced on the skin for monofilaments of different diameters. This problem was modeled as a Boussinesq problem, where there is a rigid indenter being pressed into an elastic half space. In this study, the nylon was considered rigid when compared to human skin. Sneddon took Boussinesq equations and applied Hankel transforms to derive relevant equations for a cylindrical indenter applied normal to the surface [85]. Sneddon looked at the relationships between depth of penetration and force, in addition to stress profiles as a result of the contact. The first equation derived by Sneddon (Equation 2-1) shows the relationship between load (P) and the depth of penetration (δ). Here a is the radius of the circular face and η is the Poisson's ratio of the half space. The other variable, μ, is the modulus of rigidity, also known as the shear modulus, and is defined in Equation 2-2. Additionally, E is the modulus of elasticity. Combining Equation 2-1 and 2-2 leads to a complete

expression, Equation 2-3, for the load (P) in terms of E, a, δ, and η. This theoretical equation was used to compare to the FEA results when the monofilament is applied normal to the skin. The FEA predictions were validated with analytically derived models to ensure that the simulation performed as expected [84]. The analytical model is given by the following equations:

$$P = \frac{4\mu a\delta}{1-\eta} \quad \text{Eq. 2-1}$$

$$\mu = \frac{E}{2(1+\eta)} \quad \text{Eq. 2-2}$$

$$P = \frac{2Ea\delta}{(1+\eta)(1-\eta)} \quad \text{Eq. 2-3}$$

$$\sigma_{zz} = \frac{2\mu\delta}{\pi(1-\eta)\sqrt{a^2-\rho^2}} \quad \text{Eq. 2-4}$$

$$\sigma_{zz} = \frac{E\delta}{\pi(1+\eta)(1-\eta)a} \quad \text{Eq. 2-5}$$

Sneddon derived an expression for the normal stress profile caused by the indenter, where ρ is the incremental radial distance from the center of the indenter up to the edge of the indenter (Equation 2-4). However, in this study it was necessary to set ρ equal to zero to calculate the normal stress at the center of contact, because at the edge of the indenter the stress becomes theoretically infinite [86]. This produces a singularity at the edge and as a result it is more feasible to evaluate the stress at the center of the contact. However, in practice, infinite stress will not occur due to the rounded edges of the indenter and non-linear properties, such as plasticity. This equation was rewritten to a more readily applied form in Equation 2-5 and was used to compare the normal stress found at the center of the indenter when in contact with the human skin sample.

2.3.2. Finite Element Analysis Setup

SolidWorks® Simulation was used for this modeling experiment between the monofilament evaluator and a human skin sample. Two different FEA models were analyzed: a homogenous isotropic model and a composite isotropic model, depicted in Figure 2-1. Both models used the same monofilament, which was modeled as a thin cylinder with an overall length of 40.0 mm and a diameter of 0.500 mm, equivalent to a standard 10.0-gram evaluator. The actual monofilament is made of nylon; in the simulation nylon 6/10 was used as it was already in the SolidWorks material database. The chosen nylon has an elastic modulus of 8.30 GPa, a Poisson's ratio of 0.28, a density of 1400 kg-m^3, and a yield strength of 139 MPa, as reported in the SolidWorks® material database. In the homogenous isotropic model, the specimen was a rectangular block with a Poisson's ratio of 0.49 [87] and density of 1116 kg-m^3 [88]. Four different elastic moduli were considered, 1000, 2000, 3000, and 4000 kPa [87, 88]. The overall dimensions of the specimen were 13.0 mm width, 13.0 mm height, and 13.0 mm depth. The depth was based on of the work of Thomas, Patil, and Radhakrishnan which reported that at the forefoot the thickness of the skin can be expected to be between 7.8 and 13 mm based on the health of the individual [87]. The composite isotropic model incorporated three distinct layers of skin: the epidermis, the dermis, and subcutaneous fat [88]. In Figure 2-1 the orange layer corresponds to the epidermis, the magenta is for the dermis, and the subcutaneous fat is yellow. As with the homogenous isotropic model, four values for elastic modulus of the epidermis layer were selected: 1000, 2000, 3000, and 4000 kPa [87, 88]. Likewise, five values of dermis elastic moduli were considered: 100, 150, 200, 250, and 300 kPa [88]. Only one value of subcutaneous fat elastic modulus was studied, 34.0 kPa, since it was determined that the subcutaneous fat does not vary as much as the adjacent skin layers [88]. The values of Poisson's ratio, density, and

yield strength for human skin were kept consistent between both models. In the composite isotropic model, the overall dimensions of the specimen were 13.0 mm width, 13.0 mm height, and 13.0 mm depth. The depth was subdivided based on the epidermis, dermis, and subcutaneous fat layers, which were respectively 0.6 [89], 5.0, and 7.4 mm thick. It was reported from Wang and Sanders that the dermis layer can range in thickness from 1 to 4 mm and is thicker than the epidermis [90]. In order to rationalize each layer thicknesses for the forefoot some approximations had to be made. Since the thickness of the entire specimen was 13 mm [87], the epidermis was selected to be 0.6 mm [89], and considering that Li found the subcutaneous fat region in his model to be marginally thicker than the dermis layer [88], then the dermis thickness was approximated to 5 mm. This left the subcutaneous fat layer to be 7.4 mm thick.

In both models the monofilament and specimen were arranged in a SolidWorks® assembly in which the end of the monofilament was in immediate contact with the sample. Figure 2-1 shows the monofilament (green) in contact with a human skin specimen. A static analysis was employed for all trials assuming linear elastic material properties and small displacements. The simulation was set up with a fixture on the back face of the sample, shown in green arrows, opposite that of the contacting surface with the monofilament. All of the other faces of the specimens were unconstrained and free.

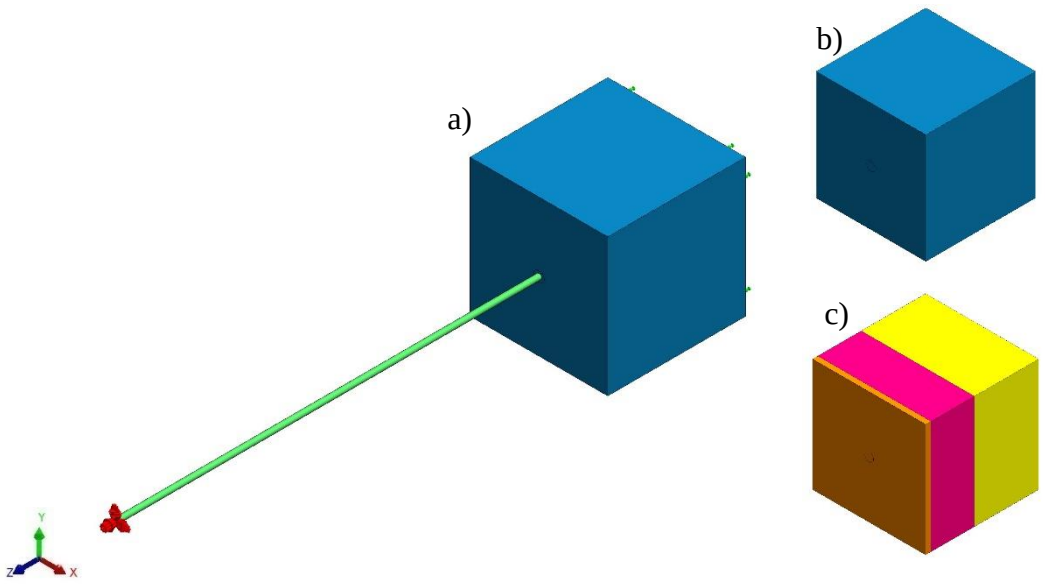

Figure 2-1: Contact Assembly- Nylon Monofilament in Initial Contact with Human Skin Specimen

a) Setup Assembly
b) Homogenous Isotropic Skin Specimen
c) Composite Isotropic Skin Specimen[2]

The monofilament was given a prescribed displacement at the opposite end of the surface-to-surface contact, shown in red arrows. The displacements considered in the homogenous isotropic model were between 0.025 and 0.3 mm spaced in equal increments of 0.025 mm apart, totaling twelve insertion depths. In the composite isotropic model seven displacements were considered between 0.1 and 0.7 mm, spaced in equal increments of 0.1 mm. These displacements were defined in the z direction, whereas the x and y directions where set to zero millimeters. It was necessary to set the x and y directions to zero in this simulation to properly define how the monofilament was supposed to interact with the specimen. The contacting surfaces between the specimen and the monofilament were given a no penetration condition, which allowed the monofilament to deform the specimen and to create an impact crater representative of the

[2] Epidermis (Orange), Dermis (Magenta), Subcutaneous Fat (Yellow)

insertion. Mesh parameters included a curvature-based mesh with a maximum element size of 0.250 mm, minimum size of 0.0833325 mm, and a minimum of twelve elements in a circle. The element size growth ratio was set to 1.5 and the mesh density was set to be fine. Mesh control settings were used at the end of the monofilament and a circular region, with a 1.00 mm diameter, on the face of the specimen to further refine the mesh. This parameter was set to have an element size of 0.050 mm and a 1.5 ratio. Dong et al. used a similar process of having an extremely fine mesh at the area of contact and a coarse mesh farther away [91]. When considering contact mechanics, it is important to have a fine mesh, which does increase the computational time. Nonetheless, mesh controls allow for areas of interest to have a much finer mesh than the surrounding areas, which are not as important and consequently the stress gradients are lower. This provided a good balance between a good quality mesh and run time. It should also be noted that an H-adaptive study was employed which served as a way to further refine the mesh at areas of interest, such as the contacting surfaces. The mesh was refined as a result of the stresses that occurred in the model in order to reach the target accuracy threshold [92]. This level of mesh refinement is similar to surface roughness; at a large scale the surface may have very little roughness, but at a smaller scale it may appear to be extremely rough.

The associated H-adaptive parameters included setting the target accuracy to 98%, or 2% error, and setting the accuracy bias to *global*. The target accuracy is a parameter for the strain energy norm [92] and was used as a criterion to justify that the simulation completed. The accuracy bias was set to *global* to prevent the presence of singularities, which meant that the FEA simulation focused on getting accurate results on a global scale [92]. Additional study parameters included selecting the options for improving the accuracy for no penetration contacting surfaces, setting

the incompatible bonding options to more accurate and using the FEEPlus iterative solver, which works well with the H-adaptive solving method. Identical mesh parameters were used for both models, where the homogenous isotropic model was validated with the theoretical equations to prove that the mesh settings yielded correct results.

After simulation, numerous results were reviewed including the contact force, normal stress, and the accuracy achieved in the simulation. Sensors were placed at the center of the specimen, where the monofilament made initial contact. Sensors were configured to measure the values of force and stress, which are automatically updated for each simulation. The contact force was calculated by the software and is shown as a set of vectors, whereas the stress is depicted with contour plots. A comparative analysis was performed between the theoretical equations and the homogenous isotropic model, while regression analysis was used to analyze results from the composite isotropic model. Linear regression analysis was first used by comparing the contact force to the insertion depth for each epidermis elastic modulus grouped by dermis elastic modulus. The coefficient of the linear regression analysis was then plotted against the epidermis elastic modulus, grouped by the dermis elastic modulus using a logarithmic relationship. Two additional coefficients were then extracted and plotted against the dermis elastic modulus using a power relationship. R^2 values were used to determine strong relationships, which in this study were all between 0.52 and 0.99 for all types of regressions performed. Once a simulation was setup it was duplicated and modified to reflect different parameters such as the insertion depth. This ensured that all settings remained the same from one simulation to another. In total 188 simulations were completed between the two models. All simulations were performed on a Dell

Inspiron 7559 with an upgraded Samsung 860 EVO m.2 solid state drive and 16 gigabytes of RAM. It also utilized a 2.6 GHz Intel Quad Core i7-6700HQ.

2.4. Results

The first set of results are based upon theoretical Equations 2-3 and 2-5, where the amount of force and stress are both functions of the depth of insertion and the diameter of the monofilament. Furthermore, when using equation 3 the units are in Newtons, however, to be consistent with neuropathy studies, which use Semmes-Weinstein monofilaments, the force is expressed in grams of force (gF). This was achieved by dividing Newtons by gravity, 9.81 $m\text{-}s^{-2}$, and then multiplying by one thousand to convert from kg to g. The values for normal stress are all expressed in kilopascals (kPa). When using Young's modulus and Poisson's ratio for human skin [87, 88] the following surface plot, Figure 2-2, was produced. It shows that as the depth of insertion increased, so did the contact force. The same was seen as the diameter of the monofilament increased. Another surface plot was created to show the normal stress as a function of insertion depth and diameter, Figure 2-3. Here, the greatest amount of stress occurred when the amount of insertion increased, while the diameter decreased. Both Figure 2-2 and Figure 2-3 are for an elasticity of 1000 kPa.

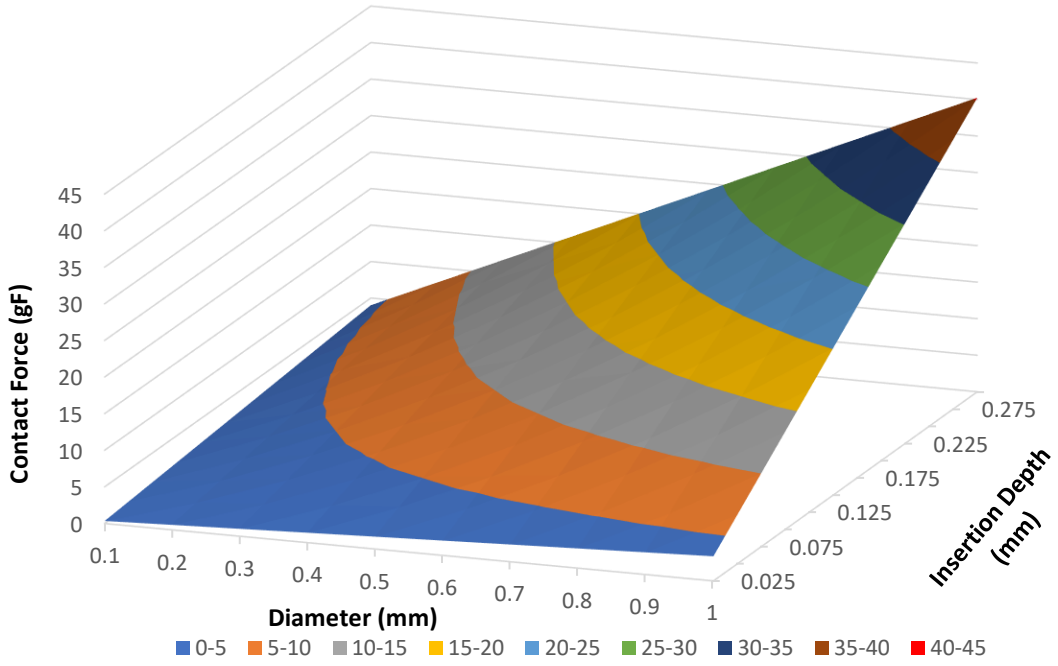

Figure 2-2: Contact Force Surface Plot- Contact Force as a Function of Insertion Depth and Diameter for Human Skin with an Epidermis Elastic Modulus of 1000 kPa

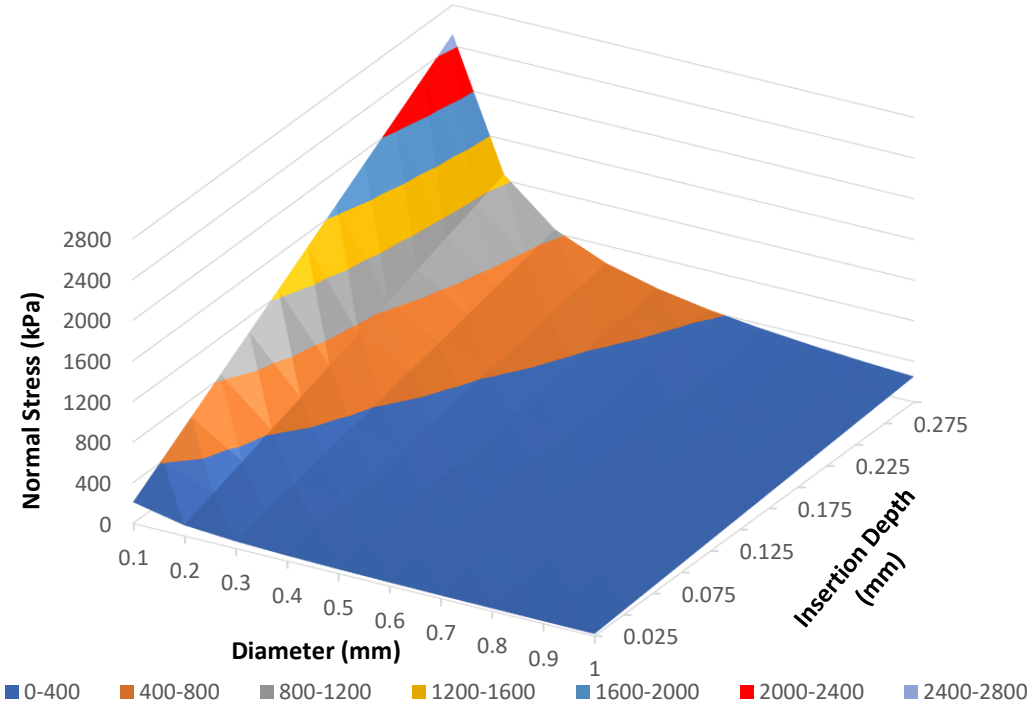

Figure 2-3: Normal Stress Surface Plot- Normal Stress as a Function of Insertion Depth and Diameter for Human Skin with an Epidermis Elastic Modulus of 1000 kPa

Direct relationships are extrapolated from the surface plots for specific monofilaments. Since the 10.0-gram monofilament is one of the most popularly used, which has a diameter of 0.5 mm, Figure 2-4 was produced to show the relationship between the contact force and normal stress versus the depth of insertion. Figure 2-4 shows a clear linear relationship for both the contact force and normal stress when grouped by elastic modulus (E). These theoretical solutions were used to validate the FEA results.

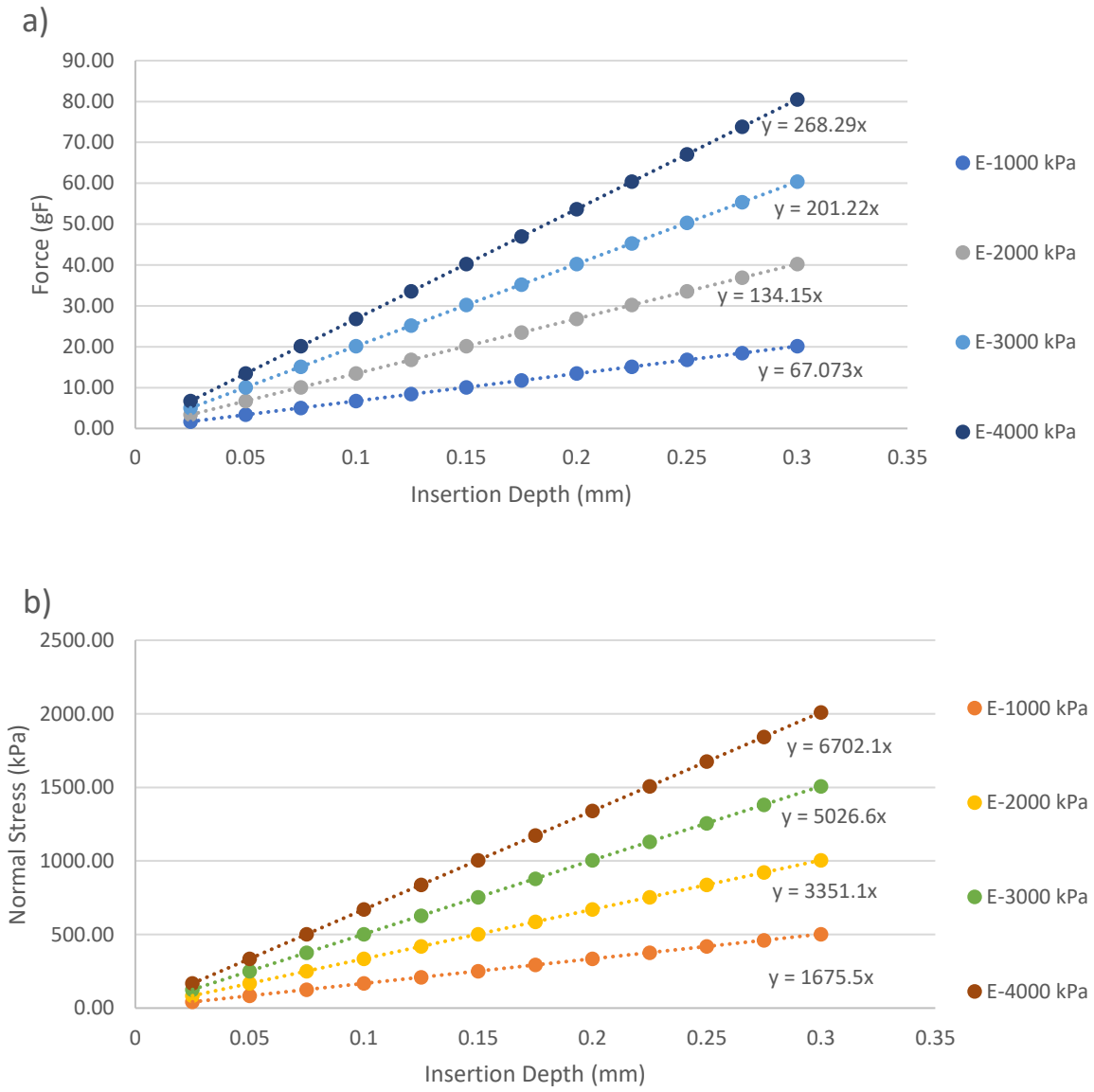

Figure 2-4: 10.0-gram Monofilament Contact Theoretical Relationships

a) Theoretical Contact Force versus Depth of Insertion for a 10.0-gram Monofilament with a 0.5 mm Diameter
b) Normal Stress versus Depth of Insertion for a 10.0-gram Monofilament with a 0.5 mm Diameter

Before going through all of the FEA results it is important to showcase the H-Adaptive mesh used during the study. Figure 2-5 showcases the detail of the mesh when the monofilament is applied to the specimen. The H-adaptive mesh refined itself at the areas of contact in order to gain an understanding of how the monofilament affected the specimen. Zooming in reveals

smaller mesh elements, which appear unclear in the overall image. Figure 2-5 also shows how the contact between the two components and the resulting stress required a finer mesh for analysis.

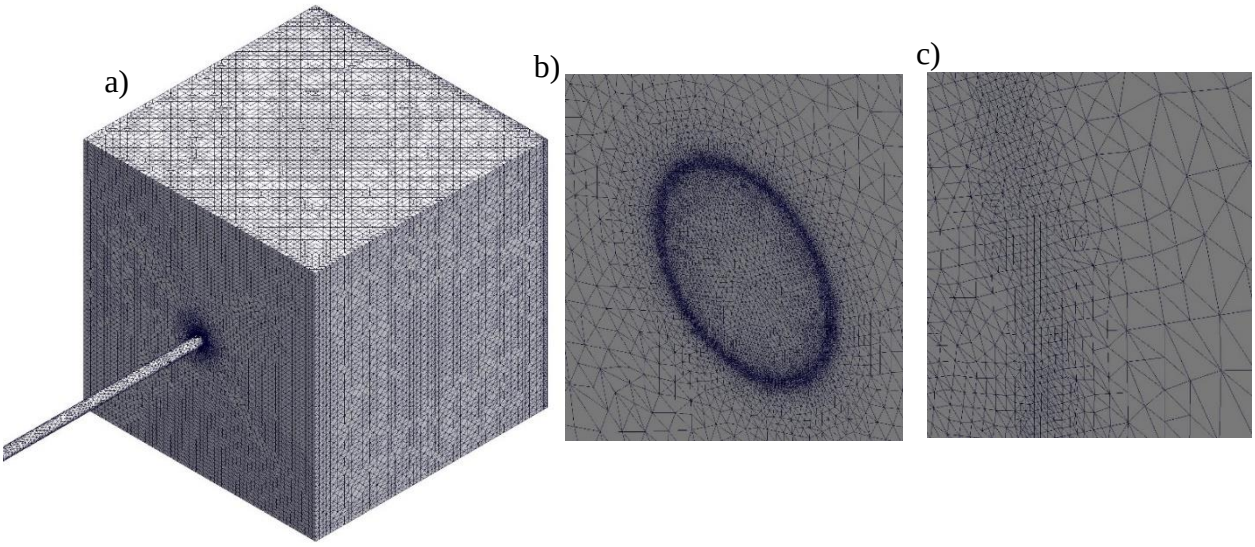

Figure 2-5: FEA H-Adaptive Contact Mesh- Mesh Utilized for 10.0-gram Monofilament for 0.600 mm Insertion Depth

a) Large Scale
b) Medium Scale
c) Small Scale

The first FEA results, for the homogenous isotropic model, are depicted in Table 2-1, which show the contact force and normal stress for a 10.0-gram monofilament applied normal to the surface of the sample at an elastic modulus of 1000 kPa. Both the theoretical contact force and normal stress are provided and are used to calculate a percent error compared to the FEA results. The FEA contact force had an average percent error of 1.97% compared to the theoretical. The normal stress average percent error was 3.32%. Likewise for moduli of 2000, 3000, and 4000 kPa the average percent errors for the contact force where 3.49%, 4.96%, and 6.39%. The corresponding average percent errors for the normal stress where 4.88%, 6.09%, and 7.56%. Also, all 48 simulations for the homogenous isotropic model achieved the 2% strain energy norm

criteria in three iterations. Each simulation completed at a value of 1.89%, 1.87%, 1.86%, and 1.86% for each modulus: 1000, 2000, 3000, and 4000 kPa, respectively. Therefore, the FEA is verified for its accuracy.

Epidermis-1000 kPa								
	FEA	Theory			FEA	Theory		Total Relative Strain Energy Norm error
Depth (mm)	Force (gF)	Force (gF)	%Error		Normal Stress (MPa)	Normal Stress (MPa)	%Error	
0.025	1.64	1.68	1.96		0.041	0.042	3.31	1.89%
0.05	3.29	3.35	1.99		0.081	0.084	3.31	1.89%
0.075	4.93	5.03	1.98		0.122	0.126	3.31	1.89%
0.1	6.58	6.71	1.97		0.162	0.168	3.31	1.89%
0.125	8.22	8.38	1.97		0.203	0.209	3.31	1.89%
0.15	9.86	10.06	1.98		0.243	0.251	3.31	1.89%
0.175	11.51	11.74	1.94		0.284	0.293	3.31	1.89%
0.2	13.15	13.41	1.97		0.324	0.335	3.31	1.89%
0.225	14.79	15.09	2.00		0.364	0.377	3.34	1.89%
0.25	16.44	16.77	1.96		0.405	0.419	3.34	1.89%
0.275	18.08	18.44	1.98		0.445	0.461	3.34	1.89%
0.3	19.72	20.12	2.00		0.486	0.503	3.33	1.89%

Table 2-1: FEA Contact Force and Normal Stress for 10.0-gram Monofilament Applied Normal to the Surface

SolidWorks® FEA also produced detailed displacement and stress plots of the results for a 10.0-gram rated monofilament. Figure 2-6a and 2-6b shows the displacement plot created as a result of the contact between the monofilament and specimen when the insertion depth was 0.150 mm, and with a 1000 kPa elastic modulus. This displacement correlated to approximately 10.0 gF produced as a result of contact. An impact crater formed at the center of contact and extends into the specimen. Likewise, Figure 2-6c and 2-6d depicts the normal stress plot. The monofilament was hidden in these plots, allowing for easy visibility of the crater formed.

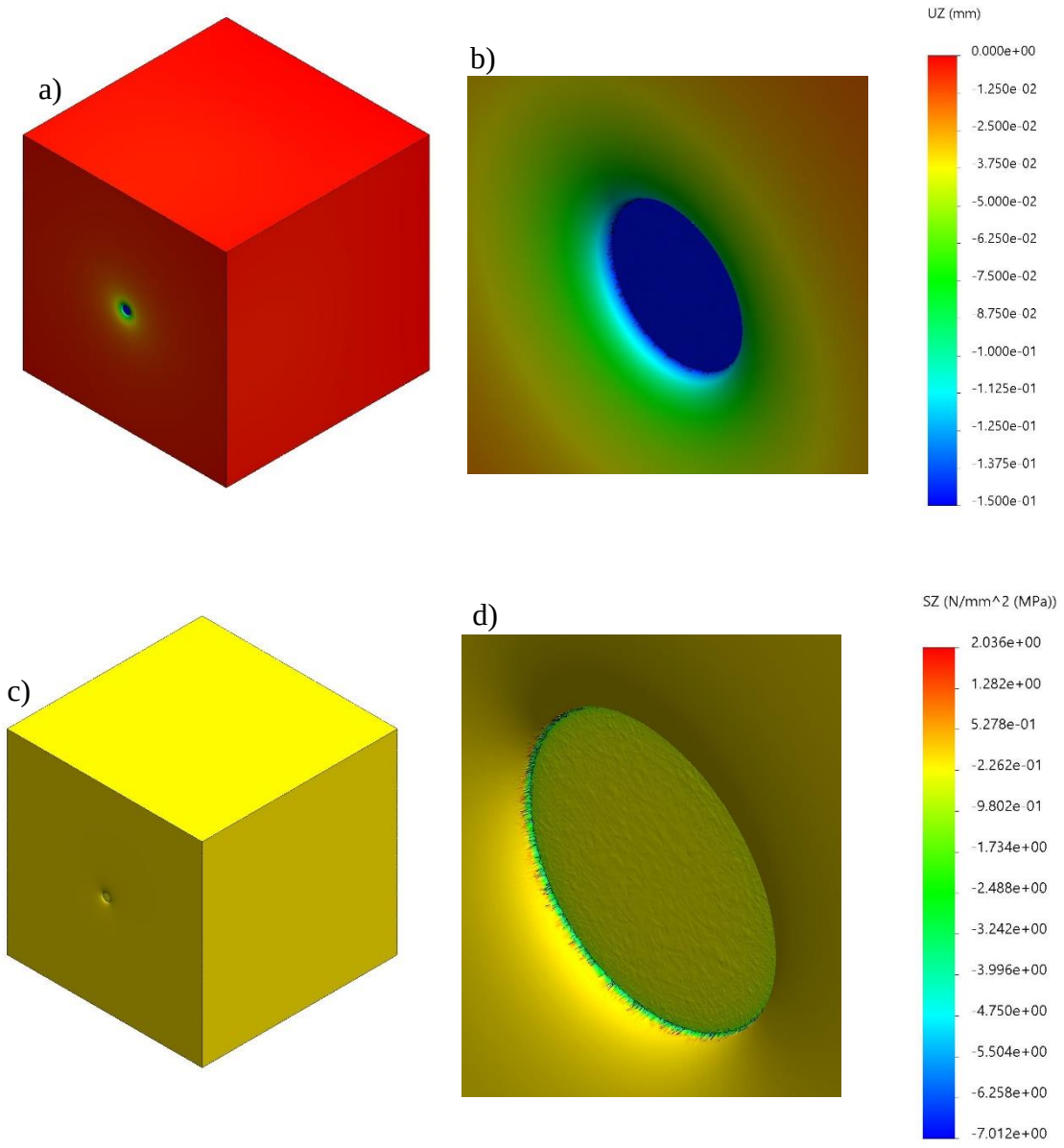

Figure 2-6: FEA Displacement and Stress Plots- Human Skin Specimen Displacement and Normal Stress Plots for 0.600 mm Insertion Depth

a) Displacement Plot
b) Displacement Plot Close-Up
c) Normal Stress Plot
d) Normal Stress Close-Up

By varying the epidermis and dermis elastic moduli and the insertion depth, the composite homogeneous model yielded 140 total simulations, accounting for 20 different ratios of epidermis to dermis elastic moduli. Contact force and normal stress plots, grouped by dermis

modulus, were generated to show the impact of both moduli. Figure 2-7 shows the contact force relationship for a dermis elastic modulus of 100 kPa and corresponding epidermis moduli. A similar plot, Figure 2-8, was generated to show the relationship between the normal stress and the displacement for a 100 kPa dermis elastic modulus. Both figures depict a linear relationship between their respective variables in the following format:

$$y = A\delta \qquad \text{Eq. 2-6}$$

In this equation y is the contact force (gF) or the normal stress (kPa), while δ is the displacement (mm). The y-intercept of these curves was manually set to zero to enforce the fact that at no displacement, i.e., no contact, there cannot be a contact force, nor normal stress. The slope of these lines, coefficient A, can then be further analyzed by taking the value and plotting it versus the epidermis modulus. Figure 2-9 and Figure 2-10 depict these plots for contact force and normal stress, respectively.

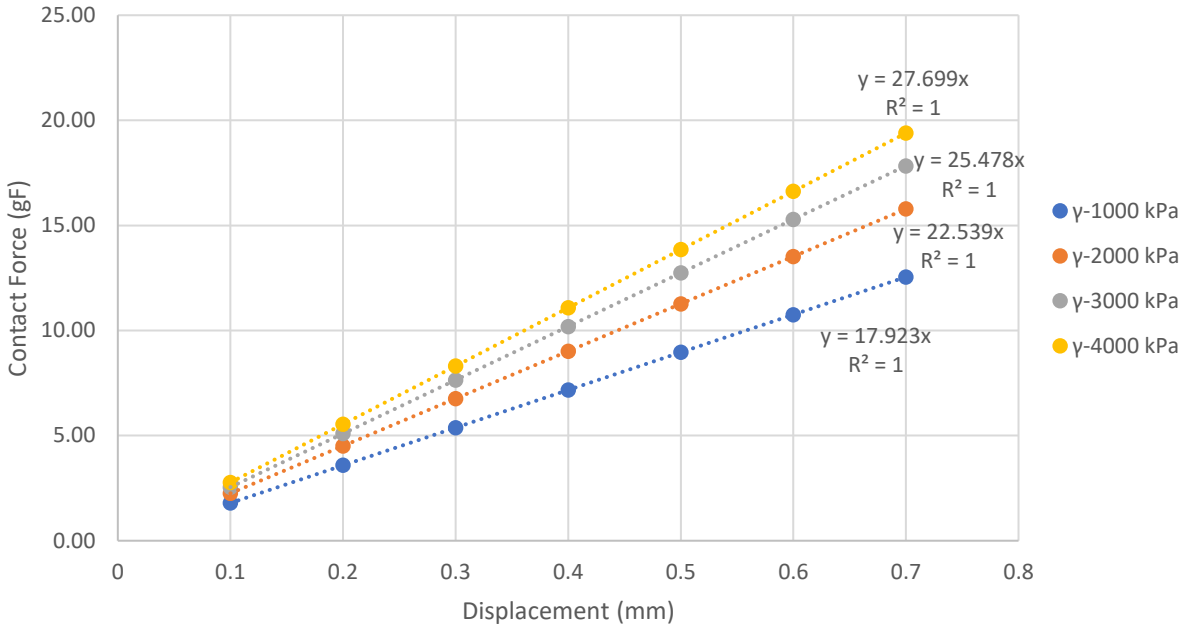

Figure 2-7: Contact Force Plot for 100 kPa Dermis Elastic Modulus versus Displacement, grouped by Epidermis Elastic Modulus (γ)

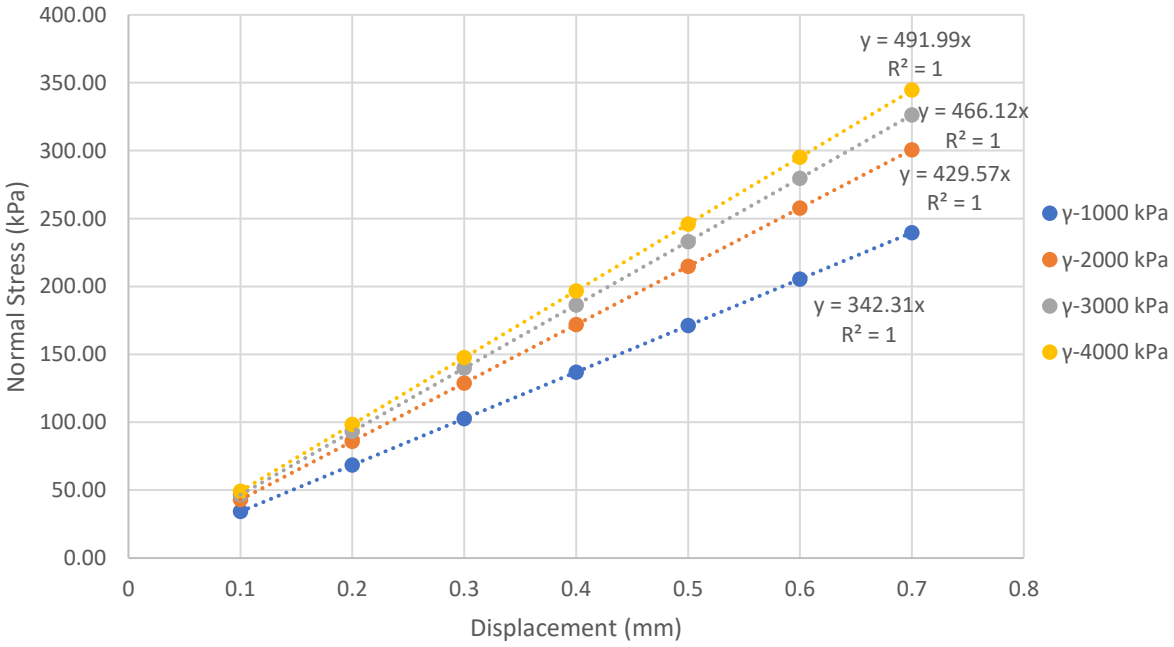

Figure 2-8: Normal Stress Plot for 100 kPa Dermis Elastic Modulus versus Displacement, grouped by Epidermis Elastic Modulus (γ)

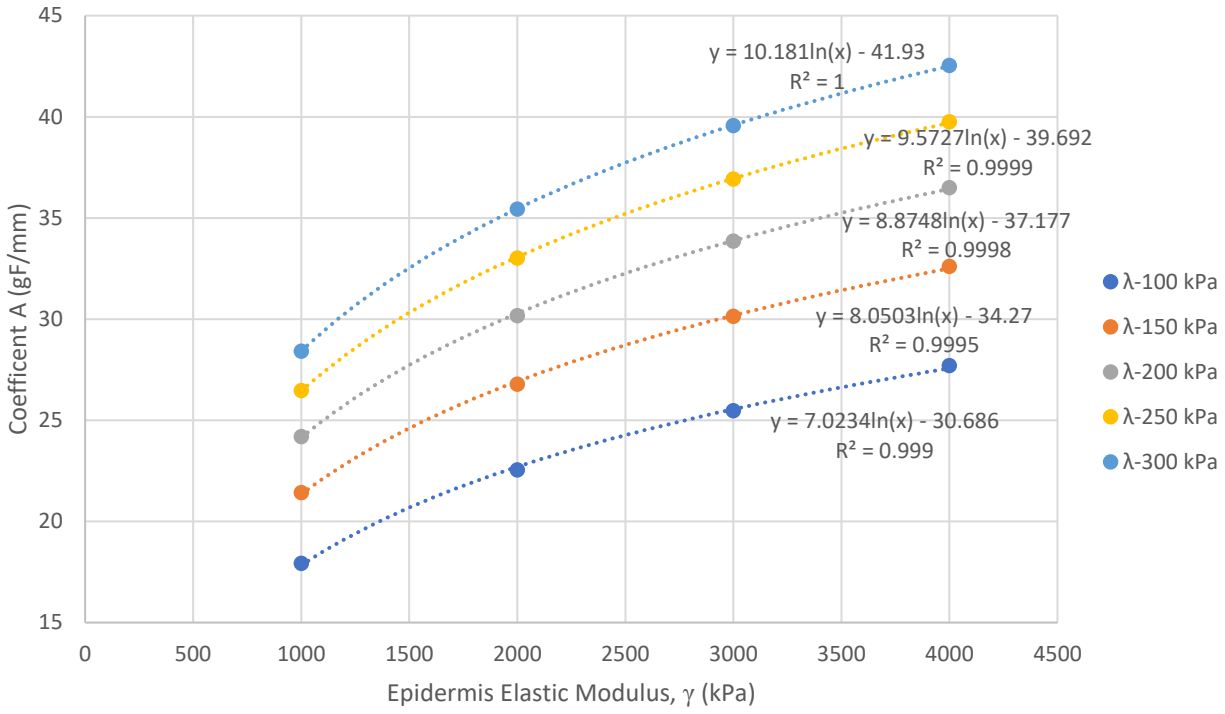

Figure 2-9: Contact Force Logarithmic Relationship Between Coefficient A and Epidermis Elastic Modulus, grouped by Dermis Elastic Modulus (λ)

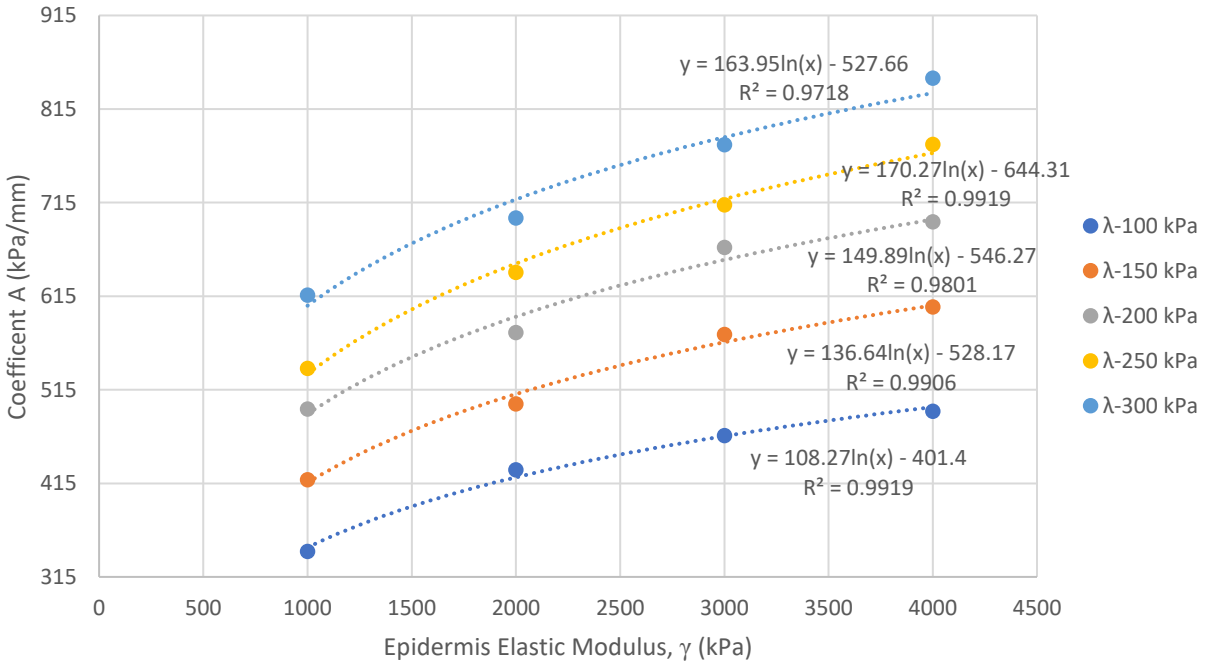

Figure 2-10: Normal Stress Logarithmic Relationship Between Coefficient A and Epidermis Elastic Modulus, grouped by Dermis Elastic Modulus (λ)

Regression analysis was used to understand the relationship between the coefficient, *A*, and the epidermis modulus; a logarithmic relationship was found to best fit the data. Two additional coefficients, *B* and *C*, were then extracted and analyzed. The following equation represents how both of these two additional coefficients, *B* and *C*, are related to coefficient *A*.

$$A = B * ln(\gamma) - C \quad \text{Eq. 2-7}$$

Coefficients *B* and *C* were then plotted versus their relative dermis elastic modulus (λ) values to further understand the relationships between these variables with further regression analysis. Figure 2-11 and Figure 2-12 show both of these coefficients for contact force and normal stress. The following equation captures these relationships for both coefficient *B* and *C*, where K_1 and K_2 are constants:

$$B, C = K_1 * \lambda^{K_2} \quad \text{Eq. 2-8}$$

All of these equations can be combined together to form empirical equations for contact force and normal stress. The variables of the equations include epidermis elastic modulus, dermis elastic modulus, and displacement. Equation 9 is for the contact force expressed in grams force and Equation 10 is for the normal stress in kPa, where γ is the epidermis elastic modulus. Furthermore, γ and λ are expressed in kPa and the displacement, δ, is expressed in mm. R^2=0.99 for both Equation 2-9 and 2-10.

$$F = [1.48\lambda^{0.3381} \ln(\gamma) - 8.282\lambda^{0.2839}]\delta \quad \text{Eq. 2-9}$$

$$\sigma = [17.579\lambda^{0.4023} \ln(\gamma) - 105.11\lambda^{0.3072}]\delta \quad \text{Eq. 2-10}$$

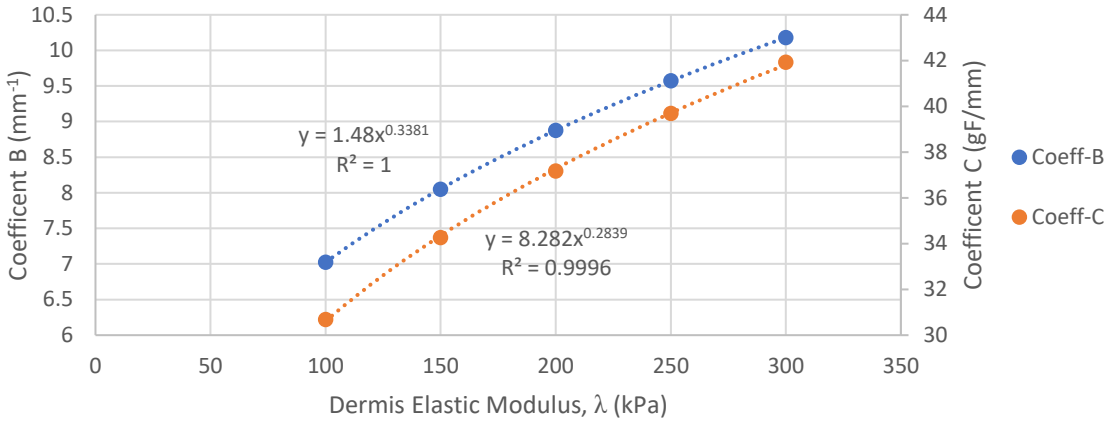

Figure 2-11: Contact Force Power Relationship Between Coefficient B & C versus Dermis Elastic Modulus

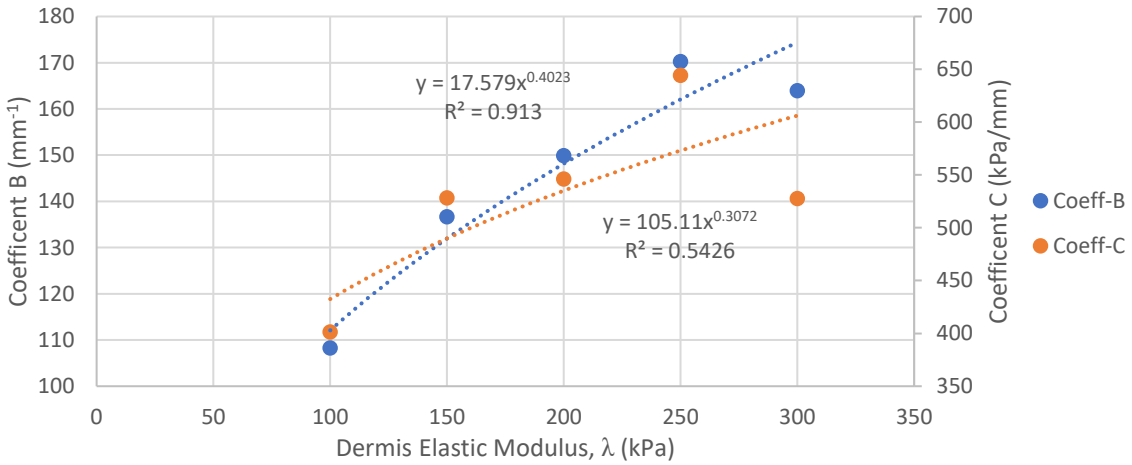

Figure 2-12: Normal Stress Power Relationship Between Coefficient B & C versus Dermis Elastic Modulus

2.5. Discussion

The results foremost show that an increase in insertion depth yielded greater amounts of contact force and normal stress. Furthermore, when evaluating the theoretical equations from Sneddon, as the diameter became larger the contact force increased, but the normal stress decreased. If the diameter decreased, the area also decreased, which allowed higher stresses to be induced. When

using the theoretical equations for the 10.0-gram monofilament, a linear relationship existed between the contact force and normal stress when evaluated versus insertion depth. The more an indenter was applied into a material the greater the force produced. Likewise, if the force increased, the corresponding normal stress increased, since the contact area did not change its physical shape. However, what is most insightful is how sensitive these equations are to differences in skin elasticity. For an elastic modulus of 1000 kPa it took exactly 0.149 mm of insertion to produce 10.0 gF when using a properly calibrated monofilament. An elasticity of 4000 kPa required 0.037 mm to produce the same force. The steeper the slope of the curve in Figure 2-4, the greater the influence that the insertion depth had on the force generated. In some cases, slight differences had a large effect on how much force was actually produced. Considering that these monofilaments are supposed to be applied by hand it would be exceedingly difficult to precisely stop applying the monofilament at exactly the right distance, even if the elasticity of the foot is known. It is also worth noting that the material properties of human skin differ from one person to another, which could influence the insertion depth required to obtain a certain amount of contact force. This would make it challenging to get the monofilament to achieve the desired force output.

The homogenous isotropic model performed very well when compared to three different validation checks. Contact force and normal stress were calculated and compared for each displacement with the theoretical contact mechanics equations for elastic moduli between 1000 kPa and 4000 kPa. The percent errors were consistent between all displacements, relative to their respected moduli. For 1000 kPa the percent error was 1.97% and was 6.39% for 4000 kPa when examining the contact force. The normal stress yielded percent errors of 3.32% and 7.56% for

1000 kPa and 4000 kPa, respectively. The reason that the results grouped by elastic modulus had approximately the same error was because the displacement is the only parameter that changed between simulations, meaning that the simulation solved the same way regardless of the initial condition applied. This consistency was seen in the strain energy norm where it was approximately the same for each displacement, for its respective modulus. The strain energy norms were 1.89%, 1.87%, 1.86%, and 1.86% for 1000, 2000, 3000, and 4000 kPa, respectively, which is within the 2% error allowed by the simulation solver.

The justification for using the same mesh settings from the homogenous isotropic model in the composite isotropic model was because of the congruency of the contact force and normal stress to the theoretical contact mechanics and the strain energy norm. The composite isotropic model provided insight into the reaction of human skin on the plantar surface of the foot to a monofilament being applied noninvasively. After analyzing all simulations for this model, empirical equations were developed that provided insight into the complexities of contact on a composite material. The empirical equations show intricate relationships between the epidermis elastic modulus, dermis elastic modulus, and the insertion depth. Although they can still be classified as linear equations, they offer a wide range of outcomes in determining the contact force and normal stress caused by insertion of a 10.0-gram monofilament. Table 2-2 details the combinations of the three variables to produce exactly 10.0 grams of force, showing that the range of displacement can vary between 0.235 to 0.559 mm to produce the correct force at specific combinations of epidermis and dermis elastic moduli. Also noteworthy was how much effect the dermis modulus had on the contact force and normal stress produced when compared to the homogenous isotropic model and theoretical contact mechanics. The amount of

monofilament insertion required to produce 10.0 gF in the composite model was between 3.75 to 6.35 times greater than previously determined from the homogenous model. All strain energy norms were between 1.01% and 1.99% and all of the 140 simulations that used the composite model ran between 2-3 iterations using the H-adaptive mesh parameters.

Variables to Produce 10.0 gF		
γ (kPa)	λ (kPa)	δ (mm)
1000	100	0.559
1000	150	0.470
1000	200	0.416
1000	250	0.379
1000	300	0.351
2000	100	0.439
2000	150	0.372
2000	200	0.331
2000	250	0.303
2000	300	0.281
3000	100	0.391
3000	150	0.332
3000	200	0.296
3000	250	0.271
3000	300	0.252
4000	100	0.362
4000	150	0.308
4000	200	0.275
4000	250	0.252
4000	300	0.235

Table 2-2: Combinations of Epidermis, Dermis, and Displacement to Produce 10.0 gF for Composite Isotropic Human Skin Model

Ultimately, regression analysis provided a means to understand the behavior of the composite model. This assertion is supported as the R^2 value of both empirical equations was approximately one. However, coefficient *C* of the empirical equation for normal stress had the poorest relationship with the data, with an R^2 value of 0.6143. Nonetheless, this coefficient had a

negligible effect on the accuracy of the empirical equation for normal stress. It was abnormal, especially since throughout the study the regression analysis showed significantly stronger correlations when curve fitting the data.

Overall, the theoretical contact mechanics and FEA results indicate that slight differences in insertion depth had large effects on the force delivered via the monofilament. FEA simulations are a powerful tool that lets users model the effects of bodies under load, or in this analysis bodies in contact with one another. It can also be used as an iterative process in order to test different combinations of fixtures, loads, and settings to compare results between simulations. Although some clinicians may be able to use a Semmes-Weinstein monofilament accurately and repeatedly, attention to application technique must be used when attempting to recreate the correct force delivered over multiple applications of the monofilament.

2.6. Limitations

The greatest limitation with this study is regarding the assumptions necessary to use the empirical equations developed. They only work with linear elastic material properties and with small displacements. The empirical equations would most likely not work with insertions depths greater than 1.0 mm as a result of the small displacement assumption; were not evaluated past 0.7 mm in this study. SolidWorks® will alert the user if the simulation needs to be solved with large displacements and for both models in this study it was verified that small displacements were adequate. Also, the fact that both the contact force and normal stress were within an acceptable percent error compared to the theoretical contact mechanics verified that small displacement simulations were appropriate for this study. Furthermore, the percent error could be

improved by setting the accuracy parameter to 99%. However, this would require more than 2-3 iterations to solve per configuration in each model. This study did not consider a range of elastic moduli for the subcutaneous fat layer and did not consider different thicknesses of the epidermis, dermis, or subcutaneous fat layers.

Although this study assumed that the nylon monofilament and human skin were linear elastic, further studies should consider using nonlinear or hyperelastic variants of the material properties. Human skin is viscoelastic, which means that loading rate will impact the stiffness response of the material. If loaded at a faster rate than the stiffness of the skin will increase. Considering these type of material models would require a nonlinear FEA which could take much effort to set up and find adequate settings. Another area of future work could involve nonlinear dynamic buckling analysis using the work of Russell and White in order to model the buckling behavior of the monofilament when it comes in contact with the skin [93]. The research of Szalai may also be useful for nonlinear simulations [94]. Nonlinear mechanical properties of human skin should be considered for future FEA [95]. It is anticipated that a similar process could be employed to determine empirical equations with the use of nonlinear material properties, or even with additional parameters such as varying the thicknesses of the epidermis, dermis, and subcutaneous fat layers, along with monofilaments with different diameters.

2.7. Conclusions

This study sought out to understand how insertion depth, monofilament diameter, and skin material properties affect neuropathy assessment on the plantar surface of the foot. The contact force and normal stress were examined using FEA and were validated using theoretical equations. The homogenous isotropic model simulations performed well compared to theoretical

contact mechanics and were shown to be an effective way of validating the mesh settings used for the composite isotropic model. Empirical equations were derived from the results of the composite isotropic model and showcased how the contact force and normal stress are affected by epidermis elastic modulus, dermis elastic modulus, and insertion depth. SolidWorks® Simulation was an effective way of running all 188 simulations and had many useful features that helped model the studies close to real life conditions. Finally, the results indicate that it would be extremely difficult to accurately apply a consistent contact force by hand for assessing neuropathy. The accuracy of the monofilament test is not only subjective of how far it is applied, but also affected by the elastic modulus of the individual's skin. As such, attention to application technique must be taken when using hand-applied monofilaments for neuropathy assessment. Furthermore the results from this chapter informed design requirements for the automated tool prototypes presented in Chapters 3 and 6.

Chapter 3: The Neuropathy Cartographer Mk1

3.1. Introduction

The findings from Chapter 2 of this dissertation demonstrate the necessity for a more reliable tool for neuropathy assessment, given the accuracy dependency on not only the insertion depth, but the material skin properties of the subject. Some clinicians may have the hand control necessary to use the hand-applied monofilament accurately and repeatedly, but there is always the potential for these variables to influence the assessment. In order to improve the relatability and accuracy of neuropathy assessment an automated tool and corresponding testing methodology have been created. Both of which can have a positive impact on neuropathy assessment on the plantar surface. The proposed solution takes the current hand-applied Semmes-Weinstein monofilament and implements robotics to automate the evaluation. Standardizing the testing procedure may allow physicians to measure the efficacy of treatments, monitor disease progression, and map out the subject's plantar threshold sensitivity more accurately.

3.2. Design Objectives

The device needed to meet certain design objectives to make it feasible. It had to be easy to manufacture, in which anyone with a technical background could assemble it within a few hours. Simple tools such as Allen wrenches, screw drivers, pliers, crescent wrenches, and a level should be the only tools required to assemble. It should ideally be built by only one individual, but no more than two should be necessary. Components should be adjustable to accommodate the different foot size of approximately 95% of the population. The machine needed to be easy to transport between exam rooms with the use of a rolling cart. The solution was required to apply a

contact force using a commercially available Semmes-Weinstein monofilament. It also had to apply at minimum three contact forces using only one monofilament between 0.2 and 10.0 grams of force. The targeted accuracy for the device needed to be within a 0.5 grams of force margin of absolute error, with a resolution of 0.1 grams of force. These requirements will be validated in the clinical study presented in Chapter 4 of this dissertation, in addition to being compared to the accuracy of both hand-applied monofilaments and other automated tool inventions. The machine needed to perform the assessment with the monofilament so that it was still noninvasive, just like the hand-applied assessment. It also needed to operate with the subject's foot out in front of them, as this is how the assessment is currently performed. Safety is always paramount, which required safety features, such as non-sharp edges and properly connecting all electrical wires. Incorporating quality power supplies with built in fault detections were necessary. The automated tool needed to evaluate one foot at a time and be comfortable for the subject during use. Ideally subjects will place their foot in the device and then in a future evaluation their foot can be relocated to the same position as before. The subject's foot had to be secured in a way to prevent excessive motion during data collection. The device had to accommodate 95% of the world's population. Multiple locations on the plantar surface were required to be evaluated during an assessment. Disinfecting surfaces between subjects was also necessary. The evaluation time per foot could take no more than 15 minutes. Lastly when manufacturing at volume the cost of the device should cost approximately $1,000.00, not including a computer.

3.3. Mk1 Design

The Mk1 solution for the automated tool took the form of a computer numerical control machine. It was designed using SolidWorks and is presented in Figure 3-1. It used a gantry system to move a Semmes-Weinstein monofilament to plantar surface testing locations. It also featured an

innovative probe system that allowed for a range of monofilament contact forces to be applied. The following sections detail the main subassemblies that make up the Mk1 diagnostic tool. The device was approximately 45 pounds, with overall dimensions being 23.5 inches in width, 29 inches in height, and 19.75 inches in depth. All components needed to manufacture the Mk1 prototype was approximately $2,300.00, which included parts from 80/20 Inc, McMaster-Carr, and Amazon. The prototype also featured 3D printed components. A $200.00 46-inch Husky workbench was also implemented, which can adjust its height to accommodate different examination tables. The device was bolted to the workbench to prevent it from falling off the table. The laptop used to run the device was a Dell Inspiron 15 3000 Touch Laptop, offered at a price of $588.00. The laptop and the workbench are not included in the $2,300.00 spent on parts and electronics. Furthermore, a nonprovisional patent application detailing the Mk1 prototype has been filed to the USPTO, under application number US 17027464.

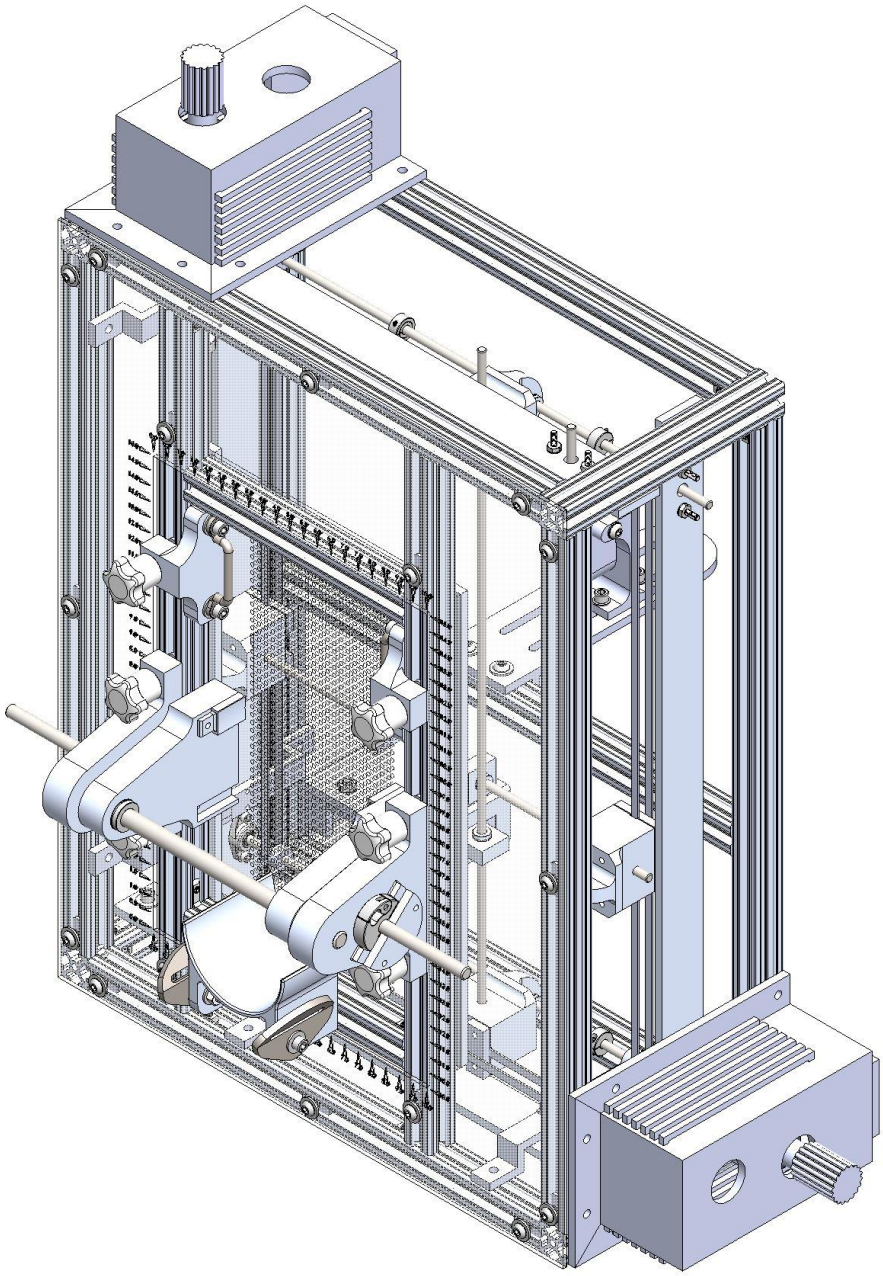

Figure 3-1: Mk1 Automated Tool Prototype

3.3.1. Mk1 Chassis Subassembly

The chassis was created out of seventeen 80/20 aluminum T-slot profiles. Its overall shape was rectangular and its generally what provided the overall shape of the device. Components and other subassemblies connected to the chassis using t-nuts. A front cover plate made of clear

acrylic was mounted to the front face of the device, in order to prevent the subject's foot from entering inside of the device. Stepper motors were mounted onto the chassis directly, in addition to cooling fans and motor covers. A camera mount and camera (Logitech Brio) were also attached at the rear of the chassis.

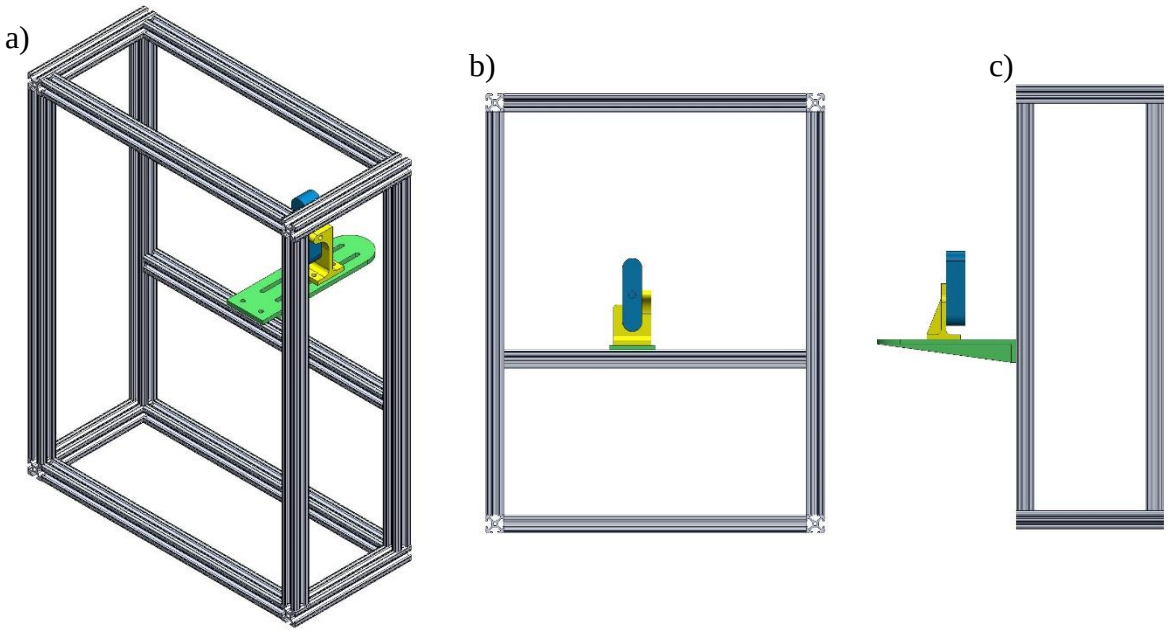

Figure 3-2: Mk1 Chassis Subassembly[3]

a) Isotropic View
b) Front View
c) Side View

3.3.2. Mk1 Foot Clamp Subassembly

Mounted in the front of the chassis was the foot clamp subassembly, Figure 3-3, which retained the only components that came in direct contact with the subject's foot, other than the Semmes-Weinstein monofilament. The clamping mechanism was based on the design of a Brannock device, often used to measure the size of an individual's foot. The subject's foot needed to be

[3] 80/20 Aluminum T-slot profiles (White), Camera Mounting Plate (Green), Camera Mount (Yellow), Logitech Brio Webcam (Blue)

placed in the device so that the plantar surface was in contact with the foot plate. The individual components of the clamp could be adjusted up and down and left and right to accommodate different size feet. Once in position these components can be locked into place using the various screw down knobs. When used in concert with the engraved ruler, Figure 3-4, on the cover plate of the device, the individual components can be relocated to specific positions. There was also a locator on the clamping mechanism to align with the ball of the foot in order to create a reference point for future use. The toes of the subject were strapped down with minimal pressure using a Velcro strap. Furthermore, the ankle was placed in a curved ankle holder and was strapped down to prevent rotation. The clamping structures were also padded with EVA foam to aid in comfort. One of the most prominent features of the device was the foot plate, which featured an array of holes. Each of the 1,029 holes functioned as potential assessment locations, each being 0.1875 inches in diameter. Each hole was evenly spaced 0.25 inches apart in a 5 inch by 7-inch rectangle and accommodated 95% of the world's maximum foot size [96]. The foot plate was made from clear cast acrylic, which permitted the camera mounted on the back of the device to take a photo of the subject's foot overlayed with the holes. The foot plate was recessed inwards below the front panel of the machine, which reduced the travel distance the monofilament needed to contact the plantar surface. All surfaces were easy to disinfect with the use of either wipes or sprays.

a)

b)

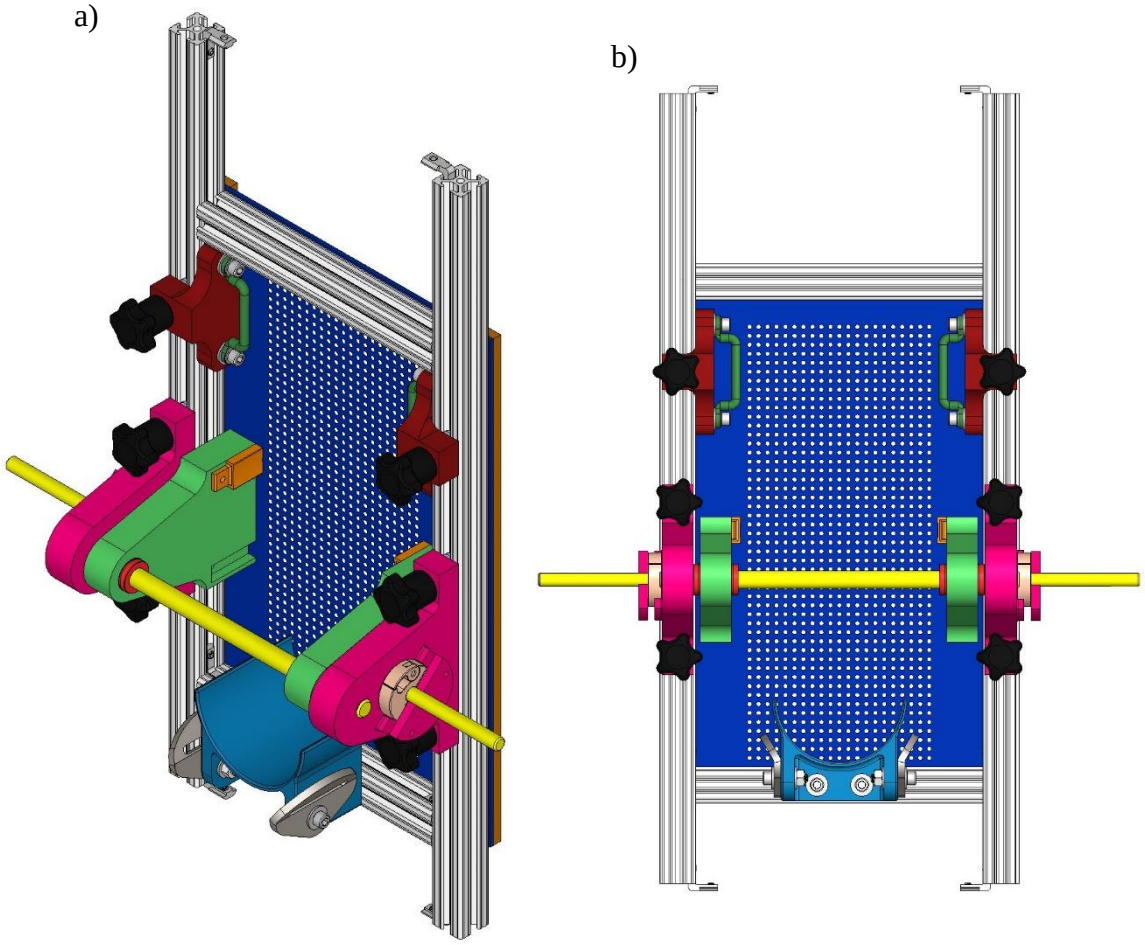

Figure 3-3: Mk1 Foot Clamp Subassembly[4]

a) Isotropic View
b) Front View

[4] Perforated Foot Plate (Dark Blue), 80/20 Aluminum T-slot profiles (White), Toe Clamp (Maroon), Foot Clamp Base (Magenta), Foot Clamp (Green), Ball of Foot Locator (Orange), Ankle Holder (Blue), Linear Sleeve Bearing (Red), Clamp Lock (Bronze), Screw Down Knobs (Black), Ankle Strap Mount (Grey) , Toe Strap Mount (Dark Green), Linear Motion Shaft (Yellow)

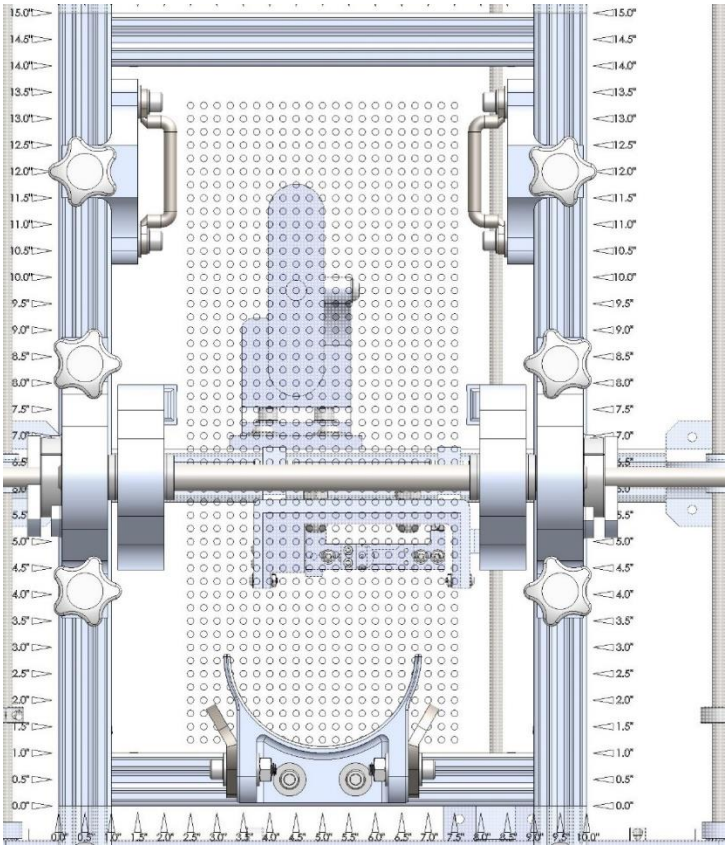

Figure 3-4: Mk1 Foot Clamp Subassembly Mounted on Front of the Automated Tool

3.3.3. Mk1 Gantry Subassembly

The gantry subassembly, Figure 3-5, translated the Semmes-Weinstein monofilament in the x and y directions of the device. It essentially moved the monofilament to one of the many holes on the foot plate for evaluation. It was comprised of belts, pulleys, linear sleeve bearings, linear mounted bearings, shaft collars, linear motion shafts, and 3D printed motion carriages, in addition to various fastening elements. There were four linear motion assembles, Figure 3-6, that made up the gantry subassembly; mounted onto brackets, directly connected to the chassis. The linear motion assemblies interconnected with each other at 90-degree intervals, outlining the rectangular chassis. The probe subassembly was connected between two perpendicular linear motion shafts and were also connected to the linear motion assemblies. The connection was

maintained by a press fit with the accompanying hole on the motion carriage, as well as with the use of self-locking retaining rings. GT2 timing belts and pulleys were incorporated into the assembly, which have become a standard in 3D printers and robotics [97]. The belts were attached to the motion carriages and the tension was maintained with the use of belt tensioners. Two stepper motors were connected at opposing corners of the device, each of which were connected to a linear motion shaft via a flexible shaft coupling. The shaft collars functioned as physical stops, which defined the total travel range in the x and y axis. 3D printed knobs were installed at the ends of the linear motion shafts for manual operation of the device, if required. It was previously determined that the gantry system had approximately a 99% accuracy in both the x and y axis [98].

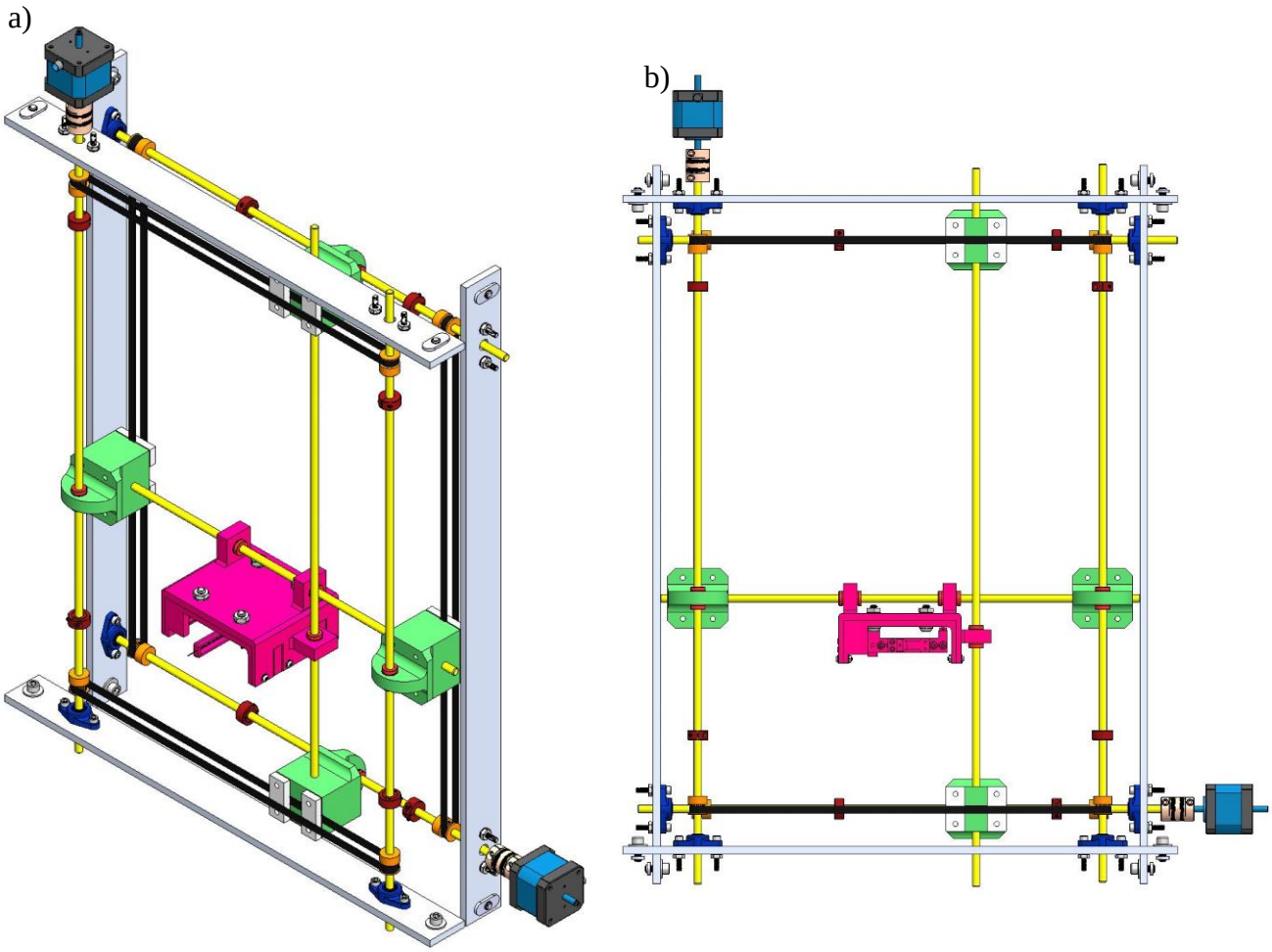

Figure 3-5: Mk1 Gantry Subassembly[5]

a) Isotropic View
b) Front View

[5] Brackets (Grey), Linear Motion Shaft (Yellow), Linear Sleeve Bearing (Red), GT2 Timing Pulley (Orange), GT2 Timing Belt (Black), Coupling (Bronze), Stepper Motor (Blue/Black), Mounted Sleeve Bearing (Dark Blue), Shaft Collars (Maroon), 3D Printed Motion Carriage (Green), Belt Tension Plate (White), Mk1 Probe Subassembly (Magenta)

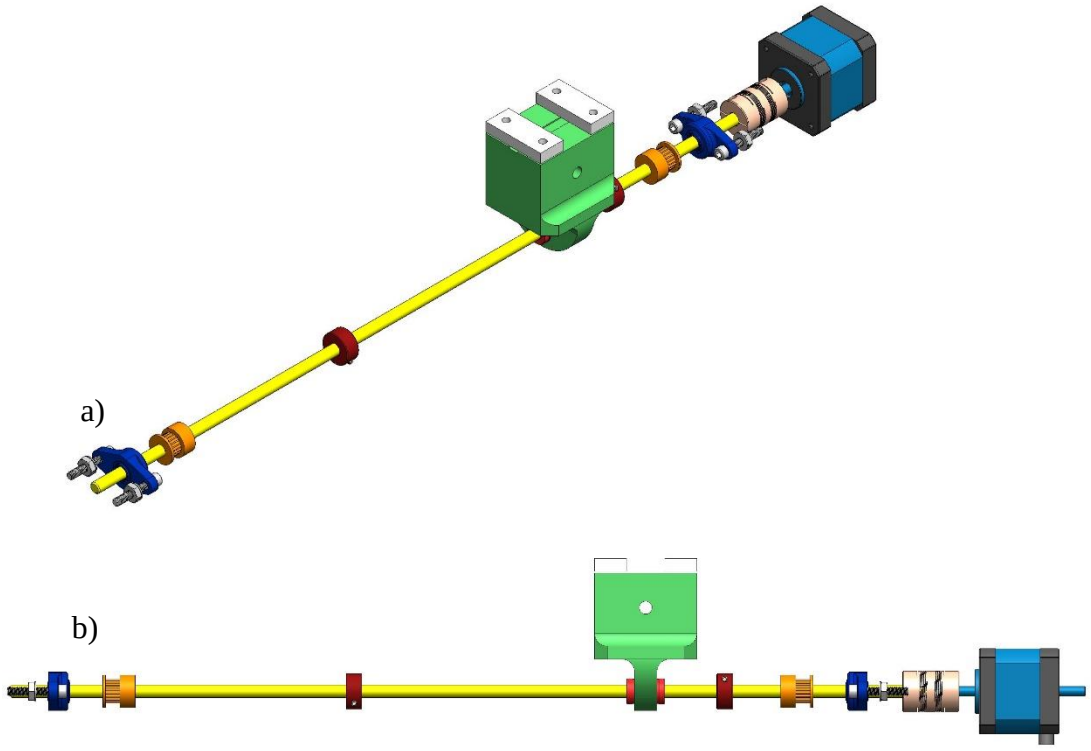

Figure 3-6: Mk1 Linear Motion Assembly[6]

a) Isotropic View
b) Side View

3.3.4. Mk1 Probe Subassembly

The probe subassembly translated the monofilament in the z-direction until it contacted the plantar surface. The monofilament was actuated through the hole of the foot plate until it made contact on the plantar surface. The probe subassembly used a commercially available 10.0 grams of force Semmes-Weinstein monofilament indirectly attached to a load cell in sequence with a stepper motor. Chapter 2 of this dissertation demonstrates the challenges of accurately driving the monofilament forward without force feedback, which lead to the implementation of a load

[6] Linear Motion Shaft (Yellow), Linear Sleeve Bearing (Red), GT2 Timing Pulley (Orange), Coupling (Bronze), Stepper Motor (Blue/Black), Mounted Sleeve Bearing (Dark Blue), Shaft Collars (Maroon), 3D Printed Motion Carriage (Green), Belt Tension Plate (White)

cell stepper motor feedback loop. As the stepper motor moved forward, the load cell continuously measured the force output until it reached a prescribed value. Once the monofilament made initial contact it began to reduce the rate of insertion, until it reached its targeted force. The monofilament itself was housed in a holder which straightened the monofilament. Furthermore, the assembly featured a miniature ball bearing carriage which provided support as the monofilament was actuated. This was essential to overcome the instability in the assembly, resulting from mounting all of the essential components to the stepper motor alone. The subassembly also featured components mainly manufactured using 3D printing, such as platform blocks, the housing, and the chassis. This subassembly and its components are presented in Figure 3-7. The accuracy of this system is presented in Chapter 4 of this dissertation.

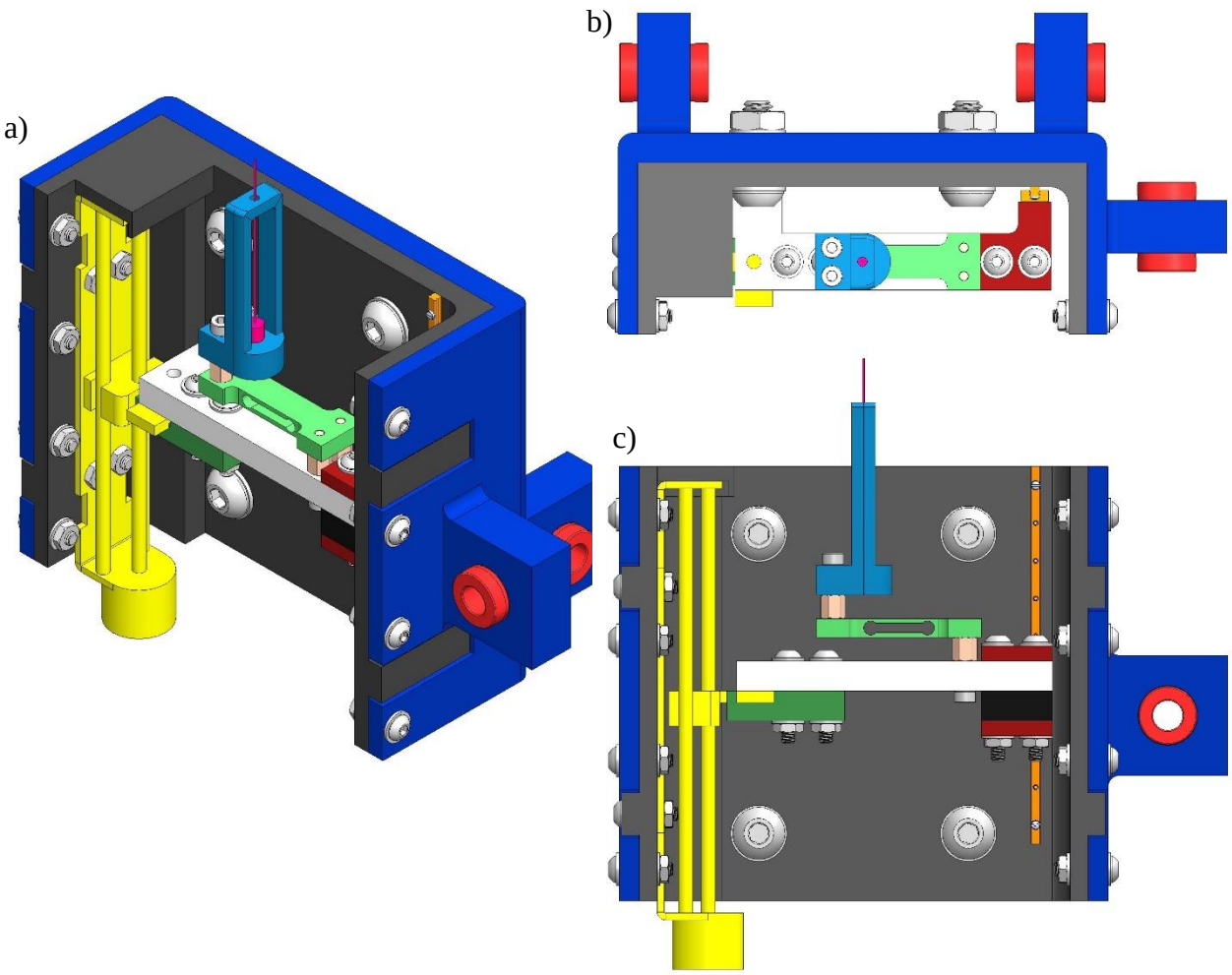

Figure 3-7: Mk1 Probe Subassembly[7]

a) Isotropic View
b) Top View
c) Front View

3.3.5. Mk1 Electronics

Electronics included three stepper motors, three stepper motor drivers, four limit switches, a load cell, a HX711 amplifier, an Arduino Mega, an Arduino Uno, a Logitech Brio webcam, a power supply, and a buck converter. Figure 3-8 presents these electronics. Two SureStep STP-MTP-

[7] Monofilament (Magenta), Monofilament Holder (Blue), Standoffs (Bronze), Load Cell (Green), Platform (White), Support Block 1 (Dark Green), Support Block 2 (Maroon), Support Block 3 (Black), Stepper Motor (Yellow), Miniature Ball Bearing Carriage (Orange), Linear Sleeve Bearing (Red), Chassis (Gray), Housing (Dark Blue)

17040D stepper motors were used in the gantry system. These NEMA 17 bipolar stepper motors have 3.81 lb-in of torque, have 1.7 amps per phase, and have 200 steps per revolution [99]. The STP-DRV-6575 stepper motor driver allowed the stepper motors to be microstepped between 200-20000 steps per revolution [99]. These specific components were powered by a STP-PWR-4805 48-volt, 5-amp, DC power supply [99]. The third stepper motor was the Walfront D8-MOTOR80, which featured a built-in lead screw driven carriage. As the motor actuated, the carriage would translate back and forth with a screw pitch of 0.5 mm [100]. It was rated at 20 steps per revolution and operates between 9 and 12 volts, with a 0.800 amps per phase rating [100]. This equated to a linear travel distance of 0.025 mm per step, which is an identical resolution considered for the homogenous isotropic model and four times the resolution considered in the composite isotropic model from Chapter 2 of this dissertation. The Walfront stepper motor was connected to a TB6600 stepper motor driver, which was powered by a buck converter. The buck converter stepped down the 48 volts supplied by the STP-PWR-4805 to 9 volts. Limit switches were mounted along the x and y axis of the machine and interacted with the gantry subassembly. These not only assisted in calibrating the gantry system before each use, but also to stop the machine if triggered. The most important electrical component was the RB-Phi-203 100-gram micro load cell. This small load cell supported weight up to 100 grams, with an error of ±50 milligrams. The rated output of the load cell was 600 μV/V and had a 1000-ohm impedance [101]. The HX711 amplifier is a 24-bit analog-to-digital converter and was set to sample data at 10 Hz [102]. The power supply, stepper motor drivers, HX711, Arduino Mega and Uno were all mounted onto a wooden board, fixed away from the subject.

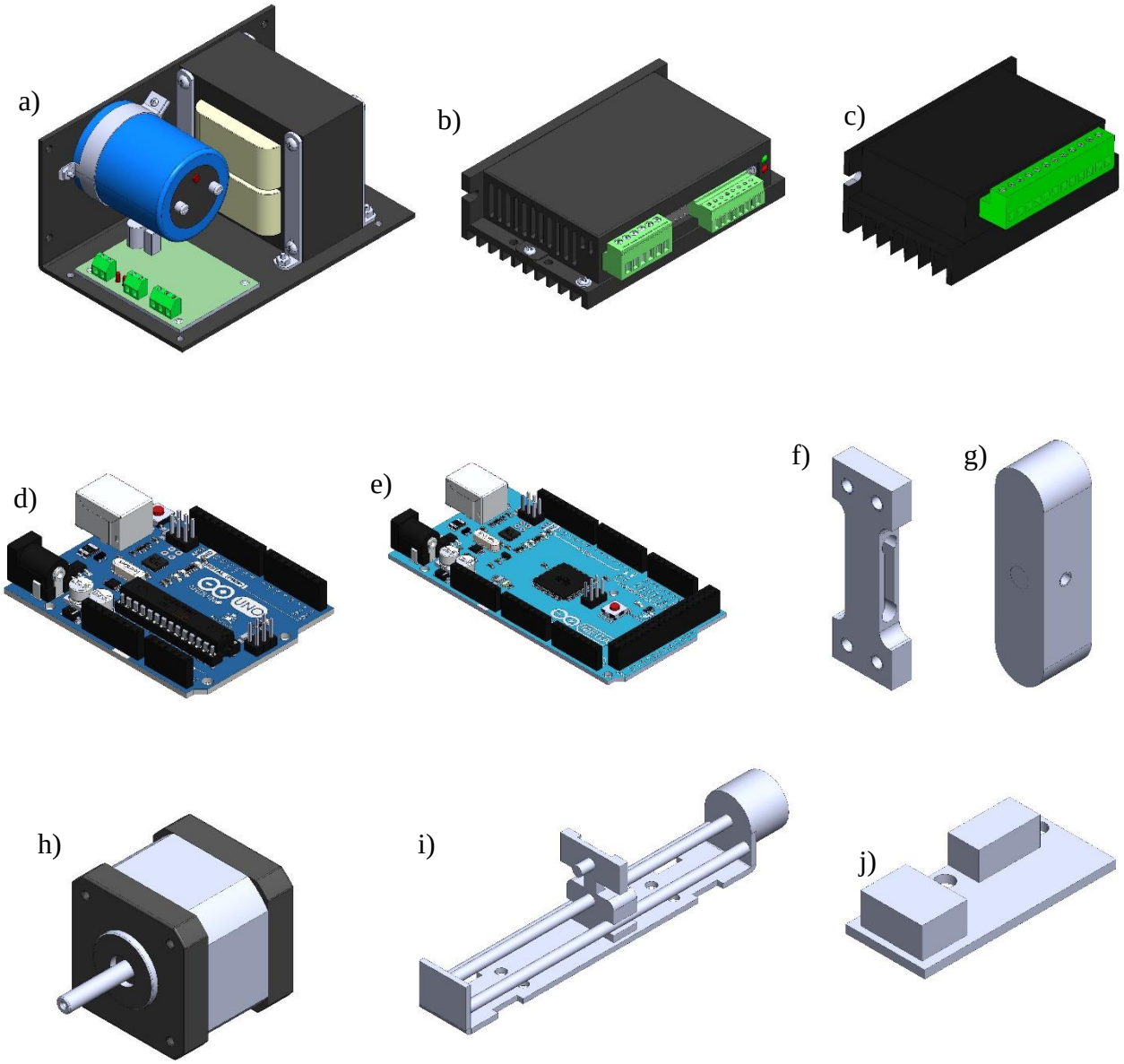

Figure 3-8: Mk1Electronics

a) STP-PWR-4808 Power Supply
b) STP-DRW-6575 Stepper Motor Drive
c) TB6600 Stepper Motor Drive
d) Arduino Mega
e) Arduino Uno
f) RB-Phi-203 100g Micro Load Cell
g) Logitech Brio Webcam
h) STP-MTR-17040D Stepper Motor
i) Walfront D8-MOTOR80 Stepper Motor
j) Limit Switch

3.4. Assessment Methodology and Features

With an automated approach for neuropathy assessment on the plantar surface came a new methodology and features that previously were not present. Following the subject's foot being placed on the device, the operator initiated the MATLAB script developed to control the automated tool. After going through positional calibrations, a picture was taken of the subject's foot through the clear acrylic foot plate with the webcam mounted on the rear of the device. The webcam was mounted vertically, which allowed for a close-up image of the foot to be taken. A grid overlay was generated over the locations of all the holes of the foot plate. The script then requested that the operator select testing locations by clicking on corresponding locations on the picture at the intersections of the grid, 13 in total. Locations were selected by region, the first region being the toe region. Each of the heads of the five toes were selected. The second region assessed was the ball of the foot region, which also had five locations. The third region was the heel region, which had three locations. After all locations were selected, the device began the assessment by randomly selecting one of four regional testing order paths. These testing paths, presented in Table 3-1, were optimized to limit the amount of travel between regions. As such, the heel region was either assessed first or last, with the other two regions occurring in the middle. Once the script had selected a testing order path, the locations within this region were assessed randomly, also determined by the script. Incorporating the use of a restricted randomization prevented the subject and the clinician from imposing biases and prevented the subject from being able to guess the order of occurrence. This was achieved using the MATLAB function `rng` shuffle. Once the locations had been randomized in the first region assessed, the gantry system moved the probe subassembly into position at the first testing location. At this point the script used a homing sequence to ascertain the location's threshold sensitivity,

illustrated in Figure 3-9. The homing sequence evaluated for the subject's threshold sensitivity to be approximated into the following categories: 0.35, 0.70, 2.0, 4.0, 6.0, 8.0, 10.0, and >10.0 grams of force. The first load the machine applied was 0.35 grams of contact force. The subject was provided a handheld led pushbutton during the assessment, Figure 3-10, which blinked for five seconds after a stimulus had been applied. If the subject perceived the stimulus they were instructed to press and hold the pushbutton for one second to document their response. If the subject felt the 0.35-gram force load, then the locations threshold sensitivity was documented as such, and the probe subassembly was moved to the next location. If the subject did not feel the 0.35-gram force stimulus, a 10.0-gram force stimulus was applied next. Should the subject still not feel the monofilament applied at 10.0 grams of force, then this location had a threshold greater than 10.0 grams of force and the next location was then assessed. If the subject indicated that they felt the stimulus, then the machine proceeded to assess the location at 4.0 grams of force, followed by the other forces included in the homing sequence. The goal of the homing sequence was to determine the location's threshold sensitivity without applying all seven contact forces, reducing the overall assessment time. This process was repeated from location to location, and from region to region, until all 13 locations on the subject's foot had been evaluated. At this point the original image of the subject's foot was then updated to show the threshold sensitivity results. The subject's second foot was then evaluated, using the same procedures. At the conclusion of the assessment the subject's threshold sensitivities on both feet were generated and ready for future analysis.

False positives checks were also included the methodology, where each location had a 10% probability of occurrence. When a false positive check occurred, the probe assembly actuated the

monofilament forward, but did not contact the plantar surface. This mimicked the sound of an actual application of the monofilament. The handheld LED pushbutton also queried the subject. A false positive check either occurred before or after the homing sequence determined the location's threshold sensitivity.

	Testing Order Paths			
Order of Occurrence	1	2	3	4
1st	Heel	Distal Phalanges	Metatarsal Heads	Heel
2nd	Metatarsal Heads	Metatarsal Heads	Distal Phalanges	Distal Phalanges
3rd	Distal Phalanges	Heel	Heel	Metatarsal Heads

Table 3-1: Regional Assessment Testing Order Paths

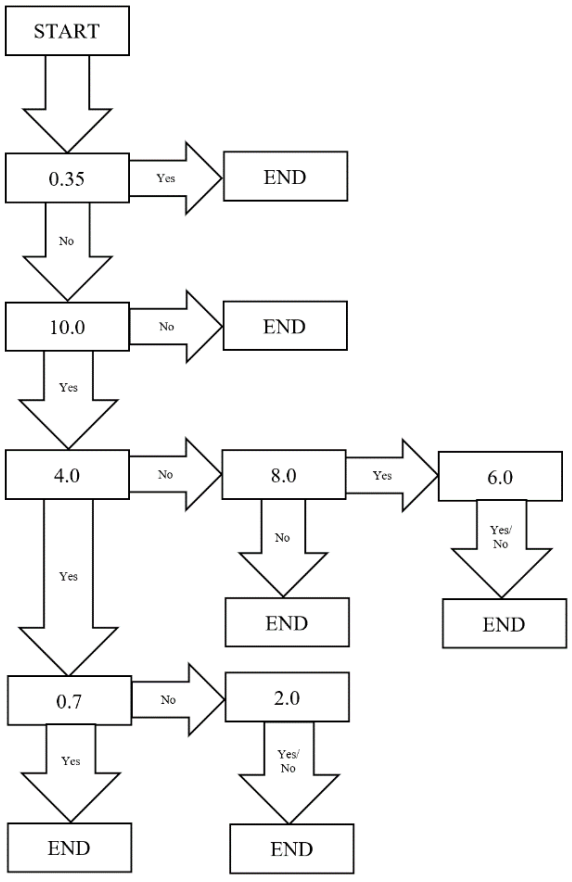

Figure 3-9: Homing Sequence

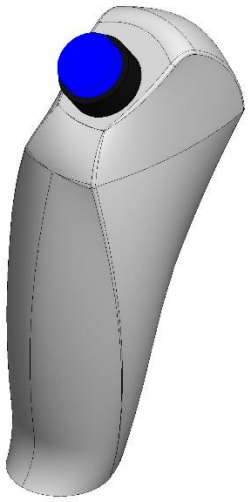

Figure 3-10: Handheld Pushbutton for Cataloging Responses

3.5. Controls and MATLAB Interface

The automated tool was controlled using a MATLAB (R2018a release) script which communicated in tandem with the Arduino Mega and Uno. The Arduino Mega operated an open-source CNC software, known as GRBL. GRBL was responsible for operating the gantry system and essential moved the probe subassembly to each location. The MATLAB script sent g-code instructions to GRBL over serial communication through one of the USB ports on the computer. These g-code instructions are the x and y locations of each of the locations. The initial homing sequence was also controlled by GRBL, in addition to any safety features related to the gantry system hitting a limit switch. The Arduino Uno operated the probe subassembly, by actuating the monofilament against the plantar surface. The MATLAB script sent the Arduino Uno the amount of force that should be applied, depending on the current homing sequence step. The monofilament was then driven forward by the stepper motor, until the load cell measured the desired force. Once initial contact was made between the subject's skin and the monofialemnt the probe subassembly begins to slow down the insertion rate of the monofilament until it finally reaches its targeted value. After the subject's response was documented, the Arduino Uno then

sent the response and the actual force applied back to the MATLAB script for further interpretation. A nonblocking stepper motor Arduino library and a nonblocking HX711 amplifier library were both used in the Arduino Uno code. These libraries made it possible accurately apply the monofilament, as they permitted a seamless data acquisition rate. All of these scripts and codes worked together to control the automated tool and to made it possible to improve the hand-applied monofilament technique.

3.6. Design Validation

The prototype developed achieved the design objectives. By using modular T-slot aluminum profiles, components could be adjusted to fit different foot sizes. This paired with the perforated foot plate made the assessment of multiple locations on the plantar surface feasible. The foot clamping mechanism not only allows for the subject's foot to be retained comfortably, but it can also be used to precisely relocate the subject's foot in the future. This allows for the assessment of the same locations over the course of multiple evaluations. This version took approximately 12 hours to assemble once all components were gathered. The weight of the device by itself was 45 pounds, and when combined with the mobile workbench, the prototype was easily transportable. The prototype also used a commercially available 10.0 grams of force Semmes-Weinstein monofilament and with the feedback loop between the stepper motor and load cell it could be applied at various contact forces. By using a typical Semmes-Weinstein monofilament in the automated tool, the assessment remained noninvasive. Preliminary pilot testing found that the device operated reliably between 0.35 and 10.0 grams of force. Its accuracy and effectiveness are discussed in Chapter 4 of this dissertation. Safety was also maintained by keeping all mechanical and electrical components away from the subject during the test, and by using quality

electronics with built-in safety settings. Although it cost $2,300.00 to manufacture this prototype, it is anticipated that if manufactured at volume the cost can be reduced closer to the targeted $1,000.00 mark. Components such as the 80/20 aluminum T-slot extrusions, motor couplings, and the miniature ball bearing carriage could be acquired for less at volume. The final assembled version of the Mk1 automated tool prototype is featured in Figure 3-11.

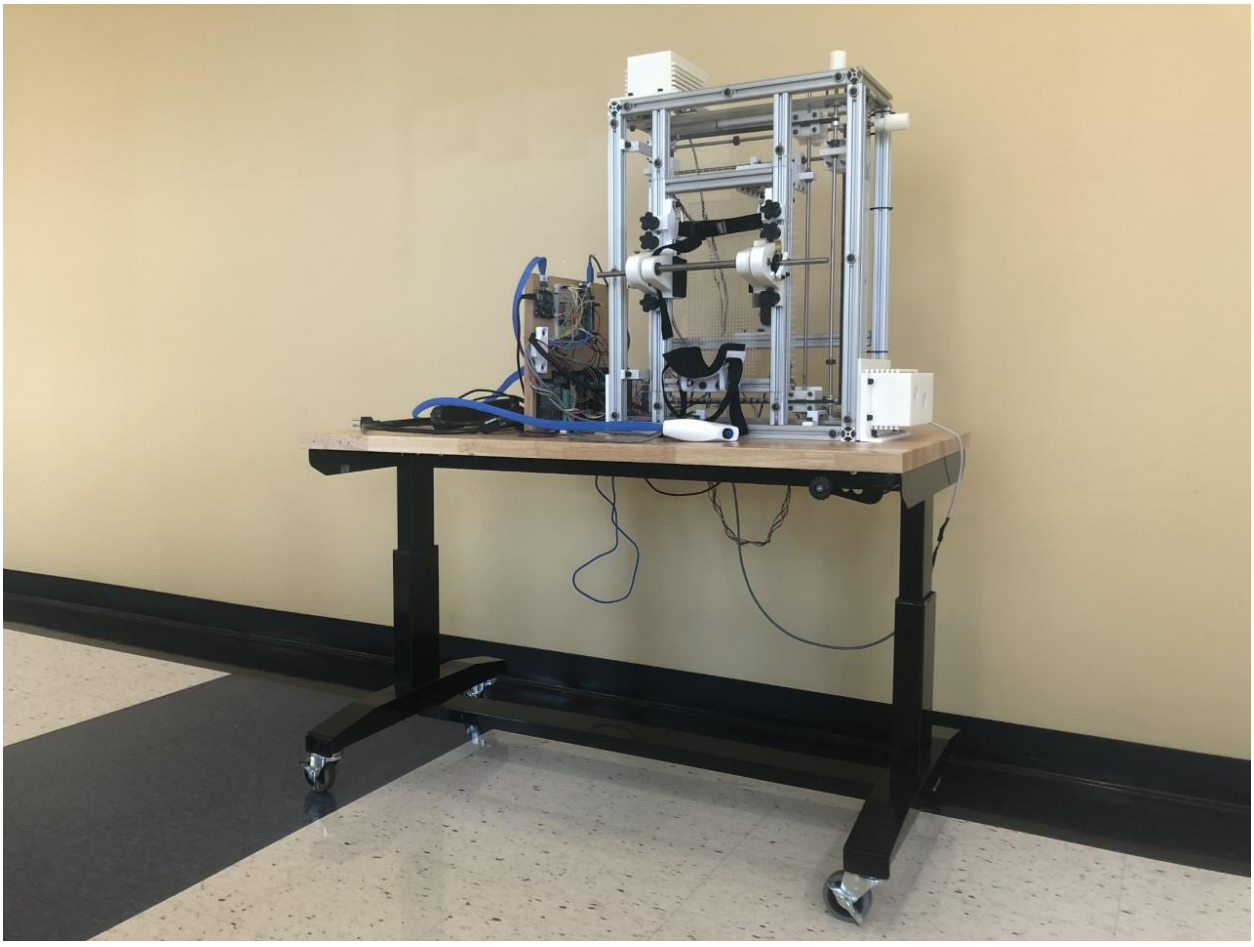

Figure 3-11: Assembled Mk1 Automated Tool Prototype

Chapter 4: Performance Analysis and Clinical Evaluation of an Automated Tool for Plantar Threshold Sensitivity Assessment in a non-Diabetic Control Population

4.1. Abstract

Neuropathy is associated with sensation loss in the extremities. Semmes-Weinstein monofilaments are common tools used to assess an individuals' sensation perception. A tool was developed to automate this testing protocol and to more accurately determine an individual's threshold sensitivity at various locations on the plantar surface. Individuals without type 2 diabetes mellitus (DM2) were classed as control subjects. They were evaluated using a hand-applied monofilament and the automated tool. The device accuracy of the automated tool was first determined, followed by subject's threshold sensitivity at each location. Twenty-six locations were evaluated per subject between 0.35 and 10.0 grams of force. A threshold sensitivity index norm was calculated based on the threshold sensitivity at each location per individual and was plotted versus age, body mass index, ankle brachial index, fasting blood sugars, and HbA1c. The device demonstrated accuracy with an absolute error less than or equal to 0.4 grams of force at most locations. Age showed the strongest relationships to sensation loss. As age increased sensitivity to touch decreased. The automated tool was shown to be effective in determining an individual's threshold sensitivity in individuals without DM2. The calculation of the threshold sensitivity index norm was useful to classify sensation loss.

4.2. Introduction

Diabetic peripheral neuropathy (DPN), oftentimes referred to as diabetic foot, affects 40-60 million people who typically experience a loss of sense to pressure and pain due to their reduced sensation in the hands and feet [4, 5, 34]. These individuals most commonly report burning feet as a symptom of neuropathy, although other symptoms include numbness, tingling, and antalgic gait [26, 28, 79]. These people also have an increased risk of infection, which can lead to ulcers, amputations, and even death [9, 10, 80, 82].

Vibratory analysis via tuning forks, applying electrical stimulation, and even measuring the reflectance spectra of human skin have all been used to study sensation loss [4, 10, 27, 29, 61]. However, force application with a hand-applied monofilament is the most common technique. In the 19th century, horsehair was used for sensation perception [50, 51]. Then, in the 1960s, Semmes and Weinstein used nylon monofilaments for neuropathy assessment on the palmar surfaces of subjects with brain injuries, which would later be called Semmes-Weinstein monofilaments (SWMs) [50, 51, 52]. The clinician applies the monofilament perpendicular to the testing site until it buckles [52, 54]. These easy-to-use devices are thought to be able to minimize movement effects of the clinician's hand while being applied and are popular because they are quick, noninvasive, and cost effective [9, 52, 53, 83].

SWMs are commonly expressed using an evaluator size which represents the amount of force they produce at buckling, often in the range between 0.008 to 300 grams of force (gF) [29]. The 10.0-gF rated SWM is the most common to assess for protective sensation loss [9, 103]. The

relationship between the evaluator size and the force applied is logarithmic, which further relates the stimulus intensity to the perceived sensation ratio via “Weber’s Law” [29, 51, 52, 54]. Hand-applied SWMs are influenced by many factors, both dependent and independent of the clinician. The force applied by the monofilament is influenced by the insertion angle and the rate of insertion [54]. The monofilaments are also subjected to fatigue in which the produced contact force can vary after as few as ten applications on the skin [54]. Moreover, the elasticity of the subjects’ skin also affects the accuracy of a SWM assessment [76]. Automated approaches have been developed to apply the monofilament, such as the work by Siddiqui et al., which used a robot to apply a SWM to the plantar surface [67]. A handheld device which used a LED to indicate when a SWM was applied at 10.0 gF was developed by Spruce and Bowling [69]. Meanwhile, Wilasrumee et al. also developed a tool to apply a SWM at 10.0 gF, which compared well with vibratory and hand-applied SWM assessments [66].

In order to improve the accuracy, reliability, and repeatability of neuropathy assessment, a diagnostic tool was developed which automates testing of threshold sensitivity at various locations on the plantar surface by using the hand-applied SWM [98]. The device has similarities to the previously mentioned automated approaches, however this device allows for the application of a variety of contact forces using only a single monofilament. This allows for the determination of an individual’s threshold sensitivity at multiple locations on the plantar surface. The first objective of this study was to conduct a performance analysis on the automated device to validate its accuracy in a control population of individuals without type 2 diabetes mellitus (DM2), followed by a comparison of results to hand-applied SWM. The second objective of this study was to observe the relationships between recorded sensation to age, body mass index

(BMI), ankle brachial index (ABI), fasting blood sugars (FBS), and HbA1c levels. Evaluating these results in a control population will support future studies of sensation loss in subjects with DM2.

4.3. Methods

4.3.1. Human Subject Demographics and Exclusion Criteria

For this study 59 human subject volunteers were recruited from the Auburn-Opelika Alabama area, ranging between 41 to 81 years of age (Mean ± Standard Deviation= 61.9±10.8 years). Two subjects did not mee the ABI criteria and were removed from the study. This left 57 subjects included in this study. There were 29 male and 28 female participants who were patients of Internal Medicine Associates (IMA) in Opelika. In this report all individuals were control subjects, meaning they were over the age of 40, had an ABI greater than or equal to 1.0 mmHg, and did not have diagnosed DM2. All subjects gave their informed consent to be a part of this research study, which was given approval by the Edward Via College of Osteopathic Medicine (VCOM-Auburn, USA) Institutional Review Board, protocol 2020-004.

4.3.2. Medical Chart Data Retrieval and ABI Screening Procedures

After an investigator explained the study to the subjects and obtained written consent to voluntarily participate, the subject's IMA medical chart was accessed. Data such as the subject's age, BMI, FBS, and HbA1c levels were retrieved and written down on the subject's datasheet for the study. In this study, up to the three most recently documented FBS and HbA1c levels were recorded, with the respective average values calculated and used for analysis. However, some of the subjects did not have FBS (n=3) and HbA1c (n=27) documented in their medical chart, due to their absence of diagnosed DM2. This lack of data did not remove the subjects from the study.

Following the retrieval of their medical data, the subject's ABI was calculated and written down. If the subject's ABI was below the 1.0 mmHg minimum, then they were excused from further analysis, and no further data were collected from them.

4.3.3. Hand-Applied SWM Application Procedures

Subjects were evaluated for threshold sensation on the plantar surface using a hand-applied SWM. Subjects were in the supine position on an exam table, with their head elevated and their legs out in front of them. Their socks were removed, and their feet hung over the end of the exam table with their toes pointing straight up. Their calves were supported underneath by the exam table. A 10.0-gram contact force monofilament was used at 13 locations per foot (Figure 4-1), as it is the most common rated monofilament used for neuropathy assessment. Locations were comprised of the five toes (distal phalanges), five on the ball of the foot (distal metatarsals), and three on the heel (calcaneus). The hand-applied SWM was applied perpendicular to the surface until it buckled and was promptly removed, after which the subject verbally stated if they felt the applied stimulus. Their response was documented on their datasheet for all locations on both feet. Locations assessed using the hand-applied SWM were evaluated anterior to posterior, where the great toe was first assessed. The great toe was followed by the first distal metatarsal (directly below the great toe), to the first heel location. The second toe was tested and succeeded by the second distal metatarsal, then to the center of the heel. This process was then used on the third toe, to the third distal metatarsal, and to the third heel location. The fourth toe was evaluated followed by the fourth distal metatarsal, then the fifth toe, and finally ending at the fifth distal metatarsal.

Figure 4-1: Plantar Surface Evaluation Locations for the Hand-Applied Monofilament and the Automated Tool

4.3.4. Automated Tool Evaluation Procedures

The other tool used in this study was an automated device that was designed to apply the standard hand-applied SWM directly to the plantar surface (Figure 4-2) [98]. The automated device used belts and pulleys to move the SWM to any location along a perforated transparent hole plate, comprising of 1,029 holes. In an upright position on the exam table, with their back supported by a backrest, the subject placed their foot against the foot plate with their toes pointing upward, while their foot was strapped into place. The machine used a load cell feedback loop with a stepper motor to accurately deploy the monofilament through the hole until it contacted the human skin at the prescribed force (RB-Phi-203 100g Micro Load Cell). Arduino

microcontrollers (Arduino Uno and Arduino Mega) were used to interface between the machine and a MATLAB script that controlled the device. The script took the force data from the automated device and interpreted it for threshold sensitivity analysis. Furthermore, the device featured a camera (Logitech BRIO) which was used to take a photograph of the subject's foot, which was used to select testing locations. The photograph also documented the results of the test at the end of the assessment, by creating a visual representation of the subject's threshold sensitivity at each location. Figure 4-3 illustrates an example threshold sensitivity map of a subject's foot evaluated using the automated tool. The automated tool applied the SWM at a range of forces: 0.35, 0.70, 2.0, 4.0, 6.0, 8.0, and 10.0 gF using a homing sequence illustrated in Figure 4-4. These values are consistent in neuropathy assessments, often with the use of individually calibrated SWMs [29]. This homing sequence allowed for the threshold sensitivity, or the subject's minimum amount of contact force sensation, at that location to be assessed as quickly as possible without having to apply the SWM all seven times. Similar to the hand-applied tool, the same 13 locations per foot were assessed. However, when using the automated tool, the locations were subdivided into three testing regions: the toes (n=5), the ball (n=5), and the heel (n=3) (Figure 4-1). Moreover, locations were randomized within each region, resulting in neither the subjects nor the clinician knowing the testing order of locations within regions. The automated device also featured a blinking push button for the subjects to catalogue an affirmative response to the prescribed force. They were instructed, before the assessment, that they must press and hold the pushbutton for one second to confirm that they felt the stimulus. A five second window was provided for the subjects to press the pushbutton. Not depressing the button designated a negative response to the subject sensing the monofilament. False positive checks were also a part of the assessment protocol with the automated device; each location

having a 10% chance of occurrence. During a false positive check, the SWM did not contact the subject's skin, but it still queried them via the pushbutton. Each foot was assessed one at a time and at the conclusion of the evaluation the data were saved in a MATLAB workspace. The collected data were used to create a threshold sensitivity map for both feet, providing the results of the automated assessment.

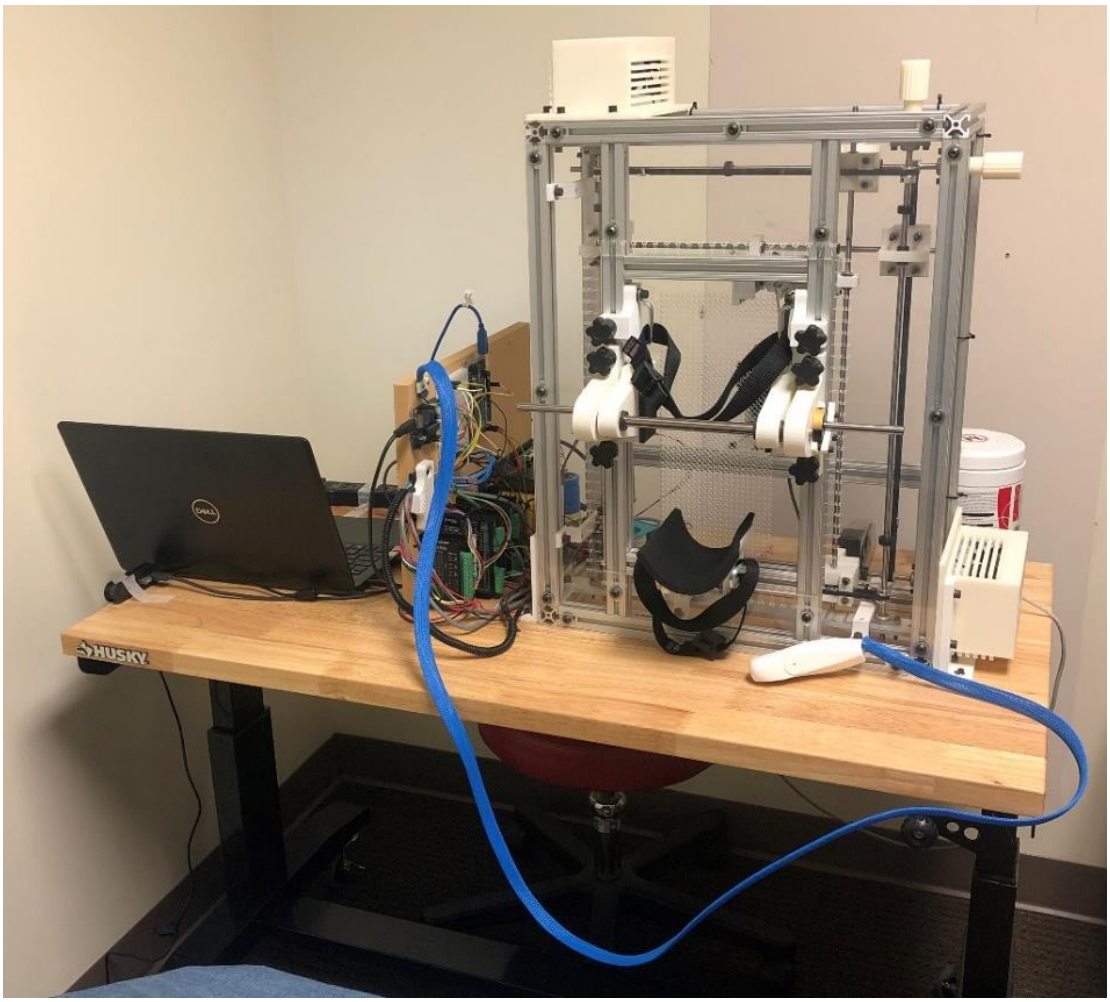

Figure 4-2: Automated Tool Experimental Device Onsight at IMA

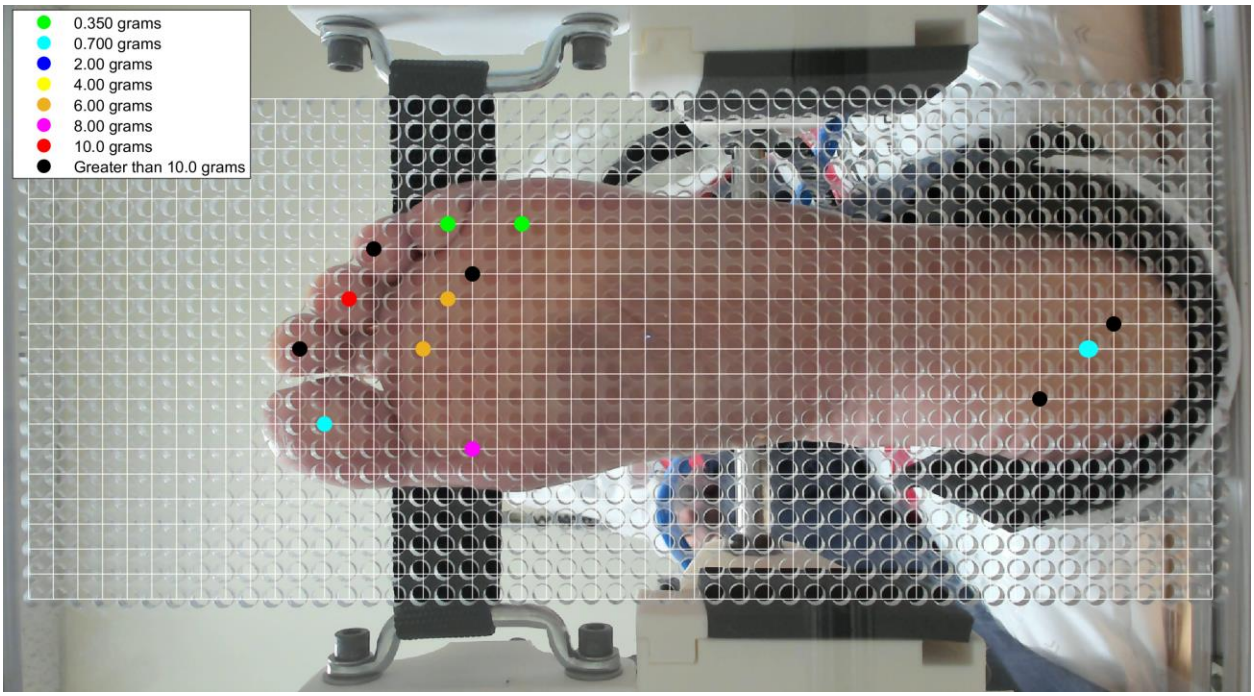

Figure 4-3: Threshold Sensitivity Map as seen in MATLAB Script Interface

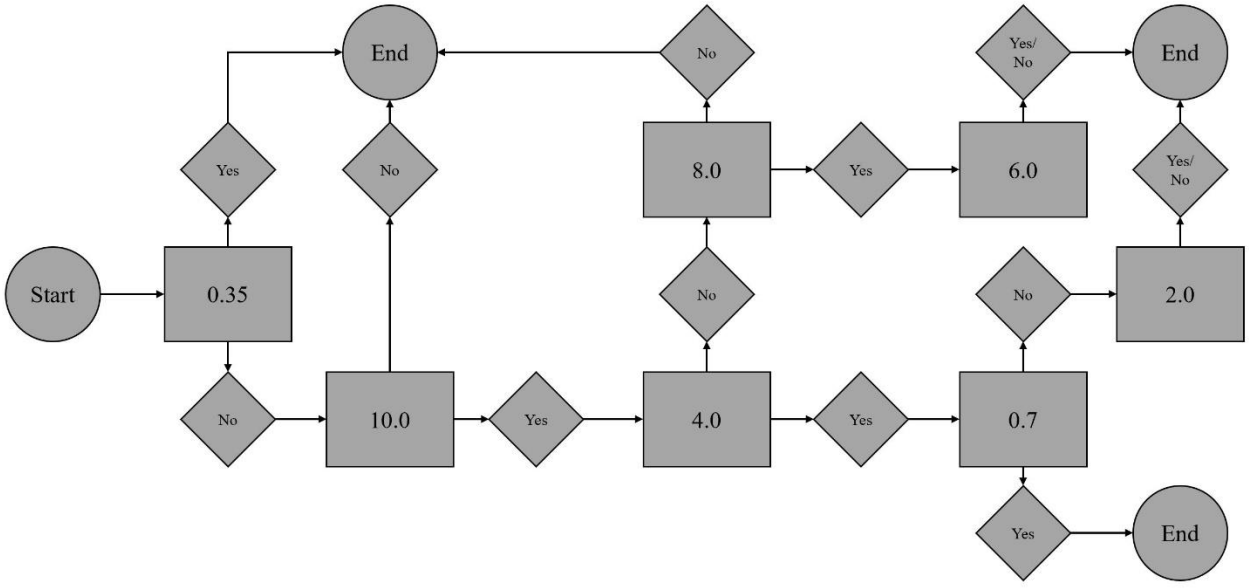

Figure 4-4: Automated Tool Homing Sequence Protocol for Threshold Sensitivity Determination

4.3.5. Accuracy Analysis Overview

Analysis was first conducted on the device accuracy, which compared the prescribed force, or the value that the device intended to deliver, to the actual amount of force applied to the skin measured by the load cell. This was carried out for all locations at all force levels by calculating the absolute error (Equation 4-1). An average absolute error was calculated for each location and at all prescribed force levels.

$$Absolute\ Error = |Actual\ Force - Prescribed\ Force| \quad \text{Eq. 4-1}$$

4.3.6. Automated Tool Data Analysis Procedures

During the study, it was discovered that a number of the subjects were pressing their foot firmly against the perforated foot plate, this likely resulted in the subject's elasticity of their plantar surface being reduced. This occurrence created inaccuracies of the device, especially at the lower prescribed forces, such as 0.35 and 0.70 gF. The load cell was not capable of processing the contact force data quickly enough to stop the advancement of the monofilament at the exact moment it reached the prescribed force. This was most apparent when the plantar surface's elasticity was reduced. This discovery led to an exclusion protocol to filter out such locations. If the actual force applied was greater than or equal to 2.0 gF above the prescribed force, then it was classed as a "device error". The two exceptions were 0.35 gF and 0.70 gF, which needed to be less than 0.70 gF and 2.0 gF, respectively, to be acceptable for analysis. Device errors meant the exclusion of data when determining the absolute error, however it did not necessarily indicate an inability of the subject's threshold sensitivity to be established at that location. Depending on the subject's responses to multiple applications of the SWM it was still possible to determine

their threshold sensitivity. Device errors impacted false positive checks, as subjects were warping the foot plate just enough to induce accidental contact.

After excluding the device errors, the threshold sensitivity at each location was determined and grouped into their respective force classifications: 0.35, 0.70, 2.0, 4.0, 6.0, 8.0, 10.0, and >10.0 gF. However, if there were not enough accurate monofilament applications of the device available to establish the threshold sensitivity, then the location was categorized as "indeterminate". Another type of "indeterminate" case was if the camera on the back of the machine was misaligned, resulting in the SWM not being applied at the correct location. MATLAB commands were used to adjust the photograph, but if it was determined that the SWM did not make contact at the correct location, due to the camera misalignment, this location was removed from the analysis.

4.3.7. Threshold Sensitivity Index Calculations

Once the threshold sensitivity of all locations was determined, a threshold sensitivity index (TSI) was calculated for each region (Equation 4-2). First, the threshold sensitivity values at each location were assigned a score based on the value they represented, ranging from one to eight (0.35 gF=1, 0.70 gF=2, 2.0 gF=3, 4.0 gF=4, 6.0 gF=5, 8.0 gF=6, 10.0 gF=7, and >10.0 gF=8). The TSI was then calculated by taking the average of all locations that did not include indeterminate data within the respective region. TSI values range from one to eight, with one representing a region that was the most sensitive to the SWM, while a value of eight represented a region that was numb to the SWM. A subject with two toes with a threshold of 0.3 gF, one toes with a threshold of 0.7 gF, and two toes with a threshold of 2.0 gF would have a TSI equal to 2.0, which signifies a region that is overall sensitive to the monofilament. A TSI Norm was then

evaluated using all three regions on both feet of the human subject (Equation 4-3). Calculated TSI and TSI Norm are unitless measurements since they are derived from a score-based average.

$$TSI = \frac{\#0.35(1) + \#0.70(2) + \#2.0(3) + \#4.0(4) + \#6.0(5) + \#8.0(6) + \#10.0(7) + \# > 10.0(8)}{\#\ Locations - \#\ Indeterminate\ Locations} \quad \text{Eq. 4-2}$$

$$TSI\ Norm = \sqrt{TSI_{R.Toe}{}^2 + TSI_{L.Toe}{}^2 + TSI_{R.Ball}{}^2 + TSI_{L.Ball}{}^2 + TSI_{R.Heel}{}^2 + TSI_{L.Heel}{}^2} \quad \text{Eq. 4-3}$$

4.3.8. Analysis Approaches and Linear Regression Analysis

The average absolute error for each location, at all prescribed force values, was first determined. The results were plotted on a histogram, which was subdivided based on the assessment regions. Results were categorized based on the frequency of locations that were the most closely related, such as the percentage of locations that were within an absolute error of 0.2 gF, 0.4 gF, and 0.6 gF. The results of these calculations did not include applications of the monofilament using the automated tool that resulted in a device error.

Furthermore, the breakdown of the threshold sensitivity at each location, grouped by region was also examined. This also used a histogram to uncover trends on how the threshold sensitivities were impacted by location and region. Percentages were calculated where the number of locations were less than a threshold sensitivity of 4.0 gF, between a threshold sensitivity of 4.0 and 10.0 gF, and where the threshold sensitivity was greater than 10.0 gF. These percentages were calculated per region.

Another analysis performed was the comparison of the results collected using the hand-applied SWM and the automated device. This was achieved by calculating the percentages where the tools performed identically and differently at each location. The potential of underdiagnosing sensitivity loss at 10.0 gF was examined by calculating the percentages in which the subjects indicated that they felt a stimulus with the hand-applied SWM but did not feel the stimulus applied by the automated tool. Also, the total number of false positive checks in the population was determined. False positive check responses were then grouped based on if subjects triggered a false positive, they did not trigger a false positive, or if a device error occurred. Percentages were calculated to disseminate these findings.

Lastly, the subject's data were analyzed using a linear regression analysis, which was performed between the subject's TSI Norm and their age, ABI, BMI, FBS, and HbA1c. R^2 and *P*-values were calculated using Microsoft Excel's regression analysis tool to infer the relationships between TSI Norms and the previously mentioned medical values. A *P*-value less than or equal to 0.05 was the criteria to be a significant standardized regression coefficient. However, in order to account for the presence of multiple indeterminate locations in the calculation of TSI Norm values, it was decided that subjects had to have at least four out of five toes, four out of five ball, and two out of three heel locations of data available on each foot to be used in the linear regression analysis.

4.4. Results

4.4.1. Automated Device Performance Results

The performance of the automated device was first analyzed. Figure 4-5 depicts the average absolute error for each location, subdivided by the prescribed force classification. The toe region

had the most accurate measurements using the device, with 81% of the locations at the seven force classifications having an average absolute error of less than or equal to 0.2 gF. Likewise, 17% of the toe locations were between an average absolute error of 0.2 gF and 0.4 gF. The remaining locations have an average absolute error less than 0.5 gF. The ball region had 34% of locations that where less than or equal to an average absolute error of 0.2 gF. Meanwhile an additional 50% had an average absolute error between 0.2 gF and 0.4 gF and 11% were between 0.4 gF and 0.6 gF. The remaining locations in the ball region where between 0.6 gF and 1.2 gF. Analysis of the heel region found that 12% of locations had an average absolute error less than or equal to 0.2 gF and an additional 48% between 0.2 and 0.4 gF. Also 36% of locations had an average absolute error between 0.4 gF and 0.6 gF; the remainder of locations were between 0.6 gF and 1.0 gF. Moreover, the maximum average absolute errors were 0.5, 1.2, and 0.9 grams of force at the toe, ball, and heel locations, respectively.

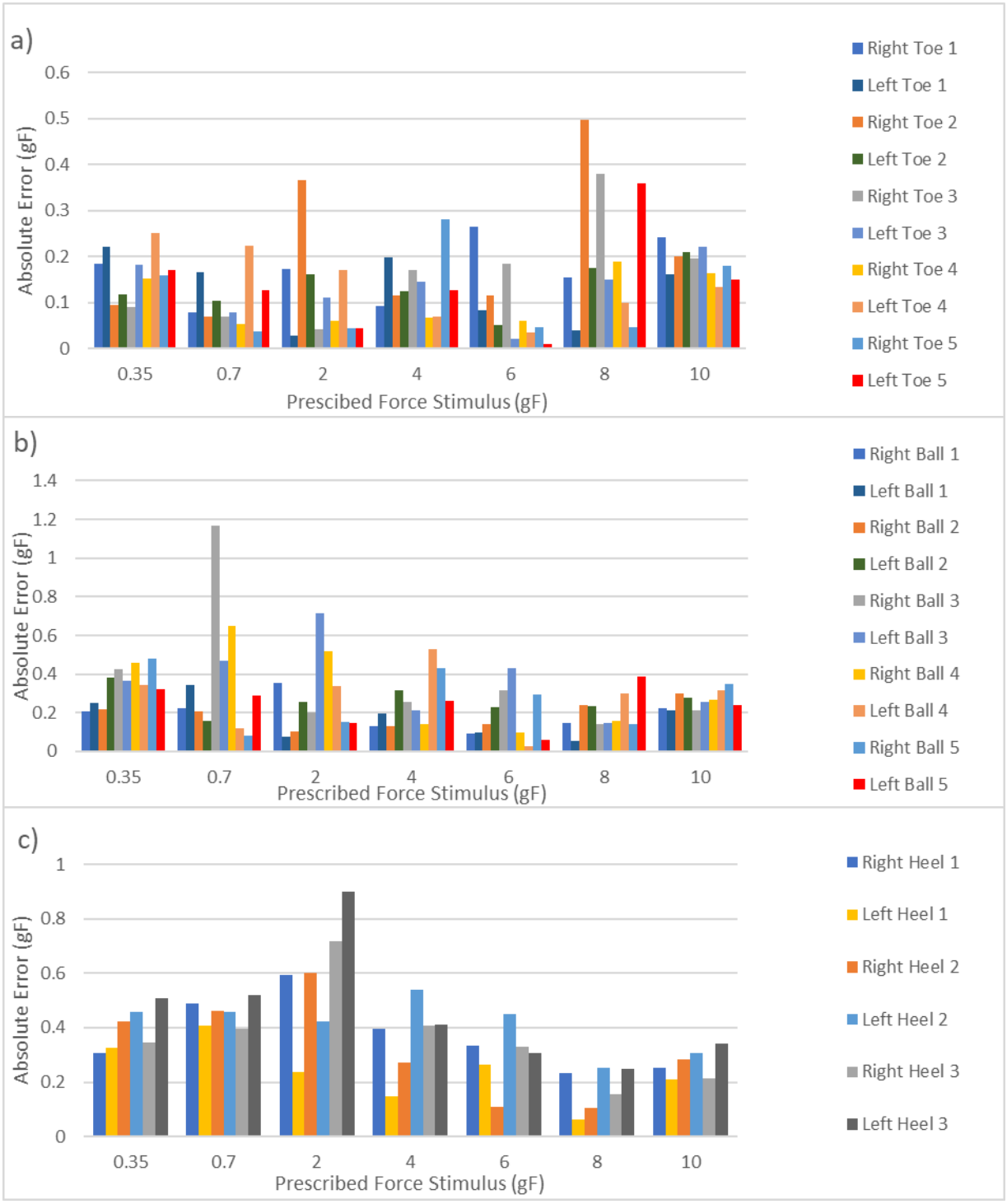

Figure 4-5: Diagnostic Tool Performance Results Categorized by Region

a) Toe Region Absolute Error
b) Ball Region Absolute Error
c) Heel Region Absolute Error

4.4.2. Automated Device Threshold Sensitivity Results

The threshold sensitivities at each location were cataloged, demonstrating the differences between the respective regions. Figure 4-6 presents these data, grouped by the force categories and subdivided by location. The toes showed the greatest sensitivity to the monofilament, with the least number of indeterminate locations. The toe data showed 63% of the locations having sensitivity less than 4.0 gF, 14% of the locations having a sensitivity between 4.0 and 10.0 gF, 15% of the locations having no sensitivity when evaluated at 10.0 gF, and 8% of the locations where the data were indeterminate. The heel results revealed the second most sensitive locations out of the complete dataset. The heel data had 38% of the locations having a sensitivity under 4.0 gF. In addition, the heel had 21% of the locations having a sensitivity between 4.0 and 10.0 gF and 35% of the locations having no sensitivity when applied at 10.0 gF. The amount of indeterminate data at the heel was only 6%. The ball region presented the most indeterminate locations, with 41% of the locations, and furthermore the least amount of sensitivity. Moreover, the ball region only had 21% of the locations having a sensitivity less than 4.0 gF, 18% of the locations with a sensitivity between 4.0 and 10.0 gF, and 20% of the locations being insensitive to a prescribed force of 10.0 gF.

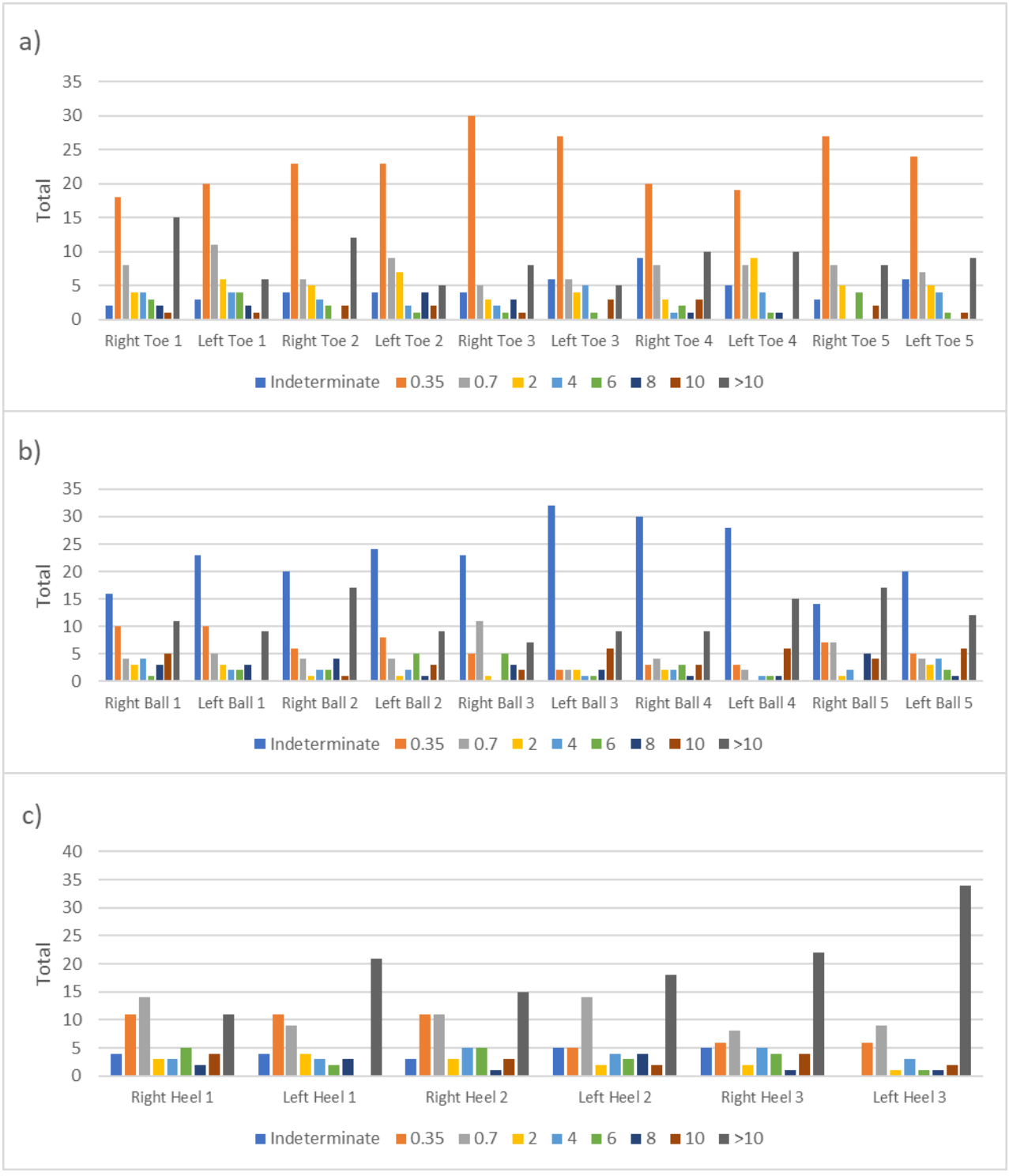

Figure 4-6: Diagnostic Tool Threshold Sensation Results Categorized by Region

a) Toe Region Results
b) Ball Region Results
c) Heel Region Results

4.4.3. Hand-Applied Semmes-Weinstein Monofilament and Automated Device Comparison

When comparing the hand-applied SWM to the machine, excluding indeterminate locations, it was observed that 64.1% of the locations had a threshold sensitivity less than 10.0 gF. The percentage of locations where the subject's threshold sensitivity was determined to be at the 10.0 gF category using the automated tool, and where they also felt the hand-applied SWM was 4.6%. The percentage of locations where the threshold sensitivity determined by the machine was greater than 10.0 gF and where the subjects could not feel the hand-applied SWM was 5.6%. Furthermore, 4.8% of locations were not sensitive to the hand-applied SWM but were to the stimulus applied by the machine. Lastly, the percentage where participants could feel the hand-applied SWM but not the machine at a contact force of 10.0 gF was 20.9%, which can be considered as the underdiagnosis rate of the hand-applied monofilament when compared to the automated tool.

4.4.4. False Positive Results

It was discovered that out of all testing locations, 10.8 % included a false positive assessment (n=160). Out of the total number of false positive checks, 57.5% of them were answered correctly by the subject, meaning they stated that they did not indicate that they felt a stimulus. 13.8% of the subjects stated that they felt the false positive check, while the remaining 28.8% of false positive checks were device errors, where a stimulus was inadvertently applied. On average each participant had 2.8 false positives per assessment, and only three individuals indicated that they felt more than two false positives.

4.4.5. TSI Norm and Medical Data Outcomes

After accounting for the prevalence of indeterminate locations, it was then possible to compare TSI Norm values to age, BMI, ABI, FBS, and HbA1c. There were 22 out of the 57 subjects who had data at four out of five toes, four out of five locations on the ball of the foot, and two out of three locations on the heel, per foot. Figure 4-7a shows the relationship between age and TSI Norm. As age increased, sensitivity decreased at a linear rate and was significant (R^2=0.34, P=0.004). The relationship between TSI Norm, BMI, and ABI, were also analyzed, but both showed non-significant relationships (Figure 4-7b and 4-7c). Next, the parallels between FBS and TSI Norm was analyzed; however, out of the 22 subjects, only 21 had data for FBS readings in their medical chart. Regardless, a linear relationship was discovered between these variables, however the result was approaching significance at the 0.05 level, Figure 4-8a (R^2=0.18, P=0.054). Lastly, the HbA1c levels were compared to TSI Norm; however, only 7 subjects had these data available in their medical profile. Although this was not enough data to make statistical claims it was still included in this study to encourage future research to examine this relationship further. Figure 4-8b shows a linear relationship between HbA1c and TSI Norm, but was also not significant (R^2= 0.41, P=0.12).

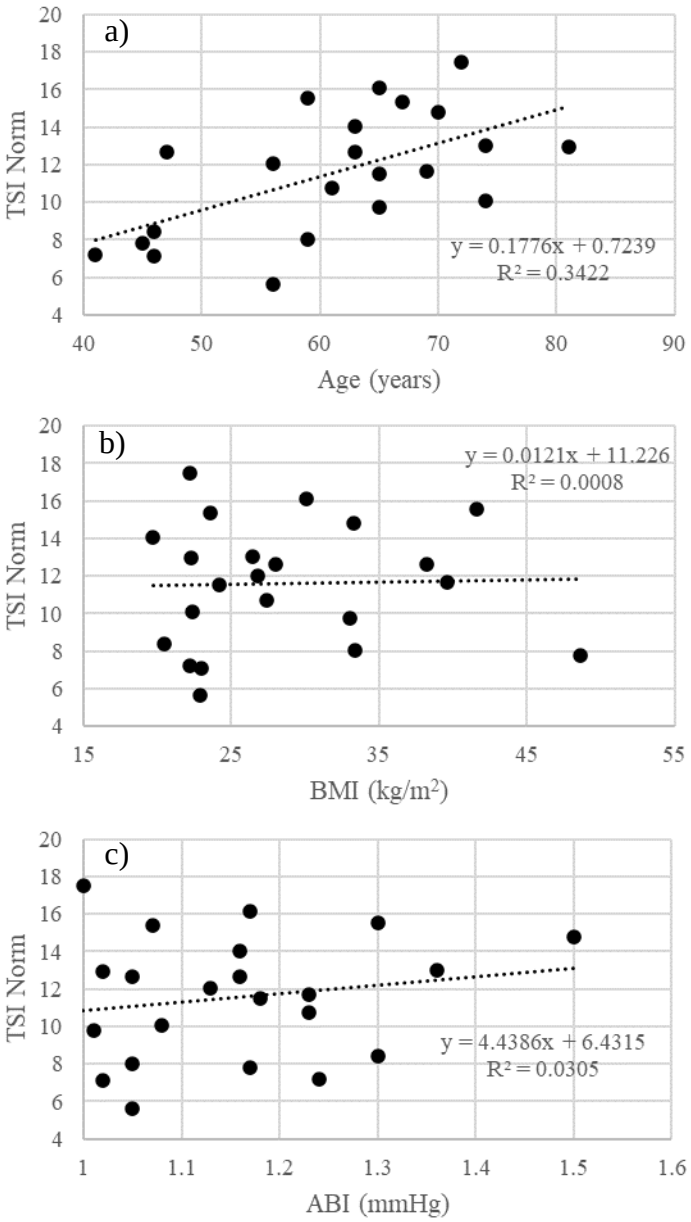

Figure 4-7: Linear Regression Analysis: TSI Norm Compared to Age, BMI, and ABI

a) TSI Norm vs Age (R^2=0.3422, P=0.004) (Age: Mean ± Standard Deviation= 61.9±10.8 years)
b) TSI Norm vs BMI (R^2=0.0008, P=0.90) (BMI: Mean ± Standard Deviation= 28.6±7.78 kg/m^2)
c) TSI Norm vs ABI (R^2=0.0305, P=0.44) (ABI: Mean ± Standard Deviation= 1.16±0.13 mmHg)

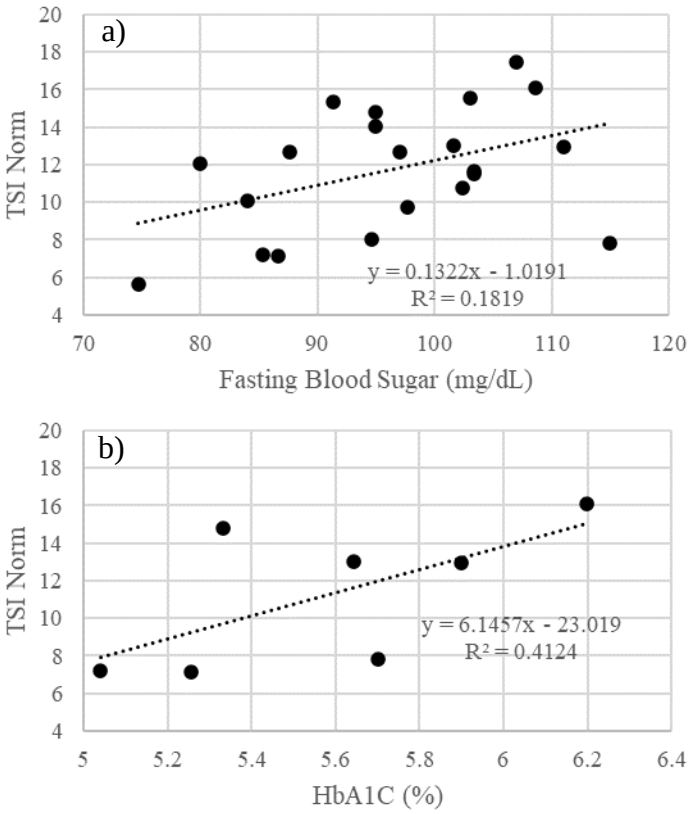

Figure 4-8: Linear Regression Analysis: TSI Norm Compared to FBS and HbA1c

a) TSI Norm vs FBS (R2=0.1819, P=0.054) (FBS: Mean ± Standard Deviation= 96.4±10.6 mg/dL)
b) TSI Norm vs HbA1c (R2=0.4124, P=0.12) (HbA1c: Mean ± Standard Deviation= 5.6±0.4 %) (TSI Norm: Mean ± Standard Deviation= 11.6±3.28)

4.5. Discussion

The device accuracy of the machine demonstrated an average absolute error less than or equal to 0.4 gF at 98%, 84%, and 60% of the locations, at the toe, ball, and heel regions, respectively. The toe region performed the best, potentially because the toes are more elastic than the ball of the foot. Overall, these results are an improvement over hand-applied monofilaments which typically are within a 1.0 to 3.0 grams of force absolute error when evaluated at 10.0 grams of force (10-30% error). These observations are identified in the studies of Lavery et al., Spruce and Bowling, as well as Chikai and Ino [54, 69, 74]. Lavery et al. found that hand-applied monofilaments would consistently underproduce the 10.0 grams of force after the first application of the

corresponding monofilament, whereas Spruce and Bowling found that hand-applied monofilaments overproduce, both had extremes upwards of 3.0 grams of force [69, 74]. Table 4-1 presents these previous studies outcomes, as well as the claimed accuracy results of some automated tools from other inventors, which had accuracy between 0.3 and 1.0 grams of force of absolute error when evaluated at the 10.0 grams of force category (3-10% error). The automated tool presented in this dissertation has an average absolute error between 0.15 and 0.35 grams of force when applied at 10.0 grams of force (1.5-3.5% error). Both the overall average absolute error and the specific results analyzed at the 10.0 grams of force category are within the initial design requirements of the automated tool presented in Chapter 3. The automated tool is not only an improvement over hand-applied monofilaments in terms of average absolute error, but is comparable to the automated tools of Siddiqui, Spruce and Bowling, and Chikai and Ino. However, one of the biggest distinctions between the automated tool presented in this dissertation and the others listed in Table 4-1 is the use of the force feedback loop, used to simultaneously measure the contact force while it is being applied. The accuracy of Lavery et al., as well as Chikai and Ino, were not based on actual human skin, and were measured using weight scales. Siddiqui et al.'s study does not state how they obtained their accuracy figure, while Spruce and Bowling used a rubber target to measure their device's accuracy. All accuracy data presented in this dissertation was calculated from each subject's skin.

Study	Type of Monofilament Assessment(s)	Notes	Accuracy
Lavery et al. [74]	Hand-Applied Tool	Examined six different brands of commercial hand-applied monofilaments	10.0 ± 1.0 gF -some can vary as much as 30%
Siddiqui et al. [67]	Automated Tool		98 mN (10.0 gF) ± 1%
Spruce and Bowling [69]	Hand-Applied and Semi-Automated Tools	Semi-Automated tool was still applied by hand until a sensor indicated targeted force was achieved 20 subjects used both tools	Hand-applied: 10.7 gF -one subject applied a 13 gF load Automated Tool: 10.5 gF
Chikai and Ino [54]	Hand-Applied and Automated Tool	Automated tool was applied at 1, 5, and 10 mm/s impact velocities	Hand-applied: 7.4 ± 0.5 gF Automated Tool (1mm/s): 9.5 ± 0.3 gF Automated Tool (5 mm/s): 9.9 ± 0.3 gF Automated Tool (10 mm/s): 10.3 ± 0.4 gF

Table 4-1: 10.0 gF Hand-Applied Monofilament and Automated Device Accuracy Comparisons from Previous Studies

The majority of device errors occurred in the ball region. It is likely that this was because subjects were inadvertently pressing too hard up against the foot plate, resulting in their ball region being artificially less elastic. The device actuated the monofilament until it reached the prescribed force. However, if the location was too rigid then it was likely unable to stop at the precise moment when the prescribed force was reached. The presence of calluses and dry skin are not only contributing factors that can influence the accuracy of the hand-applied monofilament, but also that of the device, leading to device errors. In the current iteration of the code used to control the machine, there was not a safeguard to reevaluate a location in which the monofilament was mistakenly applied at too great a force.

Currently, the medical professional operating the device cannot see the actual force applied until the end of the assessment. In order to address this in future studies the code should give the medical staff insight into the amount of force immediately after it has been applied. This would allow them to instruct the subject to adjust their foot before a remeasurement is taken. Increasing the data acquisition rate of the device's force measurement sensor and or slowing down the insertion rate of the monofilament are other techniques which may improve device performance. Currently the device will measure the load as it is being applied and will slow down incrementally until the desired force is achieved.

Additionally, it was observed that the toes were much more sensitive than the locations in the other regions, with 63% of locations having threshold sensitivities under 4.0 gF. In the heel region locations were either very sensitive or they had no sensitivity at all. It is possible that some subject's ability to sense the SWM was due to the degree of callus on the surface of the foot. Not only can calluses result in device errors in the machine, but they can impact sensitivity. The machine was able to detect threshold sensitivities less than 10.0 gF at approximately 64% of the locations. However, only approximately 5% of subjects had a sensitivity of less than 10.0 gF if they had also indicated that they did not feel a stimulus with the hand-applied SWM. One of the most substantial conclusions drawn was that the hand-applied SWM were underdiagnosing at a rate of 21% of the locations, relative to the automated tool, meaning that the subject's threshold sensitivity was greater than 10.0 gF at specific locations. However, it is possible that at threshold sensitivities below 10.0 gF, hand-applied monofilaments may have underdiagnosed less often when compared to the automated tool. It was determined that if the subject did not feel the hand-applied tool, they most likely did not feel any stimulus provided by the machine at approximately

6% of the locations. Also 5% of the locations assessed using the machine had a threshold sensitivity, but were reported to be insensitive using the hand-applied monofilament. Future work is recommended to compare how various machine operators impact the reliability of the hand-applied SWM, as it related to these percentages.

Examining the effects of age, BMI, ABI, FBS, and HbA1c revealed that the strongest relationship to sensitivity loss was the age of the subject, which was also found to be significant (P=0.004). This was especially noteworthy as the subjects in the control group did not have diagnosed DM2. Tremblay et al. found a similar relationship between threshold sensitivity to age when evaluated at the right index finger [104]. This relationship was also reported by Wickremaratchi and Llewelyn in their review on how touch perception is influenced by aging [105]. It was also described that sensation loss associated to aging affects 26% of individuals between the ages of 65 and 74, and 54% of those 85 and older [106]. FBS was the second strongest dependence on sensation loss, with its P-value of 0.054 approaching significance. BMI and ABI showed no obvious relationship in this study. Yümin et al. showed that as age and BMI increased, plantar sensation decreases in a female population of individuals without diabetes [107]. HbA1c was not a significant variable in explaining threshold sensitivity. Other studies have examined HbA1c as a biomarker for neuropathy but with mixed results from different studies, which further motivates the study of this biomarker to sensation loss [108]. Furthermore, this study should be repeated on DM2 populations with and without neuropathy symptoms in order to examine how these trends may change. Comparing data from a control population to DM2 populations is presented in Chapter 5 of this dissertation.

4.6. Conclusions

This study sought to examine the performance of an automatic tool for plantar threshold sensitivity, as well as the clinical results of this device used on a control group without DM2. It was determined that the machine had high accuracy, despite occasional problems with the foot being placed too firmly against the device's surface. This shortcoming can be addressed by improving the software of the device to allow for the reassessment of locations which cannot be evaluated due to excessive pressure caused by the subject's foot pressing firmly against the foot plate. The device showed that approximately 64% of the testing locations had a threshold sensitivity less than 10.0 gF. It was also determined that the hand-applied SWM underdiagnosed approximately 21% of the testing locations in the control group of having a threshold sensitivity category of 10.0 gF when compared to the automated tool. The formulation of a TSI Norm was demonstrated as an effective way of characterizing an individual's threshold sensation as an allocation of multiple locations per foot. TSI Norm was shown to be dependent of age and FBS, while independent of BMI and ABI. However, age showed the strongest significance to TSI Norm, while FBS was not significant with respect to TSI Norm. Future work is suggested to draw a relationship between TSI Norm and HbA1c. Finally, future investigations are recommended to not only strengthen the findings in this study, but to analyze these relationships in a population with DM2, which is the subject of Chapter 5 of this dissertation.

Chapter 5: Plantar Threshold Sensitivity Assessment Using an Automated Tool – Clinical Assessment Comparison Between a Control Population without Type 2 Diabetes Mellitus, and Populations with Type 2 Diabetes Mellitus, with and without Neuropathy Symptoms

5.1. Abstract

Aims: This study's first aim was to quantify and compare sensation on the plantar surface in healthy and Type 2 diabetes mellitus (DM2) populations with the standard Semmes-Weinstein hand-applied methodology and a tool that automates this approach. The second was to evaluate correlations between sensation and the subjects' medical characteristics.

Methods: Sensation was quantified by both tools, at thirteen locations per foot, in three populations: Group 1-Controls without DM2, Group 2-DM2s with neuropathy symptoms, and Group 3-DM2s without neuropathy symptoms. The percentage of locations sensitive to the hand-applied monofilament, yet insensitive to the automated tool was calculated. Linear regression analyses between sensation and the subject's age, BMI, ABI, fasting blood sugar, and HbA1c was performed per group. ANOVAs determined differences between populations.

Results: Approximately 22.5% of locations assessed were sensitive to the hand-applied monofilament, yet insensitive to the automated tool. Age and sensation were only significantly correlated in Group 1 (R^2=0.3422, P=0.004). Sensation was not significantly correlated with the other medical characteristics per group. Differences in sensation between the groups were not significant (P=0.063).

Conclusions: Attention to application technique is recommended when using hand-applied monofilaments. Group 1's sensation was correlated to age. The other medical characteristics failed to correlate to sensation, despite group.

5.2. Introduction

Forty to sixty million people with diabetes experience complications due to diabetic neuropathy, otherwise known as diabetic foot, globally [5]. Sensation loss in the extremities, such as the plantar and palmar surfaces, is often a complication attributed to those who have neuropathy [4, 34]. Burning of the feet is the most common symptom linked to diabetic peripheral neuropathy (DPN), in addition to antalgic gait, and tingling [26, 28, 79]. Other symptoms range from insensitivity to temperature and accidental foot trauma, which can lead to infection, ulceration, and amputations [22, 38, 109]. Painful symptoms like burning, pins and needles, and even the sensation of electrical shock are prevalent in those who have neuropathy caused by diabetes, with nighttime being the time when symptoms are at their peak [20, 47]. Aslam, Singh, and Rajbhandari have reported that hyperglycemia could be a factor attributed to painful symptoms, but other sources could be involved, such as damage to the nerves [20]. Bril reported that glycemic control is not a strong indicator for the development of diabetic neuropathy in persons with Type 2 diabetes mellitus (DM2), citing evidence that body mass index, high blood pressure, and even smoking could be additional factors [22]. In Yorek et al.'s review they reported that although glycemic control slowed down the progression of DPN in individuals with Type 1 diabetes, it did not in individuals with DM2 [21]. Noteworthy is that aging has been linked to the loss of sensation perception and affects 26% of individuals 65-74 years old and 54% of individuals 85 years of age and older [105, 106].

Semmes-Weinstein monofilaments (SWM) are the most common method used to assess for sensation loss due to being inexpensive, fast, and noninvasive [9, 52]. Developed by Semmes and Weinstein to replace the use of horsehair, these nylon monofilaments were used to assess for

sensation loss on the palmer surfaces in subjects with brain injuries [50, 51, 52]. Monofilaments are applied normal to the surface of the skin until they buckle at which time they produce a constant force, the most common of which are calibrated to produce 10.0 gF [52, 54, 110]. There is a lack of consistent methodology with monofilament assessment for neuropathy, which can factor into the diagnosis of DPN [66]. In addition to a lack of consistency, the accuracy of the assessment is also affected by fatigue, angle and rate of insertion, application technique, and even the elasticity of the subject's skin [54, 76, 111].

Novel devices and techniques have been suggested to better measure degree of sensation loss, including a laser plantar pressure sensor, a rapid current threshold detection device (Neurometer®), and measuring an individual's oxygen level in their skin [10, 61, 112]. The work of Wilasrusmee et al. created a robot to apply a SWM at 10.0 grams of force (gF) to the plantar surface which agreed well with hand-applied monofilament and vibratory assessments [66]. Similarly, Siddiqui et. al developed a robot which scanned the plantar surface through a clear medium with perforated holes, through which the device could apply a monofilament at 10.0 gF [67]. Spruce and Bowling developed a handheld electronic force sensor to mimic a typical monofilament; used an indicator light to tell the clinician when 10.0 gF had been applied upon contact [69]. This device not only had improved repeatability compared to the normal monofilament but increased resistance to fatigue [69].

This study used an automated tool, similar to the robotic instruments previously mentioned, to determine a subject's plantar surface threshold sensitivity at several locations. The tool presented in this study can apply a variety of contact forces, consistent with SWM assessments, using a

single monofilament, allowing for the mapping and documentation of the results per location. Therefore, the first aim of this study was to perform a comparison of the automated tool's findings with a standard hand-applied 10.0 gF monofilament. The second aim of this study was to compare threshold sensitivity to age, body mass index (BMI), ankle brachial index (ABI), fasting blood sugar (FBS), and HbA1c in three populations: a control group without DM2, a DM2 group with neuropathy symptoms, and a DM2 group without neuropathy symptoms. Studying how these demographics and medical characteristics relate to threshold sensitivity will reveal insights into how the presence of DM2 is related to an individual's degree of sensation loss.

5.3. Subjects, Materials, and Methods

5.3.1. Populations and Exclusion Criteria

Volunteers were recruited in the Auburn-Opelika Alabama area. The study was conducted at Internal Medicine Associates (IMA) in Opelika, Alabama and the study was given IRB approval from the Edward Via College of Osteopathic Medicine (VCOM-Auburn, USA), under record number 2020-004. All participants were required to have an ABI greater than or equal to 1.0 mmHg and had to be age forty or older. Four subjects failed the ABI screen and were excluded from the study. It should also be noted that none of the subjects had ulcers or a history of amputations on the plantar surface. Human subjects that passed the screening were categorized into three populations: Group 1. A control group without DM2 (n=57, male=29, female=28), Group 2. A DM2 group with neuropathy symptoms (n=58, male=35, female=23), and Group 3. A DM2 group without neuropathy symptoms (n=38, male=15, female=23).

5.3.2. Medical Chart Review and ABI Assessment

The subjects having given their written consent to being a part of this study, were asked if they had DM2 and if so whether they had symptoms associated with neuropathy. Their responses then placed them into the appropriate group (1, 2, or 3). The medical profiles for each subject at IMA were reviewed for their age, BMI, FBS levels, and HbA1c levels and the data were recorded on a subject datasheet. The ABI for each subject was calculated and documented on their datasheet. If the subject's ABI was less than 1.0 mmHg, they would be dismissed from the study and would not be evaluated any further. Furthermore, FBS and HbA1c would both be averaged with up to the three most current readings. These average values were used for the analysis in this report. In Group 1, three individuals did not have FBS levels documented in their charts, while 27 individuals did not have HbA1c levels documented. However, these Group 1 subjects were still included in this study.

5.3.3. Hand-Applied Monofilament Assessment

After collecting the subject's required medical data from chart review and measuring their ABI, a hand-applied monofilament was used to assess for sensitivity on the plantar surfaces. The subject laid on the exam table, with their head elevated, and their feet were stretched out in front of them. Their calves were supported by the exam table, while their feet hung off the edge of the table with their toes pointing upward. A 10.0 gF hand-applied SWM was used to evaluate for sensitivity at 26 locations, 13 locations per foot (Figure 5-1). The locations included the five toes (distal phalanges), five on the ball (distal metatarsals), and three on the heel (calcaneus). The monofilament was applied normal to each testing location by the clinician until it buckled. Subjects indicated whether or not they felt the hand-applied stimulus per location, which was then documented in their datasheet by the clinician. When using the hand-applied monofilament,

the locations were assessed anterior to posterior, starting with the great toe. Following the great toe, the first distal metatarsal and then the first heel location were evaluated. This anterior to posterior procedure was performed at all five distal phalanges, five distal metatarsals, and three locations on the heel per foot.

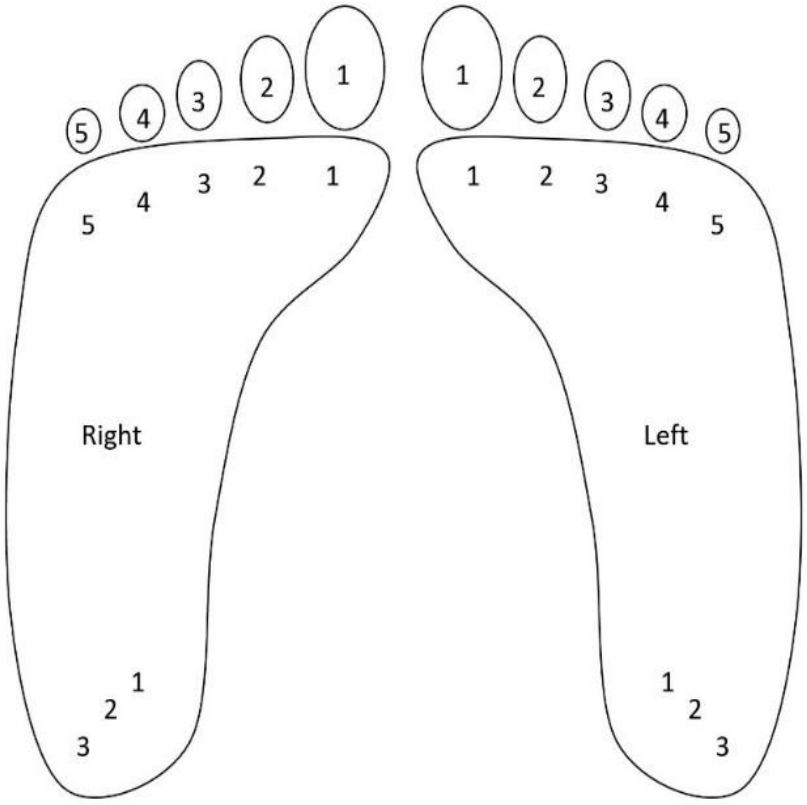

Figure 5-1: Plantar Surface Assessment Locations

Thirteen locations per foot were evaluated with both a hand-applied monofilament and the automated tool.

5.3.4. Automated Tool Assessment

Following the hand-applied monofilament evaluation, an automated diagnostic tool (Figure 5-2a) was used on the same 13 locations, one foot at a time. The diagnostic tool used a 10.0 gF rated monofilament which was mounted to a load cell feedback loop with a stepper motor. The stepper motor continues to actuate the monofilament against the skin until the load cell (RB-Phi-203 100g

Micro Load Cell) measured the prescribed force. A homing sequence (Figure 5-2b) was used to determine the individual's threshold sensitivity at each location using the following forces: 0.35, 0.70, 2.0, 4.0, 6.0, 8.0, and 10.0 gF, which are typical in monofilament assessments [29]. The subject sat on the exam table, with their back tilted against the backrest, while their calves were supported by the exam table. The subject's foot was placed against a perforated foot plate made from clear acrylic, with 1,029 holes. Their foot was secured in place with straps over the toes and over the ankle, with their toes pointing straight upward. After the subject's foot was secured in place a camera (Logitech Brio) mounted behind the device was used to take a photograph, which was then used in a MATLAB (MATLAB R2018a) script to allow the clinician to select testing locations for evaluation. Testing locations were grouped by three regions in the automated tool assessment: toe region, ball region, and heel region. The MATLAB script included randomization within regions. Furthermore, the MATLAB script communicated with Arduino microcontrollers (Arduino Uno and Arduino Mega) which controlled belts and pulleys used to translate the monofilament to each testing location. Once the monofilament was at the desired location it was actuated through the hole of the perforated foot plate until it contacted the skin at the prescribed force. After the monofilament was applied, subjects used a LED pushbutton to indicate their response to sensing the applied stimulus. Each time a stimulus was applied the LED pushbutton would start to blink, during which time the subject depressed the pushbutton for one second, only if they felt the prescribed force. Subjects were given five seconds to catalogue their response. Also, false positive assessments were randomly incorporated into the automated tool evaluation, with each of the thirteen locations per foot having a 10% chance of occurrence. During a false positive check, the automated tool actuated the monofilament forward, mimicking the sound of a standard application of the monofilament, but it did not make contact. The LED

pushbutton also blinked, at which time the subject depressed it if they perceived a sensation, although one was not applied. At the end of the exam a threshold sensitivity map was generated using the MATLAB script (Figure 5-3). These procedures were repeated for the subject's second foot.

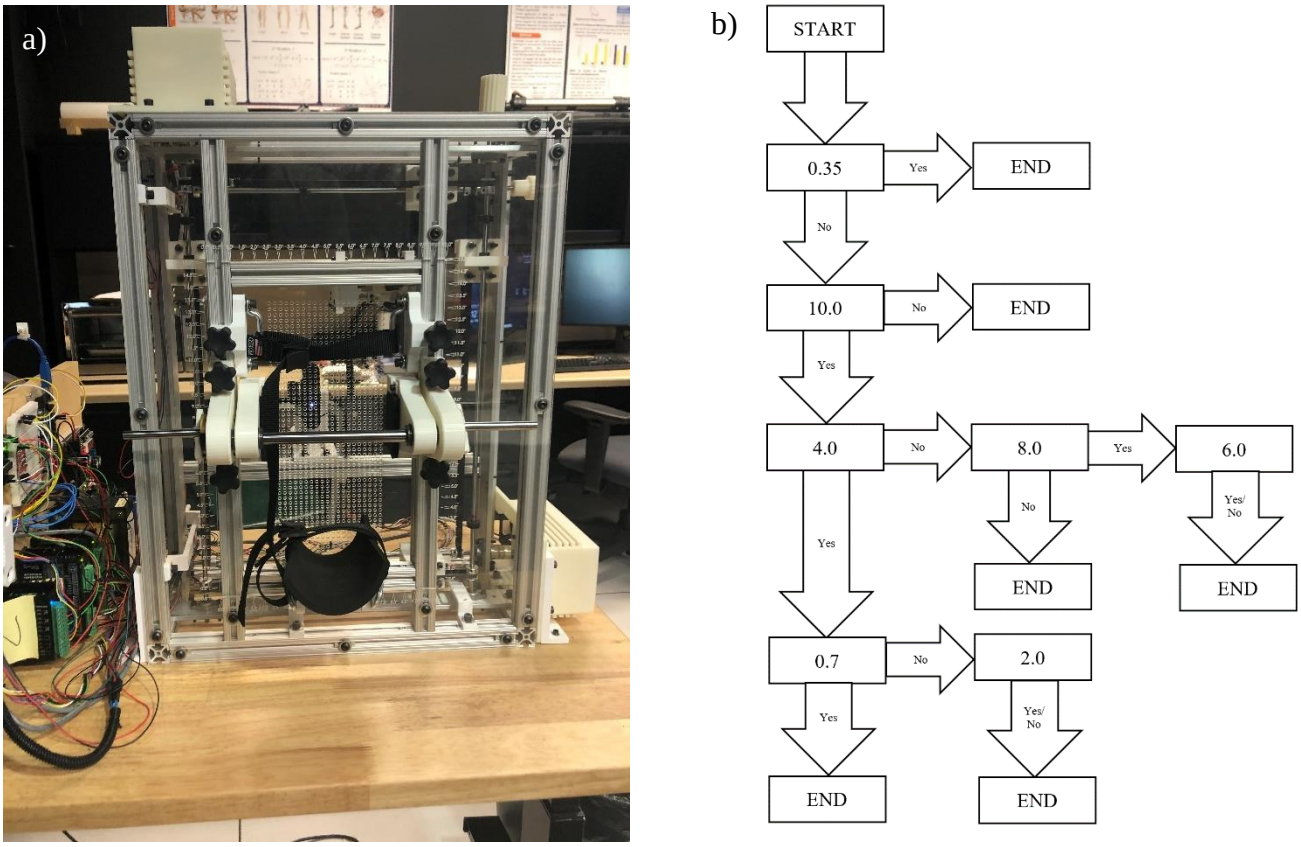

Figure 5-2:Automated Tool and Homing Sequence Protocol

a) Automated tool which applies a monofilament through the perforated foot plate until contact with the plantar surface
b) Homing sequence protocol used to determine threshold sensitivity per location. Units are in gF

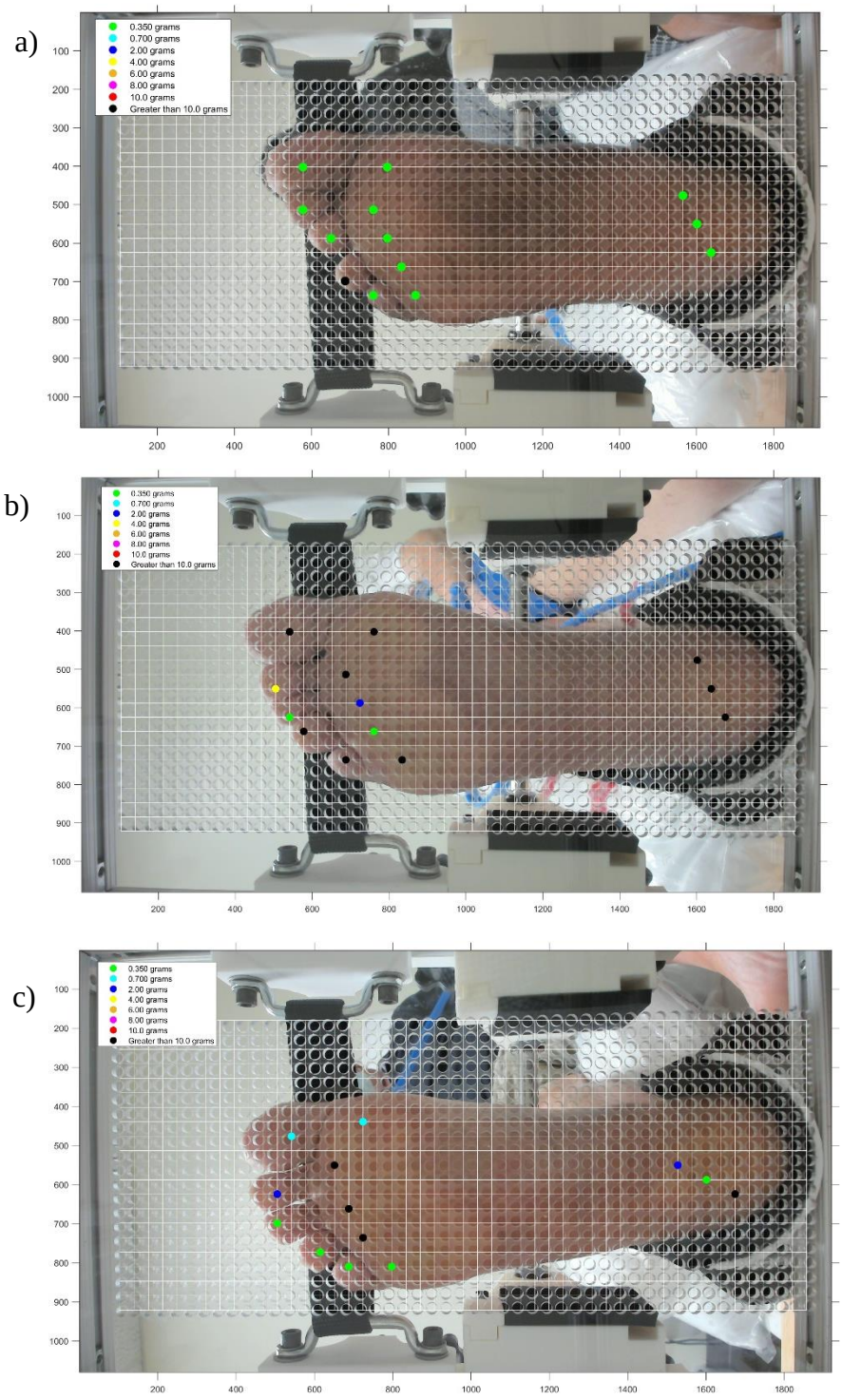

Figure 5-3: Threshold Sensitivity Maps

a) Subject from Group 1
b) Subject from Group 2
c) Subject from Group 3

5.3.5. Post Processing of Automated Tool Data

It was determined that subjects were firmly pressing their foot up against the foot plate, likely reducing the elasticity of their skin. This may have created an inaccuracy when the monofilament was applied, often resulting in a load greater than desired being administered. Although the load cell is constantly monitoring the contact force of the monofilament, the sensor's read rate prevents it from stopping the actuation of the monofilament instantaneously, especially when the subject's skin elasticity is significantly reduced. As such, every application of the monofilament via the automated tool was screened manually for accuracy in all force categories (0.35-10.0 gF). This was conducted after the subject completed the study. To ensure that accurate data were used it was decided that each location had to be within a 2.0 gF range for it to be accepted. However, at 0.35 gF and 0.70 gF, it was required that both needed to be less than 2.0 gF to be valid. If the actual force was outside of this range, then this application of the monofilament was considered to be a "device error". Although a "device error" led to the removal of data for a specific application of the monofilament, it did not always correspond to a failure in determining an individual's threshold sensitivity at this location. An example of this is if the first application of the monofilament was intended to be 0.35 gF, but was measured to had been applied at a force of 2.10 gF, then this application of the monofilament was classified as a device error. Device errors also affected false positive assessments, as some subjects were deforming the footplate such that the monofilament made accidental contact, resulting in a load being applied. Locations where the threshold could be determined were assigned to the correct force classification: 0.35, 0.70, 2.0, 4.0, 6.0, 8.0, 10.0, and >10.0 gF. If a threshold sensitivity could not be determined due to the presence of "device errors" then this location was labeled as "indeterminate". Another instance where a location was labeled as "indeterminate" was if the wrong location was evaluated, which

was caused by a camera misalignment. The photograph was realigned using MATLAB commands following the subject's evaluation, however if it was apparent that the wrong location was tested then it was excluded from future analysis.

5.3.6. Threshold Sensitivity Calculation

Using the threshold sensitivities determined with the automated tool, a regional threshold sensitivity index (TSI) was calculated, which is an average of all the locations within the specific region, excluding indeterminate locations (Equation 5-1). Points were assigned to each threshold value (0.35 gF= 1, 0.70 gF= 2, 2.0 gF= 3, 4.0 gF= 4, 6.0 gF= 5, 8.0 gF=6, 10.0 gF=7, and >10.0 gF=8). TSIs spanned one to eight, a score of one indicated a region with increased sensation perception, while a score of eight represented a region with decreased sensation perception. Using all six regions per individual a TSI Norm was calculated to assign a single value representative of an individual's overall threshold sensitivity (Equation 5-2). It should be noted that TSI and TSI Norm are unitless quantities, attributed to these metrics being calculated using score-based averages.

$$TSI = \frac{\#0.35(1) + \#0.70(2) + \#2.0(3) + \#4.0(4) + \#6.0(5) + \#8.0(6) + \#10.0(7) + \# > 10.0(8)}{\#\ Locations - \#\ Indeterminate\ Locations} \quad \text{Eq. 5-1}$$

$$TSI\ Norm = \sqrt{TSI_{R.Toe}{}^2 + TSI_{L.Toe}{}^2 + TSI_{R.Ball}{}^2 + TSI_{L.Ball}{}^2 + TSI_{R.Heel}{}^2 + TSI_{L.Heel}{}^2} \quad \text{Eq. 5-2}$$

5.3.7. Analysis Approach and Statistical Methods

A comparative analysis between the hand-applied monofilament and the automated tool was conducted for all testing locations. Percentages were calculated among all locations where the subjects stated that they felt the hand-applied monofilament but were insensitive to the 10.0 gF applied by the automated tool. This percentage was considered the underdiagnosis rate of the hand-applied monofilament at 10.0 gF, relative to the automated tool, and was calculated for all three groups.

The total number of false positive assessments were calculated per group and three percentages were calculated: fail rate, pass rate, and device error rate. The fail rate was the percentage of false positive check locations where the subject indicated that they felt a stimulus, though none was applied. The pass rate was the percentage of locations where subjects indicated that they did not feel a stimulus. The device error rate was the percentage of locations where the monofilament made accidental contact with the plantar surface.

A linear regression analysis was performed between TSI Norm and the subject's age, BMI, ABI, FBS, and HbA1c in all three populations. Furthermore, to be a part of this analysis subjects had to have data at four out of five toes, four out of five ball, and two out of three heel locations per foot. This ensured that the presence of indeterminate locations did not skew the TSI Norms. As a result, 22 Group 1 subjects, 26 Group 2 subjects, and 22 Group 3 subjects were found to have enough valid testing locations per foot to be included in further analysis. Linear regression analysis was used to analyze the TSI Norm versus the other medical chart characteristics by using Microsoft Excel regression data analysis tool, which outputted the R^2 and P-values. For

regression analysis a *P*-value of 0.05 was considered to be significant. Next, R Studio (2022.02.0 Build 443) was used to conduct all statistical tests to find trends within each metric between the populations. TSI Norms and the other five medical characteristics were first checked for normal distribution and if the variance between populations were equal (homogeneity). Normality was assessed using visual inspection with Q-Q plots and the Shapiro-Wilk normality test ($P<0.05$). The data had to pass both tests to be considered normally distributed. If the data in each metric was found to be normally distributed, then a Brown-Forsyth equal variance assessment was used ($P<0.05$). If one or more of the groups were found to fail normality, then they were assessed for homogeneity using the Flinger-Killen test ($P<0.05$). If the data between all three populations were found to be both normal and with equal variances, then a one factor ANOVA was used to find statistical significance ($P<0.05$), followed by a Tukey post hoc assessment ($P<0.05$). Furthermore, a one factor ANOVA was also considered if the data lacked normality, but had homogeneity, given that ANOVA can handle some nonnormality and that the populations were similar in number. If the data were normally distributed but lacked homogeneity then a Welch's ANOVA was used ($P<0.05$), followed by post hoc assessment with Pairwise Welch's t-test ($P<0.05$) with *P*-value adjustment using a Holm correction. If the data were not normal and did not have equal variances then a Permutational ANOVA was used to evaluate for significance ($P<0.05$), since it does not have any requirements for normality or homogeneity. This was followed by Pairwise Permutational t-Test with a P-value adjustment using a Holm correction ($P<0.05$). The Permutational ANOVA and its associated post hoc test was calculated using 10,000 iterations. Finally, Permutational ANOVA was also performed and then compared to the findings from the other ANOVA assessments.

5.4. Results

5.4.1. Comparison between the Hand-Applied Monofilament and the Automated Tool

The 57 Group 1 subjects resulted in 1,185 locations assessed, after the removal of the indeterminate locations (n=294). This yielded 21% of locations that were underdiagnosed, relative to the automated tool. There were 1,334 locations analyzed, excluding the indeterminate locations (n=172), within the 58 Group 2 subjects. Consequently only 24% of locations were underdiagnosed, compared to the automated tool. Meanwhile 38 Group 3 subjects produced 870 testing sites, not including indeterminate locations (n=118). Of these locations, 22% of them were underdiagnosed versus the automated tool.

5.4.2. False Positive Assessment Results

In Group 1, 160 locations (11%) were subjected to a false positive check. Of these locations 13.75% of them failed the assessment, 57.5% of them passed, and 28.75% of them were device errors. In Group 2, 167 locations (11%) were evaluated with a false positive assessment. Of these 18% failed the test, 72% passed, while 10% experienced a device error. Finally in Group 3, 107 locations (11%) were assessed with a false positive. Of these locations, 19.6% of them failed, 72.0% of them passed, and 8.4% experienced a device error.

5.4.3. TSI Norm and Medical Data Outcomes Compared to Populations

5.4.3.1. TSI Norm versus Age

The 22 Group 1 subjects demonstrated the strongest linear relationship between TSI Norm and age (R^2=0.3422, P =0.004), which showed that as age increased, TSI Norm also increased (Figure 5-4a). Neither the 26 Group 2 subjects (R^2=0.0014, P =0.86) or the 22 Group 3 subjects

(R^2=0.0083, P =0.69) yielded any meaningful relationship between TSI Norm and age. All groups passed both normality tests. As such a Brown-Forsyth test was used to assess for homogeneity between the groups, which found that the variances were barely equal (P=0.052). An ANOVA was used to evaluate for significance (P=0.19), but since it was borderline homogenic a Welch's ANOVA was also used (P=0.21). Both of these and the Permutational ANOVA (P=0.20) found that the difference in mean ages between the populations was not significant (Group 1: 61.9±10.8 years, Group 2: 65.0±10.1 years, Group 3: 65.9±5.85 years). The results for age are categorized in Table 5-1.

5.4.3.2. TSI Norm versus BMI

TSI Norm was compared to BMI in all three groups, however none showed any type of strong linear relationship between these variables (Figure 5-4b). Group 1 (R^2=0.0008, P=0.90) and Group 3 (R^2=0.016, P =0.58) performed the worst, while Group 2 (R^2=0.1144, P =0.091) still did not yield a significant relationship with TSI Norm. Ultimately TSI Norm was insensitive to BMI. Group 1 did not pass the Shapiro-Wilk normality assessment (P=0.014), despite passing the visual inspection using a Q-Q plot, while Groups 2 and 3 passed both. A Flinger-Killeen variance assessment was used which found that the variances were equal between groups (P=0.70). An ANOVA was used to determine significance (P=0.11), in addition to a Permutational ANOVA (P=0.12). Both found that the mean BMIs between the populations were not significantly different (Table 5-1).

5.4.3.3. TSI Norm versus ABI

TSI Norm as a function of ABI did not reveal any significant findings in the populations (Figure 5-4c). Group 1 (R^2=0.0305, P =0.44) and Group 3 (R^2=0.078, P=0.21) showed the poorest linear

relationship between TSI Norm and ABI. Group 2 (R^2=0.1208, P=0.082) yielded the best relationship but it was not significant. Furthermore, the ABIs for all three populations did pass visual inspection of the Q-Q plots, but Groups 2 and 3 were found to be nonnormal via the Shapiro-Wilk test. Flinger-Killeen test found that the populations had equal variance (P=0.34). The one-factor ANOVA and the Permutational ANOVA came to the same conclusion that the mean ABIs between the populations were not significantly different (P=0.56) (Table 5-1).

5.4.3.4. TSI Norm versus FBS

Linear regression analysis found that Group 1 showed the strongest relationship between TSI Norm and FBS (R^2=0.1819) but was insignificant (P =0.054) (Figure 5-4d). It should be noted that out of the 22 Group 1 subjects, only 21 of them had FBS levels documented in their medical charts. The results of Group 2 (R^2=0.0022, P=0.82) and Group 3 (R^2=0.0692, P=0.24) did not yield a strong linear relationship. Normal distributions existed for all groups via Q-Q plot and Shapiro-Wilk normality assessments. The Brown-Forsyth homogeneity assessment found that the populations had unequal variances compared with each other (P=0.0005). The Welch's ANOVA assessment found that the difference in mean FBS between the groups was highly significant (P<0.0001) (Table 1). Group 1 was found to be significantly different to Group 2 (P_{adj}<0.0001) and Group 3 (P_{adj}<0.0001), using Pairwise Welch's t-Test. The DM2 groups when compared to each other were not significantly different (P_{adj}=0.19). The Permutational ANOVA concluded that the mean FBS was significantly different between groups (P<0.0001). Pairwise Permutational t-Test found that Group 1 was significantly different to Group 2 (P_{adj}=0.0003) and to Group 3 (P_{adj}=0.0003). The post hoc test between the DM2 groups found that FBS was not

significantly different between them (P_{adj}=0.19). The results for FBS are documented in Table 5-1.

5.4.3.5. TSI Norm versus HbA1c

Group 1 demonstrated the strongest relationship between TSI Norm and HbA1c (R^2=0.4124), but it lacked significance (P=0.12) (Figure 5-4e). However, Group 1 only had seven individuals out of the 22 who had HbA1c values documented in their medical charts. Group 2 (R^2=0.004, P=0.76) and Group 3 (R^2=0.0628, P=0.26) did not indicate a linear relationship between TSI Norm and HbA1c. All Q-Q plots passed the visual inspection, but Group 2 did not pass the Shapiro-Wilk test (P=0.027). This resulted in the use of the Flinger-Killeen variance assessment which found that the variances were unequal between the populations (P=0.0015). Due to nonnormality and unequal variances the Permutational ANOVA was the only ANOVA performed, which found that there were significant differences in the mean HbA1c (P=0.0025) (Table 1). The Pairwise Permutational t-Test found that Group 1 was significantly different to Group 2 (P_{adj}=0.0006) and Group 3 (P_{adj}=0.0006). The DM2 groups were not significantly different from each other using this post hoc assessment, but it was close (P_{adj}=0.053). The HbA1c results are presented in Table 5-1.

5.4.3.6. TSI Norm

TSI Norms for all three groups could be approximated to follow a normal distribution using Q-Q plots and the Shapiro-Wilk normality assessment. However, the variances between the groups were unequal (P=0.030), leading to the use of a Welch's ANOVA, which found that the mean TSI Norm between the populations was not significantly different (P=0.063) (Group 1: 11.6±3.28, Group 2: 13.3±3.65, Group 3: 10.4±5.22). The Permutational ANOVA found a

contrary finding, in which there was significance between the groups, however it should be noted that upon the first run of the Permutation ANOVA the *P*-value was equal to 0.0504 which is borderline significant. Every time a Permutational ANOVA is performed there are slight changes to its output due to the randomization aspect of this statistical assessment. As such 10 iterations of the Permutational ANOVA were performed and the average *P*-value was used (*P*=0.048). Nonetheless post hoc assessment using the Pairwise Permutational t-Test did not find that any of the groups were significantly different to each other. Due to this it is more appropriate to say that the TSI Norms between the groups was not significant. Table 5-1 organizes the TSI Norm results accordingly.

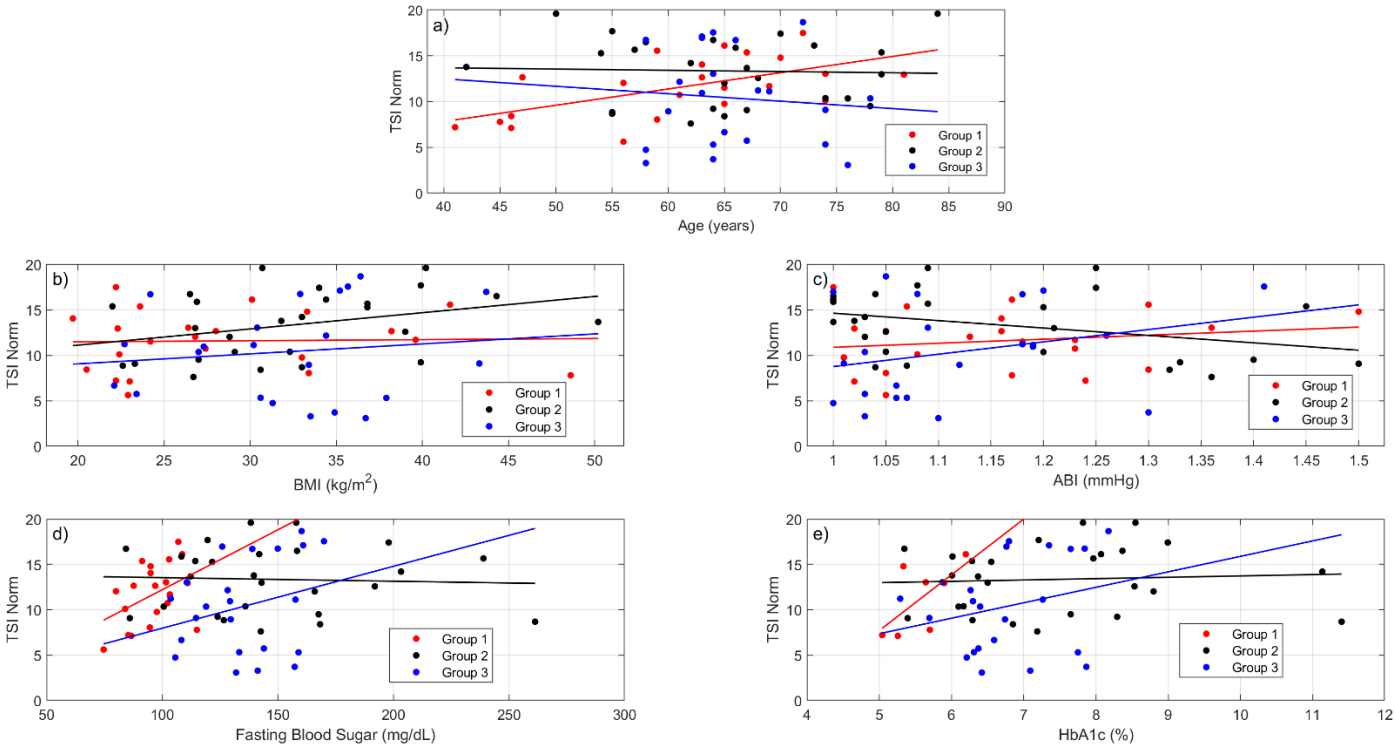

Figure 5-4: Linear Regression Plots

a) TSI Norm vs Age: Group 1 (R^2=0.3422, P=0.004); Group 2 (R^2=0.0014, P=0.86); Group 3 (R^2=0.0083, P=0.69)
b) TSI Norm vs BMI: Group 1 (R^2=0.0008, P=0.90); Group 2 (R^2=0.1144, P=0.091); Group 3 (R^2=0.0016, P=0.58)
c) TSI Norm vs ABI: Group 1 (R^2=0.0305, P=0.44); Group 2 (R^2=0.1208, P=0.082); Group 3 (R^2=0.078, P=0.21)
d) TSI Norm vs FBS: Group 1 (R^2=0.1819, P=0.054); Group 2 (R^2=0.0022, P=0.82); Group 3 (R^2=0.0692, P=0.24)
e) TSI Norm vs HbA1c: Group 1 (R^2=0.4124, P=0.12); Group 2 (R^2=0.004, P=0.76); Group 3 (R^2=0.0628, P=0.26)

			Normality Assessment		Homogeneity of Variance Assessment		ANOVA Assessment			Post Hoc Test								
Metric	Group	Mean ± Standard Deviation	Q-Q Plots (Pass/Fail)	Shapiro-Wilk (P<0.05)	Brown-Forsyth (P<0.05)	Flinger-Killeen (P<0.05)	One-Factor ANOVA (P<0.05)	Welch's ANOVA (P<0.05)	Permutational ANOVA (P<0.05)	Pairwise Welch's t-Test (P_{adj}<0.05)			Pairwise Permutational t-Test (P_{adj}<0.05)					
Age	Group 1	61.9±10.8 years	Pass	0.43	0.052		0.19	0.21	0.20									
	Group 2	65.0±10.1 years	Pass	0.91														
	Group 3	65.9±5.85 years	Pass	0.12														
BMI	Group 1	28.6±7.78 kg/m^2	Pass	0.014		0.70	0.11		0.12									
	Group 2	32.6±6.92 kg/m^2	Pass	0.42														
	Group 3	32.1±6.01 kg/m^2	Pass	0.48														
ABI	Group 1	1.16±0.13 mmHg	Pass	0.083		0.34	0.56		0.56									
	Group 2	1.16±0.16 mmHg	Pass	0.0027														
	Group 3	1.12±0.11 mmHg	Pass	0.022														
FBS	Group 1	96.4±10.6 mg/dL	Pass	0.93	0.0005			<0.0001	<0.0001		A	B		A	B			
	Group 2	148.1±43.4 mg/dL	Pass	0.11						B	<0.0001	-	B	0.0003	-			
	Group 3	135.5±20.1 mg/dL	Pass	0.32						C	<0.0001	0.19	C	0.0003	0.19			
HbA1c	Group 1	5.6±0.4 %	Pass	0.94		0.0015			0.0025					A	B			
	Group 2	7.5±1.6 %	Pass	0.027									B	0.0006	-			
	Group 3	6.8±0.8 %	Pass	0.58									C	0.0006	0.053			
TSI Norm	Group 1	11.6±3.28	Pass	0.78	0.030			0.063	0.048*					A	B			
	Group 2	13.3±3.65	Pass	0.15									B	0.17	-			
	Group 3	10.4±5.22	Pass	0.067									C	0.37	0.088			

Table 5-1: Statistical Analysis Summary

A-Group 1
B-Group 2
C-Group 3
P_{adj}-Adjusted P-value
*Permutational ANOVA average P-value after 10 iterations

5.5. Discussion

5.5.1. Hand-Applied Monofilament and Automated Tool Outcomes

The automated tool demonstrated that 21-24% of the locations assessed using the hand-applied monofilament were underdiagnosed, relative to the automated tool, regardless of cohort. This means that subjects screened for neuropathy using a 10.0 gF hand-applied monofilament could potentially be underdiagnosed for their current level of sensation. This combined with the previously discussed challenges with using hand-applied monofilaments (fatigue, angle, and rate of insertion, etc.) implies that attention to application technique should be taken when relying on them to determine an individual's degree of sensation.

5.5.2. False Positive Assessment Outcomes

Of the locations assessed 11% of them received a false positive assessment, per group. In the methodology developed for the automated tool each location has a 10% chance of having a false positive check, which compared well to this observation. Between 13-20% of locations failed the false positive assessment. Groups 2 and 3 had the greatest pass rate (72%) and the lowest device error rates for false positive assessments (10% and 8.4%, respectively). Group 1 had the greatest amount of device error rate locations (28.75%), but also had the greatest number of total device errors (n=294). This likely impacted the failure and pass rates for Group 1 locations.

5.5.3. TSI Norm and Medical Data Outcomes

The results showed that between the three groups, age, BMI, and ABI were not significantly different. It was also determined that the FBS and HbA1c between the groups were significantly different. This is not surprising considering that generally individuals with diabetes have

elevated FBS and HbA1c, which is used as a criterion to assess for diabetes [19]. However, this study failed to find a significant difference between the three groups and TSI Norm (Table 5-1). Welch's ANOVA yielded an insignificant finding (P=0.063), while the Permutational ANOVA found significance using a P-value averaged with 10 iterations (P=0.048). Yet the Pairwise Permutational t-Test post hoc assessment found that none of the comparisons were significant. Ultimately, it was concluded that TSI Norm was not significantly different between groups, which was not expected. Also surprising was that despite TSI Norm being dependent on age in Group 1 with a strong linear relationship (R^2=0.34, P=0.004), it was independent in Groups 2 and 3. Meanwhile BMI, ABI, FBS, and HbA1c produced no significant findings within each group when compared to TSI Norm. Although in Group 1, TSI Norm and FBS yielded a strong linear relationship (R^2=0.19), it was barely insignificant (P=0.054). It is apparent that Group 1 subjects attributed their current degree of sensation to their age. Meanwhile DM2 subjects' degree of sensation was regardless of neuropathy symptoms, or lack thereof. This matched well with the findings of Yorek et al., where glycemic control did not affect sensitivity [21]. The presence of DM2 in subjects makes predicting threshold sensitivity unlikely given the medical characteristics examined in this study, which encourages the necessity for not only neuropathy screening for those who currently do not express symptoms, but also continued assessment for subjects who have symptoms. The use of the automated tool developed cannot only provide a more accurate assessment for threshold sensitivity but can also document the presence of an individual's degree of sensation over the course of multiple evaluations.

Chapter 6: The Neuropathy Cartographer Mk2

6.1. Introduction

The Mk1 prototype of the automated tool was designed, built, and used in a clinical study in the Auburn-Opelika Area. The data analyzed using the control subjects indicated that the force accuracy of the device was dependent on the region assessed. The accuracy of the Mk1 prototype of the automated tool was establish in the results and discussion section of Chapter 4. The accuracy of the device had an average absolute error less than or equal to 0.4 grams force at 98% of the toe locations evaluated. This percentage dropped to 84% and 60% for locations in the ball and heel regions, respectively. Although data had to be filtered to account for the subjects that were pressing their feet against the foot plate with enough force to distort the measurement taken by the load cell, the device still showed promise. Its ability to document an individual's threshold sensitivity on the plantar surface and its new accompanying methodology allowed for an accurate and unbiased analysis of data. However, there are still some improvements that can be made, which are addressed below.

6.2. MK2 Design Improvements

The second iteration of the automated tool, Mk2, was finalized and built during the clinical study that took place from March to December of 2021. It is presented in Figure 6-1 and Figure 6-2. It had similar dimensions to the Mk1 prototype, with a width of 18.5 inches, a height of 24 inches, and a depth of 10 inches. The motor covers on the side and top of the device added an additional 5.25 inches to each dimension, respectively. The weight increased to approximately 60 pounds, attributed to the revised gantry subassembly and accompanying electronics cabinet. Although it largely remained unchanged, its improvements made it easier to assemble, more rigid, and safer.

The changes, outlined below, lead to the total cost of approximately $2,800.00, the increase largely attributed to more components required to build a separated electrical cabinet. Furthermore a $230.00 52-inch Husky workbench was used for this version for more physical space for the machine and the accompanying laptop.

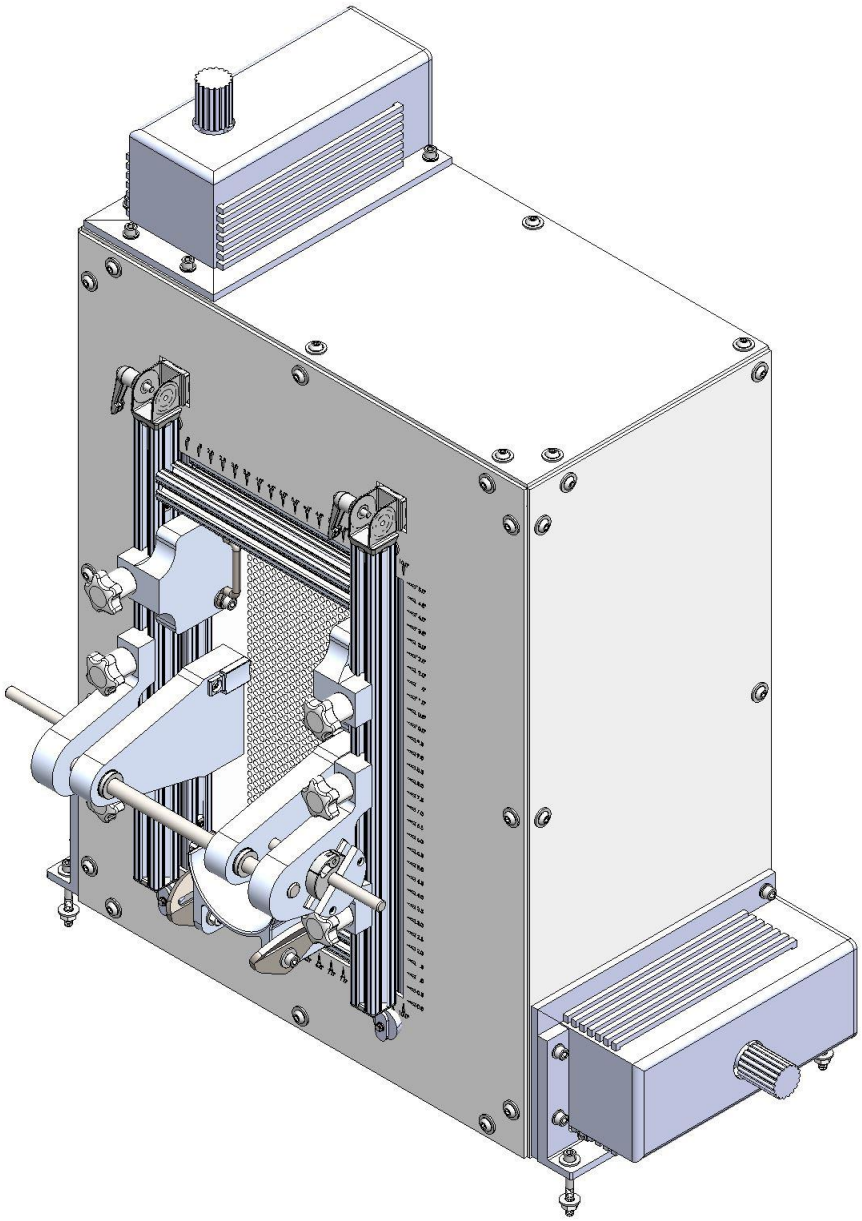

Figure 6-1: Mk2 Automated Tool Prototype

Figure 6-2: Assembled Mk2 Automated Tool Prototype

6.2.1. Mk2 Chassis Subassembly

The chassis remained largely unchanged from the Mk1 prototype, Figure 6-3. It still used the same 80/20 aluminum T-slot profiles. The biggest adaptation was the use of white acrylic panels on the front, sides, and top. These panels not only provided a more aesthetically pleasing look to the device, but also made it even more difficult for subjects and clinicians to get their hands and feet stuck inside. The back of the device remained open so that the camera still had the foot plate within its field of view. Two metal brackets were added to the center aluminum extrusion on the back of the device, where the camera was mounted. This kept the aluminum extrusion from pivoting, which could cause the camera to become misaligned.

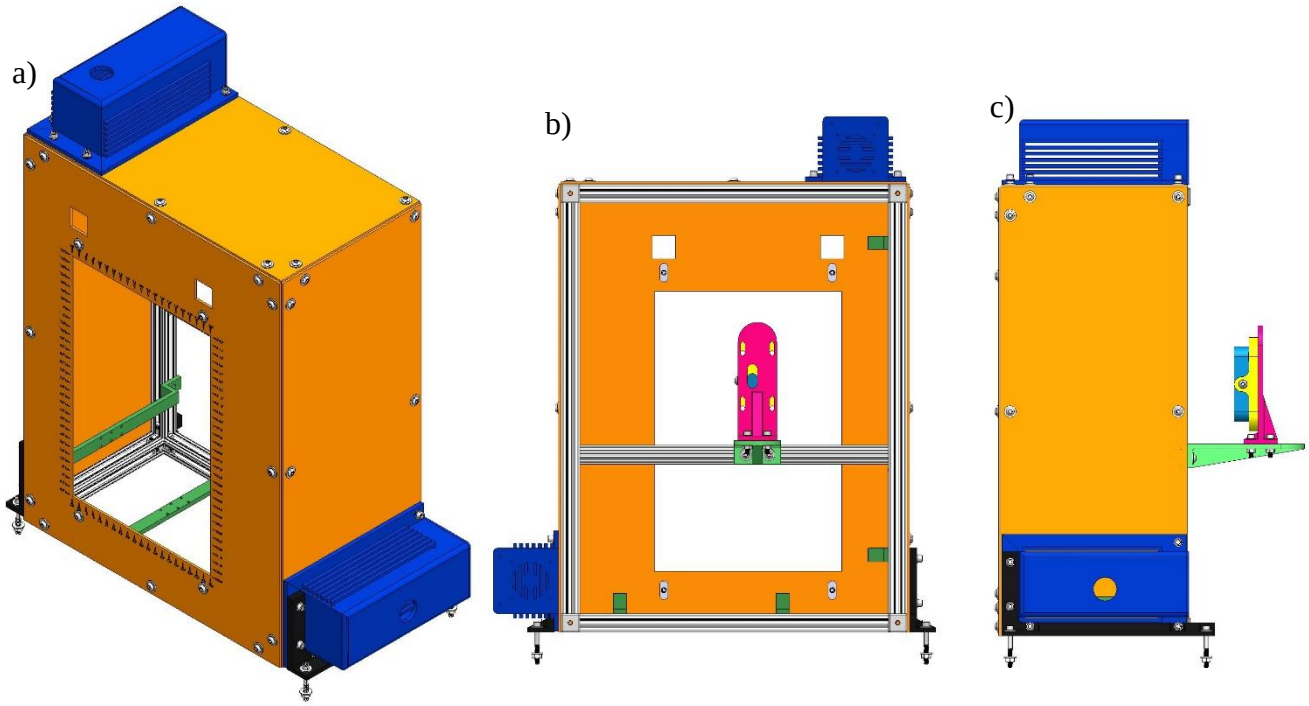

Figure 6-3: Mk2 Chassis Subassembly[8]

a) Isotropic View
b) Rear View
c) Side View

6.2.2. Mk2 Foot Clamp Subassembly

The foot clamp mechanism maintained an identical foot plate from Mk1 and similar clamping structures. The clamp subassembly, Figure 6-4, still achieved the same functionality by providing minimal compression on the medial and lateral sides of the foot. Straps kept the toes against the foot plate, and the ankle was also kept in place with a strap. In the Mk1 prototype it was difficult for some subjects to place their foot inside the apparatus. To address this, the entire foot clamp subassembly was placed on a locking pivot, illustrated in Figure 6-5. This allowed for the mechanism to be raised out of the way for the subject while they placed their foot against the

[8] 80/20 Aluminum T-slot profiles (White), Acrylic Panels (Orange), Stepper Motor Covers (Dark Blue), Camera Mounting Plate (Green), Camera Mounting Adapter (Yellow), Camera Mount (Yellow), Logitech Brio Webcam (Blue), Limit Switch Mounts (Dark Green), Mounting Brackets (Black)

foot plate and then lowered once their foot was in position. This adaptation required three additional 80/20 aluminum T-slot profiles from Mk1.

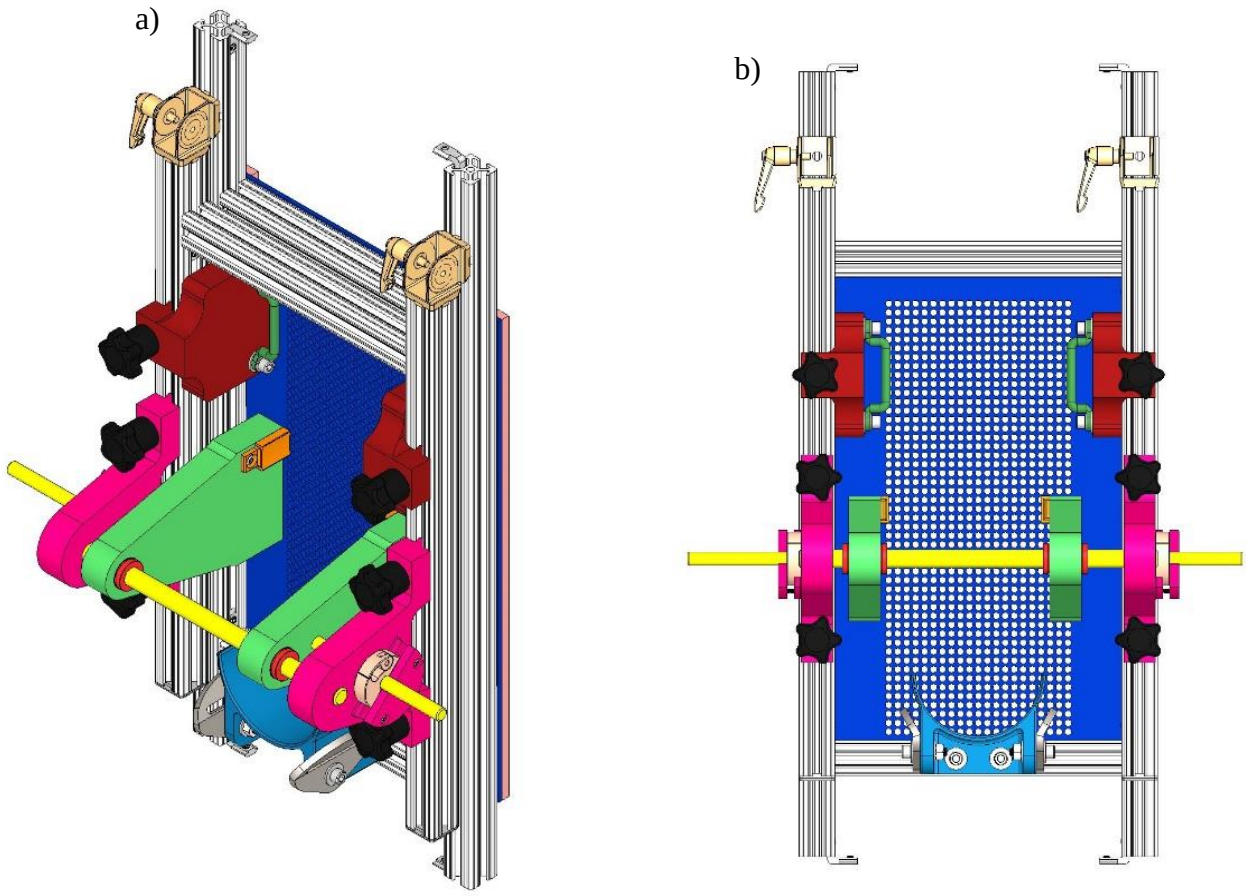

Figure 6-4: Mk2 Foot Clamp Subassembly[9]

a) Isotropic View
b) Front View

[9] Perforated Foot Plate (Dark Blue), 80/20 Aluminum T-slot profiles (White), Toe Clamp (Maroon), Foot Clamp Base (Magenta), Foot Clamp (Green), Ball of Foot Locator (Orange), Ankle Holder (Blue), Linear Sleeve Bearing (Red), Clamp Lock (Bronze), Screw Down Knobs (Black), Ankle Strap Mount (Grey) , Toe Strap Mount (Dark Green), Linear Motion Shaft (Yellow), Locking Pivot (Gold)

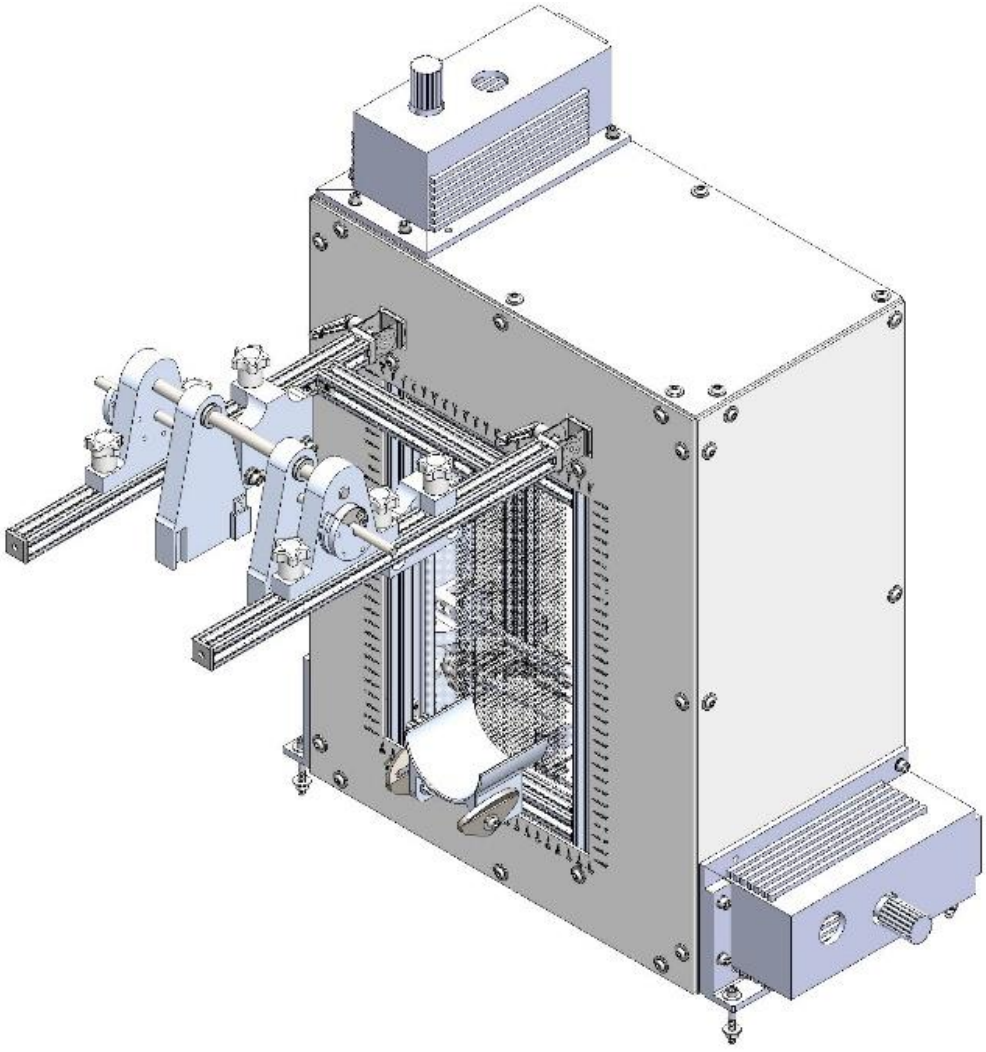

Figure 6-5: Mk2 Foot Clamp Subassembly Locking Pivot Utilization

6.2.3. Mk2 Gantry Subassembly

The gantry subassembly in Mk2 was altered to make the structure more rigid, which also had the benefit of making the device easier to assemble, Figure 6-6. The corresponding linear motion assembly is provided in Figure 6-7. The linear motion shafts were increased from 6.35 mm to 8.0 mm. Increasing the shafts required that all bearings, pulleys, retaining rings, shaft collars, and the flexible shaft couples all needed to be resourced to accept a larger diameter. The larger rods increased the overall stiffness of the assembled structure, which saved time when manufacturing

as the thinner rods had more of a tendency to warp during assembly. The motion carriages where also modified to accept a shaft holder, used to clamp onto the larger linear motion shafts. This replaced the press fit and retaining rings previously used in the Mk1 version of the automated tool. Also, a different method was used to connect the belts to the motion carriages. The belts were feed into a curved groove, which were bent back onto itself and tied off using a zip tie. A belt tensioner was still used to maintain proper tension during operation.

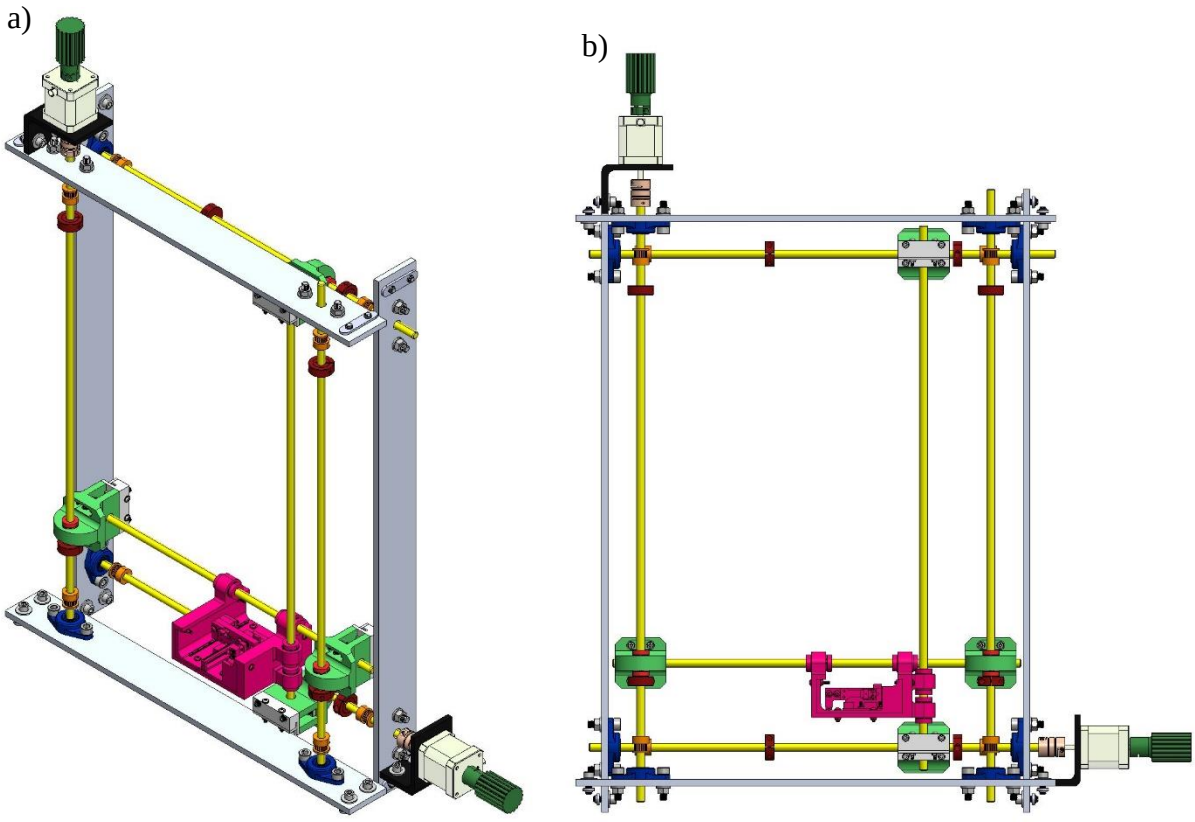

Figure 6-6: Mk2 Gantry Subassembly[10]

a) Isotropic View
b) Front View

[10] Brackets (Grey), Linear Motion Shaft (Yellow), Linear Sleeve Bearing (Red), GT2 Timing Pulley (Orange), Coupling (Bronze), Stepper Motor (Beige), Mounted Sleeve Bearing (Dark Blue), Shaft Collars (Maroon), 3D Printed Motion Carriage (Green), Belt Tension Adapter with Plate (White), Mk1 Probe Subassembly (Magenta), Manual Adjustment Know (Dark Green)

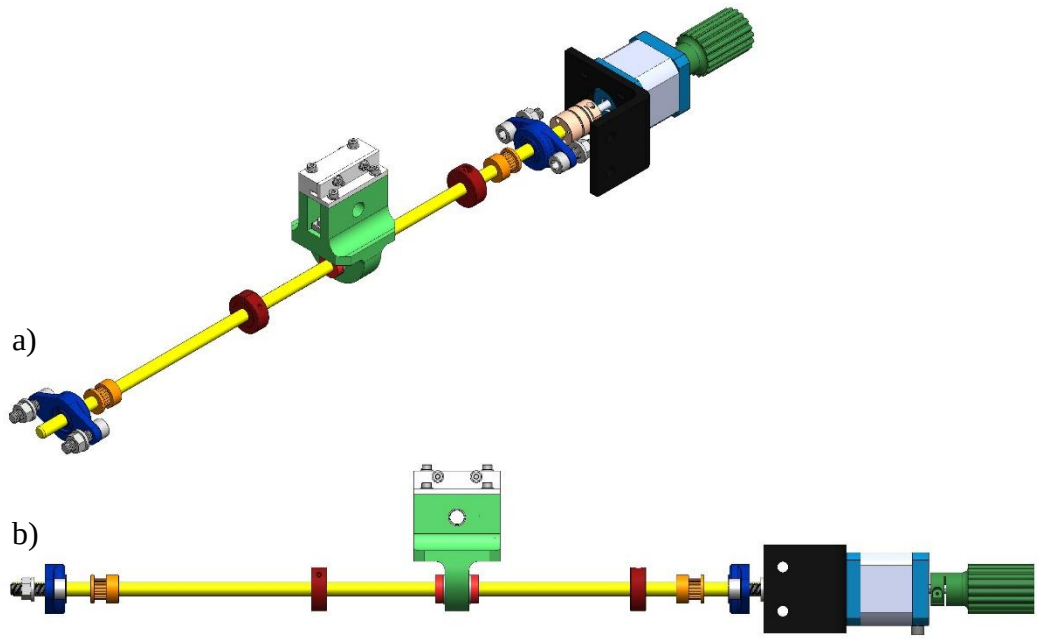

Figure 6-7: Mk2 Linear Motion Assembly[11]

a) Isotropic View
b) Front View

6.2.4. Mk2 Probe Subassembly

The probe subassembly was altered to be accessible from above, rather than below. This made servicing the probe subassembly easier, as the operator could do it while looking down onto it. This included routinely cleaning and or changing out the Semmes-Weinstein monofilament. Overall, the probe subassembly was more compact, but still featured the same load cell, Walfront stepper motor and miniature ball bearing carriage with guide rail. Limit switches, although optional, can also be implemented, which could reduce the need for the operator to manually set the origin of the z-axis. The probe subassembly featured four linear sleeve bearings, rather than

[11] Linear Motion Shaft (Yellow), Linear Sleeve Bearing (Red), GT2 Timing Pulley (Orange), Coupling (Bronze), Stepper Motor (Blue/Gray), Mounted Sleeve Bearing (Dark Blue), Shaft Collars (Maroon), 3D Printed Motion Carriage (Green), Belt Tension Adapter with Plate (White), Manual Adjustment Know (Dark Green)

the three found in the Mk1 prototype, which increase stability. This improved subassembly is provided in Figure 6-8.

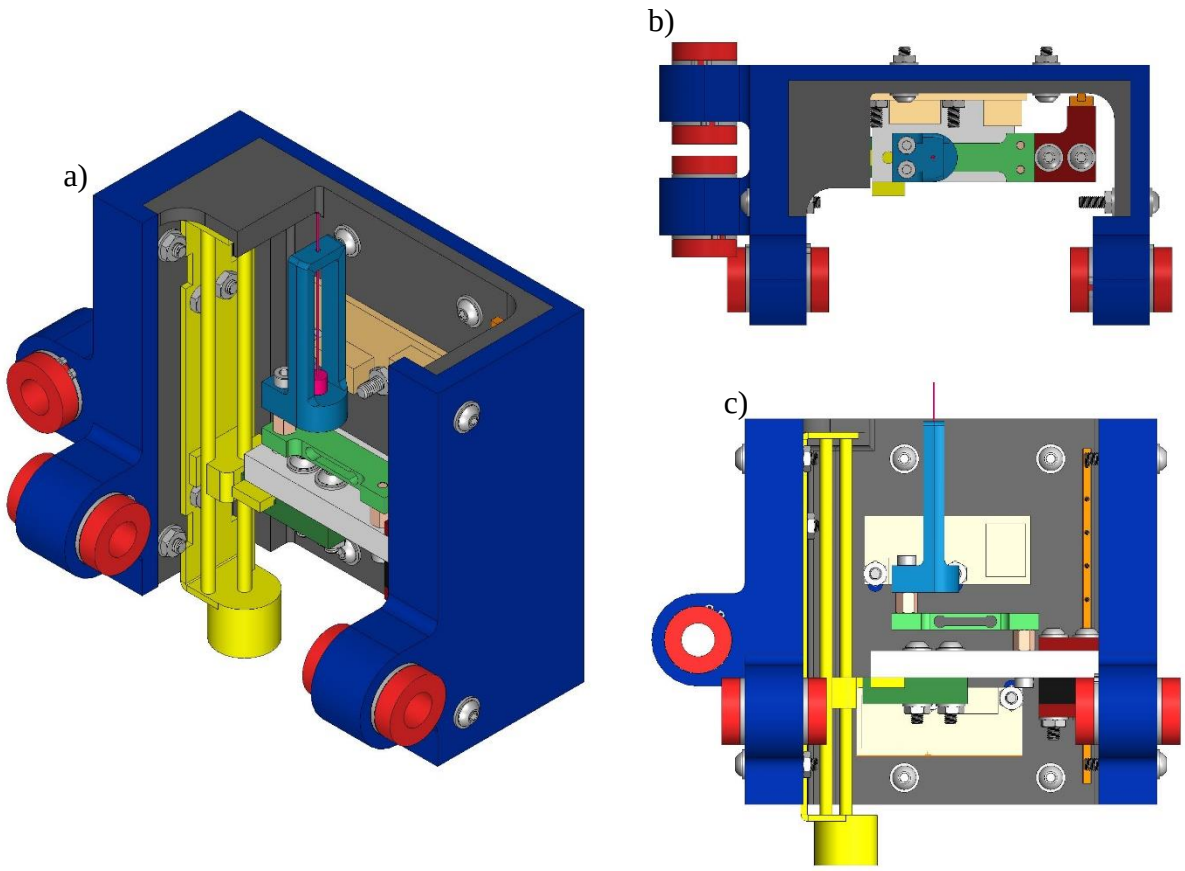

Figure 6-8: Mk2 Probe Subassembly[12]

a) Isotropic View
b) Top View
c) Front View

[12] Monofilament (Magenta), Monofilament Holder (Blue), Standoffs (Bronze), Load Cell (Green), Platform (White), Support Block 1 (Dark Green), Support Block 2 (Maroon), Support Block 3 (Black), Stepper Motor (Yellow), Miniature Ball Bearing Carriage (Orange), Linear Sleeve Bearing (Red), Chassis (Gray), Housing (Dark Blue), Limit Switch (Gold)

6.2.5. Mk2 Electronics Subassembly

One of the starkest differences between both iterations of the automated tool was the addition of a separate structure used to house the electrical components, Figure 6-9. This new structure was made out of sixteen 80/20 aluminum T-slot profiles and acrylic panels. Its dimensions were 10 inches in height, 24 inches in length, and 8 inches in depth. This version of the prototype used three dedicated power supplies. One of the power supplies was the PSB48-240S, which outputted 48 volts DC, and was used to power the stepper motors that controlled the gantry subassembly [99]. The other two power supplies were the 12-volt DC PSB12-030-P, one to power the probe subassembly, while the other powered cooling fans inside the device and the electronics cabinet. The gantry subassembly used STP-MTR-17048D stepper motors, which had a torque of 5.19 lb-in and 2.0 amps per phase [99]. The increased motor torque was necessary to counter the added weight caused by increasing the diameter of the linear motion shafts found in the gantry subassembly. All other electronics from Mk1 were carried over, including the Arduino Mega and Uno. The power supplies and the stepper motor drivers mounted on an aluminum plate to dissipate heat, as seen in Figure 6-10. The Arduinos, HX711, and a breadboard were attached to an acrylic plate at the base of the cabinet. All wiring was organized within the cabinet and was routed outside to the device.

Figure 6-9: Mk2 Electronics Cabinet[13]

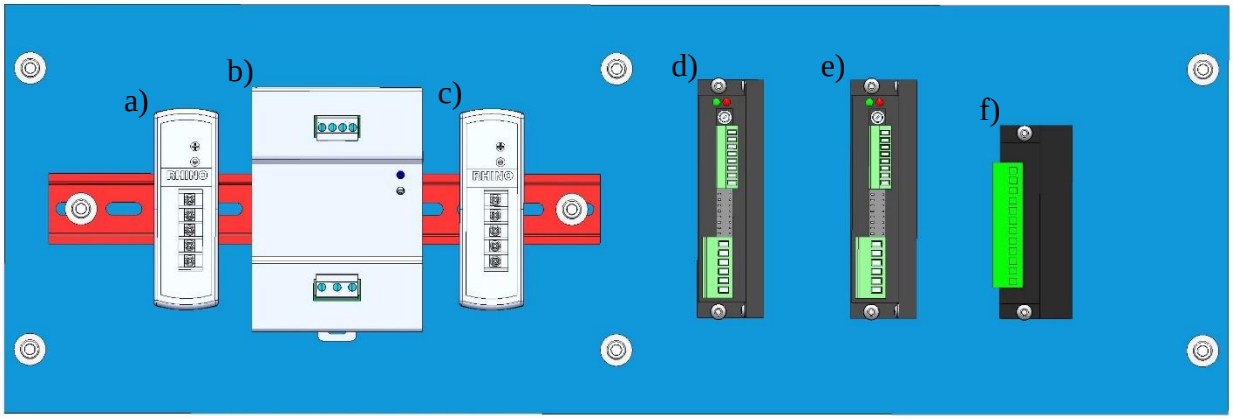

Figure 6-10: Mk2 Electronics Cabinet-Inside[14]

a) 12-volt DC PSB12-030-P
b) PSB48-240S
c) 12-volt DC PSB12-030-P
d) STP-DRW-6575 Stepper Motor Drive
e) STP-DRW-6575 Stepper Motor Drive
f) TB6600 Stepper Motor Drive

[13] 80/20 Aluminum T-slot profiles (White), Acrylic Panels (Orange), Door Hinge (Blue)
[14] Aluminum Mounting Plate (Blue), DIN Rail (Red)

Chapter 7: Future Work, Recommendations, and Improvements

7.1. Future Work

7.1.1. Threshold Sensitivity versus Sex and Time of Year

7.1.1.1. Threshold Sensitivity and Sex Linear Regression Analysis

Another direction that this research project could proceed is by evaluating how males and females experience threshold sensitivities differently, especially in the groups presented in Chapter 5. Identical methods to Chapter 5 can be considered, in which subjects would be divided into one of three groups: Group 1 (healthy subjects without type 2 diabetes mellitus), Group 2 (subjects with type 2 diabetes mellitus with neuropathy symptoms), and Group 3 (subjects with type 2 diabetes mellitus without neuropathy symptoms). However, it would be necessary to have 100 subjects in each group, each with 50 male and 50 female subjects. Threshold sensitivity in the form of TSI Norm could then be extrapolated and compared to age, BMI, ABI, fasting blood sugar (FBS), and HbA1c. These comparisons have been conducted using the limited data available from Chapter 5 of this dissertation. Table 7-1 presents the TSI Norms calculated from the male and female subjects in the three groups. The mean TSI Norm was greater in males than in females, in all three groups, which indicated that on average males in this study had a greater sensation loss. Furthermore, Table 7-2 presents the linear regression between TSI Norm and the medical characteristics, subdivided by sex. The number of males and females, as well as the respective mean and standard deviation are presented for each medical characteristic. After conducting 30 linear regressions, three have returned meaningful results. The first is that age correlated positively to sensation loss in Group 1 females (R^2=0.6399, P =0.017). This was also observed in the study by Yümin et al. [107]. Figure 7-1 presents this finding, as well as the results correlated from male subjects in Group 1. Another finding from the Chapter 5 data were

that the BMI in Group 2 males correlated strongly to threshold sensitivity (R^2=0.3208, P=0.028), Figure 7-2. In Chapter 5 this correlation between TSI Norm and BMI was not strong when considering both males and females concurrently. The last notable finding from the Chapter 5 data were that the Group 2 females had a strong linear correlation between TSI Norm and ABI (R^2=0.7688, P=0.0004), Figure 7-3. What is particularly interesting is that this relationship suggests that sensitivity threshold decreased with increasing ABI, or that female subjects with high ABI had better degree of sensation on the plantar surface. Worth mentioning was the linear regression between TSI Norm and FBS in Group 1 females, which demonstrated a linear relationship, but did not make the criteria for significance (R^2=0.4382, P=0.074).

TSI Norm			
Group	Sex	Mean	Standard Deviation
Group 1	Male	12.27	2.85
	Female	10.35	3.82
Group 2	Male	13.35	4.07
	Female	13.34	3.18
Group 3	Male	13.71	5.00
	Female	8.08	4.11

Table 7-1: TSI Norm in Males and Females per Study Group

		Male				Female			
Metric	Group	Number	Mean ± Standard Deviation	R^2	*P*-value	Number	Mean ± Standard Deviation	R^2	*P*-value
Age	Group 1	14	61.6 ±10.6 years	0.1842	0.13	8	60.3 ±11.9 years	0.6399	0.017*
	Group 2	15	64.1 ±12.3 years	0.024	0.98	11	66.2 ±6.1 years	3E-5	0.65
	Group 3	9	63.8 ±3.9 years	0.0869	0.44	13	67.3 ±6.7 years	2E-5	0.99
BMI	Group 1	14	28.9±8.6 kg/m^2	0.0264	0.58	8	28.1±6.5 kg/m^2	0.1136	0.41
	Group 2	15	31.2±5.4 kg/m^2	0.3208	0.028*	11	34.4±8.5 kg/m^2	0.0208	0.67
	Group 3	9	32.3±4.2 kg/m^2	0.0007	0.94	13	32.1±7.2 kg/m^2	0.0419	0.50
ABI	Group 1	14	1.14±0.10 mmHg	0.0289	0.56	8	1.19±0.17 mmHg	0.3286	0.14
	Group 2	15	1.17±0.15 mmHg	0.0001	0.97	11	1.14±0.17 mmHg	0.7688	0.0004*
	Group 3	9	1.18±0.12 mmHg	0.0362	0.62	13	1.08±0.08 mmHg	0.0767	0.36
FBS	Group 1	13	99.4±10.6 mg/dL	0.0183	0.66	8	91.6±9.3 mg/dL	0.4382	0.074
	Group 2	15	152.9±41.8 mg/dL	000177	0.64	11	141.6±46.5 mg/dL	0.0079	0.80
	Group 3	9	145.3±19.3 mg/dL	0.0964	0.42	13	128.7±18.4 mg/dL	0.0297	0.57
HbA1c	Group 1	3	5.93±0.25 %	0.9399	0.16	4	5.32±0.25 %	0.459	0.32
	Group 2	15	7.74±1.75 %	0.0042	0.82	11	7.06±1.22 %	0.0042	0.85
	Group 3	9	7.18±0.79 %	0.0363	0.62	13	6.49±0.64 %	0.0296	0.57

Table 7-2: TSI Norm Linear Regression to Medical Characteristics Subdivided per Sex

*Significant finding

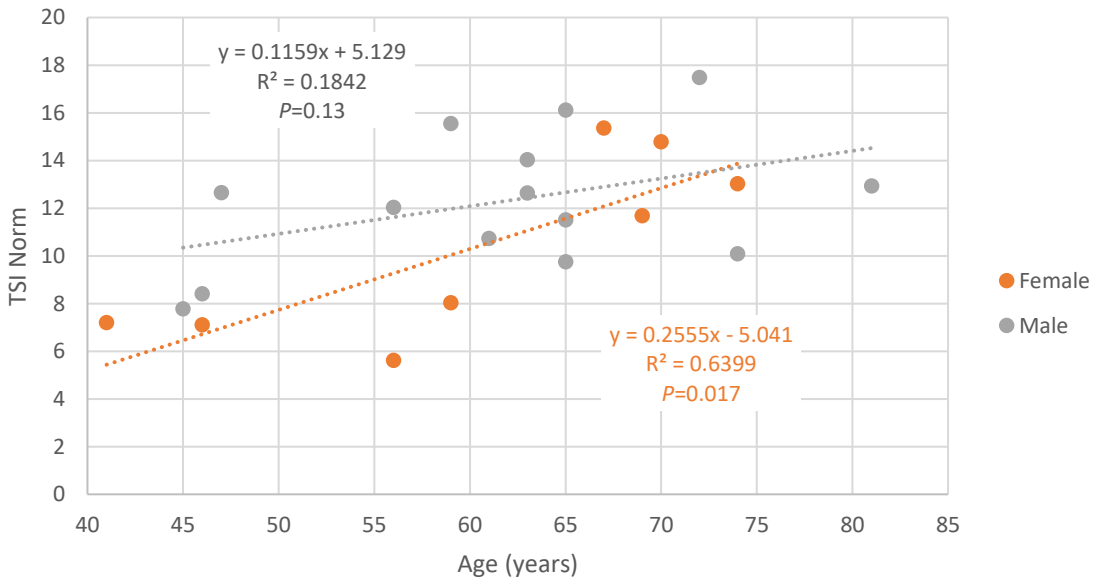

Figure 7-1: Group 1-Male and Female TSI Norm versus Age

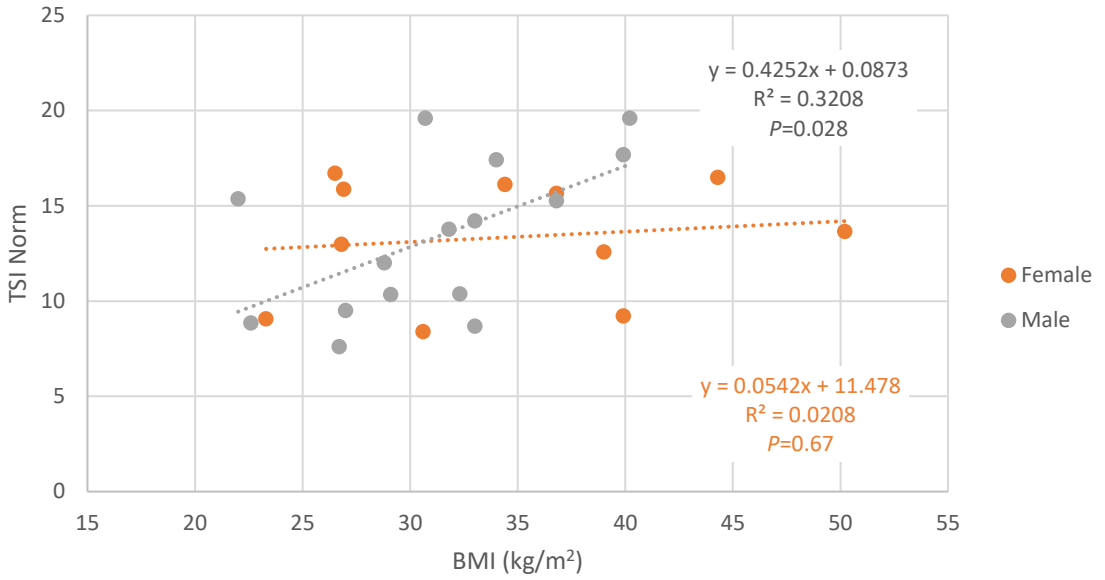

Figure 7-2: Group 2-Male and Female TSI Norm versus BMI

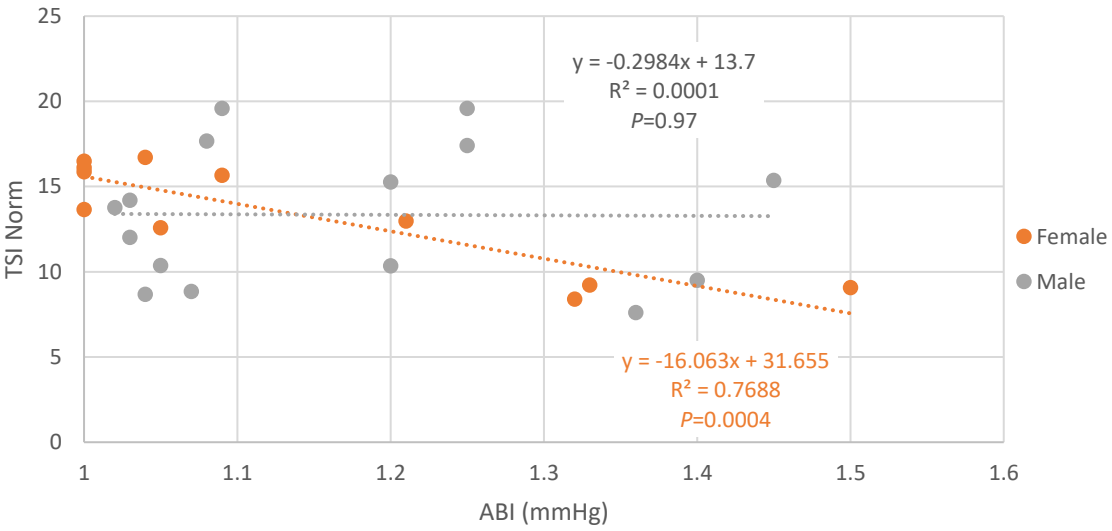

Figure 7-3: Group 2-Male and Female TSI Norm versus ABI

7.1.1.2. Threshold Sensitivity and Time of Year Linear Regression Analysis

Studying the time of year and how it can affect a subject's threshold sensitivity may also be considered in future studies using the automated tool. If the automated tool can be used on six individuals per working day, two of each from Groups 1, 2, and 3, then this would be approximately 1,500 subjects in a year, assuming 250 working days per year. A linear regression of TSI Norm versus the day of the year could then be used to see if a trend existed. However, this type of study would need to be performed every year for at least five years, and all subjects would need to be from the same geographical location. The results can also be interpreted using the group classifications, previously mentioned in Chapter 5. Preliminary data from Chapter 5 has been used to study the relationship between TSI Norm and time of year and is presented in Figure 7-4. However, it should be noted that subjects were not evaluated during July and August of 2021, which explains why there is a gap of data in Figure 7-4. When considering all subjects combined in one group the linear regression was not strong and was not significant (R^2=0.0189, P=0.26). The Group 1 subjects did have a correlation, but failed to be significant (R^2=0.1322, P=0.096). Group 3 did not present a linear relationship between TSI Norm and time of year (R^2=0.0466, P=0.35). Moreover, Group 2, which is the symptomatic DM2 group, did indicate that subjects had improved sensitivity later in the year (R^2=0.2417, P=0.011). Nonetheless these results are only based on a relatively small population scattered from March through December 2021 and are not substantial enough to draw definitive conclusions. If analyzed in a larger future study, the results could lead to a normalization of TSI Norm to account for time of year, especially if considered in multiple geographical locations.

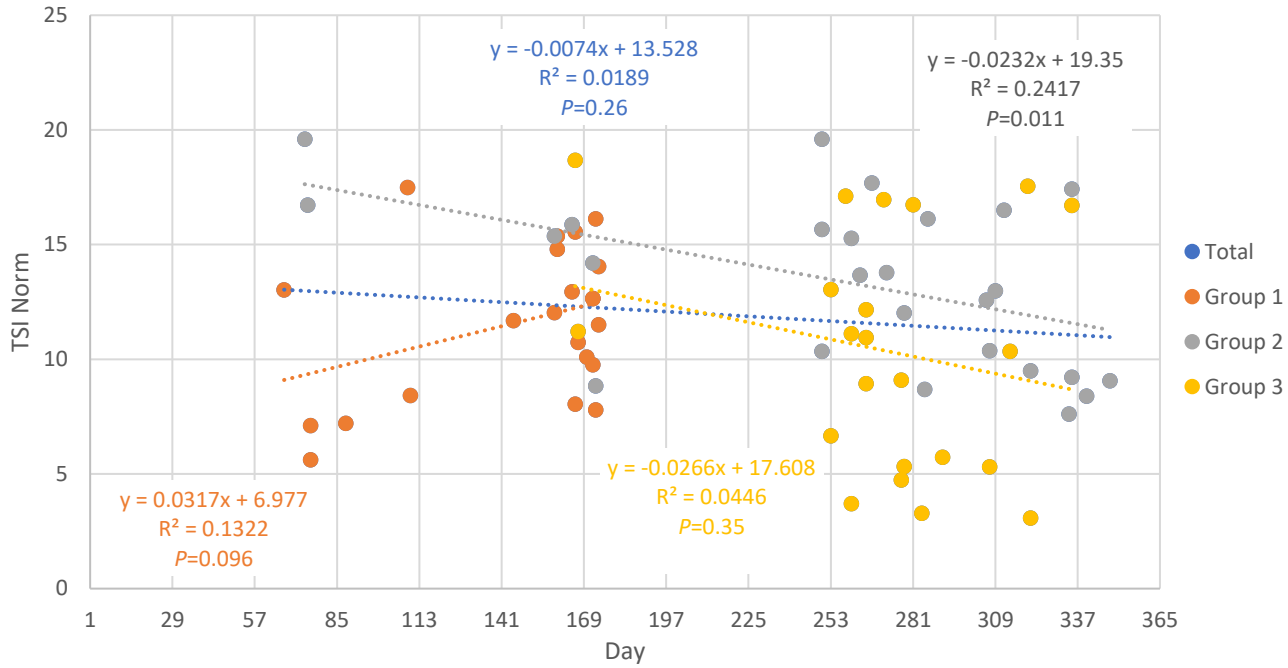

Figure 7-4: TSI Norm Linear Regression versus Time of Year

7.1.2. Threshold Sensitivity Variability versus Plantar Surface Location and Cohort

7.1.2.1. Introduction

The presented methodology used 13 locations per foot to quantify threshold sensitivity in the form of TSI Norm. However, as presented earlier, there is no standard methodology when using the hand-applied monofilament. Studies have used three, five, and ten locations to assess threshold sensitivity, but it is not clear why there are differences [9, 77]. In order to speed up the assessment it would be advantageous to find three to four locations which could be used. Finding locations with the greatest feasibility of predicting sensation loss can be achieved with a more extensive study than the one demonstrated in Chapters 4 and 5 of this dissertation.

7.1.2.2. Methods

Identical groups would be recommended, but the number of subjects required needs to be increased. In the work presented in this dissertation there were 22 healthy control subjects, 26 DM2 subjects with neuropathy symptoms, and 22 DM2 subjects without neuropathy symptoms, who all had four out of five toe locations, four out of five ball locations, and two out of three heel locations. Recruiting 100 subjects per group, matched by similar ages, ABIs, and BMIs would be the next step in understanding which locations on the plantar surface have the greatest sensitivity variability between groups. All subjects would be required to have an age greater than or equal to 50 and ABIs greater than or equal to 1.0 mmHg. It would also be beneficial to analyze all 100 subjects within the same month, by evaluating at least five subjects per day.

Instead of using TSI or TSI Norm, it would be recommended to use the point system used to derive TSI as the mechanism to study location variability. In this analysis, the subject's threshold sensitivities would be determined (0.35 to >10.0 grams of force) and then each category would be assigned a score, ranging from one to eight. Lower numbers are designated to locations with better threshold sensitivity, while larger numbers are for those with worse threshold sensitivity. From this box plots can be used per group and per locations to understand sensitivity variability.

7.1.2.3. Results and Discussion

Figures 7-5 and 7-6 show the subjects from the three groups, presented in Chapter 5. An interesting observation from the data were that the mean threshold scores found in the individuals with neuropathy symptoms were always greater than those without neuropathy symptoms for all locations on both feet. However, the data were more varied between the groups

which made observations less obvious. It is challenging to find three locations per foot and per group that performed universally the same when analyzing the data. The only location that demonstrated the greatest variability per location, per foot, and per group was the fifth toe, with the only exception being the control group versus non-symptomatic neuropathic group comparison on the right foot. Other potentially interesting locations are the second toe and the center of the heel.

When analyzing for variability between groups and locations, the neural pathways should be considered. This was not an important consideration in Chapter 4 and 5 in the calculation of TSI Norm because the plantar surface as a whole was being studied. It is not recommended to consider the fourth toe or the fourth location on the ball of the foot, since these locations share common neural pathways with the medial plantar nerve and the lateral plantar nerve. Ideally, locations that are aligned with the medial plantar nerve, lateral plantar nerve, and the medial calcaneal nerve would be considered for this variability study. This would essentially target the tibial nerve, as all of these nerves originate from it. If two locations that targeted the medial plantar nerve, one location that targeted the lateral plantar nerve, and one location that targeted the medial calcaneal nerve could be identified as the best indicators for the development of neuropathy, then this could become a new screening standard. Screenings would not only occur more quickly but would also be more meaningful for the initial assessment of diabetic peripheral neuropathy on the plantar surface.

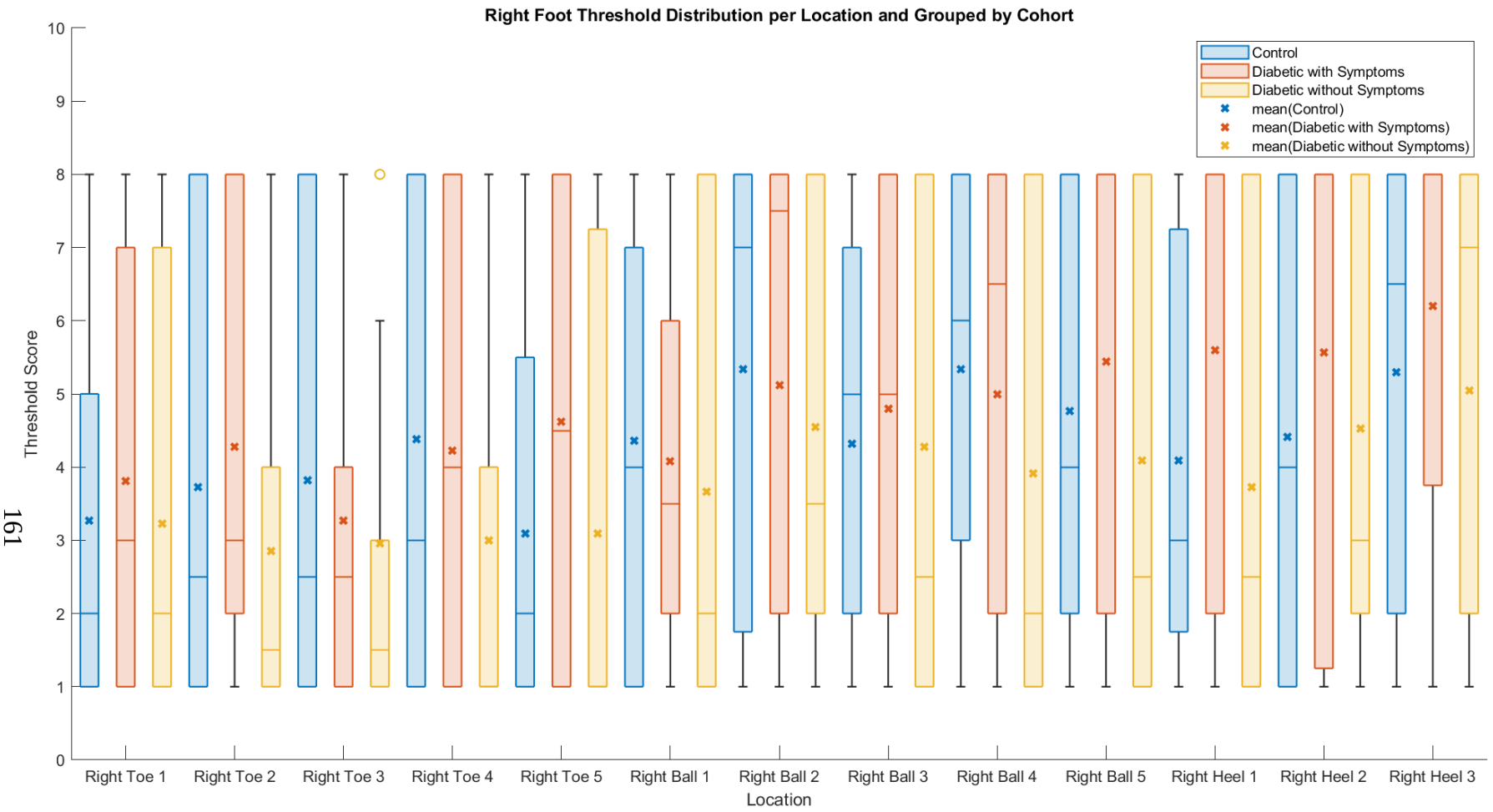

Figure 7-5: Right Foot Location Variability per Location and Grouped by Cohort

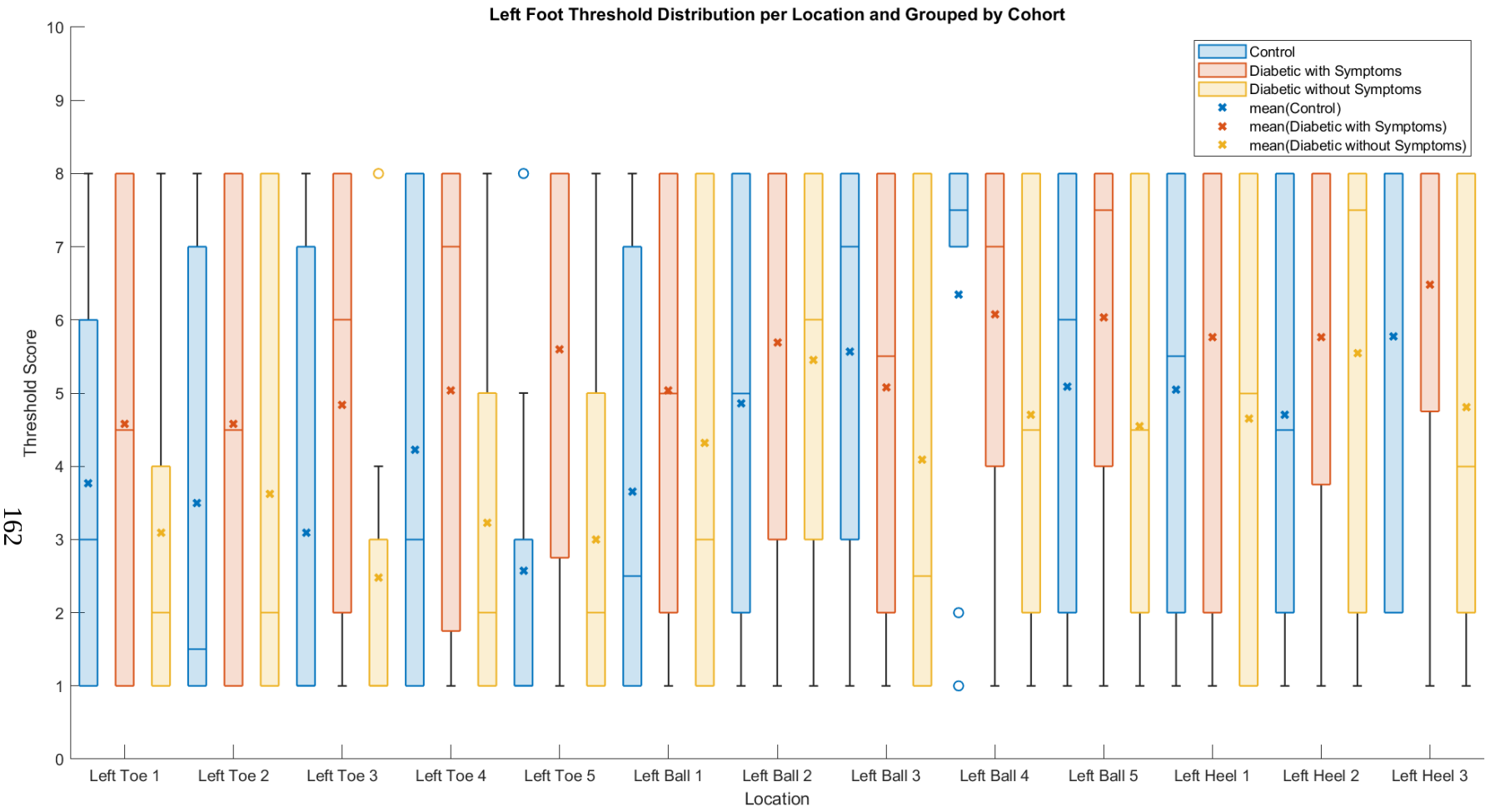

Figure 7-6: Left Foot Location Variability per Location and Grouped by Cohort

7.1.3. Utilizing the Automated Tool for Treatment Monitoring

7.1.3.1. Introduction

It has been demonstrated in Chapters 4 and 5 of this dissertation that the automated tool effectively documented plantar threshold sensitivity in healthy individuals without type 2 diabetes mellitus, as well as individuals with type 2 diabetes mellitus, with and without neuropathy symptoms. However, these subjects were only evaluated once using the device. The automated tool has the potential to document threshold sensitivity over the course of time to obtain a long-term picture of the subject's degree of sensation loss. This can either be achieved by having the machine operator reselect the locations on the plantar surface to be reevaluated, or the MATLAB script can be modified to automate this process. An accurate assessment, in addition to documentation, is necessary to effectively monitor the efficacy of treatments.

Treatments often fall into the categories of pain management or targeting underlying conditions related to diabetes [113]. Drugs for the treatment of epilepsy, antidepressants, painkillers, and anti-inflammatories have been prescribed to suppress symptoms caused by diabetic peripheral neuropathy [113, 114]. The medications: duloxetine, mexiletine, nortriptyline, and pregabalin have been used for the treatment of neuropathy, but none produced an effective reduction of symptoms [115]. Improving one's lifestyle in the forms of regularly exercising, eating healthier, and quitting smoking can be beneficial [113, 114]. However, many sources have indicated that there is currently no cure for this disease [115, 116]. The transcutaneous electrical nerve stimulation (TENS) and the frequency rhythm electrical modulation system (FREMS) have been used to treat neuropathy [117, 118]. The FREMS mechanism alleviated symptoms for up to three months after treatment [119]. Compression devices, such as compression socks have also been

studies to reduce neuropathy symptoms, as well as warm water, acupuncture, and massaging the lower extremities [120, 121] Two types of interventions are proposed with the use of the automated tool: studying activity level over the course of time and the invention of an accompanying novel treatment device.

7.1.3.2. Activity Level Compared to TSI Norm

A study using subjects with type 2 diabetes mellitus and neuropathy symptoms are recommended to study how activity level can not only improve symptoms, but potentially improve threshold sensitivity on the plantar surface. Four groups of subjects would be recommended, each with 30 individuals. The variable introduced into the study would be the number of steps per day each subject would be required to walk or run. 2,500, 3,250, 3,250, and 5,000 steps per day would be assigned to subjects placed into one of the four groups. Ideally, subjects would have similar ages, ABIs, and BMIs in order to account for outliers. Subjects would be prescreened before the study began to make sure these metrics were all similar, with an ABI greater than or equal to 1.0 mmHg and an age greater than or equal to 50. All subjects would be from the same geographical location, and all would be studied during the same time of year. All 120 subjects would start their regimen within the same week. Daily measurements would be recorded using Pedometers and the subjects would need to keep a log of their steps. Every week they would hand off their daily step log to the researchers. Subjects would be provided an Apple Watch or Fitbit to record their daily steps. Each week, subjects would be required to have a reassessment using the automated tool to document their threshold sensitivity over time. Each subject would be evaluated at the same day and time every week for three months. Furthermore, during the subject's weekly assessment, they will also report the severity of their symptoms on an index

between one to ten, with ten being the worst. Additionally, the subjects would need to provide a sample of blood to document their fasting blood sugar each week. Blood pressure readings would also be required for each office visit. Fasting blood sugars and blood pressure readings are needed to correlate these measurements with activity level and to observe these trends over time. Four automated tools would be required to evaluate six subjects per day, to study all 120 subjects within a working week. A team of eight researchers are recommended to interact with subjects every week, to operate the machine and interact with the subjects. At the conclusion of the study the results could be analyzed to understand how activity level impacted TSI Norm.

7.1.3.3. Analyzing the Efficacy of a Novel Non-pharmacological Treatment Device

The invention of this automated tool for neuropathy assessment on the plantar surface of the foot demonstrated the benefits of implementing robotics into the field of medicine. As such a novel non-pharmacological treatment device would complement the automated tool. By combining compression and temperature into a single system targeted at the lower extremities it may be possible to promote healthy circulation, preventing the buildup of edema. The proposed solution is a hot water compression boot, with multiple bladder systems, which surrounds the foot and the shank of the leg concurrently. Figure 7-6 is a representation of this device. This device could oscillate the rate in which the separate bladder systems fill with hot water, causing systematic compression of the lower extremities. Such a device can be achieved with between three and five individual bladder systems, interconnected with a system of valves and a pump. As each valve opens and closes it will compress the bladder around the area of focus. All of the bladder systems would be housed inside a fabric sleeve, which keeps the device together, yet still allows for the transmission of temperature to the subject. Arduinos, actuators, flow sensors, and temperature

sensors, would all be required to operate this device. A small pilot study with ten individuals, all with type 2 diabetes mellitus and neuropathy symptoms could be used to test the efficacy of this treatment device. Each would be trained on how to setup and use the system, while in the comfort of their own home. Subjects would be asked to use the device every day, between 30 and 45 minutes, for six months. It would also be necessary for subjects to come into the office every two weeks to be evaluated using the automated device in order to track their threshold sensitivity, in the form of TSI Norm. Subjects will also document the pain caused by their symptoms and provide that information to the research staff. At the end of the study, the results could indicate whether this novel treatment prevented further sensation loss and or alleviated painful neuropathy symptoms.

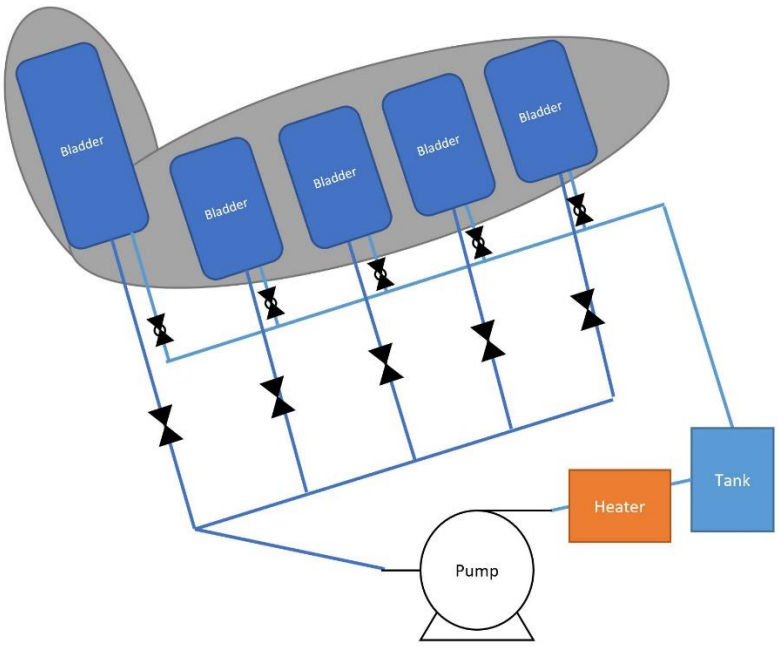

Figure 7-7: Proposed Non-Pharmacological Treatment Device

7.2. Recommendations and Improvements

7.2.1. Revised Homing Sequence Protocol

In order to speed up the assessment methodology, different procedures can be considered to determine the threshold sensitivity on numerous locations on the plantar surface. The homing sequence demonstrated in Chapters 4 and 5 was used on all subjects, regardless of group classification. This type of protocol was effective for individuals without symptoms and enabling a baseline of the subject. However, at linear approach may save more time, depending on the subject. It may be better to evaluate a healthy subject by applying the monofilament at increasing amounts of force, starting at 0.35 grams of force and ending at 10.0 grams of force, in ascending order. While a subject with painful neuropathy symptoms may benefit from starting the assessment at 10.0 grams of force and working their way down to 0.35 grams of force, in descending order. This could be used in subsequent evaluations using the automated tool once the subject's TSI Norm has been established.

An adaptive approach for follow up evaluations may also be useful, meaning that at the beginning of the reassessment each individual location can initially be tested at what the previous evaluation determined was the threshold sensitivity. Depending on their initial response, a new homing sequence could determine the specific location's new threshold sensitivity. This paired with the future work examining the threshold sensitivity variability versus plantar surface location could greatly improve the assessment time.

7.2.2. Methods for Reducing Device Errors During Assessments

One of the biggest revelations from the clinical study conducted in Chapters 4 and 5 was that subjects were able to influence the accuracy of the device by firmly placing their foot against the

foot plate. In the current versions of the MATLAB script and the code on the Arduino Uno there is no way to see the resulting contact force immediately after it has been applied. The machine operator can only view these data at the end of the assessment by going through the data results. The code can be modified to analyze for occurrences when an absolute error greater than 0.5 grams of force takes place. It can then notify the operator that a device error occurred and that a reassessment is recommended. The operator can then instruct the subject to relax their foot. The Arduino code could also be modified to decrease its insertion rate when device errors have occurred during an assessment.

Another solution would be to mount a strain gauge on the acrylic foot plate, which could be wired to either to a physical light or feedback sensor into the MATLAB script. The strain gauge could be used to indicate when subjects are distorting the foot plate. The use of a light could alert the subject and operator when the foot plate is being distorted.

The last proposal to prevent device errors is to consider mounting the automated tool on an adjustable pivot. This would allow subjects to have their foot in plantar flexion during evaluation. Some subjects may find this more comfortable and may not have the need to firmly place their foot against the acrylic plate. The pivot should allow between zero and thirty degrees of rotation but will need to be locked in place during operation.

7.2.3. Code Improvements

The code used to control the automated tool can be improved to make it more robust. The MATLAB script communicated with the Arduino Mega's GRBL code and the Arduino Uno's custom code over serial USB communication. Although this worked well in the prototypes

developed in this dissertation, a single coding environment, such as ROS or C+ would be better in a commercial version of the automated tool. In order to get the MATLAB script to communicate with the Arduinos “pauses” had to be used throughout the code to not overwhelm the serial port, which is not ideal. The script was optimized for the prototypes created, but if developed in a program that allowed for more parallel processing, the code would be more efficient, hence allowing the implementation of other improvements. Another addition to the code is incorporating variable feed rates based upon relative distances between locations. If after randomization, two locations are separated by a farther distance, then it would be prudent for the gantry subassembly to move the probe as quickly as possible. This can be achieved by modifying the g-code sent from the MATLAB script to the Arduino Mega. Moreover, a graphical user interface would be an improvement over the dialogue boxes that currently guide the operator through the device procedures. The last coding improvement would be to consider a Raspberry Pi to not only control the entire machine, but also replacing the need for a separate laptop. A display, keyboard, and mouse could be connected to a Raspberry Pi, which could also replace both Arduinos. If this action was taken, then GRBL would need to be replaced with a different g-code interpreter.

7.2.4. Probe Subassembly Improvements

One area of interest that involves the probe subassembly is analyzing the impulse of the monofilament as it contacts the plantar surface. Although the device does analyze these data to reduce its rate of insertion as it approaches the desired force, more could be done. Finding ways to correlate the impulse to the elasticity of human skin could be a way to further improve the device’s accuracy. However, one change that could be invaluable to the automated tool would be to replace the stepper motor used in the probe subassembly with a DC motor. DC motors use a

feedback loop in order to keep track of the position during use, which is not very different than what has been used in this dissertation. Yet, stepper motors are considered more accurate in position-controlled applications, such as 3D printers and CNC devices. Evaluating the feasibility of a DC motor would be a recommended next step, by investigating if the contact force accuracy can be improved.

7.2.5. Future Analysis

The data analyzed in Chapters 4, 5, and 7 have been performed by using univariate linear regressions, by comparing TSI Norm to age, BMI, ABI, FBS, and HbA1c. The influence of sex on these parameters has also been presented. However, the interactions of multiple medical characteristics on TSI Norm concurrently have not been addressed in this dissertation. Multivariate linear regression by comparing TSI Norm to different combinations of age, BMI, ABI, FBS, and HbA1c is a recommended analysis that future studies should examine. The data from Chapter 4 and 5 have been used to perform multivariate analysis considering combinations of two, three, four, and five of the medical characteristics. All of these permutations have been performed on the Group 1, 2, and 3 subjects. The results of these analyses are documented in Appendix L, M, and N. However, after 63 permutations, multivariate analysis has not provided any additional insights into the data. Although the analyses were performed within groups, additional analyses considering two-way and three-way ANOVAs are recommended, as well as MANOVA analyses.

Another recommended analysis is the calculations of sensitivity, specificity, positive predictive value, and negative predictive value when comparing the hand-applied Semmes-Weinstein

monofilaments to the automated tool. These measurements have been calculated using data available from the Group 1, 2 and 3 subjects, and are provided in Appendix O. However, in order to strengthen these findings, the automated tool should be compared to not only a 10.0 grams of force rated monofilament, but all available monofilaments between 0.35 grams of force and 10.0 grams of force. By doing this, each category that the automated tool assesses at can be directly compared to a corresponding hand-applied monofilament. This type of analysis would strengthen the findings of the automated tool.

Chapter 8: Conclusion

The purpose of this dissertation is to demonstrate the practical concerns of the hand-applied Semmes-Weinstein neuropathy assessment, present a novel diagnostic tool which automated the assessment protocol, and communicate the results of the implementation of this tool in a clinical study to ascertain subjects' current degree of threshold sensitivity on the plantar surface.

Chapter 2 of this dissertation details the results obtained considering theoretical contact mechanics and finite element analysis when modeling the contact between a nylon Semmes-Weinstein monofilament on a human skin sample. Specifically, the study examined how insertion depth, monofilament diameter, and human skin material properties affected neuropathy assessment on the plantar surface, when modeling a non-buckling monofilament. Empirical equations, which considered the epidermis and dermis elastic moduli of human skin, demonstrate the challenges associated with using a hand-applied monofilament to accurately apply 10.0 grams of force to the plantar surface. Depending on the epidermis and the dermis properties an insertion depth between 0.235 and 0.559 mm would be required to create a contact force of exactly 10.0 grams of force by hand, assuming a non-buckling monofilament.

The findings from Chapter 2 encouraged the development of an automated tool, detailed in Chapter 3, which accounted for the practical concerns of using a hand-applied Semmes-Weinstein monofilament for neuropathy assessment. The creation of the automated tool brought with it the potential for an improved assessment methodology, incorporating aspects such as documentation, randomization, and false positive assessments.

The automated tool was used in a clinical study outlined in Chapters 4 and 5. Chapter 4 analyzed control subjects who were not diagnosed with type 2 diabetes mellitus. The accuracy in terms of absolute error was calculated using the control subjects, which demonstrated that the device had an average absolute error less than or equal to 0.4 grams of force between 60% and 98% of locations, depending on the region. The toes yielded the most sensitive locations assessed, with 63% of locations having a threshold sensitivity under 4.0 grams of force. Hand-applied monofilaments were underdiagnosing sensation loss at the 10.0-gram force threshold at a rate of 21%, relative to the automated tool. TSI Norm was used to quantify a subject's threshold sensitivity at thirteen locations per foot. Control subjects significantly attributed their degree of sensation to their age (R^2=0.3422, P=0.004), but not to their BMI, ABI, fasting blood sugar, or HbA1c. Chapter 5 compared the healthy control subjects from Chapter 4 to individuals with diagnosed type 2 diabetes mellitus, with and without neuropathy symptoms. The subjects in all three groups had similar ages, BMIs, and ABIs, while only differing in their fasting blood sugar and HbA1c. However, this study failed to find a significant difference between each group's TSI Norm. Both groups with diabetes did not yield a correlation between threshold sensitivity and the other medical characteristics examined in this work.

In Chapter 6, the second iteration of the automated tool was presented and featured its various improvements over the first prototype. Chapter 7 presented three future directions this research can be taken using the automated for analyzing the effects of sex, time of year, location variability, and treatment monitoring on threshold sensitivity. Furthermore, additional recommendations and improvements to the automated tool are provided, mainly in the area of coding and controls.

This dissertation concludes with the assertion that the automated tool developed is an improved device compared to the commercially available and widely used Semmes-Weinstein monofilament. Its corresponding methodology provides the standardization needed to not only study neuropathy assessment on the plantar surface, but also studying the efficacy of future treatments.

References

[1] WebMD, "Understanding Peripheral Neuropathy -- the Basics," [Online]. Available: https://www.webmd.com/brain/understanding-peripheral-neuropathy-basics#1.

[2] American Diabetes Assoication, "Peripheral Neuropathy," [Online]. Available: https://www.diabetes.org/diabetes/complications/neuropathy/peripheral-neuropathy.

[3] American Diabetes Association, "Neuropathy," [Online]. Available: https://www.diabetes.org/diabetes/complications/neuropathy.

[4] J. J. Brown, S. L. Pribesh, K. G. Baskette, A. I. Vinik and S. R. Colberg, "A Comparison of Screening Tools for the Early Detection of Peripheral Neuropathy in Adults with and without Type 2 Diabetes," *Journal of Diabetes Research,* vol. 2017, pp. 1-11, 2017. doi: 10.1155/2017/1467213.

[5] International Diabetes Federation, "IDF Diabetes Atlas, 9th edn.," *International Diabetes Federation,* pp. 1-179, 2019. Available: https://diabetesatlas.org/.

[6] V. Skljarevski, "Historical Aspects of Diabetic Neuropathies," in *Diabetic Neuropathy Clinical Management 2nd Edition,* Totowa, Humana Press, 2007: https://doi.org/10.1007/978-1-59745-311-0_1, pp. 1-5.

[7] V. Skljarevski and A. Vladimir, "Diabetic Neuropathies," *Arch Neurol,* vol. 63, no. 10, pp. 1502-1504, 2006: doi:10.1001/archneur.63.10.1502.

[8] C. W. Hicks and E. Selvin, "Epidemiology of Peripheral Neuropathy and Lower Extremity Disease in Diabetes," *Current Diabetes Reports volume,* vol. 19, no. 10, pp. 1-13, 2019: doi:10.1007/s11892-019-1212-8.

[9] J. Dros, A. Wewerinke, P. J. Bindels and H. C. V. Weert, "Accuracy of Monofilament Testing to Diagnose Peripheral Neuropathy: A Systematic Review," *Annals of Family Medicine,* vol. 7, no. 6, pp. 555-558, 2009. doi: 10.1370/afm.1016.

[10] A. Nather, W. K. Lin, Z. Aziz, C. H. J. Ong, B. M. C. Feng and C. B. Lin, "Assessment of sensory neuropathy in patients with diabetic foot problems," *Diabetic Foot & Ankle,* vol. 2, no. 1, pp. 1-5, 2011. doi: 10.3402/dfa.v2i0.6367.

[11] B. C. Callaghan, H. Cheng, C. L. Stables, A. L. Smith and E. L. Feldman, "Diabetic neuropathy: Clinical manifestations and current treatments," *The Lancet Neurology,* vol. 11, no. 6, pp. 1-29, 2012: doi: 10.1016/S1474-4422(12)70065-0.

[12] M. Lepantaloa, J. Apelqvist , C. Setacci, J. B. . Ricco, G. de Donato, F. Becker, H. Robert-Ebadi , P. Cao, H. H. Eckstein, P. De Rango, N. Diehm, J. Schmidli, M. Teraa, F. L. Moll , F. Dick and A. H. Davies , "Chapter V: Diabetic Foot," *European Journal of Vascular and Endovascular Surgery,* vol. 42, no. S2, pp. S60-S74, 2011: DOI:https://doi.org/10.1016/S1078-5884(11)60012-9.

[13] M. Kiyani, Z. Yang, L. T. Charalambous, S. M. Adil, H.-J. Lee, S. Yang, P. Pagadala, B. Parente, S. E. Spratt and S. P. Lad, "Painful diabetic peripheral neuropathy- Health care costs and complications from 2010 to 2015," *Neurology Clinical Practice,* vol. 10, no. 1, pp. 47-57, 2019: doi:10.1212/CPJ.0000000000000671.

[14] M. Mehra, S. Merchant, S. Gupta and R. C. Potluri, "Diabetic peripheral neuropathy: resourceDiabetic peripheral neuropathy: resource utilization and burden of illness,"

Journal of Medical Economics, vol. 17, no. 9, pp. 637-645, 2014: doi:10.3111/13696998.2014.928639.

[15] A. Gordois, P. Schuffham, A. Shearer, A. Oglesby and J. A. Tobian, "The Health Care Costs of Diabetic Peripheral Neuropathy in the U.S.," *Diabetes Care,* vol. 26, no. 6, pp. 1790-1795, 2003: https://doi.org/10.2337/diacare.26.6.1790.

[16] American Diabetes Association , "Economic Costs of Diabetes in the U.S. in 2017," *Diabetes Care,* vol. 41, no. 5, pp. 917-928, 2018: https://doi.org/10.2337/dci18-0007.

[17] Mayo Clinic, "Diabetic neuropathy," Mayo Foundation for Medical Education and Research, 2022. [Online]. Available: https://www.mayoclinic.org/diseases-conditions/diabetic-neuropathy/symptoms-causes/syc-20371580#:~:text=Researchers%20think%20that%20over%20time,nerves%20with%20oxygen%20and%20nutrients.. [Accessed 22 May 2022].

[18] E. L. Feldman, B. C. Callaghan, R. Pop-Busui, D. W. Zochodne, D. E. Wright, D. L. Bennett, V. Bril, J. W. Russell and V. Viswanathan, "Diabetic neuropathy," *Nature Reviews Disease Primers,* vol. 5, no. 41, pp. 1-18, 2019: https://doi.org/10.1038/s41572-019-0092-1.

[19] "IDF Diabetes Atlas, 10th edn," *International Diabetes Federation,* pp. 1-141, 2021. Available: https://diabetesatlas.org/.

[20] A. Aslam, J. Singh and S. Rajbhandari, "Pathogenesis of Painful Diabetic Neuropathy," *Pain Research and Treatment,* vol. 2014, pp. 1-7, 2014: http://dx.doi.org/10.1155/2014/412041.

[21] M. Yorek, R. A. Malik, N. A. Calcutt, A. Vinik and S. Yagihashi, "Diabetic Neuropathy: New Insights to Early Diagnosis and Treatments," *Journal of Diabetes Research,* vol. 2018, pp. 1-3, 2018: https://doi.org/10.1155/2018/5378439.

[22] V. Bril, "Treatments for diabetic neuropathy," *Journal of the Peripheral Nervous System,* vol. 17, no. S2, pp. 22-27, 2012: https://doi.org/10.1111/j.1529-8027.2012.00391.x.

[23] E. L. Feldman, "Pathogenesis and Prevention of Diabetic Polyneuropathy," *UpToDate,* 2018: https://www.uptodate.com/contents/pathogenesis-of-diabetic-polyneuropathy#H185172517.

[24] M. Hecht, "What Is Peripheral Edema and What Causes It?," Healthline Media, 25 June 2018. [Online]. Available: https://www.healthline.com/health/peripheral-edema. [Accessed 22 May 2022].

[25] A. Veves, M. Backonja and R. A. Malik, "Painful Diabetic Neuropathy: Epidemiology, Natural History, Early Diagnosis, and Treatment Options," *Pain Medicine,* vol. 9, no. 6, pp. 660-674, 2008: DOI: 10.1111/j.1526-4637.2007.00347.x.

[26] B. A. Brouwer, M. Bakkers, J. G. J. Hoeijmakers, C. G. Faber and I. S. J. Merkies, "Improving assessment in small fiber neuropathy," *Journal of the Peripheral Nervous System,* vol. 20, no. 3, pp. 333-340, 2015. doi: 10.1111/jns.12128.

[27] A. J. M. Boulton, D. G. Armstrong, S. F. Albert, R. G. Frykberg, R. Hellman, M. S. Kirkman, L. A. Lavery, J. W. LeMaster, J. L. Mills, M. J. Mueller, P. Sheehan and D. K. Wukich, "Comprehensive Foot Examination and Risk Assessment," *Diabetes Care,* vol. 31, no. 8, pp. 1679-1685, 2008. https://doi.org/10.2337/dc08-9021.

[28] A. M. Aring, D. E. Jones and J. M. Falko, "Evaluation and Prevention of Diabetic Neuropathy," *American Family Physician,* vol. 71, no. 11, pp. 2123-2128, 2005. https://www.aafp.org/afp/2005/0601/p2123.html.

[29] R. J. Tanenberg and P. D. Donofrio, "Chapter 3-Neuropathic Problems of the Lower Limbs in Diabetic Patients," in *Levin and O'Neal's: The Diabetic Foot,* 2008, pp. 33-74. doi:10.1016/B978-0-323-04145-4.50010-7.

[30] John Hopkins Medicine, "Diabetic Neuropathy," Health, 2022. [Online]. Available: https://www.hopkinsmedicine.org/health/conditions-and-diseases/diabetes/diabetic-neuropathy-nerve-problems. [Accessed 12 May 2022].

[31] Cleveland Clinic, "Diabetic Neuropathy," 29 April 2021. [Online]. Available: https://my.clevelandclinic.org/health/diseases/21621-diabetic-neuropathy. [Accessed 12 May 2022].

[32] Y. Brazier, "What to know about diabetic neuropathy," Healthline Media, 19 March 2019. [Online]. Available: https://www.medicalnewstoday.com/articles/245310. [Accessed 12 May 2022].

[33] Cleveland Clinic, "Charcot Foot," 2022. [Online]. Available: https://my.clevelandclinic.org/health/diseases/15836-charcot-foot. [Accessed 12 May 2022].

[34] K. G. Prabhu, D. Agrawal, K. M. Patil and S. Srinivasan, "Parameters for analysis of walking foot pressures at different levels of diabetic neuropathy and detection of plantar ulcers at early stages," *IRBM,* vol. 22, no. 3, pp. 159-169, 2001. doi:10.1016/S1297-9562(01)90027-0.

[35] C. Pirri, C. Fede, N. Pirri, L. Petrelli, C. Fan, R. De Caro and C. Stecco, "Diabetic Foot: The Role of Fasciae, a Narrative Review," *Bioloigy,* vol. 10, no. 8, pp. 1-14, 2021: https://doi.org/10.3390/biology10080759.

[36] M. Tavakoli, D. G. Yavuz, A. A. Tahrani, D. Selvarajah, F. L. Bowling and H. Fadavi, "Diabetic Neuropathy: Current Status and Future Prospects," *Journal of Diabetes Research,* vol. 2017, pp. 1-2, 2017: https://doi.org/10.1155/2017/5825971.

[37] C.-P. L. Alfonso, A. Durán, A. Benedí, M. I. Calvo, A. Charro, J. A. Diaz, J. R. Calle, E. Gil, J. P. Marañes and J. Cabezas-Cerrato, "A preventative foot care programme for people with diabetes with different stages of neuropathy," *Diabetes Research and Clinical Practice,* vol. 57, no. 2, pp. 111-117, 2002: https://doi.org/10.1016/S0168-8227(02)00024-4.

[38] A. J. Boulton, "The Pathway to Foot Ulceration in Diabetes," *Medical Clinics of North America,* vol. 97, no. 5, pp. 775-790, 2013: https://doi.org/10.1016/j.mcna.2013.03.007.

[39] Orthopaedia, "Anatomy of the Foot and Ankle," Orthopaedia, 2022. [Online]. Available: https://orthopaedia.com/page/Anatomy-of-the-Foot-Ankle. [Accessed 16 May 2022].

[40] TeachMe Anatomy, "Muscles of the Foot," TeachMe Series, 2022. [Online]. Available: https://teachmeanatomy.info/lower-limb/muscles/foot/. [Accessed 16 May 2022].

[41] M. Bourne, A. Talkad and M. Varacallo, "Anatomy, Bony Pelvis and Lower Limb, Foot Fascia," National Library of Medicine, 11 August 2021. [Online]. Available: https://www.ncbi.nlm.nih.gov/books/NBK526043/. [Accessed 17 May 2022].

[42] M. De Maeseneer, H. Madani, L. Lenchik, M. K. Brigido, M. Shahabpour, S. Marcelis, J. de Mey and A. Scafoglieri, "Normal Anatomy and Compression Areas of Nerves of the Foot and Ankle: US and MR Imaging with Anatomic Correlation," *RadioGraphics,* vol. 35, pp. 1469-1482, 2015: DOI 10.1148/rg.2015150028.

[43] Physiopedia, "Basic Foot and Ankle Anatomy - Neural and Vascular," Physiopedia, 2022. [Online]. Available: https://www.physio-pedia.com/Basic_Foot_and_Ankle_Anatomy_-_Neural_and_Vascular. [Accessed 31 May 2022].

[44] T. Mete, Y. Aydin, M. Saka, H. C. Yavuz, S. Bilen, Y. Yalcin, B. Arli, D. Berker and S. Guler, "Comparison of Efficiencies of Michigan Neuropathy Screening Instrument, Neurothesiometer, and Electromyography for Diagnosis of Diabetic Neuropathy," *International Journal of Endocrinology,* vol. 2013, pp. 1-7, 2013: http://dx.doi.org/10.1155/2013/821745.

[45] A. Moghtaderi, A. Bakhshipour and H. Rashidi, "Validation of Michigan neuropathy screening instrument for diabetic peripheral neuropathy," *Clinical Neurology and Neurosurgery,* vol. 108, no. 5, pp. 477-481, 2005: doi:10.1016/j.clineuro.2005.08.003.

[46] O. Boyraz and M. Saracoglu, "The effect of obesity on the assessment of diabetic peripheral neuropathy: A comparison of Michigan patient version test and Michigan physical assessment," *Diabetes Research and Clinical Practice ,* vol. 90, no. 3, pp. 256-260, 2010: doi:10.1016/j.diabres.2010.09.014.

[47] A. Vinik, C. Casellini and M.-L. Névoret, "Chapter Thirteen - Alternative Quantitative Tools in the Assessment of Diabetic Peripheral and Autonomic Neuropathy," in *Controversies In Diabetic Neuropathy,* Cambridge, Elsvier, 2016: https://doi.org/10.1016/bs.irn.2016.03.010, pp. 235-285.

[48] Z. Yang, R. Chen, Y. Zhang, Y. Huang, Y. Hong, T. Hong, F. Sun, F. Ji and S. Zhan, "Scoring systems to screen for diabetic peripheral neuropathy," *Cochrane Database System Reviews,* vol. 2018, no. 7, pp. https://www.ncbi.nlm.nih.gov/pmc/articles/PMC6513667/#:~:text=Neuropathy%20disability%20score%20(NDS)%20and,of%20sensation%20(Dyck%201980)., 2018.

[49] A. I. Veresiu, C. I. Bondor, B. Florea, E. J. Vinik, A. I. Vinik and N. A. Gâvan, "Detection of undisclosed neuropathy and assessment of its impact on quality of life: a survey in 25,000 Romanian patients with diabetes," *Journal of Diabetes and Its Complications,* vol. 29, no. 5, pp. 644-69, 2015: https://doi.org/10.1016/j.jdiacomp.2015.04.001.

[50] M. H. Haloua, I. Sierevelt and W. J. Theuvenet, "Semmes-Weinstein Monofilaments: Influence of Temperature, Humidity, and Age," *The Journal of Hand Surgery,* vol. 36, no. 7, pp. 1191-1196, 2011. doi: 10.1016/j.jhsa.2011.04.009.

[51] M. J. G. Bradman, F. Ferrini, C. Salio and A. Merighi, "Practical mechanical threshold estimation in rodents using von Frey hairs/Semmes–Weinstein monofilaments: Towards a rational method," *Journal of Neuroscience Methods,* vol. 255, pp. 92-103, 2015. doi: 10.1016/j.jneumeth.2015.08.010.

[52] Y. Feng, F. J. Schlösser and B. E. Sumpio, "The Semmes Weinstein monofilament examination as a screening tool for diabetic peripheral neuropathy," *Journal of Vascular Surgery,* vol. 50, no. 3, pp. 675-682, 2009. doi: 10.1016/j.jvs.2009.05.017.

[53] J. A. Bell-Krotoski, E. E. Fess, J. H. Figarola and D. Hiltz, "Threshold Detection and Semmes-Weinstein Monofilaments," *Journal of Hand Therapy,* vol. 8, no. 2, pp. 155-162, 1995. doi: 10.1016/s0894-1130(12)80314-0.

[54] M. Chikai and S. Ino, "Buckling Force Variability of Semmes–Weinstein Monofilaments in Successive Use Determined by Manual and Automated Operation," *SENSORS,* vol. 19, no. 4, pp. 1-9, 2019. doi: 10.3390/s19040803.

[55] I. Willits, H. Cole, R. Jones, P. Dimmock, M. Arber, J. Craig and A. Sims, "VibraTip for Testing Vibration Perception to Detect Diabetic Peripheral Neuropathy: A NICE Medical Technology Guidance," *Applied Health Economics and Health Policy,* vol. 13, no. 4, pp. 315-324, 2015: DOI 10.1007/s40258-015-0181-6.

[56] L. Vileikyte, G. Hutchings, S. Hollis and A. Boulton, "The Tactile Circumferential Discriminator," *Diabetes Care,* vol. 20, no. 4, pp. 623-626, 1997: https://doi.org/10.2337/diacare.20.4.623.

[57] T. Ananthakumar, C. Heneghan, C. P. Price, A. Van den Bruel and A. Plüddemann, "Point-of-care devices for detecting diabetic polyneuropathy- Horizon Scan Report 0046," *National Institute for Health Research,* pp. 1-10, 2016: https://www.community.healthcare.mic.nihr.ac.uk/reports-and-resources/horizon-scanning-reports/horizon-scan-report-0046#:~:text=The%20NC%2Dstat%20DPN%20check,detecting%20abnormalities%20is%20pre%2Ddefined..

[58] N. Papanas, A. Gries, E. Maltezos and R. Zick, "The steel ball-bearing test: a new test for evaluating protective sensation in the diabetic foot," *Diabetologia,* vol. 49, pp. 739-743, 2006: DOI 10.1007/s00125-005-0111-5.

[59] D. Ziegler, E. Siekierka-Kleiser, B. Meyer and M. Schweers, "Validation of a Novel Screening Device (NeuroQuick) for Quantitative Assessment of Small Nerve Fiber Dysfunction as an Early Feature of Diabetic Polyneuropathy," *Diabetes Care,* vol. 28, no. 5, pp. 1169-1174, 2005: DOI: 10.2337/diacare.28.5.1169.

[60] M. J. Young, N. Every and A. J. Boulton, "A comparison of the neurothesiometer and biothesiometer for measuring vibration perception in diabetic patients," *Diabetes Research and Clinical Practice,* vol. 20, no. 2, pp. 129-131, 1993: DOI: https://doi.org/10.1016/0168-8227(93)90006-Q.

[61] A. P. Popov, A. V. Bykov and I. V. Meglinski, "Influence of probe pressure on diffuse reflectance spectra of human skin measured in vivo," *Journal of Biomedical Optics,* vol. 22, no. 11, pp. 1-4, 2017. doi: 10.1117/1.JBO.22.11.110504.

[62] J. Burgess, B. Frank, A. Marshall, R. S. Khalil, G. Ponirakis, I. N. Petropoulos, D. J. Cuthbertson, R. A. Malik and U. Alam, "Early Detection of Diabetic Peripheral Neuropathy: A Focus on Small Nerve Fibres," *diagnostics,* vol. 11, no. 165, pp. 1-39, 2021: https://doi.org/10.3390/diagnostics11020165.

[63] SUDOSCAN by impetomedical, "About SUDOSCAN," Impeto Medical, 23 January 2021. [Online]. Available: https://www.sudoscan.com/sudoscan/. [Accessed 12 May 2022].

[64] NEUROMetrix, "DPNCheck Overview," NeuroMetrix, Inc., 2022. [Online]. Available: https://www.dpncheck.com/overview/. [Accessed 14 May 2022].

[65] Medoc, "QST Technique," Medoc, 2020. [Online]. Available: https://www.medoc-web.com/qst-technique. [Accessed May 14 2022].

[66] C. Wilasrusmee, J. Suthakorn, C. Guerineau, Y. Itsarachaiyot, V. Sa-Ing, N. Proprom, P. Lertsithichai, S. Jirasisrithum and D. Kittur, "A Novel Robotic Monofilament Test for Diabetic Neuropathy," *Asian Journal of Surgery,* vol. 33, no. 4, pp. 193-198, 2010: https://doi.org/10.1016/S1015-9584(11)60006-7.

[67] H. U. Siddiqui, M. Spruce, S. R. Alty and S. Dudley, "Automated Semmes Weinstein monofilament examination replication using optical imaging and mechanical probe assembly," *2015 IEEE 12th International Symposium on Biomedical Imaging (ISBI),* pp. 552-555, 2015: doi: 10.1109/ISBI.2015.7163933.

[68] H. U. R. Siddiqui, "Automated Peripheral Sensory Neuropathy Assessment of Diabetic Patients Using Optical Imaging and Binary Processing Techniques," pp. 1-137, 2016: https://openresearch.lsbu.ac.uk/download/b7a6909de88733b3904e0aac85f6e97009230d200fc67a91377627dc177b59a2/3591493/2016_PhD_Siddiqui.pdf.

[69] M. C. Spruce and F. L. Bowling, "Diabetic Foot Screening: New Technology versus 10g Monofilament," *The International Journal of Lower Extremity Wounds,* vol. 11, no. 1, pp. 43-48, 2012: DOI: 10.1177/1534734612438055.

[70] W. F. W. Leung and K. T. A. Lau, "AUTOMATED TESTING FOR PALPATING DABETC FOOT PATENT". United State Patent US 9,017,266 B2, 25 April 2015.

[71] S. Ino, M. Sato, N. Takahashi and S. Yoshimura, "APPARATUS AND METHOD FOR EVALUATING DABETIC PERPHERAL NEUROPATHY". United States Patent US 2015/0182158A1, 2 July 2015.

[72] M. V. Snellenberg, A. Weiler, L. Feaster, B. Spencer, J. Chung, J. Hansen-Lund, S. Mandel, J. Bishop and G. Ray, "DEVICE FOR NON - INVASIVE DETECTION OF SKIN PROBLEMS ASSOCIATED WITH DIABETES MELLITUS". United States Patent US 2019/0021649 A1, 24 January 2019.

[73] I. J. Spruce, "Force Transducer, Medical Instrument, and Machine Implemented Method". United Kingdom Patent GB 2472168A, 26 January 2011.

[74] L. A. Lavery, D. E. Lavery, D. C. Lavery, J. LaFontaine, M. Bharara and B. Najafi, "Accuracy and durability of Semmes–Weinstein monofilaments: What is the useful service life?," *Diabetes Research and Clinical Practice,* vol. 97, no. 2012, pp. 399-404, 2012: http://dx.doi.org/10.1016/j.diabres.2012.04.006.

[75] M. McGill, L. Molyneaux and D. K. Yue, "Use of the Semmes–Weinstein 5.07/10 Gram Monofilament: the Long and the Short of it," *Diabetic Medicine,* vol. 15, pp. 615-617, 1998.

[76] V. K. Castellano, R. L. Jackson and M. E. Zabala, "Contact Mechanics Modeling of the Semmes-Weinstein Monofilament on the Plantar Surface of the Foot," *International Journal of Foot and Ankle,* vol. 5, no. 2, pp. 1-13, 2021. doi: 10.23937/2643-3885/1710055.

[77] F. Wang, J. Zhang, J. Yu, S. Liu, R. Zhang, X. Ma, Y. Yang and P. Wang, "Diagnostic Accuracy of Monofilament Tests for Detecting Diabetic Peripheral Neuropathy: A Systematic Review and Meta-Analysis," *Journal of Diabetes Research,* vol. 2017, pp. 1-12, 2017: https://doi.org/10.1155/2017/8787261.

[78] American Diabetes Assoication, "Standards of Medical Care in Diabetes—2008," *Diabetes Care,* vol. 31, no. 1, pp. 12-54, 2008: https://doi.org/10.2337/dc08-S012.

[79] E. Lindholm, M. Löndahl, K. Fagher, J. Apelqvist and L. B. Dahlin, "Strong association between vibration perception thresholds at low frequencies (4 and 8 Hz), neuropathic symptoms and diabetic foot ulcers," *PLos One,* vol. 14, no. 2, pp. 1-15, 2019. doi: 10.1371/journal.pone.0212921.

[80] L. Vileikyte, R. T. Crews and N. D. Reeves, "Psychological and Biomechanical Aspects of Patient Adaptation to Diabetic Neuropathy and Foot Ulceration," *Current Diabetes Reports,* vol. 17, pp. 1-11, 2017. doi: 10.1007/s11892-017-0945-5.

[81] R. V. Deursen, "Mechanical Loading and Off-Loading of the Plantar Surface of the Diabetic Foot," *Clinical Infectious Diseases,* vol. 33, no. 2, pp. 87-91.

[82] I. Okpe, E. Ugwu, O. Adeleye, I. Gezawa, M. Enamino and I. Ezeani, "Foot Care Education, Health-Seeking Behavior and Disease Outcome in Patients with Diabetic Foot Ulcer: Result from the Multi-Centre Evaluation of Diabetic Foot Ulcer in Nigeria Study," *International Journal of Foot and Ankle,* vol. 3, no. 2, pp. 1-8, 2019. doi: 10.23937/2643-3885/1710038.

[83] M. T. Olaiya, R. L. Hanson, K. G. Kavena, M. Sinha, D. Clary, M. B. Horton, R. G. Nelson and W. C. Knowler, "Use of Graded Semmes Weinstein Monofilament Testing for Ascertaining Peripheral Neuropathy in People with and without Diabetes," *Diabetes Research and Clinical Practice,* vol. 151, pp. 1-10, 2019. doi: 10.1016/j.diabres.2019.03.029.

[84] M. Viceconti, S. Olsen, L. P. Nolte and K. Burton, "Extracting clinically relevant data from finite element simulations," *Clinical Biomechanics,* vol. 20, no. 5, pp. 451-454, 2005.

[85] I. N. Sneddon, "The Relation Between Load and Penetration in the Axisymmetric Boussinesq Problem for a Punch Arbitrary Profile," *International Journal of Engineering Science,* vol. 3, no. 1, pp. 47-57, 1965.

[86] K. I. Johnson, "Indention by a rigid flat punch," in *Contact Mechanics 1st ed.*, Cambridge University Press, 1985, pp. 35-42.

[87] V. J. Thomas, K. M. Patil and S. Radhakrishnan, "Three-Dimensional Stress Analysis for the Mechanics of Plantar Ulcers in Diabetic Neuropathy," *Medical & Biological Engineering & Computing,* vol. 42, no. 2, pp. 230-235, 2004.

[88] C. Li, G. Guan, R. Reif, Z. Huang and R. K. Wang, "Determining elastic properties of skin by measuring surface waves from an impulse mechanical stimulus using phase-sensitive optical coherence tomography," *Journal of the Royal Society Interface,* vol. 9, no. 70, pp. 831-841, 2012.

[89] C. Y. Chao, Y. P. Zheng and G. L. Y. Cheing, "Epidermal Thickness and Biomechanical Properties of Plantar Tissues in Diabetic Foo," *Ultrasound in Medicine & Biology,* vol. 37, no. 7, pp. 1029-1038, 2011.

[90] Y. I. Wang and J. Sanders, "Skin Model Studies," *In Pressure Ulcer Research,* pp. 263-285, 2005.

[91] X. Dong, X. Yin, Q. Deng, B. Yu, H. Wang, P. Weng, C. Chen and H. Yuan, "Local contact behavior between elastic and elastic–plastic bodies," *International Journal of Solids and Structures,* vol. 150, no. 1, pp. 22-39, 2018.

[92] P. M. Kurowski, "12: Static analysis of a bracket using adaptive solution methods," in *Engineering Analysis with SolidWorks Simulation 2016*, Mission: SDC Publications, 2016, pp. 211-227.

[93] D. L. Russell and L. W. White, "An Elementary Nonlinear Beam Theory with Finite Buckling Deformation Properties," *SIAM Journal on Applied Mathematics,* vol. 62, no. 4, pp. 1394-1413, 2002.

[94] R. Szalai, "Impact Mechanics of Elastic Structures with Point Contact," *Journal of Vibration and Acoustics,* vol. 136, no. 4, pp. 1-16, 2014.

[95] H. Joodaki and M. B. Panzer, "Skin Mechanical Properties and Modeling: A Review," *Proceedings of the Institution of Mechanical Engineers Part H-Journal of Engineering in Medicine,* vol. 232, no. 4, pp. 323-343, 2018.

[96] L. Peebles and B. Norris, ADULTDATA-The Handbook of Adult Anthropometric and Strength Measurement-Data for Design Safety, 1998.

[97] B. Wang, Y. Si, C. Chadha, J. T. Allison and A. E. Patterson, "Nominal Stiffness of GT-2 Rubber-Fiberglass Timing Belts for Dynamic System Modeling and Design," *Robotics,* vol. 7, no. 4, pp. 1-8, 2018.

[98] V. K. Castellano, "A Diagnostic Tool for Neuropathy Assessment on the Plantar Surface of the Foot," *AUETD,* pp. 1-178, 2020. http://hdl.handle.net/10415/7271.

[99] Automation Direct, "Sure Step™ Stepping Systems User Manual," 29 April 2020. [Online]. Available: https://cdn.automationdirect.com/static/manuals/surestepmanual/surestepmanual.html. [Accessed 16 June 2020].

[100] Amazon, "DC 12V Drive Stepper Motor Screw with Linear Nut Slider for DIY Laser Engraving Machine," [Online]. Available: https://www.amazon.com/Stepper-Linear-Slider-Engraving-Machine/dp/B07H3XC3DD. [Accessed 16 June 2020].

[101] Robot Shop, "100g Micro Load Cell," [Online]. Available: https://www.robotshop.com/en/100g-micro-load-cell.html?gclid=Cj0KCQjwn8_mBRCLARIsAKxi0GJvlujAosrZC1mOoxS4J9px6CIAvgIlaJeF93v-4eNAoPBR2ozeNDwaAly7EALw_wcB. [Accessed 16 June 2020].

[102] Robot Shop, "HX711 Load Cell Amplifier," [Online]. Available: https://www.robotshop.com/media/files/pdf/hx711-load-cell-amplifier-datasheet.pdf. [Accessed 19 May 2022].

[103] Q. Zhang, N. Yi, S. Liu, H. Zheng, X. Qiao, Q. Xiong, X. Liu, S. Zhang, J. Wen, H. Ye, L. Zhou, Y. Li, R. Hu and B. Lu, "Easier operation and similar power of 10 g monofilament test for screening diabetic peripheral neuropathy," *Journal of International Medical Research,* vol. 46, no. 8, pp. 3278-3284, 2018. doi: 10.1177/0300060518775244.

[104] F. Tremblay, A.-C. Mireault, L. Dessureault, H. Manning and H. Sveistrup, "Postural stabilization from fingertip contact II. Relationships between age, tactile sensibility and magnitude of contact forces," *Experimental Brain Research,* no. 164, pp. 155-164, 2005. doi: 10.1007/s00221-005-2238-5.

[105] M. M. Wickremaratchi and J. G. Llewelyn, "Effects of ageing on touch," *Postgraduate Medical Journal,* vol. 82, no. 967, pp. 301-304, 2006. doi: 10.1136/pgmj.2005.039651.

[106] P. P. Breen, J. M. Serrador, C. O'Tuathail, L. R. Quinlan, C. McIntosh and G. ÓLaighin, "Peripheral tactile sensory perception of older adults improved using subsensory electrical noise stimulation," *Medical Engineering and Physics,* vol. 38, no. 8, pp. 822-825, 2016: https://doi.org/10.1016/j.medengphy.2016.05.015.

[107] E. T. Yümin, T. T. Şimşek, M. Sertel and H. Ankarali, "The effect of age and body mass index on plantar cutaneous sensation in healthy women," *The Journal of Physical Therapy Science,* vol. 28, pp. 2587-2595, 2016. doi: 10.1589/jpts.28.2587.

[108] G. Casadei, M. Filippini and L. Brognara, "Glycated Hemoglobin (HbA1c) as a Biomarker for Diabetic Foot Peripheral Neuropathy," *diseases,* vol. 9, no. 16, pp. 1-18, 2021. doi: 10.3390/diseases9010016.

[109] A. L. Calle-Pascual, A. Durán, A. Benedí, M. I. Calvo, J. P. Marañes, A. Charro, J. A. Diaz, J. R. Calle, E. Gil and J. Cabezas-Cerrato, "A preventative foot care programme for people with diabetes with different stages of neuropathy," *Diabetes Research and Clinical Practice,* vol. 57, no. 2, pp. 111-117, 2002: https://doi.org/10.1016/S0168-8227(02)00024-4.

[110] T. Costa, L. Coelho and M. F. Silva, "Automatic Segmentation of Monofilament Testing Sites in Plantar Images for Diabetic Foot Management," *bioengineering,* vol. 9, no. 3, pp. 1-18, 2022: https://doi.org/10.3390/bioengineering9030086.

[111] J. A. Bell-Krotoski and W. L. Buford, "The force/time relationship of clinically used sensory testing instruments," *Journal of Hand Therapy,* vol. 10, no. 4, pp. 297-309, 1997: DOI: 10.1016/s0894-1130(97)80045-2.

[112] R. Hughes, H. Rowlands and S. McMeekin, "A laser plantar pressure sensor for the diabetic foot," *Medical Engineering & Physics,* vol. 22, no. 2, pp. 149-154, 2000: https://doi.org/10.1016/S1350-4533(00)00019-9.

[113] H. Webberley, "What is peripheral neuropathy?," Healthline Media, 9 August 2021. [Online]. Available: https://www.medicalnewstoday.com/articles/147963. [Accessed 24 May 2022].

[114] NHS, "Treatment-Peripheral Neuropathy," Crown, [Online]. Available: https://www.nhs.uk/conditions/peripheral-neuropathy/treatment/. [Accessed 24 May 2022].

[115] R. H. Shmerling, "Treating neuropathy: Which medication is best?," The President and Fellows of Harvard College, 1 December 2020. [Online]. Available: https://www.health.harvard.edu/blog/treating-neuropathy-which-medication-is-best-202012012153 8. [Accessed 24 May 2022].

[116] John Hopkins Medicine, "Peripheral Neuropathy," The Johns Hopkins University, The Johns Hopkins Hospital, and Johns Hopkins Health System, 2022. [Online]. Available: https://www.hopkinsmedicine.org/health/conditions-and-diseases/peripheral-neuropathy#:~:text=Usually%20a%20peripheral%20neuropathy%20can,and%20other%20symptoms%20of%20neuropathy.. [Accessed 24 May 2022].

[117] D. Kumar and H. J. Marshall, "Diabetic Peripheral Neuropathy: Amelioration of Pain with Transcutaneous Electrostimulation," *Diabetes Care,* vol. 20, no. 11, pp. 1702-1705, 1997: https://doi.org/10.2337/diacare.20.11.1702.

[118] fremsLife, "APTIVA 4 & SPEEDER WH," fremsLife, [Online]. Available: https://www.fremslife.com/en/aptiva-4-speeder-wh/. [Accessed 2022 May 24].

[119] E. Bosi , G. Bax, L. Scionti, V. Spallone, S. Tesfaye, P. Valensi and D. Ziegler, "Frequency-modulated electromagnetic neural stimulation (FREMS) as a treatment for symptomatic diabetic neuropathy: results from a double-blind, randomised, multicentre, long-term, placebo-controlled clinical trial," *Diabetologia,* vol. 56, no. 3, pp. 467-475, 2013: DOI: 10.1007/s00125-012-2795-7.

[120] Doc Miller, "Are Compression Socks Good For Neuropathy?," Doc Miller, 19 Febuary 2022. [Online]. Available: https://docmillersports.com/blogs/articles/are-compression-socks-good-for-neuropathy. [Accessed 24 May 2022].

[121] J. Huizen, "Is It Possible to Reverse Diabetic Neuropathy?," Medical News Today, 9 May 2019. [Online]. Available: https://www.medicalnewstoday.com/articles/317923. [Accessed 24 May 2022].

Appendices

Appendix A (Nonprovisional Patent Application)

AUBURN UNIVERSITY | Office of Innovation Advancement and Commercialization

DATE: July 22, 2022

RE: Newly filed US Continuation Patent Application No.: **17/868,460**

Title: "**Semi-automated Plantar Surface Sensation Detection Device**"

Innovator(s): **Kenny V. Brock; Michael Edgar Zabala; Vitale Kyle Castellano; Thomas Burch; Hayden G. Burch; Jonathan Commander**

File Date: **July 19, 2022**

AU IP No.: **2019-032-03**

(Continuation of US Patent App. No. 17/027,464)

The above-referenced US patent application was filed electronically with the United States Patent and Trademark Office on July 19, 2022, and a copy of the Electronic Acknowledgement Receipt has been attached for your records. Copies of the US patent application, as filed, are available to all listed innovators upon request.

Your IAC licensing officer will continue to keep you up-dated on the progress of your patent application. If at any time you have questions or think of more information to provide us concerning your intellectual property, please feel free to contact our office.

Best Regards & War Eagle!

Misty W. Schwieker

As required by the Bayh-Dole Act (1980), Auburn University (AU) requires all AU innovators to execute the Patent and Copyright Agreement for Auburn University Personnel. Signed copies may be returned via email to iac_innovations@auburn.edu with originals to follow by campus mail. Please note that only one fully-executed agreement per innovator is required. Additional agreements will not be required on future intellectual property disclosure submissions, trademark, copyright, and/or provisional or patent application filings.

Track the status and progress of this and all your Intellectual Property (IP), Agreement(s) and MTA request(s) by logging into the AU Innovator Portal. IAC Innovator Portal ID login requests may be made via e-mail to iac@auburn.edu or by telephone to (334) 844-4977.

570 Devall Drive ▪ Suite 102 ▪ Auburn, AL 36832 ▪ P: (334) 844-4977 ▪ iac_innovations@auburn.edu

Appendix B (IRB Consent Document)

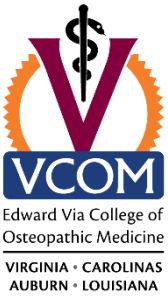

EDWARD VIA COLLEGE OF OSTEOPATHIC MEDICINE (VCOM)

CONSENT TO TAKE PART IN A BIOMEDICAL RESEARCH STUDY

Title: A Novel Clinical Tool for Neuropathic Grade Assessment

Investigator(s):
Dr. Jon Commander, MD, MS (Principle Investigator)
Dr. Michael Zabala, Auburn University
Dr. Kenny Brock, VCOM
Dr. Thomas Burch, Auburn University
Vitale Kyle Castellano, Auburn University
Hayden Burch, Auburn University
Jessica Remy, VCOM
Yousef Nikzai, VCOM
Austin Gould, VCOM
Benjamin Harman, VCOM
David McGregor, VCOM
David Axford, VCOM
Chad Gibbs, VCOM
Wesley Ortmann, VCOM
Graham Trott, VCOM
Nathan Anthony, VCOM
Katie Allen, VCOM
Bradley Louis, VCOM
Raydeer Piromari, VCOM

I. SUMMARY

Neuropathy is defined as a sensation in the body such as burning, tingling, numbness, warm or cool patches, a sensation of a sock on the foot, or a sponge under the foot.

The most common cause of neuropathy is type 2 diabetes mellitus. Neuropathic symptoms are most common in the foot but can occur in the hand, the trunk of the body or the lower back into the legs. The cause of neuropathy is not well understood. Some of the causes include an inherited trait, poor blood sugar control, and poor circulation to the feet.

The purpose of the study is to compare the standard foot exam to an examination done with a newly invented device. A standard foot exam includes hand applied monofilaments and vibratory analysis using a tuning fork. Your participation in this study is voluntary; it is your choice. You have the right to withdraw from the study at any point. The information from this research study will be confidential, kept anonymous, and maintained in a secure computer system under a coded protocol.

Our hope is that the data will give you new information about the health of your feet. The collected information will lead to better foot care for you and for all other diabetics in the future.

The study staff will explain this study in detail to you. Ask questions about anything that is not clear at any time. You may take home an unsigned copy of this consent form to think about and discuss with family or friends.

Please read this consent form carefully.

II. WHAT IS INFORMED CONSENT?

You are being asked to take part in a research study that will study that may benefit individuals who have diabetic foot neuropathy, a condition causing pain in various places on the foot. Before you decide whether to take part in the research, you should be told about the risks and benefits with this study. This process is known as informed consent. This consent form will give you information about this study and your rights as a research subject. Your decision to (or not to) participate in the voluntary study will in no way influence or affect your medical care and treatment at Internal Medicine Associates.

III. WHY IS THIS RESEARCH BEING DONE?

The purpose of this research it to develop a method of examining the sensitivity of the foot using a device using a monofilament. The research involves an office visit to examine your feet using the device.

IV. WHAT WILL HAPPEN IN THIS RESEARCH STUDY?

After you have given consent the Edward via College of Osteopathic Medicine (VCOM) student will generate a study code unique to you. All of your data and results will be deidentified using this code as to remove your identity from the results. During the exam you will be asked to remove shoes, socks, stockings, and or knee highs to expose the foot and ankle. If you have a long sleeve shirt, a gown will be provided to check your blood pressure. Your blood pressure, body mass index (BMI), and ankle-brachial index (ABI) will be evaluated and recorded on a data sheet. Your age, gender, and any symptoms related to neuropathy, such as burning, numbness, false sensation, etc., will also be recorded on the datasheet. Your medical record at IMA will be accessed for your last three fasting blood sugars and last three HgbA1c readings and will be written down on the datasheet. Your current medications will also be documented on the datasheet. Furthermore, a standard exam will be conducted using hand applied monofilaments and vibratory analysis using a tuning fork on both of your feet. After this you will be tested with the new device by a VCOM student. While you are lying on the exam table the neuropathic device will be placed up against the sole of your foot. Care will be taken to assume proper placement. Comfort is important so no part of your foot will feel excess pressure. The device will then measure 13 points from the toes down to your heel. Different pressures will be used at random locations, until your minimum threshold sensitivity is determined. You will be given a handheld pushbutton, which blinks to request a response from you. If you feel the applied

pressure, please press the button during the blinking cycle. If you are not sure if you can feel the pressure, do not hit the button. False positives are thrown into the assessment to make sure you are only pressing the button when you felt the monofilament being applied to your foot. Both of your feet will be assed using the new device A photograph will be taken of each foot for use with the device and for future analysis. You are being asked to allow the VCOM students to access your medical record and to retain a photograph of your feet.

V. WHAT ARE THE RISKS OF BEING IN THIS RESEARCH STUDY?

The examination of the foot using the monofilament should present minimal risk to you. In taking part in this research there may be other risks to you that we are not aware of at this time. As this study involves the use of your identifiable, personal information, there is a chance that a loss of confidentiality will occur. The researchers have procedures in place to lessen the possibility of this happening (see "What about confidentiality?" section below). If you choose to participate in this study, the risk for COVID-19 are about the same as those posed by similar activities while the virus is still spreading in your community. Similar activities could include grocery shopping, having your car repaired, or getting a haircut. Please refer to section XVIII COVID-19 Addendum for more information. In order to address the risk for COVID-19 face masks will be required for both the you and the investigators. Each investigator will be wearing a face shield/goggles, a gown, and a pair of gloves. A 6-foot physical distance will be maintained at all times except when the investigators are applying hand applied tools or taking vitals such as blood pressure and ABI. In the event of potential COVID-19 exposure a contact tracing log will be maintained, and you will be notified.

VI. WHAT ARE THE BENEFITS OF BEING IN THIS REASEARCH STUDY?

We cannot promise any benefits to your from taking part in the study. At the completion of the examination you will be given a copy of the datasheet with all of your results, including your threshold sensitivity of your feet using hand applied methods and the new device. However, the results using the new device cannot be used for the diagnosis of diseases, since it is not an FDA regulated device. Although you may not personally benefit from taking part in this study, the knowledge gained may benefit others.

VII. ARE THERE ANY OPTIONS TO BEING IN THIS REASEARCH STUDY?

The only alternative to participation is to choose not to participate.

VIII. WILL I RECEIVE NEW INFORMATION ABOUT THIS RESEARCH STUDY?

You will not receive any new information about this research study beyond the results of the examination.

IX. WHAT ABOUT CONFIDENTIALITY?

After you sign this consent form, the VCOM student will make a study code unique to you. This code will be used throughout this examination. This code will deidentify your data and your results collected through this study, in addition to the photographs of your feet. There will be no record that connects your name with your study code, you will be the only person who knows your own study code. At the end of the evaluation you will get a copy of this consent document and a copy of your datasheet. The investigators' copy of your signed consent form and datasheet will be keep in a locked filing cabinet and will be separated into different folders. The new machine will use your study code to save your deidentified results and data on password protected computers owned by the investigators of this study. Your datasheet will also include a summary of this results. Your identity will not be used in any sort of published report without your written permission.

Your identity in this study will be treated as confidential. The results of the study, including laboratory or any other data, may be published but will not give your name or include any identifiable references to you. This includes your blood pressure, BMI, ABI, last three fasting blood sugars, last three HgbA1c levels, current medications, age, gender, symptoms related to neuropathy, and data results from the standard foot exam and from the new device, and the photographs of your feet. However, any records or data obtained as a result of your participation in this study may be inspected by the persons conducting this study and/or The Edward Via College of Osteopathic Medicine's Institutional Review Board, provided that such inspectors are legally obligated to protect any identifiable information from public disclosure, except where disclosure is otherwise required by law or a court of competent jurisdiction. These records will be kept private in so far as permitted by law.

X. AUTHORIZATION TO USE YOUR HEALTH INFORMATION?

There is a federal law that protects the privacy of health information. This law is known as HIPAA. HIPAA stands for the "Health Insurance Portability and Accountability Act." Because of this law, your health information cannot be looked at, collected or shared with others without your permission.

Signing this consent and authorization form means you allow the Principal Investigator for this study and members of the investigator's research team to create, get, use, store and share information that identifies you for the purposes of this research.

After the VCOM student goes through this document with you and you sign it, they will go through your medical record and document the last three fasting blood sugars, and the last three HgbA1c readings on your datasheet. Your current medications will also be documented on the datasheet. The datasheet will be noted with your unique study code, used to deidentify you from your data. Your blood pressure, BMI, ABI, age, gender, and any symptoms related to neuropathy will all be evaluated and documented on your datasheet. The datasheet will also document the results of your standard foot exam and your examination using the new device.

XI. WILL IT COST ME MONEY TO TAKE PART IN THE RESEARCH?

There is no cost to you to take part in the research study. If while participating, you think you have an injury or illness related to this study, contact the study staff right away. The study staff will treat you or refer you for treatment. If referred, you will be responsible for the cost of such treatment.

XII. WILL I BE PAID FOR TAKING PART IN THIS RESEARCH?

There will be no compensation for taking part in this research study.

XIII. WHAT IF I WANT TO STOP BEING IN THE STUDY BEFORE IT IS FINISHED?

At any time during the examination, you can choose to not participate and end the examination. You can also request to be removed from this study at any time, in which case your results will be removed.

XIV. CAN I BE REMOVED FROM THIS RESARCH WITHOUT MY APPROVAL?

The person in charge of this research can remove you from this research without your approval. There are three cases where this might occur, the first is if your ABI is less than one. The second is if you hit to many false positive checks while being evaluated with the new device. The third is if you have any open wounds on your feet.

XV. ARE RESEARCHERS BEING PAID TO DO THIS STUDY?

This research study is funded by VCOM, which has paid for the development of the device, raw materials, the Auburn University graduate research assistant's salary and Auburn University undergraduate research assistant salary. Other than the Auburn University graduate and undergraduate students, none of the investigators or research staff will receive money or other types of payment from this study.

XVI. WHAT ARE MY RESPONSIBILITES IF I CHOOSE TO PARTICIPATE IN THIS RESEARCH STUDY?

If you choose to participate, an appointment will be scheduled for your examination. The examination will require that you lay still and place your foot in a device. Furthermore, you will be tested with hand applied monofilaments and a tuning fork. The examination should not take longer than 60 minutes to complete.

XVII. WHO ARE THE CONTACT PERSONS FOR THIS STUDY?

If you encounter complications or have any questions about the study, you may call:
Investigator Name: Dr. Jon Commander, MD
Address: Internal Medicine Associates, 121 North 20th St. #6, Opelika, AL 36801
Phone #: (334) 749-3385
Email Address: jcommander@imaopelika.com

This research is being overseen by the Edward Via College of Osteopathic Medicine Institutional Review Board (IRB). An IRB is a group of people whi perform independent review of research studies. You may talk with the Chairman of the IRB by calling (540) 231-4981 if:

- You have questions, concerns, or complaints that are not being answered by the research team.
- If you have questions about your rights as a research subject.
- If you need to report a research-related injury.

XVIII. COVID-19 ADDENDUM

You have agreed to participate in a research study at Edward Via College of Osteopathic Medicine. The research study involves in-person contact or procedures. Here are some things you should know about in-person research while COVID-19 remains a risk:

Risks related to COVID-19:

If you choose to participate in this study, the risk for COVID-19 are about the same as those posed by similar activities while the virus is still spreading in your community. Similar activities could include grocery shopping, having your car repaired, or getting a haircut.
In addition, participation might increase risk to your family, the community, and the research team.

You should not participate if you have any conditions or risk factors that could make a COVID-19 infection more serious. Risk factors for severe illness include having other medical conditions such as asthma, heart problems, or any other illness. Certain populations might also be at increased risk or unknown risk, including people aged 65 and older, people with disabilities, women who are pregnant or breastfeeding, people who are experiencing homelessness, and people who are part of racial and ethnic minority groups.

The information on people who need to take extra precautions is being updated regularly. We encourage you to check for the latest information before you decide whether to participate. Please visit https://www.cdc.gov/coronavirus/2019-ncov/need-extra-precautions/index.html for the most up to date information.

What we are doing to reduce risk to you:

Each lab or study has developed a process for conducting the research as safely as possible, given current knowledge about COVID-19. This process has been reviewed by the Institutional Review Board at Edward Via College of Osteopathic Medicine. A member of the research team

will review this information with you and answer any questions you might have before you agree to participate.
We will not conduct the study during times of increasing community spread or if we cannot obtain the necessary disinfecting supplies and equipment to reduce the risk of exposure.
Everyone working on the study has been instructed to stay home if they have any symptoms that could be related to COVID-19. If someone on the research team tests positive for COVID-19 and you have been exposed, someone will notify you. We will maintain a contact tracing log that is separate from your data and other details about your participation, and we will provide this log to your local health district who will conduct contact tracing in the case of a positive test. We will destroy this log 60 days after your last visit.

What you can do to reduce risk to us and to the community:

Do not participate if you have had any symptoms of COVID-19 in the past 14 days or have been in contact with someone who has symptoms. Symptoms include, but are not limited to, cough, shortness of breath or difficulty breathing, fever, chill, repeated shaking with chills, muscle pain, headache, sore throat, and new loss of taste or smell.

Do not participate if you have tested positive for COVID-19 in the past 21 days, even if you have not shown any symptoms.
Do not participate if you know you have been exposed to anyone who has tested positive for COVID-19 in the past 21 days.
Let us know if you test positive for COVID-19 within the next 14 days. We will provide your contact tracing log to the college or public health authorities who will use the tracing log to contact others who may have been exposed during your visit.
Wash your hands frequently and observe current guidance on avoiding virus spread from the Centers for Disease Control.
Wear a mask or a cloth face covering over your nose and mouth. Depending on the study, other methods may be used, such as physical distancing, a face shield, or Plexiglas barrier or multiple methods may be deployed simultaneously.
For the latest information on COVID-19 please visit: https://www.cdc.gov/coronavirus/2019-ncov/index.html

XIX. CONSENT SIGNATURES

PARTICIPANT: The research study described in this consent form, including the risks and benefits, has been explained to me and all my questions have been answered. I consent to take part in this research study. My consent is given willingly and voluntarily. I understand that I am free to withdraw my consent at any time. I will receive a signed copy of this consent form.
I give my permission to the researchers to use my medical records as described in this consent form.

_____ _____

Printed Name of Participant Signature of participant

Date

PERSON OBTAINING CONSENT: I certify I was present for the informed consent discussion. The subject or legally authorized representative had an opportunity to ask questions about the study and appeared to understand the information presented. The subject or legally authorized representative agreed to take part voluntarily in the research and I obtained his/her signature.

_____ _____

Printed Name of Person Obtaining Consent Signature of Person Obtaining Consent

Date

Appendix C (Subject Datasheet)

Patient Code: _____

Gender: _____
Age: _____
(if older than 89 indicate 90+)

Cohort

- ☐ Control
- ☐ DM2, no symptoms
- ☐ DM2, with symptoms
- ☐ DM2, history of ulcers, amputation

Sig PMH

- ☐ CKDz, Proteinuria
- ☐ Neuropathy
- ☐ Vascular Disease
- ☐ Peripheral Vascular Disease
- ☐ None

Symptoms

- ☐ Burning
- ☐ Tingling
- ☐ Numbness
- ☐ Warm Patches
- ☐ Cold Patches
- ☐ False Sensation
- ☐ Other: _____
  _____
  _____
- ☐ None

Vital Signs

BP: _____
BMI: _____
ABI Screen: _____
Last 3 Fasting Blood Sugars
_____,_____,_____
Last 3 HgbA1c
_____,_____,_____
List of Current Medications:
_____
_____
_____
_____

Patient Code: _____

Standard Foot Exam

	Right		Left	
	M	V	M	V
Toe 1				
2				
3				
4				
5				
MT 1				
2				
3				
4				
5				
H 1				
2				
3				

New Device Foot Exam*

	Right	Left
Toe 1		
2		
3		
4		
5		
MT 1		
2		
3		
4		
5		
H 1		
2		
3		

*Note: Results obtained using the new device cannot be used for the diagnosis of diseases, since this is not an FDA regulated device

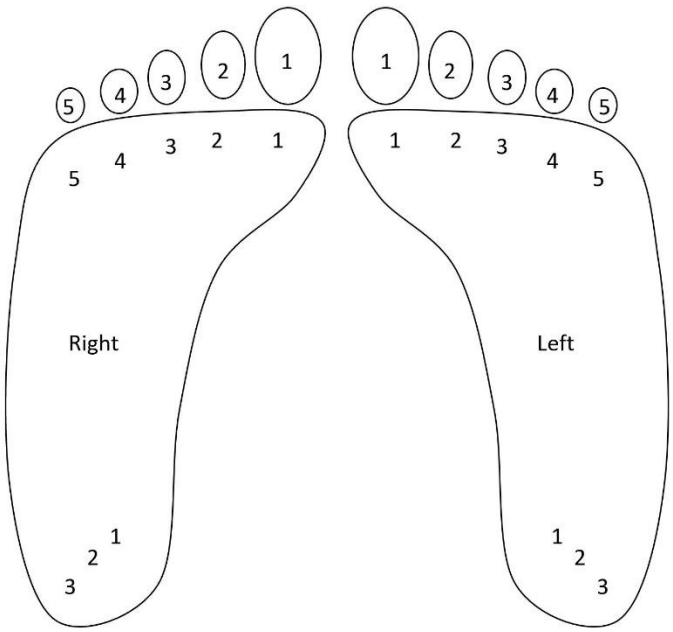

**Note: Pictorial shows the plantar surface of the foot, locations and size are not exact or to scale

Appendix D (Research Volunteer Flyer for IMA Lobby)

Dr. Jon Commander of Internal Medicine Associates

Auburn University Samuel Ginn College of Engineering's Mechanical Engineering Department

Edward Via College of Osteopathic Medicine (VCOM)

Request your participation!

A research study on diabetic neuropathy of the feet using a newly invented tool for analyzing neuropathy.

Seeking:

- 50 patients, at least 40 years-old, no health risks for diabetes/neuropathy
- 50 patients, at least 40 years-old, with type II diabetes for at least 5 years, no symptoms of neuropathy
- 50 patients, at least 40 years-old, with type II diabetes for at least 5 years, with symptoms of neuropathy
- 50 patients, at least 40 years-old, with type II diabetes and history of foot ulcers and/or partial amputation

If you meet the requirements of one of these groups, please take a flyer/request information during vital signs, and you may participate in this FREE test. Results will be provided to you. There is no compensation for this free examination. This study is not open to type I diabetics or anyone less than 40 years of age. Also if you have an Ankle-Brachial Index less than 1.0 you will be excluded from this study. Patient's with unhealed ulcers or unhealed amputations will be excluded. The entire evaluation will take no more than 60 minutes. Participates must wear a mask/face covering at all times during the study and will be responsible for bring their own.

Recruitment Script

Thank you for your interest in being included in this research on neuropathy. As a control patient you must be at least 40 years of age with no know history of peripheral vascular disease nor symptoms of neuropathy. All Type 2 DM volunteers must be at least age 40 and have had DM 2 for at least 5 years. Also if you have an Ankle-Brachial Index less than 1.0 you will be excluded from this study. Patient's with unhealed ulcers or unhealed amputations will be excluded. During the evaluation you will have a standard foot exam on each foot, which includes hand applied monofilaments and vibratory analysis using a tuning fork. You will also be evaluated using the new tool. You will also receive an ABI exam to document your blood flow to your feet. You will be given a copy of your results which you can share with your primary care physician, however since this is not an FDA approved device the results cannot be used to diagnosis a disease. There will be no compensation provided for participation. The entire evaluation will take no more than 60 minutes. An appointment time will be scheduled for the free exam.

Appendix E (GRBL Settings)

Grbl 1.1g ['$' for help]
[MSG:'$H'|'$X' to unlock]
$0=10
$1=255
$2=0
$3=0
$4=0
$5=0
$6=0
$10=3
$11=0.010
$12=0.002
$13=1
$20=0
$21=1
$22=1
$23=3
$24=25.000
$25=500.000
$26=25
$27=1.000
$30=1000
$31=0
$32=0
$100=500.000
$101=500.000
$102=100.000
$110=1000.000
$111=1000.000
$112=100.000
$120=100.000
$121=100.000
$122=1.000
$130=200.000
$131=200.000
$132=200.000

Appendix F (Neuropathy Device Start Code)

```
clc
clear all
close all

Hello=questdlg('Hello. Welcome to the Neuropathy Diagnostic Tool Assessment
Interface. Do not place the patient''s foot in the device yet. Please click
start to begin the test.', 'Welcome', 'Start', 'Start');
PSShcek=questdlg('Did you turn on the small power supply? If not please do so
now. Select begin test when completed.', 'Power Supply Check', 'Begin Test',
'Begin Test');
ExcelReminder=questdlg('Please make sure that Microsoft Excel is
closed.','Excel Reminder', 'Okay', 'Okay');

Mega=serial('COM3', 'BaudRate', 115200);
fopen(Mega);
pause(3)
Uno=serial('COM4', 'BaudRate', 9600);
Uno.Terminator= 'LF';
Uno.timeout=30;
fopen(Uno);
pause(3)
fprintf(Mega, '$X \n');
pause(3)
fprintf(Mega, '$H \n');
pause(3)
fprintf(Mega, 'G20 \n');
pause(3)
fprintf(Mega, 'G28.1 \n');
pause(3)
fprintf(Mega, 'G10 L20 P1 X0 Y0 Z0 \n');
pause(3)
mycam=webcam('Logitech');
mycam.Resolution = '1920x1080';
pause(10)


PatientData=inputdlg({'Patient Identifier:', 'Gender:', 'Age:', 'Time:',
'Date:', 'Operator Initials:'}, 'Documentation', [1 50]);
PatientIdentifierChar=char(PatientData(1));

answer=questdlg('Left Foot or Right Foot?', 'Foot Type', 'Left', 'Right',
'Left');

switch answer
    case 'Left'
        Type1st='LeftFoot';
        Type2nd='RightFoot';
    case 'Right'
        Type1st='RightFoot';
        Type2nd='LeftFoot';
end

Directory='D:\Documents\Graduate Research Neuropathy Project\Matlab Research
Files';
```

```
NewDirectory=sprintf('%s\\%s',Directory, PatientIdentifierChar);

if ~exist(NewDirectory, 'dir')
    mkdir(fullfile(Directory,PatientIdentifierChar))
end

PatientIdentifierCharType1st=sprintf('%s%s',PatientIdentifierChar, Type1st);
PatientIdentifierCharType2nd=sprintf('%s%s',PatientIdentifierChar, Type2nd);
SubDirectory1st=sprintf('%s\\%s', NewDirectory,
PatientIdentifierCharType1st);
SubDirectory2nd=sprintf('%s\\%s', NewDirectory,
PatientIdentifierCharType2nd);

if ~exist(SubDirectory1st, 'dir')
    mkdir(fullfile(NewDirectory, PatientIdentifierCharType1st))
end

if ~exist(SubDirectory2nd, 'dir')
    mkdir(fullfile(NewDirectory, PatientIdentifierCharType2nd))
end

filenamex1st=sprintf('%s.xlsx', PatientIdentifierCharType1st);
filenamex2nd=sprintf('%s.xlsx', PatientIdentifierCharType2nd);
filenamew=sprintf('%s.mat', PatientIdentifierChar);
filenamef1st=sprintf('%s.fig', PatientIdentifierCharType1st);
filenamef2nd=sprintf('%s.fig', PatientIdentifierCharType2nd);
tic

for H=1:2

    if H==1

        [T1, T2, T3, RS1]=NeuropathyScriptFunction2(Uno, Mega, mycam, 1);
        answer5=questdlg('Offer the Patient a break', 'Break', 'Okay',
'Okay');
        FigureReminder=questdlg('Please minimize the first window with
patient''s foot and results on it. Do not close the window.', 'Figure
Reminder', 'Okay', 'Okay');
        fprintf(Mega, '$X \n');
        pause(3)
        fprintf(Mega, '$H \n');
        pause(3)
        fprintf(Mega, 'G20 \n');
        pause(3)
        fprintf(Mega, 'G28.1 \n');
        pause(3)
        fprintf(Mega, 'G10 L20 P1 X0 Y0 Z0 \n');
        pause(3)
        answer6=questdlg('Place the Patient''s other foot in the machine',
'Insert Foot', 'Okay', 'Okay');
        answer7=questdlg('Click Okay to resume the test once the Patient''s
other foot has been placed in the machine', 'Resume Test', 'Okay', 'Okay');
    end

    if H==2

        [T4, T5, T6, RS2]=NeuropathyScriptFunction2(Uno, Mega, mycam, 2);
```

```
    end

end

endTime=toc;

fclose(Mega);
pause(3)
fclose(Uno);

SaveReminder=questdlg('Please press save to save the results. Do not close
out any windows.', 'Save Results', 'Save', 'Save');
writetable(T1, filenamex1st, 'sheet', 'sheet1')
writetable(T2, filenamex1st, 'sheet', 'sheet2')
writetable(T3, filenamex1st, 'sheet', 'sheet3')
writetable(T4, filenamex2nd, 'sheet', 'sheet1')
writetable(T5, filenamex2nd, 'sheet', 'sheet2')
writetable(T6, filenamex2nd, 'sheet', 'sheet3')

savefig(1, PatientIdentifierCharType1st)
savefig(2, PatientIdentifierCharType2nd)
save(PatientIdentifierChar)

movefile(filenamex1st, SubDirectory1st)
movefile(filenamex2nd, SubDirectory2nd)
movefile(filenamew, NewDirectory)
movefile(filenamef1st, SubDirectory1st)
movefile(filenamef2nd, SubDirectory2nd)
EndReminder=questdlg('The results have been saved and the files have been
moved into the patient''s folder. Please close all windows and close MATLAB.
Also please turn the machine off and unplug the usbs from the computer. Clean
the device before the next patient. Thank you for all your help -
Kyle.','Assessment Complete', 'Finish', 'Finish');
```

Appendix G (Neuropathy Script)

```
function [T1, T2, T3, rs]=NeuropathyScriptFunction2(Uno, Mega, mycam, N)


PatientFoot1=questdlg('Please place the patient''s foot in the device now.
Make sure that the foot is strapped in place and the plantar surface is
against the acylic. Adjust the table height if necessary. Hand the patient
the remote. Press Start once the patient is ready.','Place Patient''s Foot in
Device', 'Start', 'Start');

figure(N)
img=snapshot(mycam);
imwrite(img, 'PatientNew.tiff');
I=imread('PatientNew.tiff');
imshow(I);
axis on

PatientFootImage1=questdlg('Please make the window with the picture of the
patient''s foot fullscreen. Do not interact with other windows or figures
during the test', 'Fullscreen Reminder', 'Okay', 'Okay');

%[c,r]=getpts(figure(N)); %Manual selection for grid

%c1=c(1);
%c2=c(2);

c1=103;
c2=1876;
CLength=c2-c1;
xratio=12/CLength;
cd=CLength/48;

%r1=r(1);
%r2=r(2);

r1=921;
r2=180;
RLength=r2-r1;
yratio=5/RLength;
rd=RLength/20;

hold on;

for col=c1:cd:c2
    line([col, col], [r2, r1], 'Color', 'w');
end

for row=r1:rd:r2
    line([c2, c1], [row, row], 'Color', 'w');
end

%R=r1:rd:r2;
%C=c1:cd:c2;

fprintf(Mega, 'G54 X0.26 Y1.285 \n'); %Setting New Orgin at the first hole
```

```
pause(3)
fprintf(Mega, 'G30.1 \n');
pause(3)
fprintf(Mega, 'G10 L20 P2 X0 Y0 Z0 \n');
pause(0.1)
[~, ~, ~] = NeuropathyUnoFunction2("0", Uno);
pause(0.1)


for L=1:3
    if L==1
        fprintf("Region 1-Toes \n")
        answer1=questdlg('Please select locations on the heads of each toe, 5
total. Do not double click the mouse. Backspace on the keyboard will remove
the location selected. Hit Enter on the keyboard to comfirm locations.',
'Region 1', 'Okay', 'Okay');
    end

    if L==2
        fprintf("Region 2-Ball of the Foot \n")
        answer2=questdlg('Please select locations on the ball of the foot, 5
total. Do not double click the mouse. Backspace on the keyboard will remove
the location selected. Hit Enter on the keyboard to comfirm locations.',
'Region 2', 'Okay', 'Okay');
    end

    if L==3
        fprintf("Region 3-Heel \n")
        answer3=questdlg('Please select locations on the heel, 3 total. Do
not double click the mouse. Backspace on the keyboard will remove the
location selected. Hit Enter on the keyboard to comfirm locations.', 'Region
3', 'Okay', 'Okay');
    end

[x,y]=getpts(figure(N)); %Collects data on figure
hold on

Data=[x y]; %Mouse click Data stored
DataConversion=Data-[c1 r1];
DataInch=DataConversion.*[xratio yratio];

[rowInch, ~]=size(DataInch); %Determines how many points there are
NumberRows=rowInch; %Counts rows

accuracy=0.25; %rounded to nearest 0.25 inch
DataRounded=round(DataInch/accuracy)*accuracy;
DataRoundedLimit=max(DataRounded, 0); %Converts negative numbers to zero

XData=DataRoundedLimit(: ,1); %X axis data to less than or equal to 12
XData(XData>12)=12;

YData=DataRoundedLimit(: ,2); %Y axis data to less than or equal to 5
YData(YData>5)=5;

DataFinal=[XData YData];
DataFinalPixels=DataFinal./[xratio yratio];
```

```
DataPixels=DataFinalPixels+[c1 r1];
DataPixelsX=DataPixels(: ,1);
DataPixelsY=DataPixels(: ,2);
plot(DataPixelsX,DataPixelsY, 'c*');
hold on

GcodeCell=cell(1, NumberRows);
for i=1:NumberRows
    DataPoint=DataFinal(i, :); %Selects a row of data for indexed value or
rounded set
    DataPointX=DataPoint(2); %X coorrdinate for indexed value
    DataPointY=DataPoint(1); %Y coordinate for indexed value
    Gcode=sprintf('G55 X%0.2f Y%0.2f', DataPointX, DataPointY); %String
printf of Gcode
    GcodeCell{i}=Gcode;  %Stores all indexed Gcode in a Cell
end

    if L==1
        R1Gcode=GcodeCell;
        R1DataPixels=DataPixels;
        R1DataPixelsX=DataPixelsX;
        R1DataPixelsY=DataPixelsY;
        Length1=NumberRows;
    end

    if L==2
        R2Gcode=GcodeCell;
        R2DataPixels=DataPixels;
        R2DataPixelsX=DataPixelsX;
        R2DataPixelsY=DataPixelsY;
        Length2=NumberRows;
    end

    if L==3
        R3Gcode=GcodeCell;
        R3DataPixels=DataPixels;
        R3DataPixelsX=DataPixelsX;
        R3DataPixelsY=DataPixelsY;
        Length3=NumberRows;
    end
end

rng shuffle
rs=rng;

TestingOrder=randi(4);
if TestingOrder==1
    %1-2-3

    T1Gcode=R1Gcode;
    T1DataPixels=R1DataPixels;
    T1DataPixelsX=R1DataPixelsX;
    T1DataPixelsY=R1DataPixelsY;
    T1Length=Length1;

    T2Gcode=R2Gcode;
    T2DataPixels=R2DataPixels;
```

```
    T2DataPixelsX=R2DataPixelsX;
    T2DataPixelsY=R2DataPixelsY;
    T2Length=Length2;

    T3Gcode=R3Gcode;
    T3DataPixels=R3DataPixels;
    T3DataPixelsX=R3DataPixelsX;
    T3DataPixelsY=R3DataPixelsY;
    T3Length=Length3;

elseif TestingOrder==2
    %2-1-3

    T1Gcode=R2Gcode;
    T1DataPixels=R2DataPixels;
    T1DataPixelsX=R2DataPixelsX;
    T1DataPixelsY=R2DataPixelsY;
    T1Length=Length2;

    T2Gcode=R1Gcode;
    T2DataPixels=R1DataPixels;
    T2DataPixelsX=R1DataPixelsX;
    T2DataPixelsY=R1DataPixelsY;
    T2Length=Length1;

    T3Gcode=R3Gcode;
    T3DataPixels=R3DataPixels;
    T3DataPixelsX=R3DataPixelsX;
    T3DataPixelsY=R3DataPixelsY;
    T3Length=Length3;

elseif TestingOrder==3
    %3-1-2

    T1Gcode=R3Gcode;
    T1DataPixels=R3DataPixels;
    T1DataPixelsX=R3DataPixelsX;
    T1DataPixelsY=R3DataPixelsY;
    T1Length=Length3;

    T2Gcode=R1Gcode;
    T2DataPixels=R1DataPixels;
    T2DataPixelsX=R1DataPixelsX;
    T2DataPixelsY=R1DataPixelsY;
    T2Length=Length1;

    T3Gcode=R2Gcode;
    T3DataPixels=R2DataPixels;
    T3DataPixelsX=R2DataPixelsX;
    T3DataPixelsY=R2DataPixelsY;
    T3Length=Length2;

else
    %3-2-1

    T1Gcode=R3Gcode;
    T1DataPixels=R3DataPixels;
```

```
    T1DataPixelsX=R3DataPixelsX;
    T1DataPixelsY=R3DataPixelsY;
    T1Length=Length3;

    T2Gcode=R2Gcode;
    T2DataPixels=R2DataPixels;
    T2DataPixelsX=R2DataPixelsX;
    T2DataPixelsY=R2DataPixelsY;
    T2Length=Length2;

    T3Gcode=R1Gcode;
    T3DataPixels=R1DataPixels;
    T3DataPixelsX=R1DataPixelsX;
    T3DataPixelsY=R1DataPixelsY;
    T3Length=Length1;
end

for K=1:3

    if K==1
        [T1] = NeuropathyFunction4(T1Length, T1Gcode, T1DataPixelsX,
T1DataPixelsY, Mega, Uno);
    end

    if K==2
        [T2] = NeuropathyFunction4(T2Length, T2Gcode, T2DataPixelsX,
T2DataPixelsY, Mega, Uno);
    end

    if K==3
        [T3] = NeuropathyFunction4(T3Length, T3Gcode, T3DataPixelsX,
T3DataPixelsY, Mega, Uno);
    end

end

fprintf(Mega, 'G30 \n');
pause(3)
answer4=questdlg('Please remove the Patient''s foot and click okay when
done', 'Remove Foot', 'Okay', 'Okay');
```

Appendix H (Neuropathy Function)

```
function [T] = NeuropathyFunction4(TLength, TGcode, TDataPixelsX,
TDataPixelsY, Mega, Uno)

TotalNumberofTrialVector=1:TLength; %Creates row vector of total number of
points selected
VectorTranspose=TotalNumberofTrialVector'; %Creates cloumn vector of total
number of points selected
RandomizedVector=TotalNumberofTrialVector(randperm(length(TotalNumberofTrialV
ector))); %Randomizes the vector, used to randomize the test locations
RandomizedVectorTranspose=RandomizedVector'; %Takes random vector and
transposes it
Y=RandomizedVector;

GcodeCelltoString=string(TGcode); %Converts cell array Gcode to strings
GcodeCelltoStringTranspose=GcodeCelltoString'; %Transposes a Gcode string
array
Z=GcodeCelltoString;

FalsePositiveRandomizationVector=randi([1 10],1,TLength); %Flase Positive
Randmization
FalsePositiveRandomizationVectorTranspose=FalsePositiveRandomizationVector';
%Flase Positive Randomization Transpose
W=FalsePositiveRandomizationVector;
X=TLength;

TestLocationCellArray=cell(1, X);
dataout0=zeros(1, X);
dataout1=zeros(1, X);
dataout2=zeros(1, X);
dataout3=zeros(1, X);
dataout4=zeros(1, X);
dataout5=zeros(1, X);
dataout6=zeros(1, X);
dataout7=zeros(1, X);
ResponseIndex0=zeros(1,X);
ResponseIndex1=zeros(1,X);
ResponseIndex2=zeros(1,X);
ResponseIndex3=zeros(1,X);
ResponseIndex4=zeros(1,X);
ResponseIndex5=zeros(1,X);
ResponseIndex6=zeros(1,X);
ResponseIndex7=zeros(1,X);
PercentError0=zeros(1,X);
PercentError1=zeros(1,X);
PercentError2=zeros(1,X);
PercentError3=zeros(1,X);
PercentError4=zeros(1,X);
PercentError5=zeros(1,X);
PercentError6=zeros(1,X);
PercentError7=zeros(1,X);
FalsePositiveCheckIndex=zeros(1,X);
RS=cell(1,X);

for i=1:X
```

```
    TestLocation=Z(Y(i)); %Selects a random point to test at
    fprintf(Mega, '%s  \n',TestLocation); %Sends Gcode (X and Y) to the
arduino over serial usb connection
    TestLocationCellArray{i}=TestLocation; %Stores location data
    fo=0;

        while fo==0 %feedback loop
            flushinput(Mega);
            pause(1)
            fprintf(Mega, '? \n');
            C=fscanf(Mega);
            CC=strtok(C, '|');
            CCC=convertCharsToStrings(CC);

                if CCC=="<Idle"
                    fo=1;
                end
        end

    for j=1

        if W(i)==10
            %false positive code
            FalsePositiveCheckRandomizationVector=randi(2);
            FalsePositiveCheckIndex(i)=FalsePositiveCheckRandomizationVector;

            if FalsePositiveCheckRandomizationVector==2
                fprintf('False Positive Test at End \n');
                fprintf('Z axis move \n');
                pause(0.1);
                F="0.35";
                [ResponseIndex1(i), dataout1(i), PercentError1(i)] =
NeuropathyUnoFunction2(F, Uno);

                if ResponseIndex1(i)==1
                    ResponseIndex2(i)=101;
                    ResponseIndex3(i)=101;
                    ResponseIndex4(i)=101;
                    ResponseIndex5(i)=101;
                    ResponseIndex6(i)=101;
                    ResponseIndex7(i)=101;
                    dataout2(i)=0;
                    dataout3(i)=0;
                    dataout4(i)=0;
                    dataout5(i)=0;
                    dataout6(i)=0;
                    dataout7(i)=0;
                    PercentError2(i)=0;
                    PercentError3(i)=0;
                    PercentError4(i)=0;
                    PercentError5(i)=0;
                    PercentError6(i)=0;
                    PercentError7(i)=0;
                    RS{i}="0.350 grams";
                end

                if ResponseIndex1(i)==0
```

```
                    fprintf('Z axis move \n'); %Z axis moves
                    pause(0.1);
                    F="10";
                    [ResponseIndex2(i), dataout2(i), PercentError2(i)] =
NeuropathyUnoFunction2(F, Uno);
                end

                if ResponseIndex2(i)==1
                    fprintf('Z axis move \n'); %Z axis moves
                    pause(0.1);
                    F="4";
                    [ResponseIndex3(i), dataout3(i), PercentError3(i)] =
NeuropathyUnoFunction2(F, Uno);
                end

                if ResponseIndex2(i)==0
                    ResponseIndex3(i)=101;
                    ResponseIndex4(i)=101;
                    ResponseIndex5(i)=101;
                    ResponseIndex6(i)=101;
                    ResponseIndex7(i)=101;
                    dataout3(i)=0;
                    dataout4(i)=0;
                    dataout5(i)=0;
                    dataout6(i)=0;
                    dataout7(i)=0;
                    PercentError3(i)=0;
                    PercentError4(i)=0;
                    PercentError5(i)=0;
                    PercentError6(i)=0;
                    PercentError7(i)=0;
                    RS{i}="Greater than 10.0 grams";
                end

                if ResponseIndex3(i)==1
                    fprintf('Z axis move \n'); %Z axis moves
                    pause(0.1);
                    F="0.7";
                    [ResponseIndex4(i), dataout4(i), PercentError4(i)] =
NeuropathyUnoFunction2(F, Uno);

                    if ResponseIndex4(i)==1
                        ResponseIndex5(i)=101;
                        ResponseIndex6(i)=101;
                        ResponseIndex7(i)=101;
                        dataout5(i)=0;
                        dataout6(i)=0;
                        dataout7(i)=0;
                        PercentError5(i)=0;
                        PercentError6(i)=0;
                        PercentError7(i)=0;
                        RS{i}="0.700 grams";
                    end

                    if ResponseIndex4(i)==0
                        fprintf('Z axis move \n'); %Z axis moves
                        pause(0.1);
```

```
                        F="2";
                        [ResponseIndex6(i), dataout6(i), PercentError6(i)] =
NeuropathyUnoFunction2(F, Uno);

                        ResponseIndex5(i)=101;
                        ResponseIndex7(i)=101;
                        dataout5(i)=0;
                        dataout7(i)=0;
                        PercentError5(i)=0;
                        PercentError7(i)=0;
                    end

                    if ResponseIndex6(i)==1
                       RS{i}="2.00 grams";
                    end

                    if ResponseIndex6(i)==0
                       RS{i}="4.00 grams";
                    end

                end

                if ResponseIndex3(i)==0
                    fprintf('Z axis move \n'); %Z axis moves
                    pause(0.1);
                    F="8";
                    [ResponseIndex5(i), dataout5(i), PercentError5(i)] =
NeuropathyUnoFunction2(F, Uno);

                    if ResponseIndex5(i)==1
                        fprintf('Z axis move \n'); %Z axis moves
                        pause(0.1);
                        F="6";
                        [ResponseIndex7(i), dataout7(i), PercentError7(i)] =
NeuropathyUnoFunction2(F, Uno);

                        ResponseIndex4(i)=101;
                        ResponseIndex6(i)=101;
                        dataout4(i)=0;
                        dataout6(i)=0;
                        PercentError4(i)=0;
                        PercentError6(i)=0;
                    end

                    if ResponseIndex7(i)==1
                        RS{i}="6.00 grams";
                    end

                    if ResponseIndex7(i)==0
                        RS{i}="8.00 grams";
                    end

                    if ResponseIndex5(i)==0
                        ResponseIndex4(i)=101;
                        ResponseIndex6(i)=101;
                        ResponseIndex7(i)=101;
                        dataout4(i)=0;
```

```
                    dataout6(i)=0;
                    dataout7(i)=0;
                    PercentError4(i)=0;
                    PercentError6(i)=0;
                    PercentError7(i)=0;
                    RS{i}="10.0 grams";
                end

            end

            fprintf('False Positive Z \n');
            pause(0.1);
            F="0";
            [ResponseIndex0(i), dataout0(i), PercentError0(i)] =
NeuropathyUnoFunction2(F, Uno);

        else
            fprintf('False Positive at Beginning \n');
            fprintf('False Positive Z \n');
            pause(0.1);
            F="0";
            [ResponseIndex0(i), dataout0(i), PercentError0(i)] =
NeuropathyUnoFunction2(F, Uno);

            fprintf('Z axis move \n');
            pause(0.1);
            F="0.35";
            [ResponseIndex1(i), dataout1(i), PercentError1(i)] =
NeuropathyUnoFunction2(F, Uno);

            if ResponseIndex1(i)==1
                ResponseIndex2(i)=101;
                ResponseIndex3(i)=101;
                ResponseIndex4(i)=101;
                ResponseIndex5(i)=101;
                ResponseIndex6(i)=101;
                ResponseIndex7(i)=101;
                dataout2(i)=0;
                dataout3(i)=0;
                dataout4(i)=0;
                dataout5(i)=0;
                dataout6(i)=0;
                dataout7(i)=0;
                PercentError2(i)=0;
                PercentError3(i)=0;
                PercentError4(i)=0;
                PercentError5(i)=0;
                PercentError6(i)=0;
                PercentError7(i)=0;
                RS{i}="0.350 grams";
            end

            if ResponseIndex1(i)==0
                fprintf('Z axis move \n'); %Z axis moves
                pause(0.1);
                F="10";
```

```
                    [ResponseIndex2(i), dataout2(i), PercentError2(i)] =
NeuropathyUnoFunction2(F, Uno);
                end

                if ResponseIndex2(i)==1
                    fprintf('Z axis move \n'); %Z axis moves
                    pause(0.1);
                    F="4";
                    [ResponseIndex3(i), dataout3(i), PercentError3(i)] =
NeuropathyUnoFunction2(F, Uno);
                end

                if ResponseIndex2(i)==0
                    ResponseIndex3(i)=101;
                    ResponseIndex4(i)=101;
                    ResponseIndex5(i)=101;
                    ResponseIndex6(i)=101;
                    ResponseIndex7(i)=101;
                    dataout3(i)=0;
                    dataout4(i)=0;
                    dataout5(i)=0;
                    dataout6(i)=0;
                    dataout7(i)=0;
                    PercentError3(i)=0;
                    PercentError4(i)=0;
                    PercentError5(i)=0;
                    PercentError6(i)=0;
                    PercentError7(i)=0;
                    RS{i}="Greater than 10.0 grams";
                end

                if ResponseIndex3(i)==1
                    fprintf('Z axis move \n'); %Z axis moves
                    pause(0.1);
                    F="0.7";
                    [ResponseIndex4(i), dataout4(i), PercentError4(i)] =
NeuropathyUnoFunction2(F, Uno);

                    if ResponseIndex4(i)==1
                        ResponseIndex5(i)=101;
                        ResponseIndex6(i)=101;
                        ResponseIndex7(i)=101;
                        dataout5(i)=0;
                        dataout6(i)=0;
                        dataout7(i)=0;
                        PercentError5(i)=0;
                        PercentError6(i)=0;
                        PercentError7(i)=0;
                        RS{i}="0.700 grams";
                    end

                    if ResponseIndex4(i)==0
                        fprintf('Z axis move \n'); %Z axis moves
                        pause(0.1);
                        F="2";
                        [ResponseIndex6(i), dataout6(i), PercentError6(i)] =
NeuropathyUnoFunction2(F, Uno);
```

```
                        ResponseIndex5(i)=101;
                        ResponseIndex7(i)=101;
                        dataout5(i)=0;
                        dataout7(i)=0;
                        PercentError5(i)=0;
                        PercentError7(i)=0;
                    end

                    if ResponseIndex6(i)==1
                       RS{i}="2.00 grams";
                    end

                    if ResponseIndex6(i)==0
                       RS{i}="4.00 grams";
                    end

                end

                if ResponseIndex3(i)==0
                    fprintf('Z axis move \n'); %Z axis moves
                    pause(0.1);
                    F="8";
                    [ResponseIndex5(i), dataout5(i), PercentError5(i)] =
NeuropathyUnoFunction2(F, Uno);

                    if ResponseIndex5(i)==1
                        fprintf('Z axis move \n'); %Z axis moves
                        pause(0.1);
                        F="6";
                        [ResponseIndex7(i), dataout7(i), PercentError7(i)] =
NeuropathyUnoFunction2(F, Uno);

                        ResponseIndex4(i)=101;
                        ResponseIndex6(i)=101;
                        dataout4(i)=0;
                        dataout6(i)=0;
                        PercentError4(i)=0;
                        PercentError6(i)=0;
                    end

                    if ResponseIndex7(i)==1
                        RS{i}="6.00 grams";
                    end

                    if ResponseIndex7(i)==0
                        RS{i}="8.00 grams";
                    end

                    if ResponseIndex5(i)==0
                        ResponseIndex4(i)=101;
                        ResponseIndex6(i)=101;
                        ResponseIndex7(i)=101;
                        dataout4(i)=0;
                        dataout6(i)=0;
                        dataout7(i)=0;
                        PercentError4(i)=0;
```

```
                    PercentError6(i)=0;
                    PercentError7(i)=0;
                    RS{i}="10.0 grams";
                end

            end

        end

    else
        fprintf('No False Positive \n');
        fprintf('Z axis move \n'); %Z axis moves
        pause(0.1);
        F="0.35";
        [ResponseIndex1(i), dataout1(i), PercentError1(i)] =
NeuropathyUnoFunction2(F, Uno);
        FalsePositiveCheckIndex(i)=0;

        if ResponseIndex1(i)==1
                ResponseIndex0(i)=101;
                ResponseIndex2(i)=101;
                ResponseIndex3(i)=101;
                ResponseIndex4(i)=101;
                ResponseIndex5(i)=101;
                ResponseIndex6(i)=101;
                ResponseIndex7(i)=101;
                dataout0(i)=0;
                dataout2(i)=0;
                dataout3(i)=0;
                dataout4(i)=0;
                dataout5(i)=0;
                dataout6(i)=0;
                dataout7(i)=0;
                PercentError0(i)=0;
                PercentError2(i)=0;
                PercentError3(i)=0;
                PercentError4(i)=0;
                PercentError5(i)=0;
                PercentError6(i)=0;
                PercentError7(i)=0;
                RS{i}="0.350 grams";
        end

        if ResponseIndex1(i)==0
            fprintf('Z axis move \n'); %Z axis moves
            pause(0.1);
            F="10";
            [ResponseIndex2(i), dataout2(i), PercentError2(i)] =
NeuropathyUnoFunction2(F, Uno);
        end

        if ResponseIndex2(i)==1
            fprintf('Z axis move \n'); %Z axis moves
            pause(0.1);
            F="4";
            [ResponseIndex3(i), dataout3(i), PercentError3(i)] =
NeuropathyUnoFunction2(F, Uno);
```

```
            end

            if ResponseIndex2(i)==0
                    ResponseIndex0(i)=101;
                    ResponseIndex3(i)=101;
                    ResponseIndex4(i)=101;
                    ResponseIndex5(i)=101;
                    ResponseIndex6(i)=101;
                    ResponseIndex7(i)=101;
                    dataout0(i)=0;
                    dataout3(i)=0;
                    dataout4(i)=0;
                    dataout5(i)=0;
                    dataout6(i)=0;
                    dataout7(i)=0;
                    PercentError0(i)=0;
                    PercentError3(i)=0;
                    PercentError4(i)=0;
                    PercentError5(i)=0;
                    PercentError6(i)=0;
                    PercentError7(i)=0;
                    RS{i}="Greater than 10.0 grams";
            end

            if ResponseIndex3(i)==1
                fprintf('Z axis move \n'); %Z axis moves
                pause(0.1);
                F="0.7";
                [ResponseIndex4(i), dataout4(i), PercentError4(i)] =
NeuropathyUnoFunction2(F, Uno);

                if ResponseIndex4(i)==1
                        ResponseIndex0(i)=101;
                        ResponseIndex5(i)=101;
                        ResponseIndex6(i)=101;
                        ResponseIndex7(i)=101;
                        dataout0(i)=0;
                        dataout5(i)=0;
                        dataout6(i)=0;
                        dataout7(i)=0;
                        PercentError0(i)=0;
                        PercentError5(i)=0;
                        PercentError6(i)=0;
                        PercentError7(i)=0;
                        RS{i}="0.700 grams";
                end

                if ResponseIndex4(i)==0
                    fprintf('Z axis move \n'); %Z axis moves
                    pause(0.1);
                    F="2";
                    [ResponseIndex6(i), dataout6(i), PercentError6(i)] =
NeuropathyUnoFunction2(F, Uno);

                    ResponseIndex0(i)=101;
                    ResponseIndex5(i)=101;
                    ResponseIndex7(i)=101;
```

```
                    dataout0(i)=0;
                    dataout5(i)=0;
                    dataout7(i)=0;
                    PercentError0(i)=0;
                    PercentError5(i)=0;
                    PercentError7(i)=0;
                end

                if ResponseIndex6(i)==1
                   RS{i}="2.00 grams";
                end

                if ResponseIndex6(i)==0
                   RS{i}="4.00 grams";
                end

            end

            if ResponseIndex3(i)==0
                fprintf('Z axis move \n'); %Z axis moves
                pause(0.1);
                F="8";
                [ResponseIndex5(i), dataout5(i), PercentError5(i)] =
NeuropathyUnoFunction2(F, Uno);

                if ResponseIndex5(i)==1
                    fprintf('Z axis move \n'); %Z axis moves
                    pause(0.1);
                    F="6";
                    [ResponseIndex7(i), dataout7(i), PercentError7(i)] =
NeuropathyUnoFunction2(F, Uno);

                    ResponseIndex0(i)=101;
                    ResponseIndex4(i)=101;
                    ResponseIndex6(i)=101;
                    dataout0(i)=0;
                    dataout4(i)=0;
                    dataout6(i)=0;
                    PercentError0(i)=0;
                    PercentError4(i)=0;
                    PercentError6(i)=0;
                end

                if ResponseIndex7(i)==1
                    RS{i}="6.00 grams";
                end

                if ResponseIndex7(i)==0
                    RS{i}="8.00 grams";
                end

                if ResponseIndex5(i)==0
                    ResponseIndex0(i)=101;
                    ResponseIndex4(i)=101;
                    ResponseIndex6(i)=101;
                    ResponseIndex7(i)=101;
                    dataout0(i)=0;
```

```
                    dataout4(i)=0;
                    dataout6(i)=0;
                    dataout7(i)=0;
                    PercentError0(i)=0;
                    PercentError4(i)=0;
                    PercentError6(i)=0;
                    PercentError7(i)=0;
                    RS{i}="10.0 grams";
                end

            end

        end
    end
end

TestLocationCelltoString=string(TestLocationCellArray);
TestLocationCelltoStringTranspose=TestLocationCelltoString';
ResponseIndexRecordI0=ResponseIndex0';
ResponseIndexRecordI1=ResponseIndex1';
ResponseIndexRecordI2=ResponseIndex2';
ResponseIndexRecordI3=ResponseIndex3';
ResponseIndexRecordI4=ResponseIndex4';
ResponseIndexRecordI5=ResponseIndex5';
ResponseIndexRecordI6=ResponseIndex6';
ResponseIndexRecordI7=ResponseIndex7';

FalsePositiveCheckIndexTranspose=FalsePositiveCheckIndex';
ForceIndexRecordD0=dataout0';
ForceIndexRecordD1=dataout1';
ForceIndexRecordD2=dataout2';
ForceIndexRecordD3=dataout3';
ForceIndexRecordD4=dataout4';
ForceIndexRecordD5=dataout5';
ForceIndexRecordD6=dataout6';
ForceIndexRecordD7=dataout7';
PercentErrorC0=PercentError0';
PercentErrorC1=PercentError1';
PercentErrorC2=PercentError2';
PercentErrorC3=PercentError3';
PercentErrorC4=PercentError4';
PercentErrorC5=PercentError5';
PercentErrorC6=PercentError6';
PercentErrorC7=PercentError7';

NumberofTrials=VectorTranspose;
LocationSelected=GcodeCelltoStringTranspose;
RandomizedOrder=RandomizedVectorTranspose;
RandomizedLocations=TestLocationCelltoStringTranspose;

FalsePositiveCheck=FalsePositiveRandomizationVectorTranspose;
FalsePositiveOrderofOccurance=FalsePositiveCheckIndexTranspose;

RandomizedPixelsX=TDataPixelsX(RandomizedVector);
RandomizedPixelsY=TDataPixelsY(RandomizedVector);

RR=RS';
```

```
RRS=string(RR);
RRC=convertStringsToChars(RRS);
colors=[0 1 0; 0 1 1; 0 0 1; 1 1 0; 0.9290 0.6940 0.1250; 1 0 1; 1 0 0; 0 0
0];
XC=[ 0 0 0 0 0 0 0 0]';
YC=XC;

GC=[ "0.350 grams" "0.700 grams" "2.00 grams" "4.00 grams" "6.00 grams" "8.00
grams" "10.0 grams" "Greater than 10.0 grams"]';
GF=[GC; RRC];
XF=[XC; RandomizedPixelsX];
YF=[YC; RandomizedPixelsY];
gscatter(XF, YF, GF, colors, '', 30, 'on', '', '');
legend('Location','northeastoutside');
hold on

T=table(NumberofTrials, LocationSelected, RandomizedOrder,
RandomizedLocations, FalsePositiveCheck, ForceIndexRecordD0, PercentErrorC0,
ResponseIndexRecordI0, FalsePositiveOrderofOccurance, ForceIndexRecordD1,
PercentErrorC1, ResponseIndexRecordI1, ForceIndexRecordD2, PercentErrorC2,
ResponseIndexRecordI2, ForceIndexRecordD3, PercentErrorC3,
ResponseIndexRecordI3, ForceIndexRecordD4, PercentErrorC4,
ResponseIndexRecordI4, ForceIndexRecordD5, PercentErrorC5,
ResponseIndexRecordI5, ForceIndexRecordD6, PercentErrorC6,
ResponseIndexRecordI6, ForceIndexRecordD7, PercentErrorC7,
ResponseIndexRecordI7);

End
```

Appendix I (Neuropathy Uno Function)

```
function [ResponseIndex, dataoutnum, PercentError] =
NeuropathyUnoFunction2(F, Uno)


flushinput(Uno);

%Uno=serial('COM6', 'BaudRate', 9600);
%fopen(Uno);
%pause(3)

fprintf(Uno,'%s\n', F);
foo=0;

while foo==0

    if Uno.BytesAvailable>=0
        dataoutLC=fscanf(Uno,'%s\n');
        dataoutH=fscanf(Uno,'%s\n');
        foo=1;
    end
end

if dataoutH=="y"
    ResponseIndex=1;
else
    ResponseIndex=0;
end

dataoutstr=convertCharsToStrings(dataoutLC);
dataoutnum=str2double(dataoutstr);
Fnum=str2double(F);

if Fnum==0
    PercentError=0;
else
PercentError=abs((Fnum-dataoutnum)/Fnum)*100;
end

%pause(0.25)
%fclose(Uno);
%pause(0.25)
%flushoutput(Uno);

end
```

Appendix J (Arduino Uno Function)

```
#include "Arduino.h"
#include "HX711N.h"
#include "AccelStepper.h"
#include <avr/wdt.h>

HX711N scale(3, 2);  // (DOUT, CLK)

double measuredload;
char response;
bool stop_motor = false;
int calibration_factor = 13280;
int trim_in_pin = A0;
int trim_value = 0;

// Motor steps per revolution. Most steppers are 200 steps or 1.8
degrees/step
#define MOTOR_STEPS 200

// Microstepping mode. If you hardwired it to save pins, set to the same
value here.
#define MICROSTEPS 1

#define DIR 6
#define STEP 7

bool foo = 1;
bool foot = 0;
int foob = 1;
bool fee=0;
int fum=0;

AccelStepper stepper(AccelStepper::DRIVER, STEP, DIR); // Defaults to
AccelStepper::FULL4WIRE (4 pins) on 2, 3, 4, 5

float inputload;
int startt;
int endt;
int n;

void setup() {
  pinMode(8, INPUT_PULLUP);
  pinMode(9, OUTPUT);
  stepper.setMaxSpeed(1000);
  stepper.setSpeed(-100);

  Serial.begin(9600);
  //  Serial.println("HX711 calibration sketch");
  //  Serial.println("Remove all weight from scale");
  //  Serial.println("After readings begin, place known weight on scale");

  //  scale.set_scale();
  scale.tare(10); // Reset the scale to 0; Reads value 10 times, calculates
average and uses it as offset.
```

```
  //  long zero_factor = scale.read_average(); //Get a baseline reading
  //  Serial.print("Zero factor: "); //This can be used to remove the need to
tare the scale. Useful in permanent scale projects.
  //  Serial.println(zero_factor);
  //
  scale.set_scale(calibration_factor); //Adjust to this calibration factor
  stepper.setCurrentPosition(0);
}

void loop() {

  if(Serial.available()>0 && foot == 0 && foo == 1)
  {
    inputload = Serial.parseFloat();
    foot = 1;
    foo = 0;
  }
  // NOTE: LOOP HAS TO RUN QUICKLY FOR STEPPER TO MOVE SMOOTHLY. DO NOT ADD
DELAYS
  while (foot == 1){
    stepper.setSpeed(-100);
    stepper.setAcceleration(250);
    stepper.move(-300);
    stepper.runToPosition();
    foot = 0;
    delay(250);
    }

  if (scale.is_ready() && foo == 0){
    measuredload = scale.get_units_direct();

    if (measuredload < .25*inputload) {
      stop_motor = false;
      stepper.setSpeed(-20);
    }
    else if (measuredload < .5*inputload) {
      stop_motor = false;
      stepper.setSpeed(-15);
    }
    else if (measuredload < .75*inputload) {
      stop_motor = false;
      stepper.setSpeed(-10);
    }
    else if (measuredload < .9*inputload) {
      stop_motor = false;
      stepper.setSpeed(-7);
    }
    else if (measuredload < 1*inputload) {
      stop_motor = false;
      stepper.setSpeed(-5);
    }
    else {
      stop_motor = true;
      foo=1;
    }

  }
```

```
if (stop_motor) {
  Serial.println(measuredload);
  stepper.moveTo(0);
  stepper.setSpeed(200);
  fee=0;
  while (fee==0){
    stepper.runToPosition();

    fee=1;

  }

  foo=1;
  foob = 1;
  fum=0;
      startt = millis();
      endt = startt;
          while ((endt - startt) <=5000 && fum==0){
              if (foob==1){

              if (n%2==0){
              digitalWrite(9, HIGH);
              delay(250);
              }

              if (n%2!=0){
              digitalWrite(9, LOW);
              delay(250);
              }

                    if (digitalRead(8) == LOW){
                      response = 'y';
                      Serial.println(response);
                      //Serial.println("felt");
                      digitalWrite(9, HIGH);
                      foob = 2;
                      fum=1;
                    }
              endt = millis();
              n=n+1;
        }
        }
          if (digitalRead(8) == HIGH && foo == 1){
          response = 'n';
          Serial.println(response);
          foob = 0;
          digitalWrite(9, LOW);
          }

          while (foob==0 || foob==2){
          //Serial.end();
          foo=0;
          reboot();

          }
```

```
            //Serial.end();
  }

  else{
    stepper.runSpeed();
  }

}

void reboot(){
  wdt_disable();
  wdt_enable(WDTO_15MS);
  while (1) {}
}
```

Appendix K (TSI Norm and Medical Data)

Group 1 Subjects							
Patient ID	Sex	Age (years)	BMI (kg/m^2)	ABI (mmHg)	FBS (mg/dL)	HbA1c (%)	TSI Norm
C1	Female	74	26.4	1.36	101.6667	5.643333	13.02681
C2	Male	61	27.4	1.23	102.3333		10.72981
C3	Male	59	41.6	1.3	103		15.55249
C4	Female	59	33.4	1.05	94.66667		8.038518
C5	Female	70	33.3	1.5	95	5.333333	14.79399
C6	Female	67	23.6	1.07	91.33333		15.36504
C7	Male	63	19.7	1.16	95		14.04279
C8	Male	63	38.2	1.16	97		12.64349
C9	Female	46	23	1.02	86.66667	5.256667	7.11493
C10	Male	72	22.2	1	107		17.48371
C11	Male	65	24.2	1.18	103.3333		11.5075
C12	Male	81	22.3	1.02	111	5.9	12.93836
C13	Male	65	33	1.01	97.66667		9.753646
C14	Male	47	28	1.05	87.66667		12.64823
C15	Male	65	30.1	1.17	108.6667	6.196667	16.11707
C16	Female	69	39.6	1.23	103.3333		11.6838
C17	Female	41	22.2	1.24	85.33333	5.04	7.200328
C18	Female	56	22.9	1.05	74.66667		5.61449
C19	Male	74	22.4	1.08	84		10.09325
C20	Male	45	48.6	1.17	115	5.7	7.787026
C21	Male	56	26.8	1.13	80		12.03518
C22	Male	46	20.5	1.3			8.418135

Group 2 Subjects							
Patient ID	Sex	Age (years)	BMI (kg/m^2)	ABI (mmHg)	FBS (mg/dL)	HbA1c (%)	Total Norm
S1	Male	62	33	1.03	203.3333	11.13333	14.20282
S2	Female	66	26.9	1	108.3333	6.013333	15.86821
S3	Male	50	40.2	1.09	158	8.546667	19.59592
S4	Male	42	31.8	1.02	139.6667	6.006667	13.77211
S5	Male	65	28.8	1.03	166	8.796667	12.01629
S6	Male	55	33	1.04	261.3333	11.4	8.679222
S7	Male	54	36.8	1.2	121.6667	6.55	15.2754
S8	Female	67	50.2	1	112.3333	6.366667	13.66163
S9	Male	55	39.9	1.08	119.6667	7.206667	17.67937
S10	Male	76	29.1	1.2	100.6667	6.096667	10.34752
S11	Male	70	34	1.25	198	8.993333	17.41238
S12	Female	67	23.3	1.5	86	5.393333	9.068382
S13	Male	74	32.3	1.05	136	6.166667	10.37413
S14	Female	64	39.9	1.33	124	8.293333	9.219198
S15	Male	79	22	1.45	114.3333	6.283333	15.37057
S16	Male	55	22.6	1.07	126.6667	6.29	8.844835
S17	Female	57	36.8	1.09	239	7.963333	15.65815
S18	Female	68	39	1.05	192	8.533333	12.5774
S19	Female	79	26.8	1.21	143	6.5	12.98208
S20	Female	58	44.3	1	158.3333	8.366667	16.49432
S21	Male	78	27	1.4	167.6667	7.65	9.500234
S22	Female	65	30.6	1.32	168.3333	6.85	8.397949
S23	Male	62	26.7	1.36	142.6667	7.186667	7.604933
S24	Female	64	26.5	1.04	84.33333	5.346667	16.72098
S25	Male	84	30.7	1.25	138.3333	7.82	19.59592
S26	Female	73	34.4	1	142	8.07	16.12335

Group 3 Subjects							
Patient ID	Sex	Age (years)	BMI (kg/m^2)	ABI (mmHg)	FBS (mg/dL)	HbA1c (%)	Total Norm
NS1	Female	68	22.7	1.18	103.6667	5.29	11.21467
NS2	Female	58	31.3	1	105.6667	6.21	4.734742
NS3	Male	58	32.9	1.08	150	7.843333	16.73679
NS4	Female	58	33.5	1.03	141.3333	7.09	3.279566
NS5	Female	69	30.2	1.19	157.6667	7.263333	11.11775
NS6	Male	64	30.4	1.09	110.6667	5.873333	13.03244
NS7	Male	63	35.2	1.2	161	7.35	17.10672
NS8	Male	64	34.9	1.3	157.3333	7.866667	3.703452
NS9	Female	61	34.4	1.26	128.3333	6.263333	12.15529
NS10	Male	63	27.3	1.19	129.3333	6.296667	10.93882
NS11	Female	64	37.9	1.06	159	7.75	5.303248
NS12	Female	63	43.7	1	126	6.76	16.96231
NS13	Male	64	35.67	1.41	170	6.796667	17.54993
NS14	Female	76	36.7	1.1	132	6.42	3.072458
NS15	Female	74	43.3	1.01	114.6667	5.693333	9.091266
NS16	Female	74	30.6	1.07	133.3333	6.31	5.318965
NS17	Male	66	24.2	1.18	139	7.65	16.70359
NS18	Male	72	36.4	1.05	160.3333	8.173333	18.66976
NS19	Male	60	33.4	1.12	129.6667	6.74	8.936271
NS20	Female	67	23.4	1.03	144	6.373333	5.73062
NS21	Female	65	22.1	1.06	108.3333	6.59	6.657327
NS22	Female	78	27	1.03	119	6.396667	10.34988

Appendix L (Multivariate Regression-Group 1)

SUMMARY OUTPUT

Regression Statistics	
Multiple R	0.642001382
R Square	0.412165774
Adjusted R Square	0.265207218
Standard Error	2.816084696
Observations	21

ANOVA

	df	*SS*	*MS*	*F*	*Significance F*
Regression	4	88.96690131	22.24173	2.80464	0.061268503
Residual	16	126.8853283	7.930333		
Total	20	215.8522296			

	Coefficients	*Standard Error*	*t Stat*	*P-value*	*Lower 95%*	*Upper 95%*	*Lower 95.0%*	*Upper 95.0%*
Intercept	-9.576087439	7.689525033	-1.24534	0.230936	-25.87715231	6.724977427	-25.87715231	6.724977427
Age	0.124504877	0.070859464	1.757068	0.098022	-0.025710477	0.27472023	-0.025710477	0.27472023
BMI	-0.067551344	0.105109735	-0.64267	0.529538	-0.290374028	0.155271341	-0.290374028	0.155271341
ABI	5.151458546	5.264869775	0.978459	0.342411	-6.009566791	16.31248388	-6.009566791	16.31248388
FBS	0.099899904	0.076515483	1.305617	0.210145	-0.062305675	0.262105483	-0.062305675	0.262105483

SUMMARY OUTPUT

Regression Statistics	
Multiple R	0.591217461
R Square	0.349538087
Adjusted R Square	0.23475069
Standard Error	2.873854291
Observations	21

ANOVA

	df	*SS*	*MS*	*F*	*Significance F*
Regression	3	75.44857533	25.14953	3.045091	0.057213125
Residual	17	140.4036542	8.259038		
Total	20	215.8522296			

	Coefficients	*Standard Error*	*t Stat*	*P-value*	*Lower 95%*	*Upper 95%*	*Lower 95.0%*	*Upper 95.0%*
Intercept	-4.568259914	6.801322752	-0.67167	0.510818	-18.91779661	9.781276777	-18.91779661	9.781276777
Age	0.170205715	0.06287424	2.707082	0.014952	0.037552664	0.302858765	0.037552664	0.302858765
BMI	0.006983997	0.090065746	0.077543	0.939097	-0.183038117	0.197006111	-0.183038117	0.197006111
ABI	4.835580588	5.367198181	0.900951	0.380201	-6.488217744	16.15937892	-6.488217744	16.15937892

SUMMARY OUTPUT

Regression Statistics	
Multiple R	0.613996672
R Square	0.376991914
Adjusted R Square	0.26704931
Standard Error	2.812552582
Observations	21

ANOVA

	df	*SS*	*MS*	*F*	*Significance F*
Regression	3	81.37454508	27.12485	3.428988	0.040822353
Residual	17	134.4776845	7.910452		
Total	20	215.8522296			

	Coefficients	*Standard Error*	*t Stat*	*P-value*	*Lower 95%*	*Upper 95%*	*Lower 95.0%*	*Upper 95.0%*
Intercept	-4.944273947	6.052109013	-0.81695	0.425258	-17.71310782	7.824559927	-17.71310782	7.824559927
Age	0.135466961	0.069880428	1.938554	0.069343	-0.011967854	0.282901776	-0.011967854	0.282901776
BMI	-0.034656126	0.099463198	-0.34843	0.731794	-0.24450513	0.175192878	-0.24450513	0.175192878
FBS	0.096459513	0.076338783	1.263572	0.223438	-0.06460124	0.257520266	-0.06460124	0.257520266

SUMMARY OUTPUT

Regression Statistics	
Multiple R	0.630072364
R Square	0.396991183
Adjusted R Square	0.290577863
Standard Error	2.76704129
Observations	21

ANOVA

	df	*SS*	*MS*	*F*	*Significance F*
Regression	3	85.69143204	28.56381	3.730653	0.03156291
Residual	17	130.1607975	7.656518		
Total	20	215.8522296			

	Coefficients	*Standard Error*	*t Stat*	*P-value*	*Lower 95%*	*Upper 95%*	*Lower 95.0%*	*Upper 95.0%*
Intercept	-8.933623354	7.491487061	-1.1925	0.249444	-24.73927946	6.872032747	-24.73927946	6.872032747
Age	0.144236125	0.062750657	2.29856	0.034486	0.011843812	0.276628438	0.011843812	0.276628438
ABI	4.069212684	4.901422033	0.830211	0.417927	-6.271883874	14.41030924	-6.271883874	14.41030924
FBS	0.073191746	0.063127259	1.159432	0.262307	-0.059995128	0.20637862	-0.059995128	0.20637862

SUMMARY OUTPUT

Regression Statistics	
Multiple R	0.546571099
R Square	0.298739966
Adjusted R Square	0.174988195
Standard Error	2.983962445
Observations	21

ANOVA

	df	*SS*	*MS*	*F*	*Significance F*
Regression	3	64.48368772	21.49456	2.414026	0.102235304
Residual	17	151.3685418	8.904032		
Total	20	215.8522296			

	Coefficients	*Standard Error*	*t Stat*	*P-value*	*Lower 95%*	*Upper 95%*	*Lower 95.0%*	*Upper 95.0%*
Intercept	-7.646333998	8.06439089	-0.94816	0.356333	-24.66071152	9.368043529	-24.66071152	9.368043529
BMI	-0.147571074	0.100378584	-1.47014	0.159788	-0.359351375	0.064209227	-0.359351375	0.064209227
ABI	6.614069488	5.508559261	1.20069	0.246335	-5.007974653	18.23611363	-5.007974653	18.23611363
FBS	0.166312182	0.070494107	2.359235	0.030537	0.017582616	0.315041748	0.017582616	0.315041748

SUMMARY OUTPUT

Regression Statistics	
Multiple R	0.564340308
R Square	0.318479983
Adjusted R Square	0.242755536
Standard Error	2.858783883
Observations	21

ANOVA

	df	*SS*	*MS*	*F*	*Significance F*
Regression	2	68.74461436	34.37231	4.205775	0.031718128
Residual	18	147.1076152	8.172645		
Total	20	215.8522296			

	Coefficients	*Standard Error*	*t Stat*	*P-value*	*Lower 95%*	*Upper 95%*	*Lower 95.0%*	*Upper 95.0%*
Intercept	-0.373489081	4.931846179	-0.07573	0.940469	-10.73491342	9.987935257	-10.73491342	9.987935257
Age	0.179036916	0.061779787	2.897985	0.009587	0.049242399	0.308831433	0.049242399	0.308831433
BMI	0.035512904	0.083873596	0.42341	0.677012	-0.140698982	0.211724791	-0.140698982	0.211724791

SUMMARY OUTPUT

Regression Statistics	
Multiple R	0.591022856
R Square	0.349308016
Adjusted R Square	0.277008906
Standard Error	2.793378237
Observations	21

ANOVA

	df	*SS*	*MS*	*F*	*Significance F*
Regression	2	75.39891401	37.69946	4.831429	0.020911207
Residual	18	140.4533156	7.802962		
Total	20	215.8522296			

	Coefficients	*Standard Error*	*t Stat*	*P-value*	*Lower 95%*	*Upper 95%*	*Lower 95.0%*	*Upper 95.0%*
Intercept	-4.466138324	6.485749194	-0.68861	0.49985	-18.09219175	9.159915105	-18.09219175	9.159915105
Age	0.169103928	0.059532615	2.840526	0.010851	0.044030544	0.294177311	0.044030544	0.294177311
ABI	4.981904909	4.883842664	1.020079	0.321207	-5.278667784	15.2424776	-5.278667784	15.2424776

SUMMARY OUTPUT

Regression Statistics	
Multiple R	0.610362789
R Square	0.372542734
Adjusted R Square	0.30282526
Standard Error	2.743052333
Observations	21

ANOVA

	df	*SS*	*MS*	*F*	*Significance F*
Regression	2	80.4141797	40.20709	5.343606	0.015075002
Residual	18	135.4380499	7.524336		
Total	20	215.8522296			

	Coefficients	*Standard Error*	*t Stat*	*P-value*	*Lower 95%*	*Upper 95%*	*Lower 95.0%*	*Upper 95.0%*
Intercept	-5.133219	5.878815506	-0.87317	0.394069	-17.48415207	7.217714067	-17.48415207	7.217714067
Age	0.145427236	0.062190377	2.33842	0.031106	0.014770103	0.276084369	0.014770103	0.276084369
FBS	0.081608843	0.061767617	1.321224	0.202977	-0.048160105	0.21137779	-0.048160105	0.21137779

SUMMARY OUTPUT

Regression Statistics	
Multiple R	0.262944017
R Square	0.069139556
Adjusted R Square	-0.034289382
Standard Error	3.34106023
Observations	21

ANOVA

	df	*SS*	*MS*	*F*	*Significance F*
Regression	2	14.92392731	7.461964	0.668474	0.524760554
Residual	18	200.9283023	11.16268		
Total	20	215.8522296			

	Coefficients	*Standard Error*	*t Stat*	*P-value*	*Lower 95%*	*Upper 95%*	*Lower 95.0%*	*Upper 95.0%*
Intercept	4.941528062	6.770649081	0.729846	0.474876	-9.283077819	19.16613394	-9.283077819	19.16613394
BMI	-0.048114735	0.10199912	-0.47172	0.642796	-0.262406935	0.166177465	-0.262406935	0.166177465
ABI	7.100720702	6.163455649	1.152068	0.264365	-5.848219115	20.04966052	-5.848219115	20.04966052

SUMMARY OUTPUT

Regression Statistics	
Multiple R	0.489153177
R Square	0.239270831
Adjusted R Square	0.154745368
Standard Error	3.020348464
Observations	21

ANOVA

	df	*SS*	*MS*	*F*	*Significance F*
Regression	2	51.64714233	25.82357	2.830754	0.085323885
Residual	18	164.2050872	9.122505		
Total	20	215.8522296			

	Coefficients	*Standard Error*	*t Stat*	*P-value*	*Lower 95%*	*Upper 95%*	*Lower 95.0%*	*Upper 95.0%*
Intercept	-1.323237328	6.181954013	-0.21405	0.832915	-14.31104077	11.66456611	-14.31104077	11.66456611
BMI	-0.113530959	0.09746597	-1.16483	0.259295	-0.318299362	0.091237445	-0.318299362	0.091237445
FBS	0.169481692	0.071303658	2.3769	0.028756	0.019678265	0.319285119	0.019678265	0.319285119

SUMMARY OUTPUT

Regression Statistics	
Multiple R	0.457803429
R Square	0.20958398
Adjusted R Square	0.121759977
Standard Error	3.078717809
Observations	21

ANOVA

	df	*SS*	*MS*	*F*	*Significance F*
Regression	2	45.2391693	22.61958	2.386409	0.120420827
Residual	18	170.6130603	9.478503		
Total	20	215.8522296			

	Coefficients	*Standard Error*	*t Stat*	*P-value*	*Lower 95%*	*Upper 95%*	*Lower 95.0%*	*Upper 95.0%*
Intercept	-5.095947089	8.125678417	-0.62714	0.538441	-22.16736397	11.97546979	-22.16736397	11.97546979
ABI	4.326799548	5.452087285	0.793604	0.437763	-7.127610794	15.78120989	-7.127610794	15.78120989
FBS	0.122787747	0.066007572	1.860207	0.079276	-0.015889015	0.261464509	-0.015889015	0.261464509

SUMMARY OUTPUT

Regression Statistics	
Multiple R	0.637071404
R Square	0.405859974
Adjusted R Square	0.343318919
Standard Error	2.660020956
Observations	22

ANOVA

	df	*SS*	*MS*	*F*	*Significance F*
Regression	2	91.83561316	45.91781	6.489497	0.007111213
Residual	19	134.4385183	7.075711		
Total	21	226.2741314			

	Coefficients	*Standard Error*	*t Stat*	*P-value*	*Lower 95%*	*Upper 95%*	*Lower 95.0%*	*Upper 95.0%*
Intercept	-0.066212005	3.373634399	-0.01963	0.984546	-7.127309953	6.994885943	-7.127309953	6.994885943
Age	0.172961829	0.053774256	3.216443	0.004544	0.060411017	0.28551264	0.060411017	0.28551264
Sex	1.684611099	1.181067846	1.426346	0.169994	-0.787392313	4.156614512	-0.787392313	4.156614512

Appendix M (Multivariate Regression-Group 2)

SUMMARY OUTPUT

Regression Statistics	
Multiple R	0.458507806
R Square	0.210229408
Adjusted R Square	0.01278676
Standard Error	3.62576898
Observations	26

ANOVA

	df	*SS*	*MS*	*F*	*Significance F*
Regression	5	69.98786771	13.99757	1.064762	0.408878676
Residual	20	262.9240139	13.1462		
Total	25	332.9118816			

	Coefficients	*Standard Error*	*t Stat*	*P-value*	*Lower 95%*	*Upper 95%*	*Lower 95.0%*	*Upper 95.0%*
Intercept	15.04500242	9.940017248	1.513579	0.145776	-5.689510222	35.77951507	-5.689510222	35.77951507
Age	0.051236958	0.081000833	0.632549	0.534194	-0.117727819	0.220201735	-0.117727819	0.220201735
BMI	0.13346426	0.123886497	1.077311	0.294165	-0.124958445	0.391886965	-0.124958445	0.391886965
ABI	-7.393100346	5.538442399	-1.33487	0.196916	-18.94608875	4.159888053	-18.94608875	4.159888053
FBS	-0.021307273	0.029733245	-0.71661	0.481897	-0.083329736	0.04071519	-0.083329736	0.04071519
HgbAl1c	0.312904891	0.847577408	0.369176	0.715876	-1.4551106	2.080920382	-1.4551106	2.080920382

SUMMARY OUTPUT

Regression Statistics	
Multiple R	0.452600808
R Square	0.204847492
Adjusted R Square	0.053389871
Standard Error	3.55042397
Observations	26

ANOVA

	df	*SS*	*MS*	*F*	*Significance F*
Regression	4	68.1961639	17.04904	1.352507	0.28389908
Residual	21	264.7157177	12.60551		
Total	25	332.9118816			

	Coefficients	*Standard Error*	*t Stat*	*P-value*	*Lower 95%*	*Upper 95%*	*Lower 95.0%*	*Upper 95.0%*
Intercept	15.5314613	9.647556175	1.609886	0.122353	-4.531730095	35.59465269	-4.531730095	35.59465269
Age	0.054763416	0.078764137	0.695284	0.4945	-0.109035572	0.218562405	-0.109035572	0.218562405
BMI	0.144977387	0.117405507	1.234843	0.230528	-0.09918073	0.389135504	-0.09918073	0.389135504
ABI	-7.459010519	5.420532753	-1.37607	0.1833	-18.73162548	3.81360444	-18.73162548	3.81360444
FBS	-0.012407646	0.017043205	-0.72801	0.474647	-0.047850932	0.02303564	-0.047850932	0.02303564

SUMMARY OUTPUT

Regression Statistics	
Multiple R	0.435833244
R Square	0.189950617
Adjusted R Square	0.035655496
Standard Error	3.583527555
Observations	26

ANOVA

	df	*SS*	*MS*	*F*	*Significance F*
Regression	4	63.23681716	15.8092	1.231086	0.327862946
Residual	21	269.6750645	12.84167		
Total	25	332.9118816			

	Coefficients	*Standard Error*	*t Stat*	*P-value*	*Lower 95%*	*Upper 95%*	*Lower 95.0%*	*Upper 95.0%*
Intercept	14.44835657	9.789688848	1.475875	0.154815	-5.910415896	34.80712903	-5.910415896	34.80712903
Age	0.060212378	0.079094317	0.761273	0.454958	-0.104273259	0.224698015	-0.104273259	0.224698015
BMI	0.145302706	0.121349678	1.197388	0.244497	-0.107057766	0.397663177	-0.107057766	0.397663177
ABI	-7.26966355	5.471269698	-1.3287	0.198206	-18.64779176	4.108464661	-18.64779176	4.108464661
HgbAl1c	-0.179544301	0.490364323	-0.36614	0.71792	-1.199312735	0.840224133	-1.199312735	0.840224133

SUMMARY OUTPUT

Regression Statistics	
Multiple R	0.405461562
R Square	0.164399078
Adjusted R Square	0.005236998
Standard Error	3.639606698
Observations	26

ANOVA

	df	*SS*	*MS*	*F*	*Significance F*
Regression	4	54.73040641	13.6826	1.032904	0.413565909
Residual	21	278.1814752	13.24674		
Total	25	332.9118816			

	Coefficients	*Standard Error*	*t Stat*	*P-value*	*Lower 95%*	*Upper 95%*	*Lower 95.0%*	*Upper 95.0%*
Intercept	21.5654588	7.914939814	2.724652	0.012696	5.105440381	38.02547721	5.105440381	38.02547721
Age	0.036733214	0.08017902	0.45814	0.651557	-0.130008187	0.203474615	-0.130008187	0.203474615
ABI	-9.393892183	5.237682932	-1.79352	0.087304	-20.28625012	1.498465756	-20.28625012	1.498465756
FBS	-0.025578656	0.029580171	-0.86472	0.396961	-0.087093989	0.035936678	-0.087093989	0.035936678
HgbAl1c	0.542761352	0.823413729	0.65916	0.516957	-1.169621238	2.255143943	-1.169621238	2.255143943

SUMMARY OUTPUT

Regression Statistics	
Multiple R	0.440941436
R Square	0.19442935
Adjusted R Square	0.040987322
Standard Error	3.573607226
Observations	26

ANOVA

	df	*SS*	*MS*	*F*	*Significance F*
Regression	4	64.72784084	16.18196	1.267119	0.314179
Residual	21	268.1840408	12.77067		
Total	25	332.9118816			

	Coefficients	*Standard Error*	*t Stat*	*P-value*	*Lower 95%*	*Upper 95%*	*Lower 95.0%*	*Upper 95.0%*
Intercept	17.50474456	9.016213189	1.941474	0.065738	-1.245497213	36.25498634	-1.245497213	36.25498634
BMI	0.120439568	0.120405853	1.00028	0.328562	-0.12995811	0.370837246	-0.12995811	0.370837246
ABI	-6.309955551	5.191312079	-1.21548	0.23767	-17.10588002	4.485968921	-17.10588002	4.485968921
FBS	-0.024215417	0.028953041	-0.83637	0.412364	-0.084426562	0.035995727	-0.084426562	0.035995727
HgbAl1c	0.376129993	0.829554654	0.453412	0.654903	-1.349023351	2.101283337	-1.349023351	2.101283337

SUMMARY OUTPUT

Regression Statistics	
Multiple R	0.429859675
R Square	0.18477934
Adjusted R Square	0.073612887
Standard Error	3.512294275
Observations	26

ANOVA

	df	*SS*	*MS*	*F*	*Significance F*
Regression	3	61.51523792	20.50508	1.662186	0.204139704
Residual	22	271.3966437	12.33621		
Total	25	332.9118816			

	Coefficients	*Standard Error*	*t Stat*	*P-value*	*Lower 95%*	*Upper 95%*	*Lower 95.0%*	*Upper 95.0%*
Intercept	13.21643731	9.010604612	1.466765	0.15659	-5.470412924	31.90328753	-5.470412924	31.90328753
Age	0.060584797	0.077515672	0.781581	0.442791	-0.100172867	0.221342461	-0.100172867	0.221342461
BMI	0.134303435	0.115235411	1.16547	0.25631	-0.104680181	0.373287051	-0.104680181	0.373287051
ABI	-7.072957167	5.33659735	-1.32537	0.198649	-18.14038268	3.994468351	-18.14038268	3.994468351

SUMMARY OUTPUT

Regression Statistics	
Multiple R	0.364895963
R Square	0.133149064
Adjusted R Square	0.014942118
Standard Error	3.621808791
Observations	26

ANOVA

	df	*SS*	*MS*	*F*	*Significance F*
Regression	3	44.32690543	14.77564	1.126406	0.35996291
Residual	22	288.5849762	13.1175		
Total	25	332.9118816			

	Coefficients	*Standard Error*	*t Stat*	*P-value*	*Lower 95%*	*Upper 95%*	*Lower 95.0%*	*Upper 95.0%*
Intercept	6.866328568	7.456040855	0.920908	0.367087	-8.596553754	22.32921089	-8.596553754	22.32921089
Age	0.021415656	0.076450096	0.280126	0.781998	-0.137132139	0.179963451	-0.137132139	0.179963451
BMI	0.202339694	0.111962632	1.807207	0.084426	-0.029856593	0.434535981	-0.029856593	0.434535981
FBS	-0.010113306	0.01730248	-0.5845	0.56483	-0.045996454	0.025769842	-0.045996454	0.025769842

SUMMARY OUTPUT

Regression Statistics	
Multiple R	0.349071646
R Square	0.121851014
Adjusted R Square	0.002103425
Standard Error	3.645334698
Observations	26

ANOVA

	df	*SS*	*MS*	*F*	*Significance F*
Regression	3	40.5656503	13.52188	1.017565	0.403852184
Residual	22	292.3462313	13.28847		
Total	25	332.9118816			

	Coefficients	*Standard Error*	*t Stat*	*P-value*	*Lower 95%*	*Upper 95%*	*Lower 95.0%*	*Upper 95.0%*
Intercept	5.982009412	7.560327642	0.791237	0.437254	-9.697150468	21.66116929	-9.697150468	21.66116929
Age	0.026797142	0.076283026	0.351286	0.728716	-0.131404172	0.184998456	-0.131404172	0.184998456
BMI	0.199209006	0.116339311	1.71231	0.100901	-0.042063958	0.440481971	-0.042063958	0.440481971
HgbAl1c	-0.115567485	0.496411337	-0.23281	0.818064	-1.145061587	0.913926617	-1.145061587	0.913926617

SUMMARY OUTPUT

Regression Statistics	
Multiple R	0.383549764
R Square	0.147110422
Adjusted R Square	0.030807297
Standard Error	3.592524273
Observations	26

ANOVA

	df	*SS*	*MS*	*F*	*Significance F*
Regression	3	48.97480731	16.32494	1.264888	0.310812251
Residual	22	283.9370743	12.90623		
Total	25	332.9118816			

	Coefficients	*Standard Error*	*t Stat*	*P-value*	*Lower 95%*	*Upper 95%*	*Lower 95.0%*	*Upper 95.0%*
Intercept	23.50803253	7.2508022	3.242129	0.003741	8.47078913	38.54527594	8.47078913	38.54527594
Age	0.040946962	0.078889872	0.51904	0.608916	-0.122660618	0.204554542	-0.122660618	0.204554542
ABI	-9.835591783	5.127442491	-1.91823	0.068153	-20.46925667	0.798073107	-20.46925667	0.798073107
FBS	-0.009779426	0.017110298	-0.57155	0.573419	-0.045264013	0.025705161	-0.045264013	0.025705161

SUMMARY OUTPUT

Regression Statistics	
Multiple R	0.366941246
R Square	0.134645878
Adjusted R Square	0.016643043
Standard Error	3.618680504
Observations	26

ANOVA

	df	*SS*	*MS*	*F*	*Significance F*
Regression	3	44.82521257	14.94174	1.141039	0.354427323
Residual	22	288.0866691	13.09485		
Total	25	332.9118816			

	Coefficients	*Standard Error*	*t Stat*	*P-value*	*Lower 95%*	*Upper 95%*	*Lower 95.0%*	*Upper 95.0%*
Intercept	21.54312523	7.869390373	2.737585	0.012018	5.223008474	37.86324198	5.223008474	37.86324198
Age	0.046130601	0.078982371	0.584062	0.56512	-0.11766881	0.209930013	-0.11766881	0.209930013
ABI	-9.459934815	5.207014817	-1.81677	0.082903	-20.25862261	1.338752978	-20.25862261	1.338752978
HgbAl1c	-0.034190486	0.479761657	-0.07127	0.94383	-1.029155265	0.960774294	-1.029155265	0.960774294

SUMMARY OUTPUT

Regression Statistics	
Multiple R	0.190799033
R Square	0.036404271
Adjusted R Square	-0.094995146
Standard Error	3.818569861
Observations	26

ANOVA

	df	*SS*	*MS*	*F*	*Significance F*
Regression	3	12.11941439	4.039805	0.27705	0.841324128
Residual	22	320.7924672	14.58148		
Total	25	332.9118816			

	Coefficients	*Standard Error*	*t Stat*	*P-value*	*Lower 95%*	*Upper 95%*	*Lower 95.0%*	*Upper 95.0%*
Intercept	13.08018214	6.657337049	1.964777	0.062194	-0.726289865	26.88665415	-0.726289865	26.88665415
Age	-0.019752481	0.077360152	-0.25533	0.800839	-0.180187616	0.140682654	-0.180187616	0.140682654
FBS	-0.026352253	0.031031359	-0.84921	0.404909	-0.090707352	0.038002845	-0.090707352	0.038002845
HgbAl1c	0.731700286	0.856802503	0.853989	0.402314	-1.045199351	2.508599922	-1.045199351	2.508599922

SUMMARY OUTPUT

Regression Statistics	
Multiple R	0.431906362
R Square	0.186543105
Adjusted R Square	0.075617165
Standard Error	3.508492719
Observations	26

ANOVA

	df	*SS*	*MS*	*F*	*Significance F*
Regression	3	62.10241619	20.70081	1.681691	0.199992344
Residual	22	270.8094654	12.30952		
Total	25	332.9118816			

	Coefficients	*Standard Error*	*t Stat*	*P-value*	*Lower 95%*	*Upper 95%*	*Lower 95.0%*	*Upper 95.0%*
Intercept	18.30411636	8.681052302	2.108514	0.046603	0.300715787	36.30751693	0.300715787	36.30751693
BMI	0.133381425	0.114842349	1.161431	0.257914	-0.10478703	0.37154988	-0.10478703	0.37154988
ABI	-6.299424694	5.096670447	-1.23599	0.229498	-16.86927227	4.270422882	-16.86927227	4.270422882
FBS	-0.013610665	0.016754905	-0.81234	0.4253	-0.048358211	0.02113688	-0.048358211	0.02113688

SUMMARY OUTPUT

Regression Statistics	
Multiple R	0.37115429
R Square	0.137755507
Adjusted R Square	0.020176713
Standard Error	3.612172833
Observations	26

ANOVA

	df	*SS*	*MS*	*F*	*Significance F*
Regression	3	45.86044504	15.28682	1.171602	0.343133359
Residual	22	287.0514366	13.04779		
Total	25	332.9118816			

	Coefficients	*Standard Error*	*t Stat*	*P-value*	*Lower 95%*	*Upper 95%*	*Lower 95.0%*	*Upper 95.0%*
Intercept	7.840111796	4.296696836	1.824683	0.08166	-1.070692053	16.75091564	-1.070692053	16.75091564
BMI	0.180791503	0.110875097	1.630587	0.117212	-0.049149374	0.41073238	-0.049149374	0.41073238
FBS	-0.021259916	0.029162108	-0.72903	0.473676	-0.081738426	0.039218595	-0.081738426	0.039218595
HgbAl1c	0.371618838	0.838498639	0.443196	0.661952	-1.367320907	2.110558583	-1.367320907	2.110558583

SUMMARY OUTPUT

Regression Statistics	
Multiple R	0.395028299
R Square	0.156047357
Adjusted R Square	0.040962906
Standard Error	3.573652717
Observations	26

ANOVA

	df	*SS*	*MS*	*F*	*Significance F*
Regression	3	51.95001925	17.31667	1.355938	0.282197434
Residual	22	280.9618624	12.77099		
Total	25	332.9118816			

	Coefficients	*Standard Error*	*t Stat*	*P-value*	*Lower 95%*	*Upper 95%*	*Lower 95.0%*	*Upper 95.0%*
Intercept	22.90985487	7.217656382	3.17414	0.004391	7.941351688	37.87835806	7.941351688	37.87835806
ABI	-8.451332734	4.729414473	-1.78697	0.08773	-18.25953804	1.356872569	-18.25953804	1.356872569
FBS	-0.027415482	0.028776118	-0.95272	0.351085	-0.087093499	0.032262534	-0.087093499	0.032262534
HgbAl1c	0.572838268	0.805918715	0.710789	0.484683	-1.098534851	2.244211386	-1.098534851	2.244211386

SUMMARY OUTPUT

Regression Statistics	
Multiple R	0.345959001
R Square	0.119687631
Adjusted R Square	0.043138729
Standard Error	3.569596539
Observations	26

ANOVA

	df	*SS*	*MS*	*F*	*Significance F*
Regression	2	39.84543431	19.92272	1.563545	0.230846476
Residual	23	293.0664473	12.74202		
Total	25	332.9118816			

	Coefficients	*Standard Error*	*t Stat*	*P-value*	*Lower 95%*	*Upper 95%*	*Lower 95.0%*	*Upper 95.0%*
Intercept	5.330230873	6.876938594	0.775088	0.446184	-8.895800486	19.55626223	-8.895800486	19.55626223
Age	0.027626843	0.074616547	0.370251	0.714583	-0.126729244	0.18198293	-0.126729244	0.18198293
BMI	0.191112151	0.108712425	1.757961	0.092057	-0.033776634	0.416000935	-0.033776634	0.416000935

SUMMARY OUTPUT

Regression Statistics	
Multiple R	0.366668935
R Square	0.134446108
Adjusted R Square	0.059180552
Standard Error	3.53954784
Observations	26

ANOVA

	df	*SS*	*MS*	*F*	*Significance F*
Regression	2	44.75870671	22.37935	1.78629	0.190056316
Residual	23	288.1531749	12.5284		
Total	25	332.9118816			

	Coefficients	*Standard Error*	*t Stat*	*P-value*	*Lower 95%*	*Upper 95%*	*Lower 95.0%*	*Upper 95.0%*
Intercept	21.18426632	5.915143116	3.581362	0.001581	8.947860495	33.42067214	8.947860495	33.42067214
Age	0.046422396	0.07715132	0.601706	0.553255	-0.113177269	0.206022062	-0.113177269	0.206022062
ABI	-9.386396008	4.99213495	-1.88024	0.0728	-19.71341396	0.940621947	-19.71341396	0.940621947

SUMMARY OUTPUT

Regression Statistics	
Multiple R	0.066791933
R Square	0.004461162
Adjusted R Square	-0.082107432
Standard Error	3.796031725
Observations	26

ANOVA

	df	*SS*	*MS*	*F*	*Significance F*
Regression	2	1.485173922	0.742587	0.051533	0.9498814
Residual	23	331.4267077	14.40986		
Total	25	332.9118816			

	Coefficients	*Standard Error*	*t Stat*	*P-value*	*Lower 95%*	*Upper 95%*	*Lower 95.0%*	*Upper 95.0%*
Intercept	15.19574334	6.142790327	2.473753	0.021183	2.488413383	27.9030733	2.488413383	27.9030733
Age	-0.017617457	0.076863384	-0.2292	0.820736	-0.176621481	0.141386566	-0.176621481	0.141386566
FBS	-0.004748634	0.01786591	-0.26579	0.792767	-0.041707085	0.032209818	-0.041707085	0.032209818

SUMMARY OUTPUT

Regression Statistics	
Multiple R	0.069407748
R Square	0.004817436
Adjusted R Square	-0.081720179
Standard Error	3.795352422
Observations	26

ANOVA

	df	*SS*	*MS*	*F*	*Significance F*
Regression	2	1.603781533	0.801891	0.055669	0.945979497
Residual	23	331.3081001	14.4047		
Total	25	332.9118816			

	Coefficients	*Standard Error*	*t Stat*	*P-value*	*Lower 95%*	*Upper 95%*	*Lower 95.0%*	*Upper 95.0%*
Intercept	12.99569625	6.616120618	1.964247	0.061698	-0.690792018	26.68218452	-0.690792018	26.68218452
Age	-0.010478035	0.076119728	-0.13765	0.891713	-0.167943689	0.14698762	-0.167943689	0.14698762
HgbAl1c	0.138541552	0.493204876	0.280901	0.781298	-0.881730468	1.158813573	-0.881730468	1.158813573

SUMMARY OUTPUT

Regression Statistics	
Multiple R	0.402670192
R Square	0.162143284
Adjusted R Square	0.089286178
Standard Error	3.482455755
Observations	26

ANOVA

	df	*SS*	*MS*	*F*	*Significance F*
Regression	2	53.97942562	26.98971	2.225497	0.130753158
Residual	23	278.932456	12.1275		
Total	25	332.9118816			

	Coefficients	*Standard Error*	*t Stat*	*P-value*	*Lower 95%*	*Upper 95%*	*Lower 95.0%*	*Upper 95.0%*
Intercept	16.06486481	8.170685668	1.966159	0.061464	-0.837486283	32.9672159	-0.837486283	32.9672159
BMI	0.120184358	0.112843779	1.065051	0.297907	-0.113250785	0.353619501	-0.113250785	0.353619501
ABI	-5.734906035	5.011601638	-1.14433	0.264258	-16.1021939	4.632381833	-16.1021939	4.632381833

SUMMARY OUTPUT

Regression Statistics	
Multiple R	0.360634361
R Square	0.130057143
Adjusted R Square	0.054409938
Standard Error	3.548510487
Observations	26

ANOVA

	df	*SS*	*MS*	*F*	*Significance F*
Regression	2	43.29756806	21.64878	1.719259	0.201438908
Residual	23	289.6143136	12.59193		
Total	25	332.9118816			

	Coefficients	*Standard Error*	*t Stat*	*P-value*	*Lower 95%*	*Upper 95%*	*Lower 95.0%*	*Upper 95.0%*
Intercept	8.645848486	3.824510795	2.260642	0.033552	0.734245123	16.55745185	0.734245123	16.55745185
BMI	0.19347888	0.10522788	1.838666	0.078913	-0.024201576	0.411159335	-0.024201576	0.411159335
FBS	-0.010787017	0.016787748	-0.64255	0.526868	-0.045515119	0.023941085	-0.045515119	0.023941085

SUMMARY OUTPUT

Regression Statistics	
Multiple R	0.341943458
R Square	0.116925329
Adjusted R Square	0.040136227
Standard Error	3.575192609
Observations	26

ANOVA

	df	*SS*	*MS*	*F*	*Significance F*
Regression	2	38.92583117	19.46292	1.522681	0.239315279
Residual	23	293.9860505	12.782		
Total	25	332.9118816			

	Coefficients	*Standard Error*	*t Stat*	*P-value*	*Lower 95%*	*Upper 95%*	*Lower 95.0%*	*Upper 95.0%*
Intercept	8.163280443	4.230015276	1.929847	0.06605	-0.587172851	16.91373374	-0.587172851	16.91373374
BMI	0.18754638	0.109356131	1.715006	0.099789	-0.038674013	0.413766772	-0.038674013	0.413766772
HgbAl1c	-0.123714564	0.486327955	-0.25439	0.801459	-1.12976059	0.882331461	-1.12976059	0.882331461

SUMMARY OUTPUT

Regression Statistics	
Multiple R	0.369684084
R Square	0.136666322
Adjusted R Square	0.061593829
Standard Error	3.535005314
Observations	26

ANOVA

	df	*SS*	*MS*	*F*	*Significance F*
Regression	2	45.49784251	22.74892	1.820458	0.184524845
Residual	23	287.4140391	12.49626		
Total	25	332.9118816			

	Coefficients	*Standard Error*	*t Stat*	*P-value*	*Lower 95%*	*Upper 95%*	*Lower 95.0%*	*Upper 95.0%*
Intercept	25.13699756	6.431741072	3.908273	0.000706	11.83192744	38.44206768	11.83192744	38.44206768
ABI	-8.805646553	4.652209734	-1.89279	0.071038	-18.42947562	0.818182518	-18.42947562	0.818182518
FBS	-0.010857875	0.016711752	-0.64971	0.522313	-0.045428767	0.023713018	-0.045428767	0.023713018

SUMMARY OUTPUT

Regression Statistics	
Multiple R	0.348177882
R Square	0.121227838
Adjusted R Square	0.044812867
Standard Error	3.566472463
Observations	26

ANOVA

	df	*SS*	*MS*	*F*	*Significance F*
Regression	2	40.35818758	20.17909	1.586441	0.226244143
Residual	23	292.553694	12.71973		
Total	25	332.9118816			

	Coefficients	*Standard Error*	*t Stat*	*P-value*	*Lower 95%*	*Upper 95%*	*Lower 95.0%*	*Upper 95.0%*
Intercept	23.26100101	7.193756594	3.233498	0.003672	8.37958168	38.14242033	8.37958168	38.14242033
ABI	-8.260156635	4.71566169	-1.75164	0.093161	-18.01524608	1.494932808	-18.01524608	1.494932808
HgbAl1c	-0.048716685	0.472204172	-0.10317	0.918723	-1.025545439	0.928112068	-1.025545439	0.928112068

SUMMARY OUTPUT

Regression Statistics	
Multiple R	0.183163259
R Square	0.03354878
Adjusted R Square	-0.050490457
Standard Error	3.74016446
Observations	26

ANOVA

	df	*SS*	*MS*	*F*	*Significance F*
Regression	2	11.16878731	5.584394	0.399204	0.675412815
Residual	23	321.7430943	13.98883		
Total	25	332.9118816			

	Coefficients	*Standard Error*	*t Stat*	*P-value*	*Lower 95%*	*Upper 95%*	*Lower 95.0%*	*Upper 95.0%*
Intercept	11.68403096	3.719548175	3.14125	0.004577	3.989559323	19.3785026	3.989559323	19.3785026
FBS	-0.025233694	0.0300898	-0.83861	0.410318	-0.087479187	0.037011798	-0.087479187	0.037011798
HgbAl1c	0.724630308	0.838771719	0.863918	0.396553	-1.010501192	2.459761808	-1.010501192	2.459761808

SUMMARY OUTPUT

Regression Statistics	
Multiple R	0.348374852
R Square	0.121365038
Adjusted R Square	0.044961997
Standard Error	3.566194041
Observations	26

ANOVA

	df	*SS*	*MS*	*F*	*Significance F*
Regression	2	40.40386306	20.20193	1.588484	0.225838264
Residual	23	292.5080186	12.71774		
Total	25	332.9118816			

	Coefficients	*Standard Error*	*t Stat*	*P-value*	*Lower 95%*	*Upper 95%*	*Lower 95.0%*	*Upper 95.0%*
Intercept	6.832232353	3.807721913	1.79431	0.085921	-1.044640561	14.70910527	-1.044640561	14.70910527
BMI	0.189113003	0.106100497	1.782395	0.087892	-0.030372597	0.408598603	-0.030372597	0.408598603
Sex	0.620145191	1.456619582	0.425743	0.674253	-2.393101994	3.633392375	-2.393101994	3.633392375

SUMMARY OUTPUT

Regression Statistics	
Multiple R	0.349137717
R Square	0.121897145
Adjusted R Square	0.045540375
Standard Error	3.565114021
Observations	26

ANOVA

	df	*SS*	*MS*	*F*	*Significance F*
Regression	2	40.58100801	20.2905	1.596416	0.224270408
Residual	23	292.3308736	12.71004		
Total	25	332.9118816			

	Coefficients	*Standard Error*	*t Stat*	*P-value*	*Lower 95%*	*Upper 95%*	*Lower 95.0%*	*Upper 95.0%*
Intercept	22.70701131	5.349718367	4.244525	0.000306	11.6402757	33.77375	11.6402757	33.77374692
ABI	-8.214152657	4.597029281	-1.78684	0.087152	-17.72383226	1.295527	-17.72383226	1.29552695
Sex	0.238561475	1.421042534	0.167878	0.868147	-2.701088978	3.178212	-2.701088978	3.178211928

SUMMARY OUTPUT

Regression Statistics	
Multiple R	0.410396399
R Square	0.168425204
Adjusted R Square	0.055028641
Standard Error	3.547349394
Observations	26

ANOVA

	df	*SS*	*MS*	*F*	*Significance F*
Regression	3	56.0707517	18.69025	1.485276	0.24605849
Residual	22	276.8411299	12.58369		
Total	25	332.9118816			

	Coefficients	*Standard Error*	*t Stat*	*P-value*	*Lower 95%*	*Upper 95%*	*Lower 95.0%*	*Upper 95.0%*
Intercept	15.33774496	8.511910147	1.801916	0.085279	-2.314876252	32.99036617	-2.314876252	32.99036617
ABI	-5.697101477	5.105832262	-1.1158	0.276546	-16.28594949	4.891746541	-16.28594949	4.891746541
BMI	0.130705329	0.117808098	1.109477	0.279206	-0.113613713	0.375024371	-0.113613713	0.375024371
Sex	0.590777154	1.449161483	0.407668	0.687457	-2.414599815	3.596154124	-2.414599815	3.596154124

Appendix N (Multivariate Regression-Group 3)

SUMMARY OUTPUT

Regression Statistics	
Multiple R	0.372109986
R Square	0.138465842
Adjusted R Square	-0.130763583
Standard Error	5.548357315
Observations	22

ANOVA

	df	*SS*	*MS*	*F*	*Significance F*
Regression	5	79.16240406	15.83248	0.514304	0.761674086
Residual	16	492.5483023	30.78427		
Total	21	571.7107064			

	Coefficients	*Standard Error*	*t Stat*	*P-value*	*Lower 95%*	*Upper 95%*	*Lower 95.0%*	*Upper 95.0%*
Intercept	-19.85480773	28.90696883	-0.68685	0.50201	-81.13484414	41.42522868	-81.13484414	41.42522868
Age	0.014368751	0.221984558	0.064729	0.949192	-0.45621749	0.484954991	-0.45621749	0.484954991
BMI	0.109303633	0.219224607	0.498592	0.624851	-0.355431772	0.574039038	-0.355431772	0.574039038
ABI	15.36418907	14.72359362	1.043508	0.312224	-15.84843508	46.57681322	-15.84843508	46.57681322
FBS	-0.039322167	0.127390248	-0.30867	0.761552	-0.30937743	0.230733096	-0.30937743	0.230733096
HgbAl1c	2.051507522	2.938406843	0.69817	0.495094	-4.177636715	8.28065176	-4.177636715	8.28065176

SUMMARY OUTPUT

Regression Statistics	
Multiple R	0.334991239
R Square	0.11221913
Adjusted R Square	-0.096670486
Standard Error	5.464074262
Observations	22

ANOVA

	df	*SS*	*MS*	*F*	*Significance F*
Regression	4	64.15687826	16.03922	0.537217	0.710384001
Residual	17	507.5538281	29.85611		
Total	21	571.7107064			

	Coefficients	*Standard Error*	*t Stat*	*P-value*	*Lower 95%*	*Upper 95%*	*Lower 95.0%*	*Upper 95.0%*
Intercept	-6.651081376	21.53002784	-0.30892	0.761135	-52.07546951	38.77330675	-52.07546951	38.77330675
Age	-0.035631005	0.206923358	-0.17219	0.865318	-0.472201129	0.400939119	-0.472201129	0.400939119
BMI	0.087411213	0.21367453	0.409086	0.687584	-0.363402639	0.538225065	-0.363402639	0.538225065
ABI	10.69636639	12.91881969	0.827968	0.419161	-16.55996065	37.95269343	-16.55996065	37.95269343
FBS	0.033870686	0.071273518	0.475221	0.640678	-0.116503293	0.184244665	-0.116503293	0.184244665

SUMMARY OUTPUT

Regression Statistics	
Multiple R	0.365151197
R Square	0.133335396
Adjusted R Square	-0.070585687
Standard Error	5.398700457
Observations	22

ANOVA

	df	*SS*	*MS*	*F*	*Significance F*
Regression	4	76.2292737	19.05732	0.653858	0.632115288
Residual	17	495.4814327	29.14597		
Total	21	571.7107064			

	Coefficients	*Standard Error*	*t Stat*	*P-value*	*Lower 95%*	*Upper 95%*	*Lower 95.0%*	*Upper 95.0%*
Intercept	-15.082025	23.76525507	-0.63463	0.534121	-65.22233036	35.05828035	-65.22233036	35.05828035
Age	-0.003675797	0.208372719	-0.01764	0.986131	-0.443303805	0.43595221	-0.443303805	0.43595221
BMI	0.08747204	0.201905161	0.433233	0.670292	-0.338510615	0.513454695	-0.338510615	0.513454695
ABI	12.54794338	11.24437493	1.115931	0.279978	-11.17561402	36.27150078	-11.17561402	36.27150078
HgbAl1c	1.305085414	1.624338646	0.803456	0.432802	-2.121969565	4.732140393	-2.121969565	4.732140393

SUMMARY OUTPUT

Regression Statistics	
Multiple R	0.353666621
R Square	0.125080079
Adjusted R Square	-0.080783432
Standard Error	5.424351878
Observations	22

ANOVA

	df	*SS*	*MS*	*F*	*Significance F*
Regression	4	71.50962033	17.87741	0.607587	0.662625055
Residual	17	500.2010861	29.42359		
Total	21	571.7107064			

	Coefficients	*Standard Error*	*t Stat*	*P-value*	*Lower 95%*	*Upper 95%*	*Lower 95.0%*	*Upper 95.0%*
Intercept	-14.94370869	26.56963686	-0.56244	0.581161	-71.00074243	41.11332506	-71.00074243	41.11332506
Age	0.00623425	0.216436283	0.028804	0.977356	-0.45040639	0.462874891	-0.45040639	0.462874891
ABI	13.3833031	13.86057491	0.965566	0.347797	-15.85995375	42.62655995	-15.85995375	42.62655995
FBS	-0.018830545	0.117883475	-0.15974	0.87497	-0.267542936	0.229881847	-0.267542936	0.229881847
HgbAl1c	1.841951323	2.843194995	0.647846	0.525738	-4.156665768	7.840568414	-4.156665768	7.840568414

SUMMARY OUTPUT

Regression Statistics	
Multiple R	0.371806722
R Square	0.138240238
Adjusted R Square	-0.064526764
Standard Error	5.383401953
Observations	22

ANOVA

	df	*SS*	*MS*	*F*	*Significance F*
Regression	4	79.03342437	19.75836	0.681769	0.614116055
Residual	17	492.677282	28.98102		
Total	21	571.7107064			

	Coefficients	*Standard Error*	*t Stat*	*P-value*	*Lower 95%*	*Upper 95%*	*Lower 95.0%*	*Upper 95.0%*
Intercept	-18.46451158	18.77093474	-0.98368	0.339069	-58.06772209	21.13869894	-58.06772209	21.13869894
BMI	0.10826072	0.212131691	0.510347	0.616371	-0.339298028	0.555819467	-0.339298028	0.555819467
ABI	15.1061692	13.75233661	1.098444	0.287325	-13.90872481	44.12106322	-13.90872481	44.12106322
FBS	-0.037150694	0.119239969	-0.31156	0.759162	-0.288725038	0.21442365	-0.288725038	0.21442365
HgbAl1c	1.990146569	2.698602353	0.737473	0.470892	-3.703406714	7.683699851	-3.703406714	7.683699851

SUMMARY OUTPUT

Regression Statistics	
Multiple R	0.316899786
R Square	0.100425474
Adjusted R Square	-0.049503613
Standard Error	5.345280304
Observations	22

ANOVA

	df	*SS*	*MS*	*F*	*Significance F*
Regression	3	57.41431883	19.13811	0.66982	0.581534533
Residual	18	514.2963876	28.57202		
Total	21	571.7107064			

	Coefficients	*Standard Error*	*t Stat*	*P-value*	*Lower 95%*	*Upper 95%*	*Lower 95.0%*	*Upper 95.0%*
Intercept	-6.567625917	21.06124475	-0.31183	0.758749	-50.8156592	37.68040737	-50.8156592	37.68040737
Age	-0.036024384	0.202423036	-0.17797	0.860737	-0.461299402	0.389250633	-0.461299402	0.389250633
BMI	0.124416648	0.194654093	0.639168	0.530764	-0.284536426	0.533369721	-0.284536426	0.533369721
ABI	13.67975877	11.04540031	1.238503	0.231439	-9.52576619	36.88528373	-9.52576619	36.88528373

SUMMARY OUTPUT

Regression Statistics	
Multiple R	0.276439998
R Square	0.076419072
Adjusted R Square	-0.077511082
Standard Error	5.416133843
Observations	22

ANOVA

	df	*SS*	*MS*	*F*	*Significance F*
Regression	3	43.6896019	14.5632	0.496453	0.689319529
Residual	18	528.0211045	29.33451		
Total	21	571.7107064			

	Coefficients	*Standard Error*	*t Stat*	*P-value*	*Lower 95%*	*Upper 95%*	*Lower 95.0%*	*Upper 95.0%*
Intercept	4.427715577	16.71910134	0.26483	0.794149	-30.69781292	39.55324408	-30.69781292	39.55324408
Age	-0.060871016	0.202869858	-0.30005	0.767577	-0.487084772	0.36534274	-0.487084772	0.36534274
BMI	0.046304774	0.206003291	0.224777	0.824685	-0.38649208	0.479101628	-0.38649208	0.479101628
FBS	0.062547663	0.061745559	1.01299	0.324489	-0.067174941	0.192270268	-0.067174941	0.192270268

SUMMARY OUTPUT

Regression Statistics	
Multiple R	0.264290741
R Square	0.069849596
Adjusted R Square	-0.085175472
Standard Error	5.435362324
Observations	22

ANOVA

	df	*SS*	*MS*	*F*	*Significance F*
Regression	3	39.93376168	13.31125	0.45057	0.720004034
Residual	18	531.7769447	29.54316		
Total	21	571.7107064			

	Coefficients	*Standard Error*	*t Stat*	*P-value*	*Lower 95%*	*Upper 95%*	*Lower 95.0%*	*Upper 95.0%*
Intercept	0.290739185	19.49685063	0.014912	0.988266	-40.67062402	41.25210239	-40.67062402	41.25210239
Age	-0.036705104	0.20766059	-0.17676	0.861674	-0.472983814	0.399573607	-0.472983814	0.399573607
BMI	0.06626647	0.20237397	0.327446	0.747108	-0.358905464	0.491438404	-0.358905464	0.491438404
HgbAl1c	1.532172128	1.622485165	0.944337	0.357502	-1.876542714	4.940886971	-1.876542714	4.940886971

SUMMARY OUTPUT

Regression Statistics	
Multiple R	0.321682529
R Square	0.103479649
Adjusted R Square	-0.045940409
Standard Error	5.336198621
Observations	22

ANOVA

	df	*SS*	*MS*	*F*	*Significance F*
Regression	3	59.16042343	19.72014	0.692542	0.568450209
Residual	18	512.550283	28.47502		
Total	21	571.7107064			

	Coefficients	*Standard Error*	*t Stat*	*P-value*	*Lower 95%*	*Upper 95%*	*Lower 95.0%*	*Upper 95.0%*
Intercept	-3.742713747	19.84675032	-0.18858	0.852531	-45.43918892	37.95376142	-45.43918892	37.95376142
Age	-0.038102413	0.201994589	-0.18863	0.852493	-0.462477298	0.386272471	-0.462477298	0.386272471
ABI	9.468415798	12.27119438	0.771597	0.450365	-16.31240693	35.24923852	-16.31240693	35.24923852
FBS	0.044496435	0.064818724	0.686475	0.501162	-0.091682652	0.180675522	-0.091682652	0.180675522

SUMMARY OUTPUT

Regression Statistics	
Multiple R	0.351805136
R Square	0.123766854
Adjusted R Square	-0.022272004
Standard Error	5.275477183
Observations	22

ANOVA

	df	*SS*	*MS*	*F*	*Significance F*
Regression	3	70.75883529	23.58628	0.847493	0.485852563
Residual	18	500.9518711	27.83066		
Total	21	571.7107064			

	Coefficients	*Standard Error*	*t Stat*	*P-value*	*Lower 95%*	*Upper 95%*	*Lower 95.0%*	*Upper 95.0%*
Intercept	-12.91690134	22.70353844	-0.56894	0.576429	-60.61526564	34.78146296	-60.61526564	34.78146296
Age	-0.002542366	0.203600641	-0.01249	0.990174	-0.43029144	0.425206709	-0.43029144	0.425206709
ABI	12.08946121	10.93895406	1.105175	0.283638	-10.89242847	35.07135088	-10.89242847	35.07135088
HgbAl1c	1.465350783	1.545553206	0.948108	0.355631	-1.781736012	4.712437578	-1.781736012	4.712437578

SUMMARY OUTPUT

Regression Statistics	
Multiple R	0.277664379
R Square	0.077097507
Adjusted R Square	-0.076719575
Standard Error	5.414144213
Observations	22

ANOVA

	df	*SS*	*MS*	*F*	*Significance F*
Regression	3	44.07747025	14.69249	0.501229	0.686172763
Residual	18	527.6332361	29.31296		
Total	21	571.7107064			

	Coefficients	*Standard Error*	*t Stat*	*P-value*	*Lower 95%*	*Upper 95%*	*Lower 95.0%*	*Upper 95.0%*
Intercept	2.737229373	19.21567082	0.142448	0.888309	-37.63339698	43.10785572	-37.63339698	43.10785572
Age	-0.048367802	0.208525129	-0.23195	0.819192	-0.486462842	0.389727237	-0.486462842	0.389727237
FBS	0.047685285	0.095480691	0.499423	0.623531	-0.152912203	0.248282773	-0.152912203	0.248282773
HgbAl1c	0.645058583	2.553936356	0.252574	0.803459	-4.720562597	6.010679764	-4.720562597	6.010679764

SUMMARY OUTPUT

Regression Statistics	
Multiple R	0.332672048
R Square	0.110670692
Adjusted R Square	-0.03755086
Standard Error	5.314754552
Observations	22

ANOVA

	df	*SS*	*MS*	*F*	*Significance F*
Regression	3	63.27161937	21.09054	0.746657	0.538292831
Residual	18	508.439087	28.24662		
Total	21	571.7107064			

	Coefficients	*Standard Error*	*t Stat*	*P-value*	*Lower 95%*	*Upper 95%*	*Lower 95.0%*	*Upper 95.0%*
Intercept	-9.406100438	14.01318656	-0.67123	0.510596	-38.84671294	20.03451206	-38.84671294	20.03451206
BMI	0.08848543	0.207746733	0.425929	0.675209	-0.34797426	0.52494512	-0.34797426	0.52494512
ABI	11.02409019	12.42867033	0.886989	0.386783	-15.08757724	37.13575761	-15.08757724	37.13575761
FBS	0.033919783	0.069325233	0.489285	0.630549	-0.111727128	0.179566694	-0.111727128	0.179566694

SUMMARY OUTPUT

Regression Statistics	
Multiple R	0.277626809
R Square	0.077076645
Adjusted R Square	-0.076743914
Standard Error	5.414205406
Observations	22

ANOVA

	df	*SS*	*MS*	*F*	*Significance F*
Regression	3	44.06554321	14.68851	0.501082	0.686269458
Residual	18	527.6451632	29.31362		
Total	21	571.7107064			

	Coefficients	*Standard Error*	*t Stat*	*P-value*	*Lower 95%*	*Upper 95%*	*Lower 95.0%*	*Upper 95.0%*
Intercept	-1.992439205	11.3550057	-0.17547	0.862671	-25.84842095	21.86354254	-25.84842095	21.86354254
BMI	0.047597937	0.205988771	0.231071	0.819866	-0.385168411	0.480364286	-0.385168411	0.480364286
FBS	0.04018987	0.096783235	0.415257	0.682862	-0.163144161	0.243523901	-0.163144161	0.243523901
HgbAl1c	0.797050289	2.48449762	0.320809	0.75205	-4.422685519	6.016786097	-4.422685519	6.016786097

SUMMARY OUTPUT

Regression Statistics	
Multiple R	0.353606249
R Square	0.125037379
Adjusted R Square	-0.020789724
Standard Error	5.271651112
Observations	22

ANOVA

	df	*SS*	*MS*	*F*	*Significance F*
Regression	3	71.48520829	23.8284	0.857436	0.480942291
Residual	18	500.2254981	27.79031		
Total	21	571.7107064			

	Coefficients	*Standard Error*	*t Stat*	*P-value*	*Lower 95%*	*Upper 95%*	*Lower 95.0%*	*Upper 95.0%*
Intercept	-14.35765841	16.60647236	-0.86458	0.398644	-49.24656221	20.53124539	-49.24656221	20.53124539
ABI	13.27899158	13.00248666	1.021266	0.320659	-14.03821922	40.59620238	-14.03821922	40.59620238
FBS	-0.017968571	0.110812031	-0.16215	0.872991	-0.250776009	0.214838868	-0.250776009	0.214838868
HgbAl1c	1.816055944	2.621386087	0.692785	0.497287	-3.691271861	7.32338375	-3.691271861	7.32338375

SUMMARY OUTPUT

Regression Statistics	
Multiple R	0.154166395
R Square	0.023767277
Adjusted R Square	-0.078994062
Standard Error	5.419859677
Observations	22

ANOVA

	df	*SS*	*MS*	*F*	*Significance F*
Regression	2	13.58800684	6.794003	0.231286	0.79571387
Residual	19	558.1226996	29.37488		
Total	21	571.7107064			

	Coefficients	*Standard Error*	*t Stat*	*P-value*	*Lower 95%*	*Upper 95%*	*Lower 95.0%*	*Upper 95.0%*
Intercept	12.09988262	14.91549444	0.811229	0.42728	-19.11860602	43.31837127	-19.11860602	43.31837127
Age	-0.078841318	0.202231766	-0.38986	0.700979	-0.502117268	0.344434632	-0.502117268	0.344434632
BMI	0.108049727	0.196914609	0.548714	0.589593	-0.304097287	0.520196741	-0.304097287	0.520196741

SUMMARY OUTPUT

Regression Statistics	
Multiple R	0.282857474
R Square	0.080008351
Adjusted R Square	-0.016832875
Standard Error	5.26142404
Observations	22

ANOVA

	df	*SS*	*MS*	*F*	*Significance F*
Regression	2	45.74163078	22.87082	0.826181	0.452842219
Residual	19	525.9690756	27.68258		
Total	21	571.7107064			

	Coefficients	*Standard Error*	*t Stat*	*P-value*	*Lower 95%*	*Upper 95%*	*Lower 95.0%*	*Upper 95.0%*
Intercept	-1.751044424	19.35842271	-0.09045	0.928873	-42.26868882	38.76659997	-42.26868882	38.76659997
Age	-0.040283352	0.199139463	-0.20229	0.841843	-0.457087038	0.376520334	-0.457087038	0.376520334
ABI	13.2004638	10.84703699	1.216965	0.238518	-9.502645541	35.90357315	-9.502645541	35.90357315

SUMMARY OUTPUT

Regression Statistics	
Multiple R	0.271710601
R Square	0.073826651
Adjusted R Square	-0.023665281
Standard Error	5.27907099
Observations	22

ANOVA

	df	*SS*	*MS*	*F*	*Significance F*
Regression	2	42.20748658	21.10374	0.757259	0.482588157
Residual	19	529.5032198	27.86859		
Total	21	571.7107064			

	Coefficients	*Standard Error*	*t Stat*	*P-value*	*Lower 95%*	*Upper 95%*	*Lower 95.0%*	*Upper 95.0%*
Intercept	5.344107103	15.80408738	0.338147	0.73896	-27.73422793	38.42244214	-27.73422793	38.42244214
Age	-0.060632379	0.197733244	-0.30664	0.762455	-0.474492816	0.353228057	-0.474492816	0.353228057
FBS	0.066654234	0.057488234	1.159441	0.26064	-0.053670022	0.186978489	-0.053670022	0.186978489

SUMMARY OUTPUT

Regression Statistics	
Multiple R	0.253592127
R Square	0.064308967
Adjusted R Square	-0.034184826
Standard Error	5.306126456
Observations	22

ANOVA

	df	*SS*	*MS*	*F*	*Significance F*
Regression	2	36.76612495	18.38306	0.652924	0.531812378
Residual	19	534.9445814	28.15498		
Total	21	571.7107064			

	Coefficients	*Standard Error*	*t Stat*	*P-value*	*Lower 95%*	*Upper 95%*	*Lower 95.0%*	*Upper 95.0%*
Intercept	1.51630839	18.67927149	0.081176	0.936151	-37.57985615	40.61247294	-37.57985615	40.61247294
Age	-0.034916332	0.202652916	-0.1723	0.865027	-0.459073759	0.389241094	-0.459073759	0.389241094
HgbAl1c	1.648327885	1.545587421	1.066473	0.299574	-1.586623766	4.883279535	-1.586623766	4.883279535

SUMMARY OUTPUT

Regression Statistics	
Multiple R	0.314392479
R Square	0.098842631
Adjusted R Square	0.003983961
Standard Error	5.207289001
Observations	22

ANOVA

	df	*SS*	*MS*	*F*	*Significance F*
Regression	2	56.50939039	28.2547	1.041999	0.372054074
Residual	19	515.201316	27.11586		
Total	21	571.7107064			

	Coefficients	*Standard Error*	*t Stat*	*P-value*	*Lower 95%*	*Upper 95%*	*Lower 95.0%*	*Upper 95.0%*
Intercept	-9.352983652	13.72942472	-0.68124	0.503941	-38.08899984	19.38303253	-38.08899984	19.38303253
BMI	0.125556975	0.189526226	0.662478	0.515621	-0.271125974	0.522239924	-0.271125974	0.522239924
ABI	14.0154784	10.60216451	1.321945	0.201882	-8.175106951	36.20606376	-8.175106951	36.20606376

SUMMARY OUTPUT

Regression Statistics	
Multiple R	0.267954551
R Square	0.071799641
Adjusted R Square	-0.02590566
Standard Error	5.284844681
Observations	22

ANOVA

	df	*SS*	*MS*	*F*	*Significance F*
Regression	2	41.04862364	20.52431	0.734859	0.492715759
Residual	19	530.6620828	27.92958		
Total	21	571.7107064			

	Coefficients	*Standard Error*	*t Stat*	*P-value*	*Lower 95%*	*Upper 95%*	*Lower 95.0%*	*Upper 95.0%*
Intercept	0.209457696	8.829730208	0.023722	0.981322	-18.27138002	18.69029542	-18.27138002	18.69029542
BMI	0.045981303	0.201006939	0.228755	0.821504	-0.374731056	0.466693662	-0.374731056	0.466693662
FBS	0.064167724	0.060018033	1.069141	0.298402	-0.061451463	0.189786911	-0.061451463	0.189786911

SUMMARY OUTPUT

Regression Statistics	
Multiple R	0.261218573
R Square	0.068235143
Adjusted R Square	-0.029845369
Standard Error	5.294982455
Observations	22

ANOVA

	df	*SS*	*MS*	*F*	*Significance F*
Regression	2	39.01076159	19.50538	0.695705	0.510987294
Residual	19	532.6999448	28.03684		
Total	21	571.7107064			

	Coefficients	*Standard Error*	*t Stat*	*P-value*	*Lower 95%*	*Upper 95%*	*Lower 95.0%*	*Upper 95.0%*
Intercept	-2.513886138	11.0368504	-0.22777	0.822257	-25.6142795	20.58650722	-25.6142795	20.58650722
BMI	0.065325472	0.197079002	0.331468	0.743919	-0.347165619	0.477816564	-0.347165619	0.477816564
HgbAl1c	1.593792982	1.543663044	1.032475	0.314814	-1.637130901	4.824716866	-1.637130901	4.824716866

SUMMARY OUTPUT

Regression Statistics	
Multiple R	0.318916051
R Square	0.101707448
Adjusted R Square	0.007150337
Standard Error	5.199005318
Observations	22

ANOVA

	df	*SS*	*MS*	*F*	*Significance F*
Regression	2	58.14723676	29.07362	1.075619	0.360968322
Residual	19	513.5634696	27.02966		
Total	21	571.7107064			

	Coefficients	*Standard Error*	*t Stat*	*P-value*	*Lower 95%*	*Upper 95%*	*Lower 95.0%*	*Upper 95.0%*
Intercept	-6.653084263	12.16271189	-0.54701	0.590742	-32.10993282	18.80376429	-32.10993282	18.80376429
ABI	9.803018846	11.83013091	0.828648	0.417592	-14.95772971	34.5637674	-14.95772971	34.5637674
FBS	0.044688741	0.063144428	0.707723	0.487709	-0.087474066	0.176851547	-0.087474066	0.176851547

SUMMARY OUTPUT

Regression Statistics	
Multiple R	0.351794348
R Square	0.123759263
Adjusted R Square	0.031523396
Standard Error	5.134794674
Observations	22

ANOVA

	df	*SS*	*MS*	*F*	*Significance F*
Regression	2	70.75449577	35.37725	1.341769	0.285051072
Residual	19	500.9562106	26.36612		
Total	21	571.7107064			

	Coefficients	*Standard Error*	*t Stat*	*P-value*	*Lower 95%*	*Upper 95%*	*Lower 95.0%*	*Upper 95.0%*
Intercept	-13.13191712	14.40242578	-0.91179	0.373306	-43.27654072	17.01270648	-43.27654072	17.01270648
ABI	12.10911382	10.5364667	1.149258	0.264712	-9.943964436	34.16219208	-9.943964436	34.16219208
HgbAl1c	1.469124065	1.475305384	0.99581	0.331856	-1.618725591	4.556973722	-1.618725591	4.556973722

SUMMARY OUTPUT

Regression Statistics	
Multiple R	0.272651733
R Square	0.074338967
Adjusted R Square	-0.023099036
Standard Error	5.277610717
Observations	22

ANOVA

	df	*SS*	*MS*	*F*	*Significance F*
Regression	2	42.50038361	21.25019	0.762936	0.480058126
Residual	19	529.2103228	27.85317		
Total	21	571.7107064			

	Coefficients	*Standard Error*	*t Stat*	*P-value*	*Lower 95%*	*Upper 95%*	*Lower 95.0%*	*Upper 95.0%*
Intercept	-0.99520558	10.23791767	-0.09721	0.923579	-22.42341354	20.43300237	-22.42341354	20.43300237
FBS	0.044824692	0.092293214	0.485677	0.63275	-0.148347224	0.237996608	-0.148347224	0.237996608
HgbAl1c	0.783005853	2.421091566	0.32341	0.749917	-4.284397033	5.850408739	-4.284397033	5.850408739

Appendix O (Sensitivity, Specificity, Positive and Negative Predictive Values)

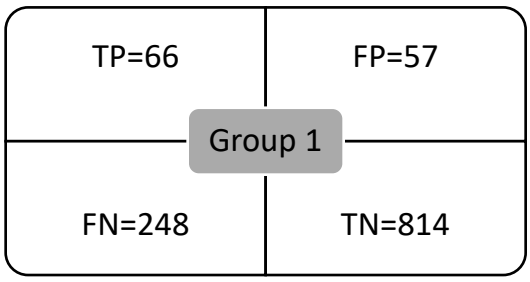

Sensitivity=21.0%
Specificity= 93.5%
PPV=53.7%
NPV=76.6%

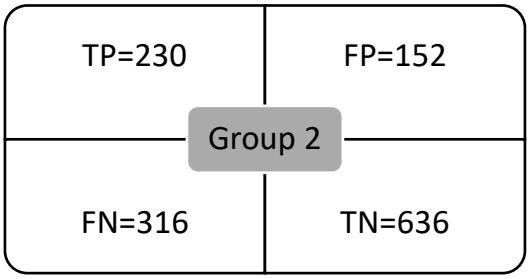

Sensitivity=42.1%
Specificity= 80.7%
PPV=60.2%
NPV=66.8%

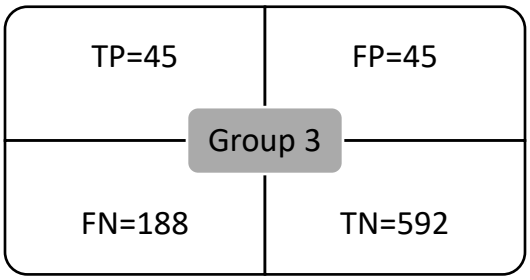

Sensitivity=19.3%
Specificity= 92.9%
PPV=50.0%
NPV=75.9%

[15]

[15]

TP-True Positive
FN-False Negative
FP-False Positive
TN-True Negative
PPV-Positive Predictive Value
NPV-Negative Predictive Value